Identification of Therapeutic Targets and Molecular Markers for Glioblastoma Stem Cells

A thesis

submitted by

Shreya Kulkarni

In partial fulfillment of the requirements
for the degree of

Doctor of Philosophy

in

Cellular and Molecular Physiology

TUFTS UNIVERSITY

Sackler School of Graduate Biomedical Sciences

May, 2016

Advisor: Dr. Brent Cochran

Thesis Chair: Dr. Gary Sahagian
Committee Member: Dr. Michael Forgac
Outside Examiner: Dr. Charles Stiles

Abstract

Glioblastoma Multiforme (GBM) is the most common type of malignant brain cancer with a median survival of only 14 months post diagnosis. The current standard of care for all the patients is maximal surgical resection followed by radiation and chemotherapy with temozolomide, a DNA alkylating agent. This treatment reduces the tumor bulk, but is not curative as recurrence is very common. The GBM tumor cell population is heterogeneous and a small percentage of the tumor cell population, known as GBM stem cells (GBM-SCs), has the capacity to initiate and sustain tumor growth as well as the ability to survive in hypoxic tumor niches. Hypoxia drives clonogenicity of GBM-SCs and increases their ability to resist chemo and radiotherapy. GBM-SCs can be isolated using cell surface markers such as CD133. However, these markers are not ideal, as they do not detect all the cancer stem cell populations and their expression can change in response to the external microenvironment, which may lead to confounding results.

Due to the high mortality associated with these tumors, there is an urgent need for the development of new therapeutics against GBM and especially ones that specifically target the GBM-SC population. Further, the lack of good GBM stem cell markers is a hindrance to our ability to identify and study these cells. In this thesis, I have identified novel therapeutic targets for GBM-SCs and have characterized novel molecular markers for GBM-SCs.

First, I have used a genome-wide RNAi approach (~10,000 genes) to screen and identify genes important for cellular growth and survival, which could potentially be used to target the GBM stem cell population. Using this unbiased RNAi screening approach, I identified several genes important in GBM stem cell growth and survival in hypoxic (1%

oxygen) and normoxic (21% oxygen) conditions. I identified 81 essential genes, which are required for GBM-SC growth under both normoxic and hypoxic conditions in two different GBM-SC cell lines. Interestingly, only about a third of the essential genes were common to both cell lines. This indicates a high degree of variability between the cell lines and suggests that for a given tumor the majority of potential targets may be tumor specific highlighting the need for personalized therapies. 30% of the hits under hypoxic conditions were specific to this oxygen environment suggesting that some genetic targets are dependent on the oxygen environment. In addition to revealing genetic hits that are essential genes already implicated in GBM such as CDK4, KIF11 and Ran, the screen also identified genes that have not been previously implicated in GBM stem cell biology. One such gene, the Serum and Glucocorticoid regulated Kinase -1 (SGK1) was selected for further investigation. SGK1 scored as a hit in two different GBM-SC lines in the pooled RNAi screen. I have validated SGK1 as a gene important in GBM-SC survival using shRNA mediated knockdown, CRISPR/Cas9 gene modification, as well as pharmacological inhibition of the kinase. I show that SGK1 depletion induces cell death specifically in the GBM-SCs and not in traditional serum-dependent glioma cell lines. This effect is also exclusive to the undifferentiated state of the GBM-SCs.

Finally, to address the need for identification of better molecular markers for GBM-SCs, I characterized a panel of GBM-SC specific monoclonal antibodies that our laboratory had generated previously in a collaborative effort with Douglas Jefferson's laboratory and Cell Essentials. The antigen for these antibodies is lost upon differentiation of GBM-SCs and a similar pattern was observed for staining of undifferentiated and differentiated embryonic stem cells for mAb 7-18. We have

identified the antigen for mAb 7-18 by immunoaffinity purification and mass spectrometry to be the Coxsackie virus and Adenovirus Receptor (CXADR), which is currently being investigated for its utility as a stem cell marker for GBMs. All these antibodies have also been evaluated for their possible use as toxin conjugated mAb therapeutics. We have shown that these antibodies bind cell surface antigens, are internalized, and can detect their antigen in human GBM tissue samples. Thus, these antibodies may be novel drug development candidates for identifying and possibly targeting GBM-SC in human GBMs. The results of this thesis have advanced our knowledge of GBM biology by identifying new genetic targets, which may be therapeutically relevant and by characterizing new molecular markers to further our understanding of GBM stem cells.

Acknowledgements

I would like to gratefully acknowledge various people without whom this dissertation would not have been possible. First and foremost, I would like to thank my thesis advisor Dr. Brent Cochran. I knew his was the lab I wanted to join within the first week of my rotation and it was absolute pleasure to work under his tutelage. I have not met someone as excited as Brent is about science and he pushed me to test the boundaries of my knowledge. I will forever be grateful for the guidance and support he has provided through these crucial years of my scientific training. I would also like to thank my thesis committee members Dr. Gary Sahagian and Dr. Michael Forgac for all their input and guidance on my project and keeping me focused towards completing my PhD. Gary has been very supportive ever since I had interviewed with him to join the program at Tufts. I would also like to extend my gratitude to Dr. Charles Stiles for agreeing to serve as the outside examiner for my defense. I would also like to thank Dr. Douglas Jefferson and Dr. Shelley Grubman for all the encouragement they have provided during my time in lab. I was lucky to be able to work on a very interesting project, which makes Chapter 5 of this thesis, in collaboration with Douglas Jefferson's lab and Cell Essentials.

My experience in graduate school would not have been the same without the many people I have had the pleasure to work and hang out with at Tufts. I would like to sincerely thank the members of the Cochran lab, Sejuti Sengupta and Surbhi Goel-Bhattacharya for all their help and the great company they have provided. I look forward to maintaining that relationship for many years to come. I also would like to take this opportunity to thank some of the people who made key contributions in the projects during my thesis, especially for work in Chapter 5. Many strides had already been made

by Mike Boncaldo, Forrest White, Maureen Sherry-Lynes, Caitlyn Synder, Douglas Jefferson, Shelly Grubman, Willem Louis and Brent Cochran, before I joined the lab. During my PhD, I have had the pleasure of collaborating with Alex Neil, Sean Koerner, Colleen Flannagan, Dorjee Norbu and Brendan Waldoch. All these people have contributed immensely to the work in Chapter 5.The great collegial environment in the department is thanks to the great students and post docs who have worked on the Jaharis 7th floor lab space and in the CMP department. It was great to hang out and relax with everyone at Tea after a busy week in lab.

I would like to thank my friends outside of Tufts, who have been crucial throughout this whole process. My "DC and Boston family" have made living in the US worthwhile and I am grateful for all their support and all the memories we have created together over the years. I would like to thank my parents Rajeshwary and Avinash Kulkarni, my sister Bakuli, my brother-in-law Chandrasekhar and my grandfather, Madhusudan Joshi for all their love and affection over many years. I would also like to thank my in-laws Vineeta and Murari Lal Aggarwal and Kaushu for their kind words of encouragement. My uncle and aunt, Dhananjay and Ruchi Joshi and Sunil and Jyoti Sood have been a great support system ever since I travelled here for the very first time. I would not have been able to pursue my interests without their unwavering support. Last but certainly not the least, I could not have done it without the love and support of my wife, Shiuli Agarwal, who has always been there to cheer me up when the chips are down and to encourage me to keep going. Our 1 year old daughter, Saisha Kulkarni, keeps us both going and is the best alarm clock I could hope for to start off every day in the best possible way.

Table of Contents

List of Figures

List of Tables

List of Abbreviations

GBM	Glioblastoma Multiforme
GBM-SCs	Glioblastoma Multiforme Stem Cells
TMZ	Temozolomide
EGF	Epidermal Growth Factor
bFGF	basic Fibroblast Growth Factor
HIF	Hypoxia Inducible Factor
PDGFR	Platelet Derived Growth Factor Receptor
VEGF	Vascular Endothelial Growth Factor
IDH1	Isocitrate dehydrogenase 1
PI3K	Phosphoinositide 3 Kinase
RNAi	RNA interference
shRNA	Short hairpin RNA
sgRNA	Small guide RNA
MAD	Median Absolute Deviation
BAGEL	Bayesian Analysis of Gene EssentiaLity
CRISPR	Clustered regularly-interspaced short palindromic repeats
SGK1	Serum and Glucocorticoid regulated Kinase 1
mAb	Monoclonal Antibodies
CSCs	Cancer Stem Cells
TAC	Transit Amplifying Cells
CXADR	Coxsackie virus and Adenovirus Receptor
IPA	Ingenuity Pathway Analysis
RBX1	Ring box protein 1
KIF11	Kinesin 11
FAK	Focal Adhesion Kinase
FOXO3a	Forkhead Transcription Factor 3a
NF-κB	Nuclear Factor Of Kappa Light Polypeptide Gene Enhancer In B-Cells-1

Chapter 1

Introduction

Primary malignant brain tumors affect around 7.23 per 100,000 people, and almost 17,000 deaths are expected to be attributed to it in 2016 (CBTRUS 2015), indicating the high mortality rate of this cancer. Gliomas are the most common primary tumors of the central nervous system [1, 2].Within this group, astrocytomas account for almost 66% of all malignant tumors of the CNS. Depending on the ability of the tumors to invade into the surrounding brain tissue, gliomas can be classified as diffuse tumors, which invade the surrounding brain parenchyma, and circumscribed tumors having a much clearer boundary between cancerous and normal brain tissue[3]. Diffuse gliomas can be further classified into different grades I-IV, based on their histopathology and clinical presentation[4]. Grade I gliomas are benign and are often non-lethal due to their lack of progression. Grade II and III tumors are more invasive and aggressive and can progress to grade IV, which are considered to be incurable. Grade IV astrocytomas are termed as Glioblastoma Multiforme (GBM), named so due to each tumor's varied appearance both grossly and microscopically. GBMs make up more than 90% of all astrocytoma cases[4].

Glioblastoma Multiforme and Clinical Relevance

GBM is the most common type of primary tumor of the brain, accounting for ~45% of malignant gliomas[5, 6]. The hallmark histological features of this tumor include high mitotic index, diffuse brain infiltration, presence of necrotic regions as well as microvascular proliferation in the tumors [4, 7]. The current standard of care for GBM patients is maximal safe resection surgery of tumor from the brain, followed by a regimen of radio and chemotherapy and adjuvant chemotherapy[8]. Chemotherapy consists of administration of temozolomide (TMZ), a cytotoxic DNA alkylating agent. Even with this aggressive treatment regimen, the prognosis for GBMs remains poor with median

survival of 14-15 months post diagnosis and a low 5.3% 5-yr survival rate for the patients[8, 9]. Due to its diffuse invasive pattern of growth, the surgical removal of tumor tissue remains incomplete, leading to relapse within a mean of 6-7 months post surgery, usually close to the boundary of the original tumor[10, 11]. Recent clinical trials have tested the use of bevacizumab in GBM, both as standalone therapy and as cotreatment with TMZ and radiation. Although bevacizumab does increase progression free survival, there is no effect on overall survival of the patients [12, 13].

80% of all diagnosed GBMs arise de novo, known as primary GBMs, and present with no previous history of lower grade tumors in the patients [1]. This is in contrast to secondary GBMs, which are typically diagnosed 5-7 years after the patient has been diagnosed and treated for a lower grade glioma [14]. Although clinically and histopathologically indistinguishable, primary and secondary GBMs differ greatly in the genetic landscape of the tumor cells, with each possessing mutations uniquely present in one or the other[14]. Due to their progression from low grade gliomas, secondary GBMs possess many of the mutations found in those tumors, the most common being the mutation in isocitrate dehydrogenase 1/2 (IDH1/2), which is present in almost 90% of secondary GBM cases[15, 16]. Additionally, other mutations such as in tumor protein p53 (TP53), Alpha Thalassemia/Mental Retardation Syndrome X-linked (ATRX) genes and the deletion of 1p/19q chromosomal arms are typical in various low grade gliomas [17]. However, these mutations are not as common in primary GBMs, which possess prevalent mutations in Epidermal Growth Factor Receptor (EGFR) and Phosphatase and Tensin Homolog (PTEN) genes, amongst others, not found in secondary GBM tumors [3, 14]. The co-occurrence of mutations in TP53 and EGFR are rare, indicating the independent

evolution of these tumors and may present a case for classification of these into different disease groups [14, 18]. A recent TCGA analysis of the mutational profiles of lower grade gliomas (LGG) revealed that the molecular landscape and not histology was the best predictor of survival and progression in LGGs. The mutations divided LGGs into 3 subtypes based on the IDH1, 1p/19q and TP53 mutational status. Patients with IDH1 mutation and 1p/19q codeletions had TERT promoter mutations and the most favorable prognosis from the 3 groups. IDH1 mutants without 1p/19q codeletions, histologically present as LGGs similar to ones with the deletion, however, almost exclusively possess mutations in TP53 (94%) and ATRX (87%) and a poorer prognosis [19]. This indicates the importance and need for molecular classifications for aiding in diagnosis and treatment.

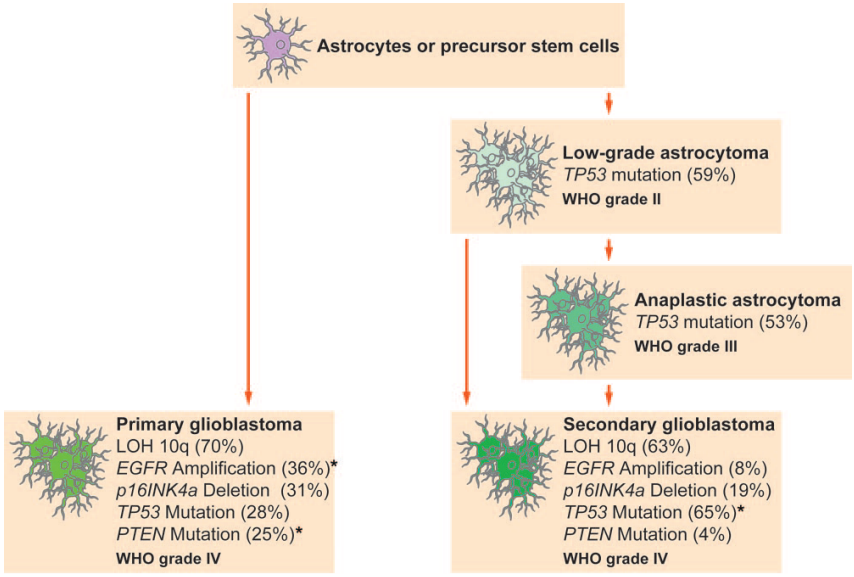

Figure 1.1: Distinct molecular evolution of primary and secondary GBMs. Different molecular and genetic events drive the pathogenesis of primary and secondary GBMs, with rare overlap of predominant mutations in each type. Adapted from Raudino et al. ISBN: 978-953-51-0989-1, InTech, DOI: 10.5772/52782[20].

Molecular Characterization of GBMs

The intertumoral heterogeneity in GBMs, as in many other cancer types, is clear[9, 19, 21, 22]. The physiological and genetic differences between each patient tumor presents with a clinical challenge of personalizing therapy to the patient. Although each GBM presents with similar clinical and histological features such as microvascular proliferation and necrosis, the genetic and transcriptional landscape of each tumor may be quite different [2, 7].

The differences between gliomas have been previously utilized to segregate the tumors into different subtypes based on patient survival, histological features as well as specific mutations such 1p/19q deletion, $IDH1^{R132H}$ and EGFRvIII mutations[18, 19, 23–26]. Phillips et al utilized an unbiased classification approach to segregate grade III and grade IV gliomas, using the transcriptional profile of the tumors [21]. Using k-means clustering, the authors were able to segregate 76 tumor samples into 3 subgroups; Proneural, Proliferative and Mesenchymal. The tumors within a subclass were similar in expression of 32 genes defined for each subclass. Analysis of each subtype revealed the enrichment of tumors with lower grades in the proneural subtype and lower survival of the patients with tumors in the mesenchymal or proliferative subtypes[21].

IDH1 was identified as a frequent mutation in grade I-III gliomas and in 85% of secondary glioblastomas. Patients with tumors possessing this mutation have a better disease prognosis [15, 16]. However, this mutation is not frequently detected in primary GBMs (<10%), indicating the distinct molecular origins of the different grades of gliomas [16, 22]. Classification of gliomas has been performed utilizing the mutation in the IDH1 gene and TERT promoter methylation as well as taking into account the

epigenetic differences in tumors[27]. The loss of specific DNA repair enzyme O-6-methylguanine-DNA-methyltransferase (MGMT) has been reported in various cancers, especially in GBMs, where this protein loss is due to methylation of its promoter [28]. MGMT repairs the alkyl adducts on the guanine residue of the DNA, which is the main mechanism of action of TMZ, the frontline chemotherapy used in GBMs[29, 30]. The efficacy of treatment by TMZ is reduced when MGMT is expressed due to its ability to repair the lesions made by the drug. The presence of promoter methylation at the MGMT locus has been used to group GBMs, and the patients with unmethylated MGMT promoter have been shown to be at a significantly higher risk of death from GBM due to lack of response to TMZ [31, 32]. As MGMT successfully predicts the response to TMZ in patients, this stratification has been proposed as a selection criteria for receiving adjuvant TMZ therapy [8, 31, 32].

Global DNA methylation profiling and clustering of GBM tumors has led to the identification of the Glioma CpG Island Methylator Phenotype or G-CIMP+ subclass of GMBs. This group features hypermethylation of CpG sites in specific subset of genes, and offers a significant survival benefit. Patients having G-CIMP+ tumors survive almost 3 times longer compared to the G-CIMP- subgroup. Interestingly, the occurrence of G-CIMP is highly correlated with the presence of IDH1 mutations in these tumors (87.5%) and almost all IDH1 mutant tumors possess this hypermethylation [9, 33].This co-occurrence has been attributed, in part, to the epigenetic effects of neo-metabolite 2-hydroxyglutarate (2-HG), produced by the $IDH1^{R132H}$ mutant protein [34]. One of the targets of 2-HG are the ten-eleven-translocation (TET) family of DNA hydroxylases

which are inhibited by the oncometabolite and this inhibition may result in the G-CIMP phenotype observed in IDH1 mutant tumors [35, 36].

The Cancer Genome Atlas (TCGA) consortium profiled more than 500 GBM tumors by performing microarray and DNA sequencing analysis of the tumors. This has led to a comprehensive cataloging of the genomic and transcriptional landscape of GBM tumors [9, 18, 22]. Using the transcriptional profile of the tumors, unassisted hierarchical clustering was able to separate all tumors in 4 robust subgroups; Neural, Proneural, Mesenchymal and Classical, similar to the previously described classification[21]. In addition, mutations identified in each sample were also segregated into each of these subsets.

(A) (B)

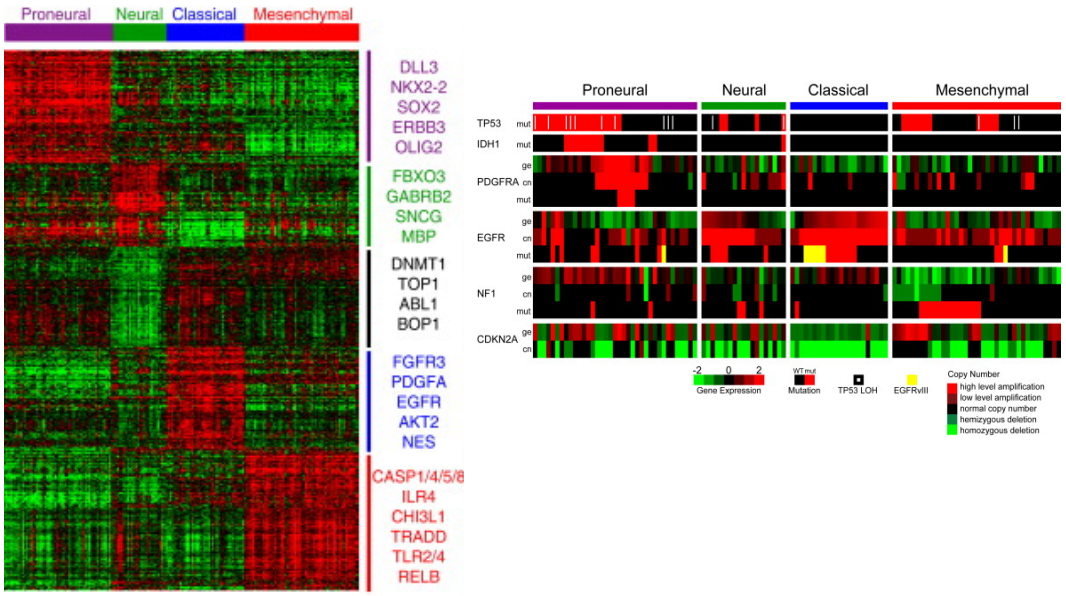

Figure 1.2: TCGA Classification of GBMs. (A) Hierarchical clustering of tumors based on gene expression groups the tumor into 4 subtypes: Proneural, Neural, Mesenchymal and Classical. Key proteins in the gene expression signatures are shown for all subtypes. (B) Mutations cluster into the four subgroups with distinct mutational profile for each subtype. Adapted from Verhaak et al. Cancer Cell. 2010 Jan 19; 17(1): 98-110[22].

The classical subgroup consisted of tumors with increased expression of stem cell and precursor markers such as nestin, and of genes in the Notch and Sonic hedgehog pathways. The defining feature of the classical subtype is an enrichment of EGFR amplification, a common genetic event in GBM tumors, which is present in almost all tumors in this subtype as well as a stark absence of TP53 mutations in this group. More than half the tumors in the mesenchymal subgroup had mutations in the NF1 gene and an enrichment of mesenchymal markers YKL40 and MET. The neural subtype was characterized by the expression of neural markers like SLC12A5 and NEFL. The proneural subtype featured increase in expression of oligodendrocytic genes like NKX2-2 and OLIG2 as well as alterations in PDGFRA, TP53 and the point mutation in IDH1[22]. Interestingly, G-CIMP+ tumors are enriched in the proneural subgroup and almost exclusively contribute to the increased overall survival benefit of the proneural group, which is lost upon separation of the G-CIMP+ and G-CIMP- proneural tumors[9, 18].

Recent single cell analysis studies have shown the significant amount of intratumoral heterogeneity present in GBM tumors with tumor cell populations with different mutations and gene expression signatures belonging to the different subtypes present in each tumor [37, 38]. Furthermore, increasing heterogeneity in the tumor was negatively associated with disease survival [38]. This indicates that the subtyping of entire or part of GBM tumors may not be representative of the entire tumor population and would be an average of the different transcriptional profiles present within a single tumor[3]. Furthermore, although recurrent GBMs almost always maintain the subtype of the original tumors, the switching of subgroups has also been reported post-treatment in

gliomas [9, 21]. Thus, interpretation of subtypes of the tumors must be performed with care during separation of GBM tumors into groups by their gene expression profiles.

Important Pathways in GBM Etiology

Cells require dysregulation of various pathways in order to grow uncontrollably to form a tumor including increase in proliferation, escaping cell death and ability to sprout vessels for nutrient supply [39]. The disruption of these processes is observed in GBMs with the tumors accumulating mutations in key signaling nodes to modulate these pathways [18].

p53 and Retinoblastoma protein (Rb) pathway are regulators of cell cycle control and are critical tumor suppressor genes whose function is disrupted in 87% and 78% of GBM tumors respectively [18, 40, 41]. In GBMs, the function of these proteins is compromised either by direct mutation in the gene itself, or through indirect inhibitory mutations and gene expression changes in regulatory proteins. p53, the gatekeeper of the genome, is responsible for a variety of key functions in the cell such as cell cycle regulation, apoptotic control and DNA repair and damage response[42]. p53 is inactivated in GBMs by either point mutation to disrupt its DNA binding or deletion of the TP53 gene locus. Although the mutation is present at a much higher frequency in grade II, III gliomas (~65%), its ~25% mutational rate in GBMs is significant[9, 19]. Independent of TP53 mutations, amplifications of CDK4, MDM2 and MDM4, upstream negative regulators of p53 have been observed in a fraction of GBMs[7]. Furthermore, the CDKN2A locus, encoding the Ink4a and Arf proteins, which function as crucial regulators for p53 as well as the Rb pathway, is observed to be homozygously deleted in ~49% of GBMs [18, 41].

These mutations would represent an alternate mechanism for functional suppression of p53.

In a similar vein, the Rb pathway is also affected by a number of mutations in key genes and regulators. Rb is the cell cycle regulation checkpoint, and is phosphorylated by a number of cyclin dependent kinases (CDKs), which in turn triggers the release of the E2F transcription factor from binding with the RB1 protein, resulting in expression of key cell cycle proteins. This results in progression through the cell cycle [43, 44]. RB1 is mutated in ~10% of GBMs, but is modulated further by CDKN2A locus deletion, and amplification in CDK4 and CDK6 [18, 22, 45].

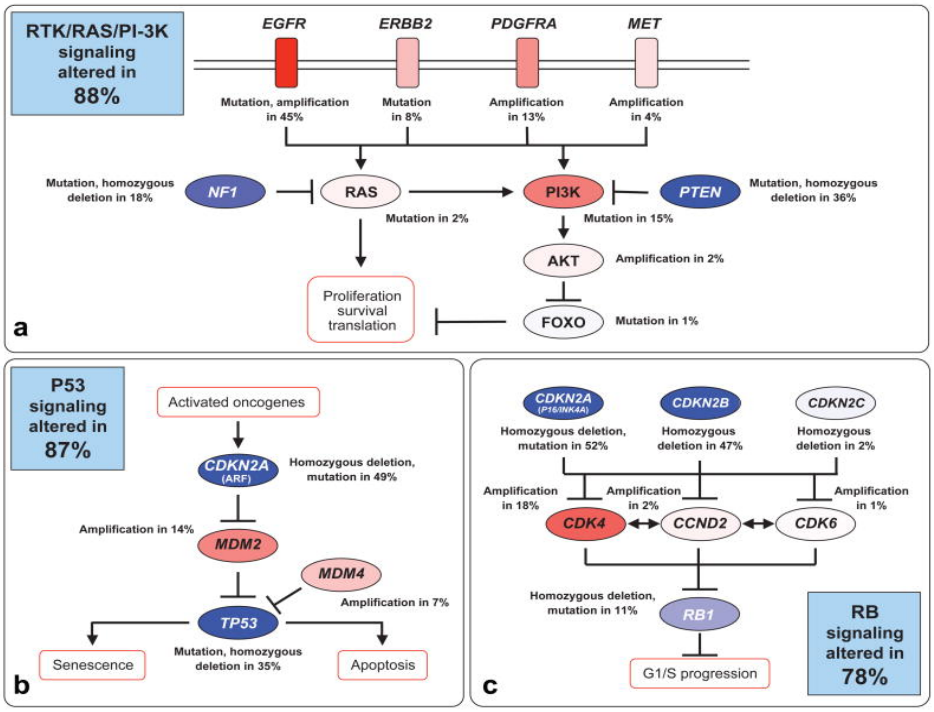

Figure 1.3: Commonly Mutated Pathways in GBMs. (A) Genomic characterization of GBM tumors shows striking enrichment of mutations in key regulatory pathways. Adapted from TCGA. Nature. 2008 Oct 23; 455(7216): 1061–1068

Receptor Tyrosine Kinases (RTK) are involved in the regulation of various important cellular processes often abrogated during cancer development such as cell proliferation, survival and invasion[46]. Various RTKs have been found to be deregulated on the genomic as well as on the proteomic level in GBMs [18, 47]. The most common mutation in this family occurs in the epidermal growth factor receptor (EGFR)[9, 18]. Focal amplifications of the gene and specific extracellular domain mutations are found in ~60%GBM tumor samples[18, 48]. Almost 50% of EGFR amplified tumors (~13% total) also possess the EGFRvIII mutation. This mutant is an in-frame deletion of exons 2-7,which results in the loss of the extracellular binding domain of the receptor[18, 49, 50]. This leads to the constitutive activation of EGFR signaling in these tumors and presence of EGFRvIII is a prognostic indicator of poor patient survival[51, 52]. Furthermore the presence of this mutation is found to be heterogeneous within the tumor, and although it is present only in a subset of cells, it can lead to increased proliferation of neighboring cells, not possessing this mutation through paracrine effects [53, 54]. Platelet Derived Growth Factor Receptor - α (PDGFRA) amplifications are present in 15% of GBMs [22]. Similar to EGFR, a constitutively active mutant of PDGFRA with in frame deletion in exons 8-9 is present in ~40% of tumors possessing PDGFRA amplification [3, 18, 55]. Although PDGFRA mutants account for a relatively small fraction of GBMs, the signature for activation of the downstream pathways is found in ~30% of GBMs [47]. This indicates that the importance of the role PDGFRA is underestimated if only mutation data is taken into consideration. The activation of this pathway drives the proneural subtype gene signature in GBMs [22]. The proneural subtype, once the IDH1/2 mutants are ungrouped, has the poorest prognosis of the four subclasses[9]. It's role is

highlighted by the fact that overexpression of PDGF in the subventricular zone of mice using retroviruses is sufficient to produce large diffuse gliomas, similar in phenotype to human GBM tumors[56]. Mutants of other RTKs such as c-MET have also been identified although they are not as common. Interestingly, the majority of GBMs display activation of 3 or more RTKs in a single tumor, giving rise to redundancy in signaling and often crosstalk between the kinases [57]. This cooperativity indicates the importance of this pathway in tumor development leads to the limited effectiveness of inhibitors targeting single RTKs.

In addition to receptor kinases, other non receptor tyrosine kinases can also play a key role in gliomagenesis [58]. Src family kinases, PTK2 (or Focal Adhesion Kinase) and TNK2 are tyrosine kinases activated in various GBM cell lines and may represent a subset of non-mutated proteins in the tumors which are important for the development of the tumor[58]. PTK2 is downstream of integrin proteins, which have been shown to play a critical role GBM biology [59, 60].

The Phosphoinositide-3-Kinase (PI3K) and Ras pathways are important pathways often activated in GBMs. Mutations in the PIK3CA catalytic subunit and PIK3R1 regulatory subunit of PI-3Kinase enzyme in ~15% of GBMs indicates its importance in tumor formation and maintenance [18]. Downstream of PI3K, PDK1 and AKT have been shown to be critical effectors in the pathway that are often activated in GBMs. Activation of these pathways regulates key functions such as cellular survival through FOXO proteins and cell migration by modulation of the cytoskeletal system [61, 62]. Although mutations in these proteins are not frequent, Phosphatase and Tensin Homolog (PTEN) is deleted, mutated or silenced in 40-50% of GBM tumors. PTEN is the major negative

regulator of the PI3K pathway and its loss by any means leads to an overactivation of PDK1 and AKT, which then enhances tumorigenicity. The PTEN locus may be deleted by the loss of chromosome 10q, a common genomic lesion in GBMs [18, 63]. Further, NEDD4-1, an E3 ubiquitin ligase which regulates PTEN abundance in the cell has been shown to be overexpressed in GBMs [64]. The importance of PTEN has been demonstrated using various mouse models in which PTEN is either deleted or is lost in progressive models of grade III astrocytomas lacking NF1 and p53 [65–67].

Activation of the Ras pathway has been shown to be important in majority of cancers. Although GBMs don't exhibit overt mutations in the Ras oncogene, there is frequent deletion in a key negative regulator of Ras, Neurofibromin-1 (NF1) [18]. 15-18% of GBMs have NF1 either deleted or mutated to the inactive form and resulting in the activation of Ras and the Mitogen Activated Protein Kinase (MAPK) pathway, which is important in progression of the cell cycle and for cancer cell proliferation and survival [9, 68]. NF1 mutations are featured in the mesenchymal subtype of GBMs and regulate downstream pathways such as hyperactivation of mTOR and 4EBP-1, S6Kinase as well as Signal Transducer and Activator of Transcription 3 (STAT3) [69, 70]. Many genetically engineered mouse models rely on the deletion of NF1 for tumor formation although deletion of NF1 alone is not sufficient for glioma formation [71]. Loss of NF1 and p53 with PTEN deletion in glial cells and neural progenitor cells is required for the formation of malignant astrocytomas in mice resembling GBMs [66, 72].

Various genes involved in the growth and survival of tumor cells often do not possess mutations, but are activated by upstream mutated effectors, or signals from the microenvironment. Analysis of TCGA and other gene expression data using network

analysis algorithms identified various transcription factors important for maintenance of the tumor, including STAT3, C/EBPβ, RUNX1 and FOSL[73]. STAT3 is a critical regulator of the stem cell state of the glioma initiating cells and is a key anti-apoptotic protein in GBMs[74, 75]. The activation of STAT3 and C/EBPβ is enriched in the mesenchymal subtype of GBMs [73]. Dysregulation of YAP and TAZ have also been identified using this approach, along with the disruption of the Hippo pathway in the mesenchymal subtype. Interestingly, TAZ has been found to be hypermethylated in the proneural subtype of GBM, indicating the difference in signaling dependencies of the subtypes [76]. Constitutively active transcription factor, NF-κB, has been identified in glioblastomas. Importance of the NF-κB pathway in cell survival is highlighted by the presence of mutations in the inhibitory NFKBIA gene, which codes for the NF-κB inhibitory protein[77]. This mutation occurs exclusively in EGFR wild type tumors [78] indicating that the NFKBIA and EGFR mutations may be affecting similar pathways during tumorigenesis. This is particularly interesting given that NF-κB has been shown to function downstream of EGFR [79]. Activated NF-κB can transcribe pro-survival target genes leading to disruption of apoptotic death in these tumors.

It is clear that although mutations play an important role in development of GBM tumors, activated downstream pathways present an important avenue for targeting the dependencies of the tumors. Identification of key signaling nodes in GBM biology will be important in understanding the intricacies of the signaling pathways involved. These core pathway components may represent novel potential targets for the treatment of GBM.

Cancer Stem Cells in Glioblastoma

GBMs possess a high degree of intratumoral heterogeneity. This heterogeneity is driven, in part, by the genetic changes occurring during tumor growth as well as by the microenvironment of different sections of the tumor [80]. Two proposed models may be used to explain the propagation and the organization of the tumor as a whole. The stochastic model of tumor growth postulates that all tumor cells maintain their ability to initiate tumorigenesis. Although the tumor cell cycling is asynchronous and some cells proliferate at lower frequency, the majority of the cells are contributing to tumor growth [80, 81]. Alternatively, the hierarchical model proposes that a distinct cellular hierarchy is present within the tumor where a subset of tumor stem cells has the ability to propagate and generate new tumors. The bulk of the tumor population in this model are either differentiated cells or progenitor cells in various stages of differentiation [82, 83].

The cancer stem cell hypothesis as an explanation for the source of heterogeneity in tumors remains controversial. Evidence supporting the stochastic model of cancer heterogeneity has also been presented [84]. Although the cancer stem cell hypothesis does not posit the transformation of a normal stem cell, the driver mutations and the location of the initiator cells help define the hierarchical organization of the tumor [85, 86]. The identification of a cellular lineage in a tumor depends on the identification of the hierarchy using various markers. In the case of Acute Myeloid Leukemia (AML) and GBMs, two cancers with a well defined CSC phenotype, CD34+/CD38- cells and CD133+ cells respectively were the defined CSC populations [87, 88]. The cells in this population were exclusively shown to possess tumor initiation ability. However, some AMLs with CD34-/CD38+ cells and some CD133- GBM cells, have been shown to

possess tumorigenic properties as well [89, 90]. Similar results were demonstrated for melanoma with the inability of the putative cancer stem cell marker, CD271, to separate between tumorigenic and non tumorigenic populations [84]. This brings into question the use of these markers, as well as whether indeed there is a subpopulation in the tumors which is exclusively tumorigenic. High heterogeneity and diversity between patient samples makes it challenging to consistently tease apart CSC populations from cells which are not stem-like [91]. A key assay performed for CSC characterization is the mouse xenograft experiments. This assay tests the ability of the cells to form a tumor but does not directly evaluate their ability to recreate a hierarchy in the transplanted tumor. Further, this method may be enriching for cells which are capable of tumorigenesis under xenograft conditions, and not necessarily assay for cancer stem cells from the tumor[91]. Enzymatic dissociation, cell sorting, transplantation site and recipient mouse strain may all influence the ability of cells to form tumors [91, 92]. Quintana et al showed that by using a NOD/SCID IL2Rγ null mouse rather than NOD SCID mice, they were able to significantly increase tumorigenic frequency of the tumor cells. They showed that approximately 30% of melanoma tumors cells are able to form tumors in mice compared to only 1 in 10^6 cells in NOD/SCID mice[93].This suggests there is an immunological restriction to the xenograft even in NOD/SCID mice. Further, implantation into mice is not an ideal microenvironment for the human cells to grow, and thus this assay may select for cells which grow in mice rather than being more tumorigenic [91]. This argues against the CSC hypothesis as we might be significantly underestimating the tumorigenic ability of the cells in mice. Interconversion between non-tumorigenic cells to a tumorigenic phenotype in culture has been previously described [94, 95]. Tumor cells

may be able to convert due to genetic or epigenetic changes or factors in the microenvironment [91, 92]. The frequency of this conversion would define whether it is compatible with the cancer stem cell hypothesis. If this conversion occurs at a higher efficiency and frequency, it would make it difficult to distinguish between the populations tumorigenic and non-tumorigenic populations [91]. The CSC population within the tumors have been hypothesized to be resistant to therapeutics, and thus lead to recurrence [96]. Although this may be true in some cancer types, other cancer types such as in testicular cancer, tumor stem cells have been shown to be more sensitive to chemotherapy in some cases [97]. Further, mutations in key proteins may drive resistance and recurrence such as in V600E Braf mutant tumors treated with Braf inhibitor, Vemurafenib [98, 99]. This supports the stochastic hypothesis of tumor progression as chemoresistance is a feature of mutation possessing cells which are driving growth and recurrence, and not of a cellular subpopulation of with an inherent chemoresistant properties[92].

Although not all cancers have a well described cancer stem cell population and hierarchy, various lines of evidence have been presented for GBMs in support of the cancer stem cell hypothesis [91]. Studies have isolated cells with neural stem cell like properties from many human GBMs. It has also been shown that normal neural stem cells can be mutated to form GBM-like tumors in mice [72, 88, 100–104]. Evidence has also been presented for dedifferentiation of mature cells into stem-like cells that form tumors in mice [66, 105]. Expression of stem cell transcription factors in non-tumorigenic tumor cells is able to convert these cells to a tumorigenic phenotype, indicating the importance of the stem cell state in GBM tumor formation [94]. The various lines of evidence supporting the

cancer stem cell hypothesis in GBMs are described in the next sections. The tumors that follow the cancer stem cell hypothesis are also subject to clonal evolution driven by mutations and the microenvironment and thus these two hypotheses may be either independent or interacting phenomena to produce heterogeneity in the tumor population [91].

The hierarchical stem cell theory is modeled on the cellular organization delineated in various different normal cellular tissues. Particularly in the brain, there is a small population of neural stem cells residing in specialized niches of the adult brain known as the subventricular zone and the subgranular zone [106, 107]. Neural stem cells are highly plastic, undifferentiated and quiescent population of cells. These specialized cells have a capacity to self renew and to give rise to multiple lineages of differentiated neural cells. Lineage tracing experiments have captured the generation of brain-specific differentiated cellular subtypes arising from fluorescent-tagged stem cell populations [108]. Persistent neurogenesis throughout the human lifetime is required for maintenance of the preexisting neural circuitry as well as the production and integration of new cells into the network. This enables maintenance of tissue integrity and organ function [109]. In order to generate more differentiated cell lineages, NSCs must undergo asymmetric cell divisions, which entails giving rise to two non identical daughter cells, one of which retains the stem cell phenotype of the parent cell whereas the other does not acquire those traits [110]. This not only results in the maintenance of the undifferentiated NSC population, but the resulting progenitor cell may undergo further division and differentiation. Neural stem cells have been successfully isolated and cultured as neurospheres, which have the capacity to be passaged and expanded indefinitely without

a significant loss in their ability to differentiate into neurons, astrocytes and oligodendrocytes [111–113].

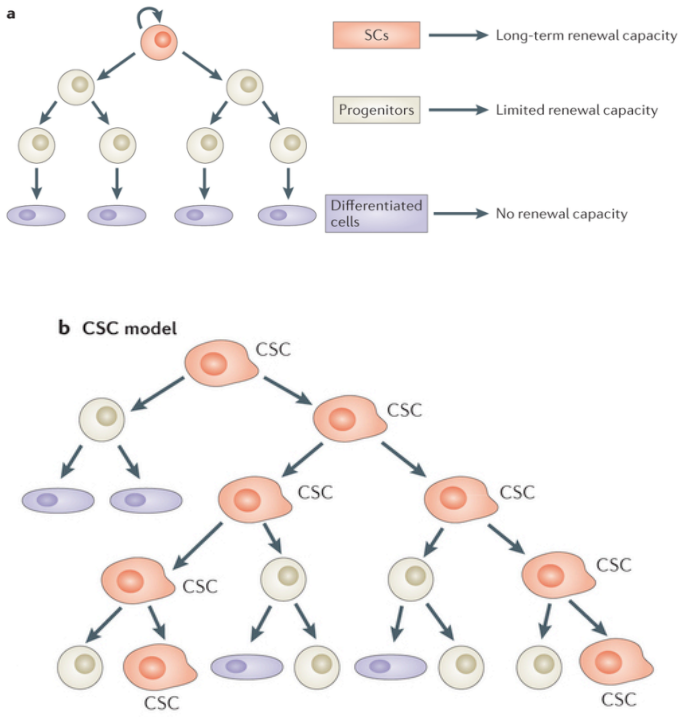

Figure 1.4: The normal neural and cancer stem cell hierarchy. Normal neural cells possess a hierarchy of self-renewing stem cells. Cancer stem cell hypothesis postulates that such as hierarchy also exists within the tumor. Adapted from Beck et al. Nature Reviews Cancer 13, 727-738 (2013).

Many tumors, including GBMs, have been attributed to possess distinct population with differential tumorigenic ability. Similar to normal NSCs, a subpopulation of cells in the tumor have the ability to initiate and maintain tissue growth, in this case the tumor mass [96]. Cancer stem cells (CSCs) were first isolated from the bone marrow of AML patients. These cells were a minor subpopulation of the tumor and expressed markers found on hematopoietic stem cells viz. $CD34^{+}CD38^{-}$. These cells were able to form

tumors in SCID mice upon serial transplantation and these tumors had features similar to the parental AML tumor. Further, other cellular populations were not able to form tumors on serial transplantation[87]. This instigated the isolation of cancer stem cells from various different cancers, including GBMs.

Cancer stem cells have been isolated from various brain tumors using CD133 as a stem cell marker as well as by the ability to form neurospheres in culture[88, 100–102, 114]. CD133 or Prominin-1 is a cell surface glycoprotein, which has been used a marker for the isolation of normal neural stem cells (for more information, see molecular markers section below). Singh et al demonstrated that CD133+, but not CD133-, cells from glioblastomas and medulloblastoma tumors were able to form tumors in SCID mice upon serial transplantation[88, 100].Further, CD133+ cells isolated from the implanted tumor and serially transplanted into a secondary mouse also formed a tumor in the xenograft[100]. In addition to using CD133 as a marker for GBM stem cells, primary human tumor stem cells were also isolated and cultured in serum-free media supplemented with Epidermal Growth Factor (EGF) and Fibroblast Growth Factor (FGF2), similar to the conditions described for NSC cultures[102, 111]. This condition is not amenable for the survival of differentiated or differentiating cells in the tumor but enriches for the cells possessing stem cell like characteristics. These cells display the full complement of features attributed to stem cell cultures such as self-renewal in vitro and in vivo, as measured using markers and serial xenograft transplantations respectively as well as the ability to differentiate into different brain specific progeny viz. astrocytes, neurons and oligodendrocytes [102]. Both these methods, the marker based as well as the

phenotypic selection, are routinely used in isolation of the GBM stem cell populations from patient tumors [96].

The enrichment of cells using CD133 as a marker or their ability to form neurospheres does not reliably ensure that the isolated cells are tumor stem cells [115, 116]. Evidence for variation in CD133 as a marker is published, and transit amplifying cells, a more differentiated cell type which still possess some stem cell qualities, may also form neurospheres in culture (See below) [116]. Thus, strict functional assays are used to characterize the isolated primary GBM stem cells (GBM-SCs). In addition to possessing the genomic lesions characteristic of the tumor, the most important functional test is the ability of the cells to form a tumor in nude mice. The tumor formed should phenotypically resemble the parental tumor as well as contain cells which have properties of self -renewal in vitro by serial passaging, and tumorigenesis in vivo by serial transplantation [100, 102, 117, 118]. Additionally, GBM-SCs in culture should express proteins such as Nestin, Olig2, Sox2, BMI1, CD133 and L1CAM, which are present in various undifferentiated cell types. These cells should also give rise to terminally differentiated brain specific lineages upon differentiation [96, 101, 119, 120].

In order to study GBM in vitro, various cell culture models have been utilized to represent the biology of tumor cell growth. The two popular preclinical models are the traditional patient derived serum lines and the cancer stem cells isolated from GBM tumors. The primary difference between the two models is the use of serum in the growth medium, with the traditional lines requiring 10% fetal bovine serum for their propagation [121]. Addition of serum to GBM stem cell neurospheres induces differentiation and loss of stem cell phenotype, as observed in the case of normal NSCs [102, 122]. Using serum

glioma lines as a preclinical model poses several disadvantages. Firstly, the characteristic genetic aberrations in the parental tumors are not preserved in serum glioma cell lines, leading to misrepresentation of the predominant signaling pathways in effect in GBMs [123]. Furthermore, the implantation of these cell lines intracranially or subcutaneously do not phenocopy the parental tumor or the general characteristics of GBMs, which are seen in tumors derived from GBM-SCs. In contrast, GBM-SCs maintain the genetic landscape of the tumor in culture as well as give rise to tumors similar to the parental tumors upon implantation into mice [88, 102, 124]. Additionally as few as 100-1000 CD133+ cells are required for form a tumor in mice upon serial transplantation, highlighting the tumorigenic capacity of the cancer stem cell population. CD133- tumor cells, although detected in the mouse brain upon xenografting, are usually unable to form a tumor and many more cells of the serum glioma lines are required for formation of tumors intracranially in mice [88].

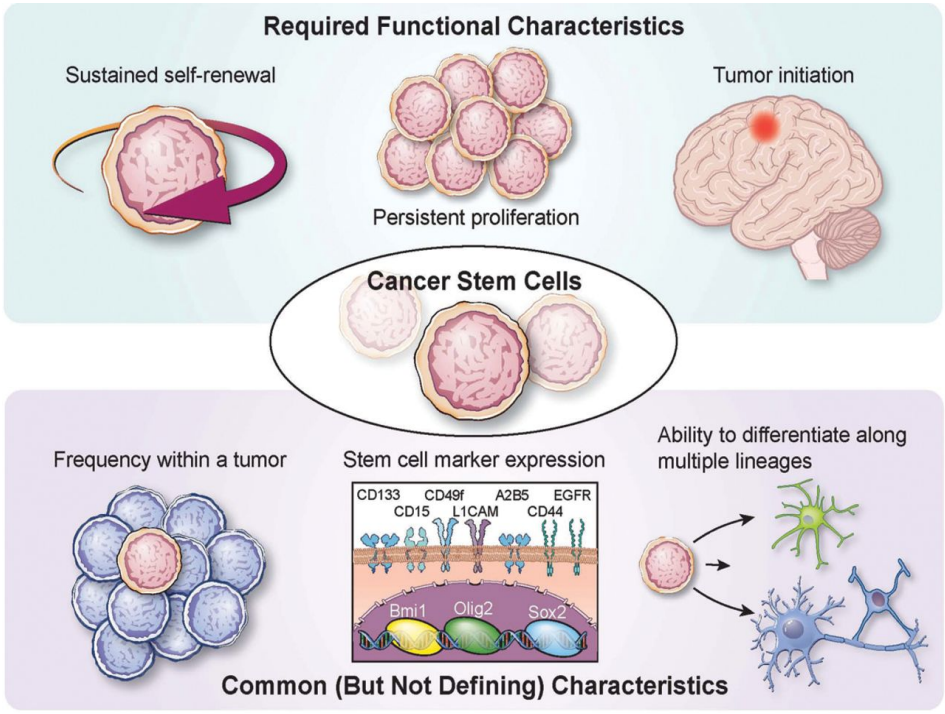

Figure 1.5: Key Characteristics of Cancer Stem Cells. Cancer stem cells isolated from tumors should possess key properties of self-renewal, and tumor initiation and ability to differentiate into multiple lineages.

To demonstrate the difference between serum glioma lines and GBM-SCs, Lee et al isolated serum derived glioma lines and neurosphere cultures from the same glioblastoma tumors [121]. They found critical differences in the growth patterns and tumorigenic potential upon comparison of the two cell lines derived from the same tumor. The serum lines although showing fast growth in vitro had significantly reduced tumorigenic potential compared to the neurospheres and did not phenocopy the parental tumor. Interestingly, early passage serum lines were non-tumorigenic. On a global scale, gene expression signatures were compared between the parental tumor, the neurosphere and serum derived tumor lines as well as with the traditional glioma lines. The parental tumor and the neurospheres were separated from the lines grown in serum, both traditional and

patient derived, based on the gene expression profiles by unsupervised clustering. This indicated that the neurosphere cultures more closely represent the biology of the parental tumors[121]. Others have also demonstrated that the mutational landscape in a given GBM-SC line closely resembles the parental tumor from which it was derived. In addition, GBM-SCs may be cultured as adherent lines on laminin coated plates, which preserves their stem-like state and thus is useful for performing various phenotypic and functional assays on these lines [115, 123, 124]. These considerations encourage the use of patient derived GBM-SC lines as a preclinical model for GBM tumor growth.

Tumor stem cells could arise from either direct mutagenesis of the cells in the stem cell niche of the brain or through the process of dedifferentiation of more mature cell types [125]. The undifferentiated progenitor cells in the brain have been suggested as an initiator cell for the tumors in a number of mouse models [126]. Expression of activated Ras and Akt in nestin expressing progenitor cells, but not in GFAP expressing astrocytes, formed high-grade gliomas in mice having features similar to GBM tumors. Interestingly, the tumor incidence in mice was increased after deleting the Ink4a/Arf locus in addition to the expression of activated Ras and Akt in either the progenitor cell or astrocytic populations [127]. By knocking out three important tumor suppressors, p53, NF1 and PTEN, from nestin expressing neural progenitors, astrocytomas were formed at a 100% penetrance in the mutant mice [66, 72]. Lineage tracing experiments using similar p53, NF1 co-deletion identified the oligodendrocytic precursor cells (OPC) as the initiator clones, which are the largest pool of cycling cells in the brain that may be marked by Olig2 and NG2 [128–130]. Further, expression of EGFR and PDGF in the neural progenitor cells by orthotopic gene transfer also led to the formation of malignant

gliomas especially in the Ink4a-Arf null genetic background [56, 131]. Although there is mounting evidence for the involvement of stem cells in cancer initiation, dedifferentiation of astrocytes and surprisingly neuronal cells has also been shown to initiate and form glial tumors in mice [105, 127, 132]. The possibility of transformation driven dedifferentiation implies a more complex system of brain tumor initiation. This is also supported by evidence of on non-transformation driven dedifferentiation of cycling progenitor cells into somatic stem cells under physiological conditions [80, 133].

Neovascularization is a critical factor in the pathogenesis of GBM and GBM-SCs have been shown to play a key role in this process [134]. In a p53+/- mouse model as well as in tumor xenografts, tumor cells demonstrated the ability to transdifferentiate into endothelial cells to support the angiogenic development in the tumor. Growth of GBM-SCs in media for endothelial cell also produced a endothelial like phenotype [135]. Endothelial cells lining the vessels in GBM tumors were found to posses the genomic landscape typical to the tumor, and were costained with CD31 and GFAP, indicating that some endothelial cells were indeed formed from a glial tumor lineage, further supporting this hypothesis [136]. Various studies have now corroborated the ability of GBM-SCs to transdifferentiate into endothelial cells in culture using matrigel. They are able to produce tubular and flagstone phenotype typical to endothelial cells in culture as well as expressing the appropriate endothelial cell markers [137, 138].

GBM-SCs and Therapy Resistance

The current standard of care therapy includes radiation and treatment with temozolomide and even with aggressive treatment, recurrence is common [11]. This resistance may be

attributed to the high intratumoral heterogeneity within the tumors, which includes the presence of the cancer stem cell population. Gene expression and single cell RNA-seq analysis revealed the presence of multiple molecular subtypes within the tumors and each subtype may possess differential sensitivity to chemo or radiotherapy [37, 38, 139]. By subcloning and culturing cells from different locations in the tumors, Meyer et al were able to demonstrate the differential TMZ sensitivity of certain clones compared to others, indicating the presence of a preexisting population of TMZ resistant cells within the tumor[139]. GBM-SCs present within the tumor may be the source of the resistance to TMZ treatment.

Several other studies have demonstrated a similar resistance of GBM-SCs to TMZ. Using lineage tracing methods, the tumor stem cell were shown to repopulate the tumor bed upon ablation of the tumor with TMZ chemotherapy in p53-/pten-/nf1- mutant mice leading to re-growth of the tumor. Targeted depletion of this population significantly decreased the tumor cellularity [140]. Several other cancer types have shown similar phenomena, indicating the importance of these cells in resistance to the standard therapies and in recurrence of the tumors. GBM neurosphere cultures and GBM-SCs identified by CD133 marker selection, showed a marked resistance to TMZ treatment, even at a high concentration of 200μM [141–143]. In contrast, several other studies demonstrating the sensitivity of GBM-SCs in culture to TMZ have also been published [144, 145], highlighting the requirement of future studies on this topic. Interestingly, long term TMZ treatment of PDGF driven mouse glioma stem cells enriched for the presence of GBM-SCs as assayed by side-population analysis [146], however this claim remains controversial as well [141, 147]. MGMT expression in GBM-SCs predicted

resistance of GBM-SC lines to TMZ and imparted ~10 fold lower sensitivity to TMZ than MGMT non expressors [144, 148]. MGMT remains the key factor in the prediction of TMZ responsiveness in both tumors and in GBM-SC cultures [31, 33, 149].

Ionizing radiation (IR) is used as a primary therapeutic approach for the treatment of GBMs until TMZ was added as the cotreatment arm. The treatment with radiation alone had even shorter time to recurrence in the GBM patients and alluded to the presence of resistant tumor cells in the brain [11]. Radioresistance of GBM tumors may be attributed to the presence of radioresistant GBM-SCs within the tumor population. Indeed the radiation treatment increases the number of CD133 positive in human tumors, as measured by performing tumor resection before and after radiation [150]. In cell culture models, treatment of patient derived GBM-SC cultures with 5 Gy IR, lead to an increase in the number of CD133+ GBM-SCs within the population. This was also observed in vivo when a mix of CD133+ and CD133- cells were implanted into mice, which were then treated with 5Gy IR. This resulted in an enrichment of the CD133+ cells from 5% of the population to 80%, whereas this increase was only up to 25% in the mice that were not irradiated. The ability of GBM-SCs to survive this insult was due to the lower amount of apoptosis in response to radiation compared to CD133- cells which in turn may be due to upregulation of checkpoint proteins CHK1 and CHK2 as well as other DNA damage repair enzymes [151]. Ropolo et al observed a similar increase in checkpoint proteins upon IR treatment but not in DNA damaging agents [152]. Although, CD133+ cells have been shown to be resistant to IR, this resistance may be inherent in the cell line studied, due to the genomic and transcriptional landscape of the cells [153].

Various pathways have been implicated in resistance to therapies in GBMs. Segregation of GBM-SCs into 2 groups, Proneural and Mesenchymal based on gene expression, led to detection of differential sensitivity of the cells to IR in mouse xenograft models. Mesenchymal cells were less sensitive to radiation dependent inhibition due to the expression of various cytokines such as IL6, TNFα and TGFβ and their activation of the NF-κB pathway [154]. Notch pathway inhibitors, γ secretase inhibitors, have been used as radiosensitizers in the context of GBM-SCs as well as for cotreatment with TMZ, which work through inhibition of radiation induced Akt activation. Thus, Notch functions in resistance by upregulating key anti-apoptotic signaling nodes, to prevent cell death and promote cell propagation. [155]. Due to the increase in DNA damage repair proteins, the activation of PARP may be a mechanism of resistance. This was indeed shown to be the case, and when PARP inhibitors were used it decreased self renewal of the GBM-SCs as well as sensitized them to IR treatment [156].

Many alternate targeted therapies are being tested for clinical use. These include inhibitors targeting specific receptor kinases. However due to the high redundancy of RTK functions, single inhibitors may not be effective due to compensation from other receptor molecules leading to resistance to that drug [57]. Due to the vast intra and inter-tumoral heterogeneity, tumors may co-opt different pathways to survive specific chemo and radiotherapeutic agents and further work is needed to elucidate this in detail to develop more effective therapeutics.

Molecular Markers of GBM-SCs

Discovery and enrichment of the cancer stem cell population in GBMs has resulted in a better understanding of disease progression and tumor maintenance due to their transcriptional similarity to the parental tumors as well as their ability to create phenotypically similar intracranial xenograft tumors in mice [88, 102, 121]. Use of stem cell specific markers have aided in the isolation and enrichment of this population of cells, many of which have been adopted from their application in the neural stem cell field [117].

Hierarchical organization of neural stem cells in the brain has been studied in the Subventricular Zone (SVZ) and Subgranular Zone (SGZ) [157]. In the proposed model, a small subpopulation of quiescent neural stem cells with the ability of self renewal, named Type B cells, are at the top of the lineage hierarchy and can be identified using Glial Fibrillar Associated Protein (GFAP) and Nestin as markers [158]. Other markers specific to stem cells are Sox2, Olig2 and BMI1. These cells give rise to different progenitor transit amplifying cell (TAC) populations. Type C progenitor cells are derived from Type B cells and possess limited self-renewal ability and progressive lineage determination. The less differentiated TAC still expresses nestin, which is lost when the TAC differentiates further into a more lineage restricted TAC. The TAC population can be marked using Doublecortin and Polysialylated neural cell adhesion molecule (PSA-NCAM) proteins as molecular markers [106]. This population can then give rise to a migrating type A neuronal lineage restricted cell. These cells can then migrate and terminally differentiate into a mature neuron and integrate into the existing neuronal network [80, 109].

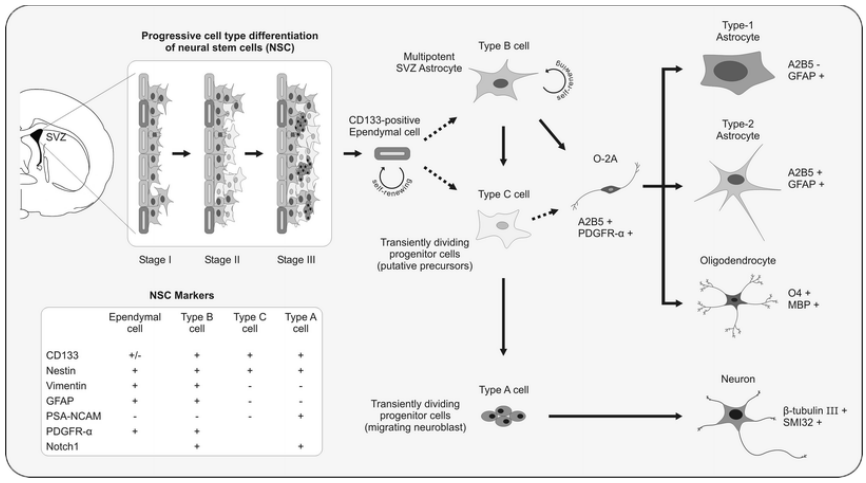

Figure 1.6: Molecular Markers for Detection of Normal Neural Stem Cells. Lineage specific markers of neural stem and progenitor cells allow the evaluation of each cellular population independently. Such a lineage marker system is not known for GBM-SCs.

Several proteins have been used to evaluate the undifferentiated nature of GBM-SCs in culture which are known to be expressed in neural stem cells [96]. Transcription factor Sox2, one of the four Yamanaka factors, is known to drive stemness and is suppressed in differentiated cells [159, 160]. GBM-SCs that show higher expression of Sox2 in culture are more tumorigenic and knock down of Sox2 by shRNA decreases of cell viability. Moreover, treatment of cells with TGF-β increased expression of Sox2 leading to increased tumorigenecity in mice [161]. Musashi-1 and Olig2 are other markers which are used to assay the undifferentiated phenotype of GBM-SCs as their expression is well-studied in other undifferentiated cell types [162]. Furthermore, Suva et al demonstrated that expression of SOX2, Olig2, POU3F2 and SALL2 into differentiated, non tumorigenic GBM cells, were able to convert them into tumor propagating cells, indicating the importance of these stem cell factors in GBM biology [94]. These are all however, internal markers, that are not useful in enrichment of GBM-SCs from tumors. A

number of cell surface markers have been used to identify and enrich the GBM-SC population within the tumor, the most widely used being CD133.

CD133, or Promnin-1, is a 120 KDa cell surface glycoprotein discovered in the CD34+ hematopoietic stem cell population [163]. This was then subsequently discovered in leukemic cells in both CD34+ and CD34- cells from patients [164, 165]. The protein for CD133 is heavily glycosylated and that is putatively detected by the AC133 and AC141 CD133-specific antibodies used in the literature, with overlapping populations stained by the antibodies recognizing the two epitopes [163, 164, 166, 167]. Although the presence of the glycosylated cell surface antigen is restricted to few tissues like bone marrow and progenitor cells, the CD133 mRNA is widely expressed in various tissues including placenta, pancreas, kidney and liver [164, 166]. The presence of the AC133 antigen for CD133 has been utilized in the isolation of the neural stem cell progenitors as well as cancer stem cell populations from various cancer types such as colon cancer [163, 168, 169]. Singh et al first demonstrated the ability to use surface expression of CD133 as a marker for enrichment of a highly tumorigenic population from GBM and medulloblastoma patient tumors. A small number cells from the CD133+ population, even as few as 100 cells, were able to form tumors in mice as opposed to CD133- cells which were non-tumorigenic [88, 100]. Various studies have now corroborated the enrichment of GBM-SC population using cell sorting by CD133 detection which have confirmed their stemness using phenotypic assays and by gene expression [96]. The amount of CD133 positive cells found in the gliomas is relatively high with 20-30% of the tumor cells staining positive, whereas a smaller fraction was stained in grade III medulloblastoma. This difference has been speculated to be linked to the aggressiveness

of the tumor [100], which has been corroborated by observing the staining pattern in low grade and high grade gliomas [170, 171]. Further, immunostaining with CD133 also demonstrated variable staining patterns, either as islands of positive cells or as single positives [100]. Interestingly, the frequency of CD133+ clusters was correlated with increasing malignancy [172]. A hallmark of stem cells is the ability to divide asymmetrically giving rise to 2 daughter cells, one of which retains stem cell properties and the other possesses more differentiated characteristics. CD133+ cells were shown to divide asymmetrically and the distribution of CD133 varied between the two daughter cells, with more CD133 present in the stem-like daughter cell [173]. Although there is a decrease of the cell surface antigen of CD133 with differentiation, CD133 is still expressed at the mRNA and protein level and no change is observed upon differentiation [167, 174]. This indicates that the glycosylation and surface presentation of the antigen may be more important for GBM-SC identity than mRNA expression, which has been shown to be widely expressed even in non-transformed and non-stem populations [164, 166, 167, 175].

AC133 positivity has since been shown to have prognostic value, with increased CD133 staining independently linked to poor progression-free and overall survival [90, 172, 176]. Further, the ability to isolate GBM-SCs using CD133 was itself a negative prognostic indicator [176, 177]. Costaining of CD133 and other stem cell markers has also been studied. CD133 and nestin coexpression in gliomas, has shown that the amount of staining observed inversely correlates with survival in glioma patients [178] and, in a different study, the CD133 expression was highly correlated with the expression of stem cell marker Musashi-1 [171]. However, other studies have rejected the use of CD133 as a

prognostic indicator as they found no correlation of CD133 expression with survival or tumor grade in GBM and other gliomas [179–181].

Although CD133 antigen expression is widely used in the GBM-SC field to isolate and enrich for stem cells, various studies show that in some tumors, tumorigenic cells are not restricted to the CD133+compartment of the tumor [149, 182, 183]. Similar observations have been made in neural stem cells as well with isolation of stem cells which are CD133-negative [184]. Cultures grown from CD133-negative populations, although less frequent to grow than neurospheres from CD133-positive cells, also recapitulated the phenotypic characteristics of GBM-SCs demonstrated by the latter [185]. Although both populations have the ability to enrich for GBM-SC neurospheres, the resultant cells possess different transcriptional profiles indicating that different pathways may be co-opted by these cells to produce the stem-like phenotype [185]. Using the AC133 epitope, this group was able to group the AC133+ as type 1, resembling the expression pattern of fetal neural stem cells and AC133- cells, possessing a transcriptional profile similar to adult neural stem cells [185]. Wang et al engrafted CD133- neurospheres into rats and upon subsequent analysis of xenograft tumors, found an upregulation of AC133 epitope as well as CD133 mRNA. These cells also possessed the characteristics attributed to stem-like cells [182]. In another study, tumors with deleted PTEN, usually by chromosome 10 alteration and not CD133 positivity, was demonstrated as the primary factor influencing the ability of the cells to grow in culture as neurospheres [183]. Additionally the authors provided evidence of 3 distinct types of neurosphere cultures which included neurospheres which were separated into CD133- and CD133+ neurospheres, but were able to give rise to spheres with mixed CD133 expression

(positive and negative) and CD133- cultures which only produced CD133- progeny upon propagation. All 3 types expressed stem cell markers, had ability to differentiate as well as to form tumors upon engraftment. Although Type 1 CD133- neurospheres formed the most aggressive tumors and type 3 tumors possessed a more differentiated phenotype and could exclusively be marked by TBR2, CULX2, DLX2 and DLX1 progenitor markers. The authors proposed a hierarchy where type 1 CD133+ may arise from type 2 CD133- stem cells, and give rise to type 3 CSCs, and a tumor may be a mix of all three types of GBM-SCs [183]. CD133, in GBM-SCs as well as neural stem cells, has been shown to be significantly lower in slower cycling cells, with the expression of the epitope and mRNA increasing when cells are released from cell cycle arrest [184, 186]. This perhaps explains its inability to detect the different stem-like cell population within the tumor, and as GBM-SCs are believed to be quiescent, CD133 may not be able to detect the population with most stem-like properties.

Given the application of CD133 as a marker for stem-like cells, it is surprising that its role in GBM-SCs is not well understood [174]. Recently, studies have demonstrated a functional role for CD133 in self-renewal of GBM-SCs with knockdown of CD133 leading to decreased self-renewal capacity but no increase in apoptosis [187]. Further, CD133 can respond to environmental stimuli via the PI-3-Kinase pathway to affect downstream signaling [188]. Many different stimuli and pathways have been associated with the upregulation of CD133, such as hypoxia, mitochondrial stress and TGF-β1 [189], [190], making it's expression dependent on the culture conditions used to grow the cells. Altogether, these studies demonstrated that CD133, although a useful tool in enrichment of GBM-SC for in vitro culture, is not a marker for all GBM-SC populations

and other markers are required for use with or instead of CD133 to detect the stem cell populations in the GBM tumor samples.

In view of this evidence, several alternative markers for enrichment of GBM-SCs have been suggested. Stage-specific embryonic antigen 1 (SSEA-1 or LeX or CD15) is a neural stem and progenitor cell marker widely used to mark mouse embryonic stem cells and is expressed in the developing CNS of mice [191, 192]. However, SSEA-1 marks more differentiated human cells and its absence is considered a marker for human embryonic and induced pluripotent stem cells [193]. Son et al evaluated CD15 as a marker for GBM-SCs comparing it to CD133 [194]. Unlike CD133, which was unable to identify CD133+ cells in 40% of the tumors tested, CD15+ was able to isolate GBM-SCs from all but one tumor and from all tumors without a CD133+ population. This enriched population co-expressed many stem cell markers and was highly tumorigenic. Importantly, they also demonstrated the exclusive ability of CD15+ cells to differentiate into various brain specific cell types [194]. CD15 expression was also utilized for marking cells derived from primitive neuroectodermal tumor-like subgroups of GBMs, although it did identify cancer stem cells in the CD133-/CD15- compartment [195]. However, the utility of CD15 as a marker has been called into question by a study showing that there was no difference between CD15+ and CD15- cells in the properties that define GBM-SCs [196]. Integrin α-6 is a cell surface receptor for laminin, a major extracellular matrix protein in the brain and is known to play a key role during development of the brain [197]. It was shown to be expressed in 3 undifferentiated cells viz. embryonic, hematopoietic and neural stem cells [198]. Integrin α-6 is key for growth of neural stem cells in laminin based cultures [199]. Integrin α-6 has been proposed as a

marker for enrichment of GBM-SCs from tumors [59]. Costaining with CD133 identifies double positives for both markers as well single positives for each antigen. Integrin α-6 + cells were able to form spheres at a significantly higher efficiency than integrin α-6 negative cells. Further, depletion of the protein resulted in loss of self-renewal and tumorigenesis. High expression of integrin α-6 correlated with shorter survival for xenografted mice. Cells staining positive for Integrin α-6 were enriched in the perivascular niche in the tumor, which is known to be an important microenvironment for GBM-SCs [59, 200]. A2B5, a glial progenitor marker, was also evaluated as a stem cell marker by its ability to identify CD133- cancer stem cells. Twenty-five tumors could be divided into 3 groups of cells with the following populations: $A2B5^{+}CD133^{+}$, $A2B5^{+}CD133^{-}$, and $A2B5^{-}CD133^{-}$. Between these populations, A2B5+/CD133- stained populations were the most tumorigenic in mice, followed by A2B5+/CD133+ and lastly double negative cells. However, A2B5 marked a majority of the cells in the tumor (~65%), calling into question the specificity of the stem cell population isolated [201]. A2B5 has also been used to separate different populations of cells from neurosphere cultures derived from primary GBMs [202]. Double staining with CD133 was also performed with Tenascin-C (TNC), an extracellular matrix glycoprotein, upregulated in several diseases, stained gliomas progressively with grade and was able to isolate tumorigenic, neurosphere forming cells from the tumor population [203]. CD90, a glycophosphotidylinositol (GPI) anchored cell surface protein, was downregulated upon differentiation of GBM-SCs and was also able to identify cells which were CD133 negative but were clonogenic in culture compared to CD90 negative cells [204]. To identify novel markers for GBM-SCs, Liu et al performed a phage display screen in vivo,

by injecting the bacteriophage library into a subcutaneous tumor growing in the mouse. CD133+ GBM-SCs were isolated from this tumor by FACS and subsequent enrichment of the bound phages was performed. VAV3, a Rho GEF and CD97, cluster of differentiation marker 97, were identified as the top screening hits. Both these hits were overexpressed in GBMs and were shown to be important for GBM-SC self renewal and tumorigenecity in mice [205]. Isolation of cells using these markers enriched for the classical subtype of GBM-SCs indicating that these may be used to differentiate between the different GBM tumor subtypes in vitro [205]. Cell surface protein CD44, which has been used as a marker for breast cancer and prostrate carcinomas, was also used in GBMs to isolate GBM-SCs. CD44/Id1 double positive cells were tumorigenic and were found in the endothelial niche of the tumor. These markers were also prognostically relevant in GBMs, with higher expression of CD44/Id1 correlated with poor survival [206]. Comparison of the gene expression signatures of CD133 and CD44 isolated cells found that the CD133 population was enriched for the proneural signature whereas the CD44 cell population were more mesenchymal in gene expression. Thus, these markers may be able to independently identify different subtypes of cells within the tumor [207] The potential of CXCR4 as a marker should also be evaluated as it was coexpressed with various stem cell markers in primary and recurrent GBMs, whereas a receptor family member, CXCR7 did not show this same enrichment [208].

Marker Type	GBM-SC Marker	Description	Reference
Internal	NES	Nestin	[178]
	Olig2	Oligodendrocyte Lineage Transcription Factor 2	[120]
	MSI1	Musashi RNA Binding Protein 1	[209]
	Sox2	SRY Box 2	[161]
	Bmi1	Bmi Polycomb Ring Finger	[210]
	Id1	Inhibitor of DNA Binding 1	[211]
	ALDH1A3	Aldehyde dehydrogenase	[212]
Cell surface	CD133	Prominin 1	[88]
	CD15 or SSEA-1	Fucosylltransferase 4	[194]
	ITGA6	Integrin α-6	[59]
	A2B5	Cell surface ganglioside	[201]
	CD44	CD44 Adhesion Molecule	[207]
	TNC	Tenascin-C	[203]
	CD90	Thy-1 Cell Surface antigen	[204]

Figure 1.7: Table of putative stem cell marker for GBM-SCs. List comprises of both internal and external markers used for GBM-SC identification in the literature. Cell surface markers would be most useful in isolation of GBM-SCs form tumors.

The heterogeneous nature of GBMs makes it a challenge for identification of a 'one size fits all' marker for the stem cell population. The expression of marker proteins may vary between patient tumors. Further identification and rigorous experimentation is required to ensure that the enriched population is GBM-SCs using clonogenicity and tumorigenicity assays. It is clear that it is unlikely that a marker will be identified which is unaffected by cellular processes and environmental stimuli, especially in the case of cell surface proteins. The expression of these proteins may start changing as soon as the tumor is dissociated for GBM-SC isolation, further complicating our ability to correctly identify these cells. Further, single marker studies may be over-estimating the cancer stem cell populations in the tumor and multiple markers may need to be utilized for better

characterization of these cells. We are indeed limited by our ability to accurately mark these cells before their antigen profile on the surface is disrupted upon tumor resection [96, 213]. Intracellular markers are useful in mouse experiments, but do not allow for enrichment of human GBM-SCs from the tumor population. Thus, investigation should also be focused on the expression of various proteins in their niche on GBM tumor sections in order to identify markers, which may indeed mark the initiator cells in the tumor.

The Hypoxic Niche in GBMs

Solid tumors such as GBM usually outgrow the normal nutrient supply available. As the tumor grows larger, the interiors of the tumor are not as well vascularized as the rest of the neoplastic mass, leading to a depletion of nutrient and oxygen content. This physiological reduction of oxygen content is termed hypoxia and is a prominent feature in many types of cancers [214]. Physiological oxygen concentration in the brain ranges from ~5-10% [215, 216]. Hypoxic regions are required during development and influence survival and differentiation of embryonic and neural stem cells by notch signaling mediated mechanisms [217]. Tumors may possess oxygen concentrations ranging from 0.1-5%. This is usually in the form of a gradient, with higher amount of oxygen available to regions near vasculature, and this oxygen availability decreases as a function of distance from the blood vessel [216, 218]. Necrotic regions are formed in niches exhibiting severe hypoxia/anoxia and lack of nutrient supply [2]. The presence of a disorganized vascular network also leads to the significant variation in the blood flow to the region of the tumor, resulting in the intermittent oxygen delivery to the tissues, termed as cycling hypoxia. In such lesions, oxygen may be delivered to the tissue either

at a high frequency (usually in hours) or at low frequency (in days), which contributes to the degree of hypoxia present in each tissue, and changes the mechanism of cellular response to this stress[214, 219].

Hypoxic regions are a hallmark of GBM pathogenesis with the tumors exhibiting necrotic cores termed as psuedopalisades [4]. This region is characterized by the presence of hypercellularity surrounding a necrotic core formed due to cellular migration away from the anoxic regions of the tumor [220]. Due to increase in growth of the tumor mass, hypoxic niches within the tumor increase due to the lack of vasculature in the interior. This results in the upregulation of various angiogenic factors, such as angiopoietin-2 and Vascular Endothelial Growth Factor (VEGF), to give rise to new blood vessels for nutrient supply. However, due to the absence of adequate regulation, capillaries formed possess various structural and functional abnormalities, including irregular architecture and absence of basement membrane [221]. This further, leads to leakiness and irregular blood flow, which in turn again upregulates angiogenic signals. This cycle eventually leads to exacerbation of hypoxia, apoptosis in the cells residing in the niche, and migration of surrounding tumor tissue, giving the appearance of psuedopalisades[222, 223]. The physiological importance of tumor hypoxia is underscored by the poor prognosis associated with the increasing volume of necrotic and hypoxic niches found in the tumor [224, 225]. These niches are not dependent on the size of the tumor as even smaller sized tumors possess necrotic cores [226]. Further, the presence of these niches negatively impacts the effectiveness of the radiation therapy, which is based on the generation of free radicals using tissue oxygen [214]. Radiation affects the tumor cells by creating DNA lesions as well as by utilizing intracellular oxygen to produce reactive

oxygen species (ROS). These ROS species can cause further oxidative damage to the DNA as well as other components of the cell machinery. Limited amount of oxygen in the hypoxic tissues restricts the damage by radiation to mostly direct DNA damage. This is efficiently by the DNA damage and repair response. Three times the amount of radiation is required to produce the same toxicity in hypoxic niches compared to surrounding normoxic tissue [225, 227]. In addition to contributing to radioresistance, hypoxia also drives an increase in MGMT, the DNA repair enzyme which repairs the lesions formed due to TMZ treatment, in the resident GBM-SC population. This increased expression hampers the cytotoxic effects of TMZ leading to chemoresistance in the tumors [228]. Furthermore, hypoxia also maintains the cells in a quiescent state and upregulates various DNA damage pathway proteins including checkpoint proteins, CHK1 and CHK2, leading to an increase in resistance to both radio- and chemo-therapy [229, 230]. Samples of tumor cells from the tissue surrounding hypoxic regions, were shown to possess invasive mesenchymal properties driven by the transcriptional program of STAT3 and p300 compared to cells away from that niche [231].

The Hypoxia Inducible Factors or HIFs primarily mediate the molecular changes in the cells due to hypoxia. These proteins are transcription factors which are regulated by the oxygen content available to the cells [232]. HIFs are heterodimeric comprising of an oxygen sensitive α-subunit and a constitutive β-subunit also known as aryl hydrocarbon receptor nuclear translocator or ARNT. There are 3 HIF complexes formed in the cells, HIF1, HIF2 and HIF3, which possess the HIF1α, HIF2α, or HIF3α subunit respectively. Although, these isoforms are moderately similar to each other (~50% homology), their downstream function and regulation are distinct. In the presence of sufficient oxygen,

prolyl hydroxylases (PHDs) hydroxylate HIFs within its oxygen dependent domain, which facilitates the binding of von Hippel-Lindau protein (pVHL), an E3 ubiquitin ligase [233–235]. pVHL ubiquitinates the HIF subunit leading to its proteolytic degradation [236, 237]. Under hypoxic conditions, the PHD activity is inhibited, leading to stabilization of HIF α-subunit, its dimerization with the constitutive β-subunit and translocation to bind hypoxia responsive elements (HREs) with consensus sequence 5'-RCGTG-3', (where R is any purine) on the genome [238]. HIFs activate a transcriptional program which influences key cancer processes such as angiogenensis, cell survival and proliferation [239]. HIF1α is ubiquitously expressed in all tissues whereas HIF2α is restricted to particular cell types such as the endothelium and neural crest derivatives [240]. Although, HIF1α and HIF2α share many downstream targets such as GLUT1, VEGF, TIE2, and ANG-2, targets such as ALDA and PGK are specific to HIF1α whereas HIF2α specifically regulates TGF-α, Oct4 and cyclin D1 [239, 241, 242]. This regulation occurs post DNA binding as the consensus sites of the two proteins is identical [243].Thus the roles of the HIFs are considered complementary and not redundant, which is strongly supported by the different mechanisms of embryonic lethality in HIF1α and HIF2α null embryos [244, 245]. The expression of HIF1α and HIF2α in GBMs has been linked to tumor aggressiveness and poor prognosis [246]. They have been shown to be present in the tissue surrounding the necrotic core as well as in other hypoxic regions [220, 228, 247]. Although, HIF1α was present in the tumor as well as the normal brain, HIF2α was preferentially expressed in the tumor cells [214].

Hypoxia, HIFs and GBM-SCs

The hypoxic niche has been found to impact the functional properties of GBM-SC population. Using marker data, the GBM-SC population has been shown to be enriched in the hypoxic niches of the tumors [228]. Furthermore, cells isolated from the hypoxic core were found to possess more immature characteristics, and were more clonogenic and tumorigenic under neurosphere growth conditions [228, 248]. Using CD133, Sox2 and Oct4 as a marker for stemness, incubation at 7% O_2 (hypoxic, but physiological oxygen) was shown to increase the number of CD133+ cells in the population. Furthermore, hypoxia conditions further aided in the self-renewal of these GBM-SC lines. This effect was transient and was able to be reversed when cells were incubated back at 20% [153]. Daoy medulloblastoma cells also exhibit an increase in CD133+ cells upon exposure to hypoxia [249]. Siedel et al made a similar discovery when incubating the cells at 1% oxygen, and observed an increase in the percent of CD133+ cells. Increase in stemness was also characterized by other markers such as CXCR4 and A2B5 [250]. In addition to this, there is a reported increase in size and the total number of neurospheres isolated in hypoxia, but 1% hypoxia also inhibits a downregulation of the gene makers expressed during differentiation of GBM-SCs, such as GFAP and Tuj1. This increase was dependent on the PI3Kinase, ERK and mTOR pathway, as was tested using specific inhibitors for these important cellular pathway, which attenuated the CD133+ fraction [189]. GBM-SCs also showed an increase in expression of HIF2α in the CD133+ population of the cell compared to the CD133- cells, and this signature was associated with an upregulation of c-Myc, Nanog and Oct4 mRNAs [95]. Hypoxia is a critical factor in the neovascularization of the tumors [134]. The transdifferentiation of GBM-SCs has

been demonstrated in various studies and hypoxic conditions are key in this transdifferentiation process. GBM-SCs were shown to transdifferentiate to the endothelial lineage in xenograft tumors and were enriched in the hypoxic niches [135].

Specific roles of HIF1 and HIF2 are unclear in GBM with studies showing contrasting results. CD133+ GBM-SCs were more responsive to hypoxia, forming larger and more spheres compared to CD133-cells. Furthermore, expression of a degradation resistant HIF1α construct, lead to the increase in clonogenicity of the GBM-SC line, which was not further affected by hypoxia, indicating that the effect of hypoxia in these cells is mediated through HIF1α [251]. Soeda et al used three neurosphere lines to show that HIF-1α but not HIF-2α protein was responsive to 1% hypoxia and knocking down HIF1α only resulted in decreased clonogenicity in vitro [189]. In contrast to these studies, others have elucidated the role of HIF2α exclusively in these cells. Increased clonogenicity observed in CD133 negative cells cultured long term at 2% hypoxia was shown to be mediated by HIF2α. Use of oxygen stable form of the HIF2α increased the number of CD133 positive cells in the population as well as increasing the clonogenicity, stemness and tumorigenicity of CD133 negative GBM-SCs [95, 252]. A separate study demonstrated that knock down of HIF-2α but not HIF-1α was sufficient to reduce the hypoxia induced expression of stem cell markers and clonogenicity [250]. These data were supported by Li et al, who showed that HIF2α gene expression is higher in CD133-positive than in CD133-negative cells. Further, HIF2α mRNA levels were responsive to hypoxic conditions in CD133+ cells, whereas HIF1α was ubiquitously expression in both CD133 positive and negative cells. However, the authors do show that both factors influence tumorigenicity with mice injected with GBM-SCs containing HIF2 or HIF1

knock down surviving for longer time. Clinically patients with higher expression of HIF2α are correlated with a poor prognosis [253]. Taken together, this indicates that HIF2α may be the more clinically and biologically relevant in GBM-SC biology. However, the disparate in vitro results are likely reflective of the heterogeneity of GBM-SC cell lines.

Given the importance of the HIFs in the etiology of GBM, the tumor cells may use several different pathways to influence the expression of HIFs. Mutations in the pVHL tumor suppressor would stabilize the HIFs due to the its inability to degrade it leading to accumulation [254]. IDH1/2 produces neometabolite 2-hydroxyglutarate which may inhibit the PHD proteins responsible for hydroxylation of HIFs at proline residues as the first step of the degradation of HIFs [35]. Other major pathways influencing hypoxia signaling include the EGFR and Ras mitogenic pathway as well as the PI3 Kinase pathway. All 3 pathways, which may include mutations in key nodes such as EGFR and PTEN deletion, deregulate mTOR leading to stabilization of HIF1α even under normoxic conditions [229]. Further, MDM2 also regulates HIF1α levels by influencing its degradation [255]. Aberrations in these pathways may lead to stabilization of HIFs and the development of a psuedohypoxic state, which is amenable for mutagenesis and tumorigenesis. Targeting hypoxic signaling may be done by either targeting these upstream pathways, targeting the HIFs directly through inhibitors or by using cytotoxic drugs which work specifically under hypoxic conditions such as TH-302 [256–258].

Summary

GBM stem cells are considered to be the major cause of GBM recurrence contributing to its poor prognosis, due to its ability to survive the current standard of care therapies and its ability to thrive under hypoxic conditions. Our knowledge about this population is further limited by the dearth of cell surface markers to identify these cells within the tumor population. This thesis attempts to address both these important issues in the field. In chapter 3, we aim to identify novel molecular vulnerabilities of GBM stem cells under different oxygen availability conditions using a pooled RNAi screening approach for growth and elucidate the underlying mechanism regulated by the identified gene. Chapter 4 aims to identify novel molecular cell surface biomarkers to distinguish GBM stem cells from differentiated cells, which do not possess stem like characteristics. To this end, we performed a monoclonal antibody screen to identify and evaluate these antibodies as potential markers and therapeutics for targeting GBM-SCs.

Chapter 2

Materials and Methods

Culture of GBM-SC Lines

Primary GBM stem cell (GBM-SC) lines, GS6-22, GS7-2, GS11-1, GS13-1 and MGG 8 were cultured in serum-free and growth factor rich stem cell media (SCM) and passaged by an acid base sphere dissociation protocol using accutase enzyme (Invitrogen, CA) as previously described [74]. SCM was made using Dulbecco's modified Eagle's medium (DMEM)/F12 (Invitrogen, CA) with 1% Penicillin/Streptomycin and supplemented with neural supplement Gem21 (Gemini Bioproducts, CA), Epidermal Growth Factor (EGF) (20 ng/ml; Peprotech, NJ), and human basic-Fibroblast Growth Factor 2 (bFGF-2) (20 ng/ml; Peprotech). MGG8 lines was kindly provided by Hiroaki Wakimoto, PhD (Massachusetts General Hospital, MA) [124].Glioma serum cells, U251, A172, U373 and human fibroblast line, Hs27 were cultured and passaged in DMEM with 10% Fetal Bovine Serum and 1% Penicillin-Streptomycin. H04 and SW06 normal human neural progenitor cells were kindly provided by Dr. Dennis Steindler and were grown in DMEM with 5%FBS, N2 Supplement (Invitrogen) and 20ng/ml EGF and bFGF. For growing cells on laminin and for differentiation, plates are coated with poly-L-ornithine for 1 hour at 37°C followed by washing and coating with 2µg/ml Laminin for 2 hrs at 37°C. To induce differentiation, GBM-SCs are plated in DMEM/F12 media with Gem21 only (no EGF, bFGF) and cultured for 48 hrs. Following aspiration of media, DMEM with 2% FBS is added to the cells for 7-10 days for complete differentiation. GBM-SCs can also be grown on laminin in stem cell media as undifferentiated stem cell cultures [115].For hypoxia experiments, C-chambers with a custom gas mix (5%CO2, balance nitrogen; Airgas, MA) was setup and used as per manufacturer's instructions (Biospherix, NY). Following inhibitors and drugs were used in this thesis: SGK1 inhibitor GSK650394

[259] (Tocris, MN), KIF11: Monastrol [260], Proteasome inhibitor MG132,pan-caspase inhibitors z-VAD-FMK and q-Vd-OPh [261, 262] (Sigma, MO), JNK inhibitor SP600125 [263] and p38 MAPK inhibitor SB239063 [264] (SelleckChem, MA).

siRNA and Plasmid Transfection

Cells were dissociated and plated in 96 well plates (for growth curve) or 6- well plates (for RNA or protein isolation) at 50% confluence and placed in standard culture conditions overnight. For siRNA transfection, RNAiMax (Invitrogen, CA) was diluted at a concentration of 0.2µl per well (for 96 well plates) or 6µl per well (for 6-well plates) in opti-MEM (Invitrogen, CA). The siRNA was separately diluted to achieve a final (in well) concentration of 10nM or 25nM and mixed with prepared RNAiMax solution. After incubation for 15 mins, the RNAiMax:siRNA mixture was applied to the plated cells dropwise. Cells were subsequently allowed to grow for 4 days for the growth assay or 2 days for RNA or protein extraction. The following siRNAs were used in this study; siKIF11 (SMARTpool L-003317-00-0005), siCXADR (SMARTpool L-003650-00-0005) (Dharmacon, CO).

For plasmid transfection experiments, GBM-SCs were plated at 50,000 cells per well in a 6 well plate and grown overnight in standard culture conditions. 10µg of constitutively active IKK-β plasmid was diluted in opti-MEM media and Trans-IT transfection reagent (Mirius Bio, WI) was separately diluted to 3 times the amount of plasmid in opti-MEM. These mixtures were combined and after 30 min incubation at room temperature, it was applied to the cells. Protein was collected 3 days post-transfection. For the growth assay, transfected cells were counted and equal numbers of cells were plated into 96 well plates

24 hours post-transfection. Cell viability was assayed 5 and 10 days after plating. A control RFP plasmid (kindly provided by Ira Herman's laboratory) was utilized to check for efficiency of transfection, which was determined by FACS (data not shown).

Plasmid and Lentivirus Preparation

Lentiviral constructs expressing Scramble-shRNA, SGK1-shRNA ((1) TRCN0000312568, (2) TRCN0000010432, (3) TRCN0000194957), and RBX1-shRNA (TRCN0000272521) in the PLKO.1 vector backbone were obtained (Sigma, MO). The p53-shRNA plasmid was kindly provided by the Charlotte Kuperwasser laboratory. PLKO.1 plasmids were transformed, amplified and purified in chemically competent DH5α E. Coli using Plasmid Miniprep Kits. The plasmids of interest were co-transfected with VSVG and VPRΔ8.2 plasmids into 293T cells using Trans-IT transfection reagent (Mirius Bio, WI). After 24 hours, transfection media was removed and replaced with DMEM with 30% FBS. Virus containing supernatant was removed 48 hours and 72 hours post-transfection. Polyethylene Glycol (PEG) was added to collected viral supernatant to final concentration of 5%, mixed thoroughly and incubated overnight. The mixture was then centrifuged for 15 minutes at 3000 rpm at 4°C, and pellet re-suspended in DPBS to 1/10th the original volume.

Preparation of the lentiviruses used for the pooled shRNA screening was performed according to manufacturer's instruction (Cellecta Inc, Decipher Project, CA). Plasmids for the viruses were provided as 3 modules, each containing ~27,500 unique hairpin constructs. Virus preparation was performed in six 15 cm dishes and 10μg for pooled library (Module 1,2 or 3) was used per plate (total of 60μg per experiment). Library

constructs were cotransfected with VSVG and VPRΔ8.2 plasmids into 293T cells using Trans-IT transfection reagent (Mirius Bio, WI). Virus was collected and concentrated as described above.

LentiCrispr V2 plasmid was obtained and amplified using standard techniques in Stbl3 competent E. Coli cells (Addgene, MA). LentiCrispr V2 plasmid was digested with Bsmb1 for 10 minutes, followed by inactivation at 80°C for 20minutes and treated with alkaline phosphatase for 20minutes (Thermo Fisher, MA). The digests were run on 0.75% agarose gel and digested plasmid was eluted using GeneClean DNA Elution kit (MP Biomedicals, CA). DNA Oligos designed based on methods recommended in the Crispr protocol and small genomic guides used in previous study [265]. Oligos were annealed in BioRad Thermocycler by increasing temperature to 95°C for 10 minutes and slowly ramping down temperature by 5°C/min until temperature reached 25°C. Annealed oligos were then diluted and ligated using Quick Ligation Kit (New England Biolabs, MA). Stbl3 cells were transformed with ligated plasmid and colonies selected on LB-Ampicillin plates. The cloning was confirmed using standard sequencing methodology.

Lentiviral Titration and Cell Line Viral Transduction

Prepared and concentrated lentiviruses (except Screening Library plasmids) were titered using U251 glioma cell lines. U251 cells were plated at density of 12,500 cells/well in 24 well plates in media with polybrene (2ug/ml). 6 dilutions were prepared for each lentivirus with the most concentrated dilution containing 1µl of concentrated virus and 10 fold subsequent dilutions. Viruses were applied on the cells for 24hrs, after which media was changed. 48hrs post transduction, puromycin is added at a final concentration of

1μg/ml and cells are allow to grow until colonies are observed in the most diluted wells. Cells are subsequently fixed with ice-cold methanol for 10mins (Sigma, MO) before staining with 0.5% crystal violet in 25% methanol. Plates are washed with DI water, and colonies are counted to estimate virus titer.

For viral transduction of GBM-SCs and other glioma lines, cells were plated at required confluence and viral particles are added at an MOI of 2 (for lenticrisprv2) or 10 (for PLKO) in media containing polybrene (GS6-22 and cell lines: 2μg/ml; MGG 8: 1μg/ml). Media was changed after 24 hours and puromycin added 48 hours post transduction (Serum glioma lines, H04, SW06: 2μg/ml; GS6-22, HS27: 1μg/ml; MGG 8: 0.1μg/ml). Cells were allowed to grow for 7-10 days for growth assays and 2-4 days after selection for RNA and protein isolation.

Pooled shRNA screening of GBM-SCs

Genome-wide pooled shRNA lentiviruses were prepared as per manufacturer's protocol (Cellecta Inc, CA). The screen was performed on GBM-SC lines to identify gene essential for cell growth. Cells were infected with lentivirus in media with polybrene (2ug/ml) at MOI of 0.5 to ensure maximum number of single viral integrants per cell. Number of cells was adjusted to allow for at least 200 integrations per shRNA construct to maintain the complexity of the library. After 48 hours post infection, cells were selected for infection using puromycin (0.1-1ug/ml) for further2 days. Genomic DNA was isolated from one-third of the infected cells as a reference time point for infection. Remaining cells were placed under normoxic (21%) or hypoxic (1%) conditions. Cells were expanded as and when required. After 10 and 18 days following growth in

normoxic and hypoxic conditions respectively, genomic DNA from cells from both treatment conditions was isolated using ethanol precipitation. Two-step Polymerase Chain Reactions (PCR) was setup up as described and primers were designed and synthesized (IDT, IA) according to manufacturer's instructions (See Primer Table). PCR was used to amplify unique 18-nucleotide bar-code specific to each shRNA construct. Briefly, for the first round of PCR, 200ug of genomic DNA from the cells was amplified using Taq polymerase (Clontech, CA) using the following cycling conditions: 94°C for 3mins, 16 cycles of (94°C for 30 sec, 65°C for 10sec, 72°C for 20 sec), and 1 cycle of 68°C for 2 mins. Custom index sequences were inserted in forward primer of the second PCR step in order to multiplex different samples in a sequencing run. PCR product from the previous round was used as a template. Following PCR amplification (Qiagen, MD) and gel extraction (GeneClean, MP Bio, OH), Next Generation Sequencing (NGS) was performed in the Tufts University Core Facility (TUCF, MA) using Illumina HiSeq 2500 High Throughput Sequencer. Data was analyzed using Galaxy software and bar codes were resolved and identified using Decipher Deconvolution software according to manufacturer's instruction (Cellecta, CA).

Data Analysis

After deconvolution and enumeration of the samples, each hairpin was normalized to the total number of reads for that sample. Normoxic and hypoxic sample hairpins were compared with the reference sample hairpins and fold change and subsequently $\log_2$ fold change was calculated. Median Absolute Deviation (MAD) score of the population was derived and then a Z score based on MAD score was calculated for each hairpin [266]. MAD analysis minimizes the effect of outliers on the population by calculating a robust Z

score. A cutoff of median ± 3 MAD and <0.5 fold change was applied to the hairpins and at least 2 hairpins targeting a gene needed to meet this criteria for a gene to be considered a hit. Bayesian Analysis of Gene EssentiaLity (BAGEL) algorithm is a python based program which was available online through the referred paper [267]. After downloading necessary files, the analysis was run on the screening data using WinPython32 program to produce an output containing the Bayes Factor score for each tested gene. BF>5 was applied as a criterion for essentiality. Gene lists were analyzed for enriched canonical pathways and functions with Ingenuity Pathway Analysis (IPA) (Qiagen, CA).

Prestoblue and MTS Cell viability assays

To measure viability of GBM-SC lines in response to shRNA or inhibitor treatment, cells were dissociated and plated with virus or inhibitor at 3000-5000 cells per well concentration in 96 well plates (Corning, NY). Lentiviral particles (for transduction protocol see above) and inhibitors are added to the wells containing the cells and the cells were allowed to grow for 5-7 days. GBM-SC neurospheres were dissociated to single cell suspension by trypsin (Sigma, MO) and cell viability was assessed using the membrane permeant, resazurin based Prestoblue Cell Viability reagent (Life Technologies, NY). Metabolically active cells reduce Prestoblue to yield a red fluorescent resorufin product, which was quantitatively measured in a Spectrafluor Plus plate reader (Ex 544nm/Em590nm) to determine relative numbers of live cells. No trypsin treatment is required for adherent cells H04 and SW06, which may be directly assayed by addition of prestoblue in the wells.

Glioma line cell viability was assessed using CellTiter 96®AQ_{ueous} One Solution Cell Proliferation (MTS) assay (Promega, WI). Cell were plated and treated with inhibitor or lentiviral particles as described above, and MTS assay was performed at 72 hours according to the manufacturer's protocol

Western Blotting

Cells were lysed in RIPA buffer containing protease and phosphatase inhibitor cocktails. Protein concentrations were determined using BCA method (Thermo Fisher, MA). Lysates were separated using ready-made SDS-polyacrylamide (SDS-PAGE) gels and transferred onto nitrocellulose membrane (Thermo Fisher, MA). Nitrocellulose membranes were blocked with 5% non-fat dry milk, in TBS-T (10 mMTris-HCl pH 7.5, 100 mMNaCl, and 0.05% Tween 20), and incubated with primary antibody overnight. The following antibodies were utilized in this study: SGK1, total and cleaved PARP, cleaved caspase 3, total p53, phospho-Ser258-FOXO3a, Bcl2, Bcl-xL, Mci-1 (Cell Signaling, MA); β-catenin, total Caspase 3 and cleaved caspase 9 (Abcam, MA); β-Actin (Sigma, MO). phospho-Ser315 FOXO3 was a gift from Dr. Michael Greenberg and anti-FLAG antibody was a kindly provided by Dr. Ira Herman. Blots were then washed with TBST and incubated with a horseradish peroxidase conjugated secondary antibody (BioRad, CA). Bands were visualized with high-sensitivity chemiluminescence reagent (Pierce Biotechnology, IL) using autoradiography film (Denville Scientific, NJ).

SYPRO RUBY staining

Protein samples were collected and quantified and protein were resolved by SDS-PAGE as stated above. Following gel electrophoresis, the gel was transferred into a fix solution

(50% methanol, 7% acetic acid) for 30 minutes. This was repeated once with a fresh fix solution. Gel was then incubated in SYPRO® Ruby gel stain (Invitrogen, CA) overnight on an agitator at room temperature. Following this, the gel was incubated in wash solution (10% methanol, 7% acetic acid) for 30 minutes and then imaged using the BioRad Gel Doc XR+ gel imaging system. For mass spectrometry analysis in chapter 5, once the bands to be isolated were identified, they were cut from the gel using clean razor and stored in an eppendorf tube for shiiping to the Taplin Mass spec facility.

Annexin V/ Propidium Iodide Apoptosis Assays

shRNA or drug treated cells were stained using an Annexin V-GFP/PI staining kit (BD Pharmigen) according to the manufacturers protocol. Briefly, $1x10^4$ cells were infected in 6-well plate with control and targeted shRNA and selected with puromycin. Cells were accutased, washed twice with 0.1% BSA in PBS and resuspended in PBS at $1x10^6$ cells/ml density. FITC conjugated Annexin V and/or Propidium Iodide (PI) was added to the cells and incubated for 15 minutes at room temperature. Control lentivirus infected cells, which were unstained or stained with only FITC Annexin V or PI, were used as controls. Cells were analyze using FACSCalibur flow cytometer and data were analyzed using Summit software.

RNA Extraction and Real time PCR

Cells were lysed with Trizol extraction reagent, with 1ml Trizol used per 10 million cells. Phenol chloroform extraction was performed as previously described. RNA quantity and purity was determined using NanoDrop Spectrophotometer (Thermo, DE). For each condition, 1μg of RNA was used to set up a reverse transcription (RT) reaction to

produce cDNA using iScript cDNA synthesis kit (BioRad, CA). 2µl from the RT reaction was used as a template for qPCR. Qiagen SyBr Green Mastermix reagent was used for qPCR and samples were run using Agilent Mx3000p qPCR machine using standard protocol with dissociation curve. Data were analyzed using ΔΔCt method of quantification of fold change to compare samples. Primers used are listed in Table 2.1.

in vivo Xenograft Mouse Injections and Luciferase Assay to Follow Tumor Growth

Eight-week or older NCR nude athymic mice were injected with established cell lines infected with non-targeting control or SGK1 knockdown shRNA construct. Stereotactic injection was performed using previously described protocol [268]. Briefly, mice were anaesthetized using Ketamine:Xylazine (100mg/kg; 20mg/kg respectively) and placed in stereotactic frame. An incision was made using an 11-0 blade to expose the bregma. A small hole was drilled in the skull using a 22 gauge needle, followed by injection of cells 2mm deep into the brain using Hamilton syringe (Hamilton Company, NV). The rate of injections were controlled to 1µl/min using the World Precision nanoinjector apparatus. Mice were then sutured and allowed to recover and monitored daily. A post injection luciferase assay was performed the next day and then once a week, to assess tumor growth by injecting Vivoglo luciferin (Promega, WI) and imaging the mice using a Xenogen IVIS-200 small animal imaging system.

Live cell staining by Flow Cytometry

GBM-SCs were dissociated using accutase as described above and 1 x 10^5 - 1 x 10^6 cells were resuspended in PBS with 1% BSA. Fc binding sites were blocked using Fc Block (Miltenyi Biotech) for 10 mins at 4°C. After 1x PBS wash, cells were incubated with the

primary antibody (undiluted supernatant for mAbs) for 20 mins. After washing the primary antibody with PBS, cells are incubated with AlexaFluor488 secondary antibody for 20 mins. Cells were washed twice with PBS and resuspended in 300µl PBS. Cells were analyzed by FACS using MoFlo sorter and data analysis using Summit software.

Immunoflorescence

GBM-SCs were seeded into 96 well plates coated with laminin (Corning, NY) and treated with shRNA or inhibitors. For IF staining, cells were washed with ice-cold PBS and fixed in 4% paraformaldehyde (Signma) for 10 min at RT followed by permeabalization with 0.1% Triton X-100 in 1% BSA. Cells were then blocked with 10% goat serum (Abcam, MA) in PBS. Overnight staining with the primary antibodies was performed (at 1:100 dilution unless otherwise noted). After washing away primary with cold PBS 3 times, cells were incubated with Alexa488 or Alexa 536-labeled anti-rabbit secondary antibody (1:500) (Invitrogen) at room temperature for 1 h. The cells were washed with cold PBS, and counterstained with DAPI (Invitrogen). Plates were examined for fluorescence intensity using EVOS fluorescence microscope.

Immunohistochemistry

Unstained paraffin section slides were de-paraffinized using a xylene-ethanol washing protocol starting with 100% Xylene, 50% Xylene - 50% Ethanol, 100% Ethanol and subsequent decreasing amount of alcohol content till slides were finally in DI water. Antigen retrieval by heating was performed on slides in sodium citrate buffer and allowed to subsequently cool down to RT. Sections were blocked with 10% normal goat serum (Abcam, MA) for 1 hour, followed by overnight incubation with primary antibody

(mAb undiluted supernatant) in the cold room. After washing with PBST 3 times, sections were incubated with 3% w/v H_2O_2 for 10 min. After serial washing, bound primary antibody was detected by adding a HRP conjugated secondary antibody 3,3'-diaminobenzidine (DAB) (Abcam). Sections were counterstained with hematoxylin and dehydrated using the protocol for de-paraffinization in reverse order. Slides were mounted with coverslips and observed under the EVOS light microscope.

Caspase 3/7 activity assay

GBM-SCs were seeded into 96 well plates coated with laminin (Corning, NY) and treated with shRNA or inhibitors.The Caspase-Glo® 3/7 Assay was performed according to manufacturers instruction. Caspase-3/7 released by the cell acts on the tetrapeptide sequence DEVD which is cleaved to induce luciferase signal which was detected using the Tecan spectrophotometer and luminometer.

Immunoaffinity Purification

GBM-SCs and other cell lines were lysed using RIPA buffer as previously described. Immunoaffinity purification was performed by scaling up Crosslink Immunoprecipitation (IP) Kit protocol, which was used previously according to the manufacturers instruction. 10 ml Protein G beads were added into a 50ml conical tube and washed using PBS containing 0.01M sodium phosphate, 0.15M NaCl; pH 7.2 buffer which enables effective coupling of antibody to the beads. 0.1mg of mAb 7-18 antibody was applied to the beads at a concentration 10µg/ml for 2 hours. Following centrifugation and washing away unbound antibody, the coupled antibody-beads were crosslinked by Disuccinimidylsuberate (DSS) at a concentration of 250 µM DSS crosslinker. The

reaction was performed for 1 hour at room temperature and subsequent washing with 0.1M glycine elution buffer pH 2.8 stopped the crosslinking reaction. The lysate was applied to the crosslinked antibody-bead complex overnight in the cold room. Prior to application, lysate was precleared using G-beads by incubating them for 1 hour at RT. The following day, the lysate-beads mix was poured into 15ml titration column and the lysate was allowed to flow through after the beads settled. The column was then thoroughly washed with PBS. Elution with Glycine buffer was performed and 200 µl fraction were collected which were run on a gel for western blotting and SYPRO Ruby staining.

(A)

Primer Name	Sequence
FwdHTS PCR1	TTC TCT GGC AAG CAA AAG ACG GCA TA
RevHTS PCR1	TGC CAT TTG TCT CGA GGT CGA GAA
FwdGex PCR2	CAA GCA GAA GAC GGC ATA CGA GA
RevGex PCR2*	AATGATACGGCGACCACCGAGATCTACA CTCTTTCCCTACACGACGCTCTTCCGATCT **NNNNNN** AGTCCGAAACCCCAAACGCACGAA

*** NNNNNNN: Barcode Sequence**

(B)

Barcode Number	Sequence
BC1	ATCACG
BC2	CGATGT
BC3	GATCAG
BC4	TCGGTA
BC5	ACAGTC
BC6	TGACCA
BC7	CAGATC
BC8	AGTCAA
BC9	TAGCTT
BC10	ATGTCA
BC11	CCGTCC
BC12	GGCTAC
BC13	CTTGTA
BC14	ACAGTG

Table 2.1: Primers used in Pooled shRNA Screening. (A) The list of forward and reverse primers for the two step PCR reaction. The N position in RevGex PCR2 change according to the barcode inserted.(B) Index Barcode sequences for RevGex PCR2 primers

Gene Name	Forward Primer	Reverse Primer
SGK1	ACCCTGTTAGGGCTTGGTTT	GGCACTCTAACGCTCGTTTC
β-2-Microgloblulin	GTGTCTGGGTTTCATCCATC	GGCAGGCATACTCATCTTTT
Fas/CD95	GCAGGCCAAGTTGCTGAATC	ACTCCCCAGAAGCGTCTTTG
FASL	CTACTGGGTGGACAGCAGTG	CTCTTCTTCAGGGGTGGCAG
BIM	GCCTGGTCTGCAGTTTGTTG	GAACGCAGCGAACCGAATAC
BCL-xL	ATCCACTCTACCCTCCCACC	GTGTGGGGGTCTCACAGAAG
TRAIL	GAGCTGAAGCAGATGCAGGA	ACGGAGTTGCCACTTGACTT
GADD45	TCAGCAAAGCCCTGAGTCAG	CATCTCTGTCGTCGTCCTCG
FLIP/CFLAR	AGAGAACGGCATGAACCTGG	CCCAGGGATGAAGCCAACAT
XIAP	CTCCACGGTGCCCAGTTAAT	CCGCGAAACCAGTCACTACT
Survivin	TCTGTCACGTTCTCCACACG	CAGTAGGGTCCACAGCAGTG
Oct4	CTTGAATCCCGAATGGAAAGGG	GTGTATATCCCAGGGTGATCCTC
Olig2	GGACAAGCTAGGAGGCAGTG	ATGGCGATGTTGAGGTCGTG

Table 2.2: qPCR Primers: List of the qPCR primer sequences used in this thesis.

Guide Name	Sequence
Non Targeting Guide	GATCCATGTAATGCGTTCG
SGK1 Guide 1	CTTGAAGATCTCCCAACCTC
SGK1 Guide 2	TTCAAGATGGACTGAACTTC

Table 2.3: Guide Sequences Targeting SGK1: Guide sequence for non-targeting control and SGK1 specific test guides.

Chapter 3

Identification of targets for GBM-SCs using Pooled shRNA screening under normoxia and hypoxia

Figure Contributions:

TRC Screening Part of Figure 3.7 was contributed by

Surbhi Goel-Bhattacharya and Sejuti Sengupta.

Introduction

GBM is the most aggressive form of primary brain cancer with a very poor prognosis of only 14 months post diagnosis and with treatment [3, 11]. The standard of care therapy does not completely ablate all the tumor cells and thus, tumor recurrence is almost inevitable [269]. This is attributed to a small subpopulation of cells within the tumor which are resistant to frontline therapy and are responsible for tumor maintenance and growth[140, 151, 200]. These cells, known as tumor or GBM stem cells, also have a unique ability to thrive in hypoxic niches, with the microenvironment driving clonogenicity and ability of the cells to resist therapy [228, 251, 270].

There is extensive heterogeneity between and within GBM's [9, 38]. There has been an effort to characterize the mutations occurring in GBMs and other gliomas, in order to identify vulnerabilities in these tumors. However, a mutation based inquiry does not identify the non-mutated genetic targets and an unbiased approach is required to systematically identify genetic dependencies. In order to find genes that are not only important in growth and maintenance of the bulk of the tumor, but also can be used to target cancer stem cell growth under hypoxic conditions, we have used an unbiased pooled shRNA screening approach to identify genes which are important in GBM-SC growth and survival under both normoxic and hypoxic conditions. Using this negative selection screen, we have screened ~10,000 genes in the two different patient derived GBM-SC lines.

Results

Pooled shRNA Screening of GBM-SCs

To identify genes important for the proliferation and survival of GBM stem cells under normoxic and hypoxic conditions, we utilized a near genome-wide pooled shRNA screening approach to target ~10,000 genes. The 10,000 genes are divided into 2 module sets with each module containing ~27,500 lentiviral hairpins targeting 5,000 genes. Each gene is targeted with a minimum of5 unique hairpin sequences to control for potential off-target effects of a single shRNA sequence. Each shRNA construct contains an 18-nucleotide barcode sequence unique to the hairpin. Next Generation Sequencing enables identification and enumeration of the barcodes for each shRNA, which is integrated in the genomic DNA of the transduced cells.

The pooled lentiviral transduction was performed on GBM-SCs considering two important factors. First, the library was transduced at a multiplicity of infection (MOI) of 0.5. The low MOI ensures the presence of a single viral integrant per cell in the majority of the population. This decreases the probability of the phenotype occurring due to the combined effect of knockdown of multiple genes in a cell. Second, to control for position specific integration effects and to average out behavior differences between individual cells, 200 unique cells were infected per shRNA. This also reduces the phenotypic effects of co-occurrence of multiple hairpins in a given cell, as the probability of the same two genes getting co-transduced more than once is low.

Identification of Essential Genes in GS6-22 and MGG 8 Cell Lines

The GS6-22 and MGG 8 GBM stem cell lines were each transduced with the lentiviral library and infected cells were selected with puromycin for 48 hrs. Following selection, the cells were pooled and divided into 3 equal groups. One group served as the reference sample for the distribution of transduced shRNAs in the library, and genomic DNA was isolated immediately. The other two groups of cells were grown either under normoxic conditions (21% oxygen) for 10 days or under hypoxic conditions (1%) for 18 days. This time difference was due to the fact that GBM-SCs grow at a slower rate under hypoxic conditions. The slower doubling times require increasing the assay length to achieve at least 4 population doublings so that inhibitory shRNAs will be significantly depleted from the population. Genomic DNA was then isolated from the cells grown under both oxygen conditions. For all the three samples (reference, normoxia and hypoxia), the viral integrants containing the shRNA barcodes were amplified by PCR and the products were sequenced using Illumina HiSeq next generation sequencer (Figure 3.1A). Sequencing of the reference, normoxia and hypoxia, enumerated the relative abundance of each 18-nt barcode from each sample. These barcodes were mapped to specific shRNAs and further to the targeted genes. Knockdown of essential proteins by the shRNA would lead to the loss of cellular viability for the cell, resulting in its dropout from the population and hence the reduction in the abundance of the shRNA barcode in that cell population. Following sequencing, to normalize for the different numbers of total reads from the sequencing of each sample (reference, normoxia or hypoxia for a given GBM-SC line), the abundance of each hairpin was normalized to the total number of reads for the entire

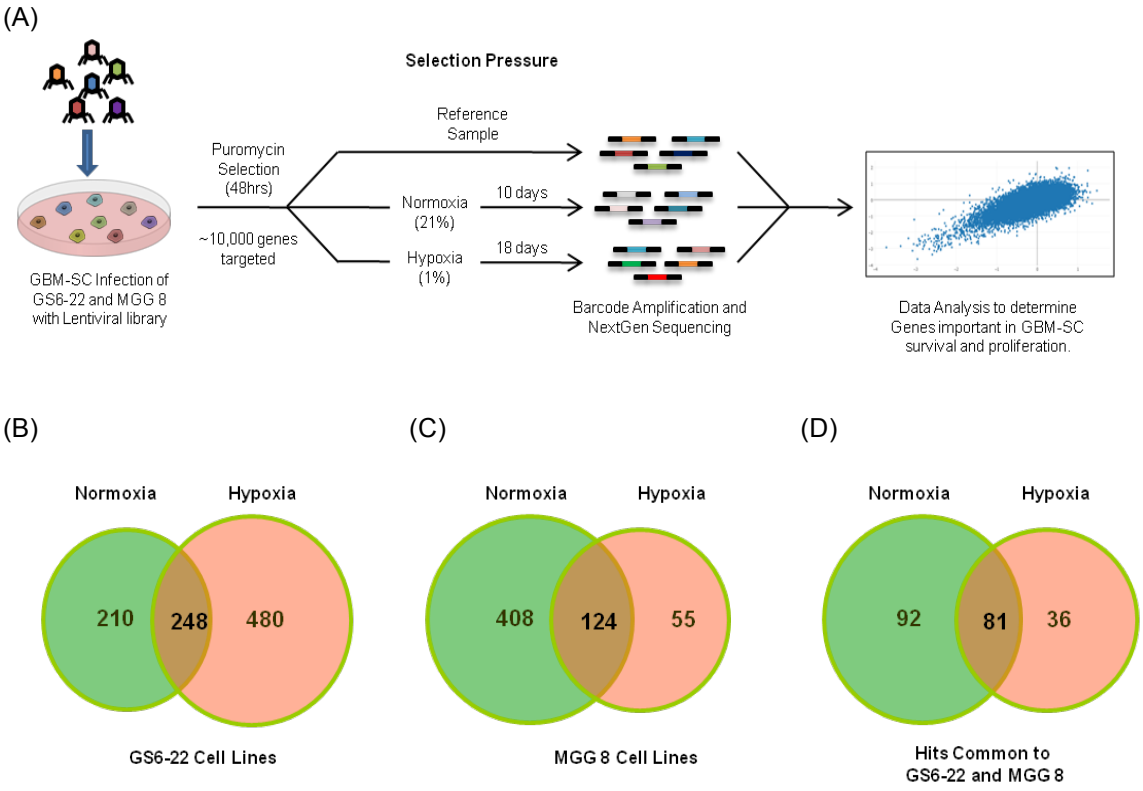

Figure 3.1: Identification of Essential Genes in GBM-SCs. (A) Schematic of screening methodology used to screen GS6-22 and MGG 8 Cell Lines. (B-D) Comparison of hits in different conditions as determined by MAD Analysis of screening data in both cell lines in Hypoxia (1% Oxygen) and Normoxia (21% Oxygen). A 3 MAD and <0.5 fold change cutoff was applied to all hairpins. Genes with at least 2 qualifying hairpins was scored as a hit. Comparison between normoxia and hypoxia hits (B) in GS6-22, (C) in MGG 8 and (D) common to both cell lines.

population of that sample. The barcode depletion in the normoxic and hypoxic samples was quantified for all hairpins tested by comparing the abundance of the same barcode in to the aforementioned reference control sample. This was done by calculating the fold change of abundance between the test condition and the reference control. Hairpins that were not detected in the reference sample were excluded from further analysis, which was a rare occurrence in the screens.

Hit Selection

GBMs exhibit high inter-tumoral heterogeneity and likely possess varying genetic dependencies based on the mutations and expression profiles of the individual tumors. In order to identify core essential genes, we screened two different patient derived GBM-SC lines; GS6-22 and MGG 8. Both cell lines were screened in triplicate for essential genes in normoxia and hypoxia. By comparing the gene hits from two cell lines, we aimed to identify key growth and viability factors common to different tumors. Once the screening was completed, the analysis to determine essential genes was performed using two published methodologies; Median Absolute Deviation (MAD) method and the Bayesian BAGEL algorithm.

Median Absolute Deviation (MAD) score is a robust statistical parameter which is less sensitive to the presence of outliers in the population compared to the Z- Score [266]. The MAD score is calculated for every hairpin separately and for the population as well. The population MAD is used to determine the cutoff to be used for the screening data. Fold change was determined for all replicates individually and then the median fold change of the replicates was calculated for further analysis. To test the concordance between the

replicates, we compared the $\log_2$(fold change) values of the hairpins in each replicate in a cell line and condition with one another, and found a concordance ranging from 0.6 to 0.75 between the samples. The Median Absolute Deviation (MAD) score was calculated for each hairpin in the population. A hairpin was considered a hit if its MAD score was >3 median absolute deviations from median of the population. Due to the detection of hairpins with less than 50% loss of abundance in the conditions compared to the control using this criterion, we applied an additional cutoff of fold change of <0.5 to ensure that the effect of the hairpin was biologically relevant. A gene was considered a candidate hit if at least 2 hairpins targeting the gene, matched the above criteria. This helps minimize false positives due to off-target effects.

Using the MAD analysis, we identified 448 (~4.5%) and 728 (~7%) genes, which were essential for GS6-22 cells under normoxic and hypoxic conditions respectively. Of these, 248 genes were important to maintain viability under both conditions in this cell line (Figure 3.1 B). MGG 8 cells required 532 (~5%) genes and 179 (~2%) genes for survival or proliferation in normoxia and hypoxia respectively, out of which 124 genes were essential in both conditions (Figure 3.1C). The variable hit rate may be a function of the genetic (such as mutations) as well as physiological (rate of proliferation) difference in these cell lines, which presumably represents the variations observed between distinct tumors. Comparison between the hits in the two cell lines was performed under both conditions. Under normoxic conditions, 174 genes are essential to both cell lines, which represents 32% and 38% of the total normoxia hits in GS6-22 and MGG 8 cells respectively. 118 genes (~1.2%) are required for the growth of both cell lines under

	Gene Symbol	Description
Selected Hits Common to Normoxia and Hypoxia	EIF3A	Eukaryotic Translation Initiation Factor 3
	KIF11	Kinesin family member 11
	RBX1	Ring Box-1
	PLK1	Polo-Like Kinase 1
	RBL2	Retinoblastoma-Like 2
	SAP18	Sin3A-Associated Protein
	CKAP5	Cytoskeleton Associated Protein 5
	ACACA	Acetyl-Coenzyme A Carboxylase α
	CDC2L1	Cell Division Cycle 2-Like 1
	GRIP1	Glutamate Receptor Interacting Protein 1
	SMC2	Structural Maintenance of Chromosomes 2
	CDC2L2	Cell Division Cycle 2-Like 2
	ADIPOR2	Adiponectin receptor 2
	CHAF1A	Chromatin Assembly Factor 1
	CXCL12	Stromal Cell-Derived Factor 1
	GRB2	Growth Factor Receptor-Bound Protein 2
	SGK1	Serum/Glucocorticoid Regulated Kinase 1
	SPTLC1	Serine Palmitoyltransferase, Long Chain Subunit 1
	STK36	Serine/Threonine Kinase 36
	TERF2IP	Telomeric Repeat Binding Factor 2, Interacting Protein
Selected Hypoxia Specifc Hits	BCL2L1	BCL2-like 1
	CDR2	Cerebellar Degeneration-Related protein 2
	HYOU1	Hypoxia Up-Regulated 1
	MAPK6	Mitogen-Activated Protein Kinase 6
	MCL1	Myeloid Cell Leukemia Sequence 1
	MEN1	Multiple Endocrine Neoplasia 1
	MKRN1	Makorin Ring Finger Protein 1
	MSH6	MutS Homolog 6
	MYF5	Myogenic Factor 5
	NT5C3	5'-Nucleotidase, Cytosolic III
	PFKFB4	6-PhosphoFructo-2-Kinase/Fructose-2,6-Biphosphatase 4
	SF3B4	Splicing Factor 3b, subunit 4
	YWHAE	Tryptophan 5-Monooxygenase Activation Protein, Epsilon Polypeptide

Figure 3.2: Selected Essential Genes for GS6-22 and MGG 8 in Both Conditions as well as Hypoxia Exclusively. Gene hits between GS6-22 and MGG 8 under normoxia and hypoxia were compared to find gene hits in both conditions. Hypoxia specific hits represent genes, which score as a hit in hypoxia but not under normoxic conditions.

hypoxic conditions (Supplementary Figure S1). The 81 core essential genes, i.e. genes important for both cell lines under both normoxic and hypoxic conditions, were identified (Figure 3.1D). Selected essential genes are listed in Figure 3.2 and are annotated if they are known to be relevant in cancer biology. Approximately 50% of the normoxia genes are also essential for survival under hypoxic conditions. By contrast, close to 70% of the genes important for survival under hypoxic conditions are also essential for survival under normoxia (Figure 3.1D). Selected hypoxia specific genes are listed in Figure 3.2. This analysis indicates that most survival genes are common to both conditions and relatively fewer genes are required for hypoxic survival exclusively. Identification of these pathways that these genes regulate may be important in understanding the biology of GBM stem cells in the hypoxic microenvironment. The core essential gene list represents the best candidates for drug discovery for targeting GBM stem cells across multiple GBMs under both normoxia and hypoxia.

The core list of essential genes consists of various proteins involved in key housekeeping functions of the cells. Indeed many of these genes, almost 50%, were previously known to be important for cell viability and have been identified by various screens as a part of the core set of essentiality genes for different cell lines [267, 271]. Top hits of the screen, include genes important in transcription (eg. POLR2B), translation (eg. RPS6, RPL30) as well as part of the proteasomal machinery (eg. PSMA1, PSMB2) (Supplementary Table S1). These key functions are important for all cell types and enrichment of these hits confirms the validity of the screen.

Analysis of the core essential gene list using Ingenuity Pathway Analysis (www.ingenuity.com) likewise revealed the enrichment of canonical pathways involved

(A) Pathways Affected by Core Essential Genes

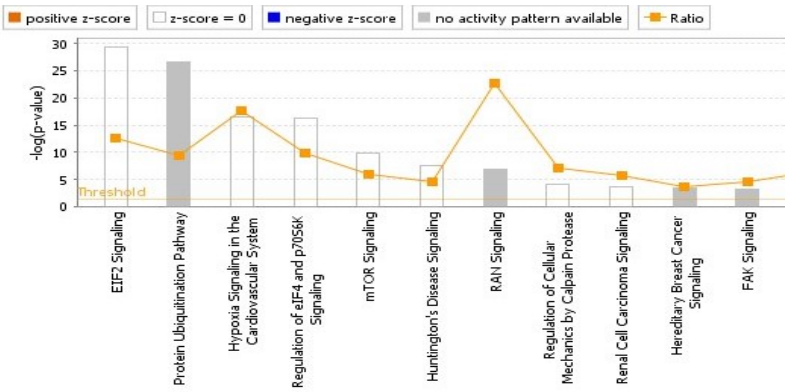

(B) Comparison between pathways when known essential genes are excluded

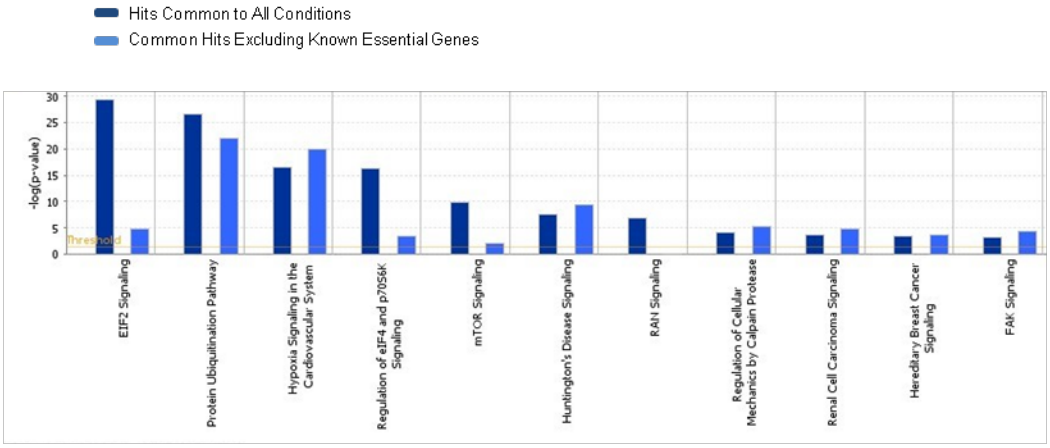

(C) Top Pathways and Networks represented by Hypoxia Specific Gene Hits

Top Canonical Pathways

Name	p-value	Overlap
PI3K/AKT Signaling	4.45E-06	3.9 % 5/128
14-3-3-mediated Signaling	7.82E-05	3.4 % 4/119
Regulation of eIF4 and p70S6K Signaling	1.91E-04	2.7 % 4/150
Ephrin B Signaling	3.99E-04	4.0 % 3/75
EIF2 Signaling	4.42E-04	2.1 % 4/187

Top Networks

ID	Associated Network Functions	Score
1	Cell Death and Survival, Embryonic Development, Organismal Development	36
2	Cell Death and Survival, Cellular Compromise, Connective Tissue Disorders	34
3	Cancer, Hematological Disease, Immunological Disease	24
4	Carbohydrate Metabolism, Small Molecule Biochemistry, Cellular Assembly and Organization	2

Figure 3.3: Ingenuity Pathway Analysis of essential genes from screen. (A) Top canonical pathways enriched by analyzing 81 genes essential to both cell lines under both conditions. (B) Comparison between (A) and the common hits after removing known essential genes. (C) Top canonical pathways and networks enriched by analyzing hypoxia specific gene hits.

in translation and proteasomal degradation. This was mainly on account of a number of elongation factors and proteasome subunits that were scored as hits in the screen, as was to be expected (Figure 3.3A). Removal of these known essential genes did not significantly change the pathway enrichment (Figure 3.3 B). However, a few pathways important in GBMs such as Ran signaling, which is known to play a role in various cancers including GBM, were no longer enriched after removal of the known essential genes from the list of hits, indicating its core function in various cell types. (Supplementary Figure S3.2) [272]. A number of calpain proteases and GRB2 contributed to the enrichment of FAK signaling, which was unchanged in the comparative analysis in Figure 3.3 B. (Supplementary Figure S3.3). Interestingly, known important GBM pathways such as MAPK or RTK signaling pathways were not enriched in this list. This may be due to redundancy in the proteins present in these pathways as well as due to the compensation by other signaling pathways involved in survival of these cells. Interestingly, hypoxia signaling was enriched as a canonical process in the hits that were common to both conditions. This may be due to the HIF genes being activated in normoxia in these cells lines and their role in the induction of stemness. This was not observed in the analysis of hypoxia-specific gene hits from the screen (Figure 3.3C). Although hypoxia relevant genes were not overrepresented in this analysis, the top networks regulated by these genes are known to be important in cancer biology.

Data Analysis Using BAGEL algorithm and Comparison with MAD

To compare and contrast the genes that are identified using 2 distinct published statistical methods, we performed a second data analysis using the Bayesian Analysis of Gene EssentiaLity (BAGEL) algorithm [267, 271]. This algorithm calculates a Bayes Factor

for each gene to estimate the probability of its essentiality utilizing two gene lists to train the algorithm; an essential and a non-essential gene list. Using data from previously published screens across different cancers and cell lines, the essential gene list comprised of genes commonly scored as hits across various cell lines in different screens and the non essential gene has genes with no effect on cellular proliferation or survival. The Bayes Factor (BF) determines whether a test gene is more likely to be an essential gene than a non-essential gene. BF>5 for a gene indicates that it is likely to be essential for maintaining cellular viability. In contrast to the MAD analysis, the bayes factor combines the effects of all targeting hairpins to generate a common score for each tested gene.

The bayes factor was calculated for each gene in the pooled screen of GS6-22 and MGG 8 cell lines by the BAGEL algorithm and a cutoff of BF>5 was applied. We were able to identify 152 core essential genes (2% of library) common to both cell lines under normoxic as well as hypoxic conditions (Figure 3.4A). 42 hypoxia specific genes were identified by this analysis method. Comparing the hits using BAGEL to the 3 MAD analysis, we observed that almost all genes (66 hits out of 81 genes; 82%) identified using the MAD analysis were also detected by BAGEL (Figure 3.4B). However BAGEL missed 15 genes that were detected using MAD analysis, likely due to high number of ineffective hairpins targeting those genes (Figure 3.4C). At least some of these genes were validated (see below) suggesting that the BAGEL method is overly strict and misses some true positives. Only 4 hits were common between the hypoxia specific genes determined by both analysis methods (Figure 3.4D).

(A)

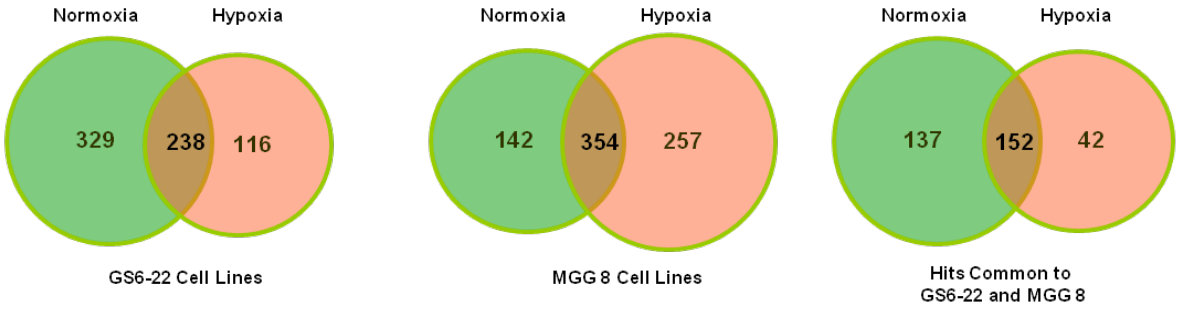

(B)

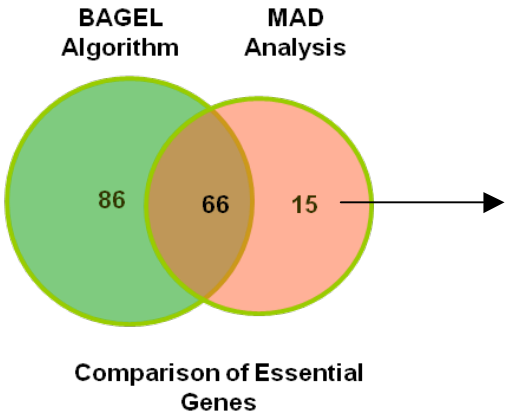

(C)

Gene Symbol	Description
ADIPOR2	Adiponectin Receptor 2
CHAF1A	Chromatin Assembly Factor 1, Subunit A
CXCL12	Stromal Cell-Derived Factor 1
EIF4G3	Eukaryotic Translation Initiation Factor 4 Gamma, 3
FBL	Fibrillarin
GNPNAT1	Glucosamine-Phosphate N-Acetyltransferase 1
GRB2	Growth factor Receptor-Bound protein 2
HSPE1	Heat Shock 10kDa protein 1
ISCU	Iron-Sulfur Cluster Scaffold Homolog
PLK1	Polo-Like Kinase 1
RBL2	Retinoblastoma-Like 2
SGK1	Serum/Glucocorticoid Regulated Kinase 1
SPTLC1	Serine Palmitoyltransferase, Long Chain base subunit 1
STK36	Serine/Threonine Kinase 36
TERF2IP	Telomeric Repeat Binding Factor 2, Interacting Protein

(D)

Gene Symbol	Description
BCL2L1	BCL2-like 1
RBM8A	RNA binding motif protein 8A.
PRKRIR	50KDa Interferon-Induced Protein Kinase-Interacting Protein
SPACA3	Sperm Acrosome Associated 3

Figure 3.4: Analysis using BAGEL Algorithm and Comparison with MAD Analysis. Pooled screening data was analyzed using BAGEL algorithm and a cutoff of BF>5 was applied. (A) Comparison of the hit under normoxic and hypoxic conditions in GS6-22 and MGG 8 cell lines separately and hits common to both lines under both conditions. (B) Comparison of core essential genes from BAGEL and MAD Analysis. (C) Gene hits detected by MAD analysis but not by the BAGEL algorithm. (D) Hypoxia specific hits detected by both BAGEL and MAD analysis methods.

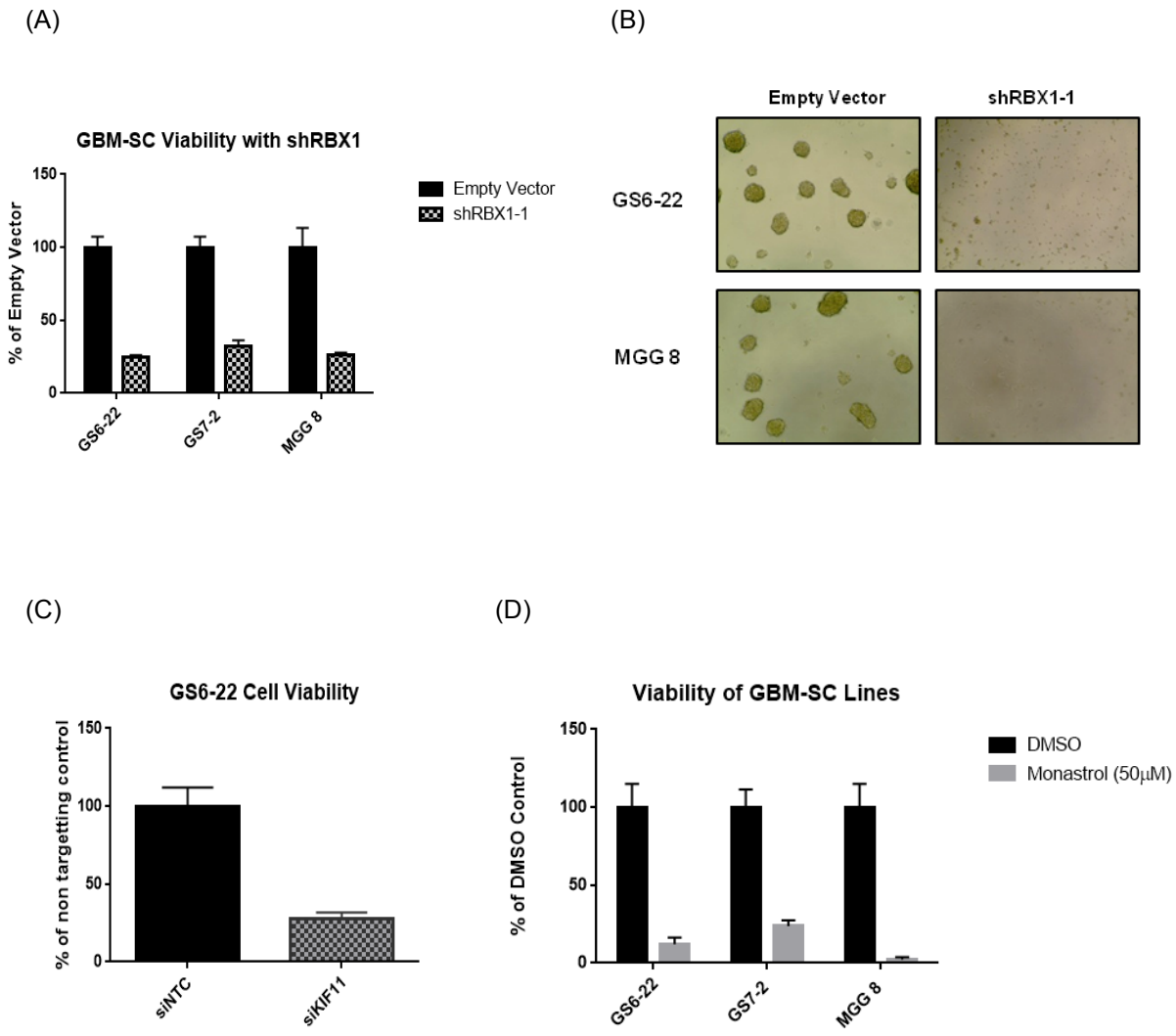

Figure 3.5: Validation of RBX1 and KIF11 Hits from Screen. (A) Viability in response to shRNA targeting RBX1 was determined in 3 different GBM-SC cell lines. (B) Images showing the inhibitory effect of knockdown of RBX1 on growth of GS6-22 and MGG 8 cell lines. (C) Cell viability was measured after knocking down KIF11 protein by siRNA in GS6-22 cell lines and by using KIF11 specific inhibitor, Monastrol (50μM) in 3 GBM-SC lines.

Validation of the Top Targets from the Pooled Screen

To validate the top hits of the screen, we utilized gene depletion using siRNA and shRNA, independent from the targeting sequences used in the pooled shRNA library. Multiple GBM-SC lines were used to validate gene hits including GS6-22 and MGG 8, which were used in the screen. Ring Box -1 (RBX1), an E3 ubiquitin ligase and Kinesin 11 (KIF11) play critical roles in cell cycle progression and were the top screening hits in GS6-22 and MGG 8 cells under both conditions. Depletion of RBX1 protein by shRNA resulted in a significant decrease in cell viability of three GBM-SC lines tested (Figure 3.5 A-B). KIF11 was also validated as an essential gene using siRNA and Monastrol, a specific KIF11 inhibitor [260]. Both depletion of KIF11 protein and inhibition of its activity led to a significant decrease in GBM-SC viability (Figure 3.5 C-D).

Analysis of Essential Kinases

Kinases are among the most attractive targets for drug development. They represent key signaling nodes regulating various processes critical for survival and functioning of the cells and are quite druggable. Inhibitors targeting kinases have shown efficacy in the clinic. Small molecular inhibitors for various kinases have been developed, many of which are commercially available [273, 274].

We identified the kinases, which are important in cellular proliferation and survival of GBM-SCs in normoxic and hypoxic conditions. Out of 600 kinases tested, 64 kinases (10.6%) were hits in GS6-22 or GBM 8 in either oxygen conditions. Comparisons were performed between 4 different groups/conditions viz. GS6-22 Normoxia, GS6-22 Hypoxia, MGG8 Normoxia and MGG 8 Hypoxia. 40 kinases out of the 64 (~63%) hits

(A)

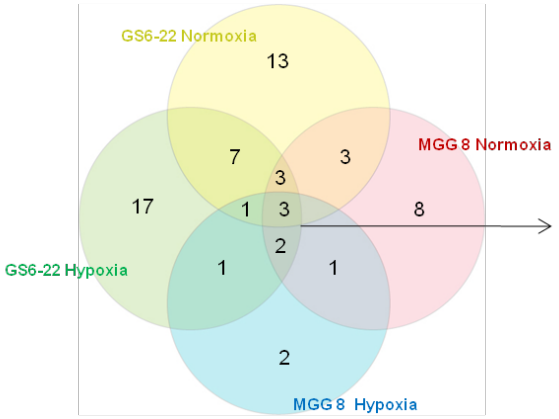

(B)

Essential Kinase for GS6-22 and MGG 8 in Normoxia and Hypoxic conditions

Gene Symbol	Entrez ID	Definition
PLK1	5347	Polo-like kinase 1
SGK1	6446	Serum/glucocorticoid regulated kinase 1
STK36	27148	Serine/threonine kinase 36

(C)

Top Canonical Pathways

Name	Overlap
Glioma Signaling	12.3 % 13/106
Role of NFAT in Cardiac Hypertrophy	5.4 % 10/186
Breast Cancer Regulation by Stathmin1	5.1 % 10/197
Molecular Mechanisms of Cancer	3.2 % 12/373
Pyridoxal 5'-phosphate Salvage Pathway	9.5 % 7/74

(D)

Top Diseases and Bio Functions

Diseases and Disorders

Name	#Molecules
Cancer	50
Organismal Injury and Abnormalities	50
Tumor Morphology	15
Neurological Disease	21
Gastrointestinal Disease	46

Figure 3.6: Analysis of Kinase Hits from Pooled shRNA Screen. Kinase hits in each condition were identified and then comparisons were performed between the hits in the various condition (A) Venn diagram representing the number of kinase hits in each sample as well as common hits. If value for an intersection was zero, the number is not included in the diagram. (B) List of 3 kinases essential under all conditions. (C-D) Top canonical pathways and diseases by IPA analysis of all kinase hits, unique to any condition or common to the conditions.

were unique to a single condition whereas 15 (23%) were present in two conditions. 6 (~9%) kinase hits were observed in 3 out of 4 conditions tested (Figure 3.6A). Only three Serine/Threonine kinases, Polo-like Kinase 1 (PLK1), Serine/Threonine Kinase 36 (STK36) and Serum and Glucocorticoid regulated Kinase 1 (SGK1) were identified as essential for both GS6-22 and MGG 8 cell lines under both normoxic and hypoxic conditions (Figure 3.6B). As the common essential kinases were few in number, we performed pathway analysis on all the kinases scored as a hit in the screen, by combining kinases which were unique and common to either condition or cell line (Figure 3.6C). The top represented pathways included glioma signaling and metabolic salvage pathways. The glioma signaling network included gene hits which are present in the growth factor signaling cascade important in GBM growth, proliferation and survival (Supplementary Figure S3.4). Analysis of various published RNAi screens shows the high discordance of identified hits when screening with different libraries using the same cell lines in contrast to the same library [275, 276]. In view of this, comparison of the hits determined by the kinase analysis from the Cellecta pooled shRNA screen was performed with the hits identified by an independent arrayed shRNA kinome screen using TRC library. This arrayed screening was performed by other members of the laboratory on GS6-22 cell lines under normoxia. Using 2 independent shRNA libraries, should decrease the probability of identification of a false positive kinase hits due to screen specific conditions. Using this approach, we identified only 4 kinases, which were scored as essential in both screens (Figure 3.7). Of the 4 kinases, CDK4 and KDR are well studied

kinases with known roles in GBM as well as other cancers[18, 22]. Only SGK1 was identified as a common kinase in both screening hit analyses.

(A)

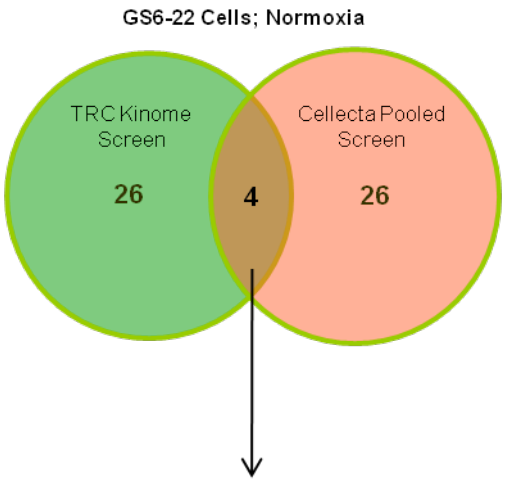

Gene Symbol	Description	Fold Change
CDK4	Cyclin Dependent Kinase 4	0.20
CDKL5	Cyclin Dependent Kinase Like 5	0.17
KDR	Vascular Endothelial Growth Factor Receptor 2	0.48
SGK1	Serum/Glucocorticoid Regulated Kinase 1	0.46

Figure 3.7: Comparison between Arrayed and Pooled shRNA screen. Gene hits from pooled and arrayed shRNA library screening forGS6-22 cell line under normoxic conditions were compared. These independent screens were performed using the same GS6-22 cell line.

Dataset	Download Link
Core Essential Genes	http://bit.do/bUGcN
Core Essentials Excluding Known Viability Genes	http://bit.do/bUGea
Hypoxia and Normoxia Specific Genes	http://bit.do/bUGei

Supplementary Table S1: List of hits under different conditions. Table contains links, which will allow access to list of genes scored as hits in the MAD analysis in the mentioned datasets.

(A)

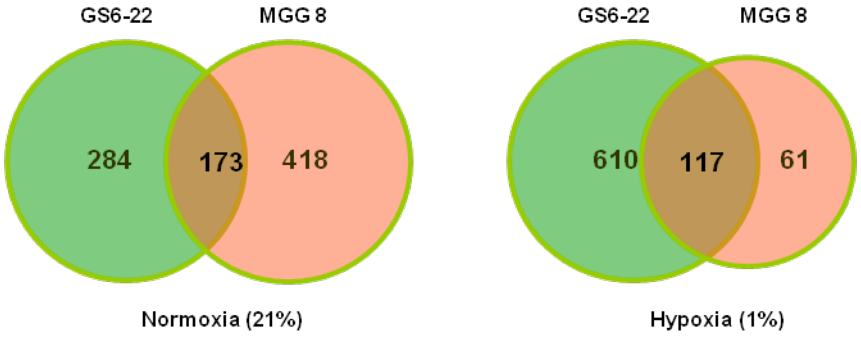

Supplementary Figure S3.1: Comparison of hits from different GBM-SC lines. Essential genes from GS6-22 and MGG 8 were compared by condition of growth in the screen, viz. normoxic and hypoxic conditions.

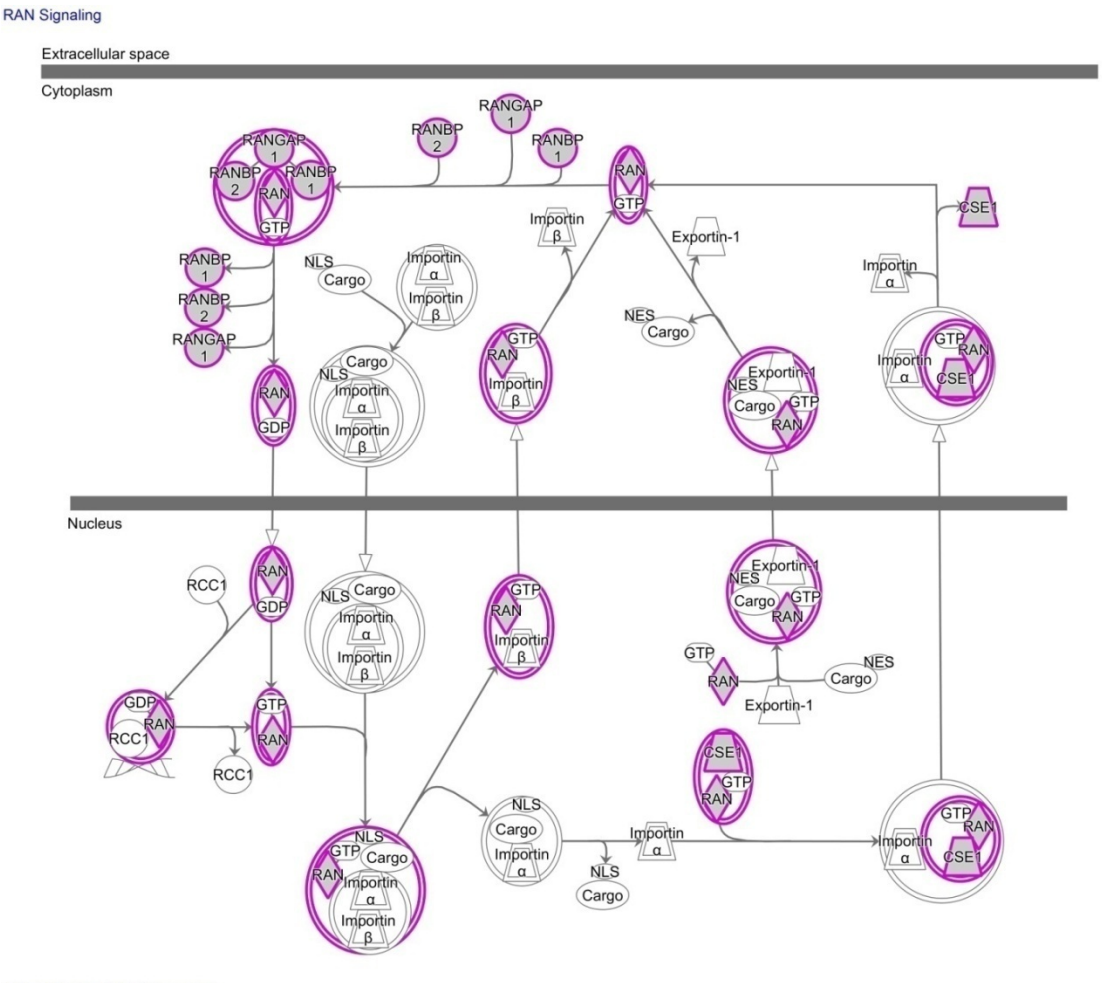

Supplementary Figure S3.2: Ran Signaling Network was one of the top canonical pathways enriched by analyzing top essential genes from both cell lines identified by the shRNA screen. Highlighted nodes represent hits identified in the screen.

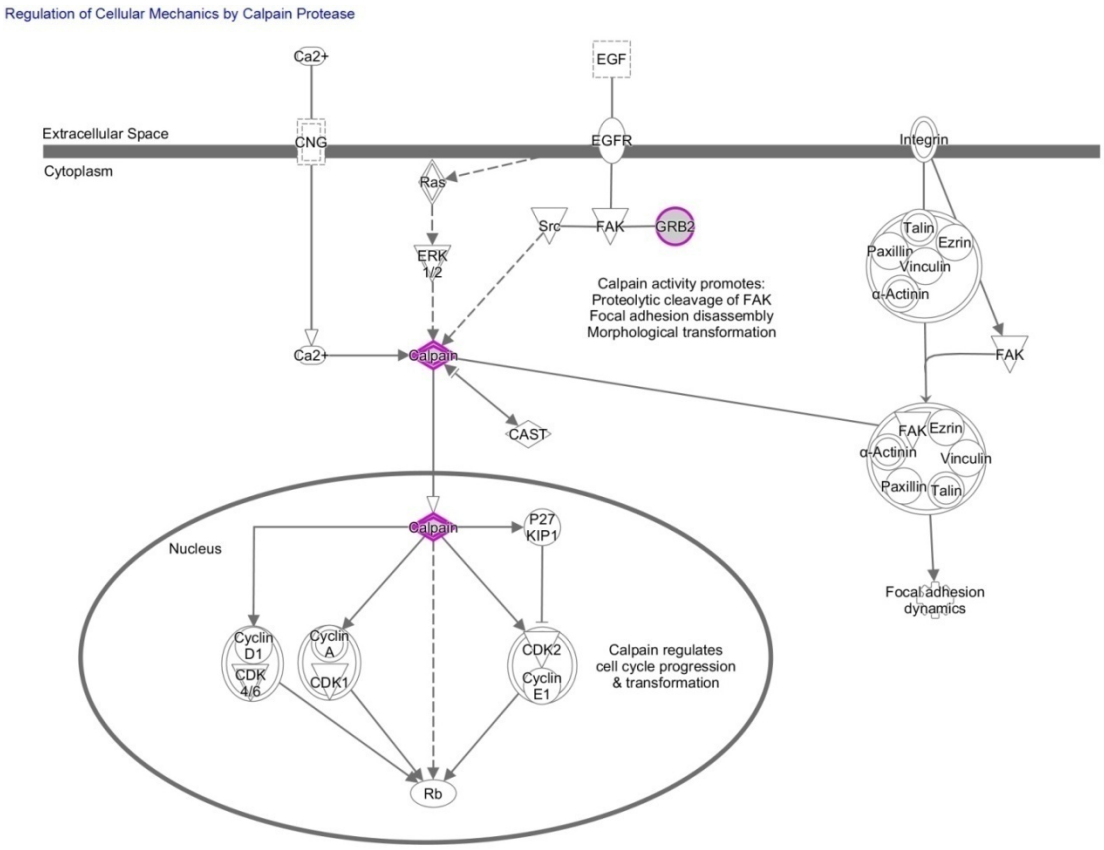

Supplementary Figure S3.3: Focal Adhesion Kinase Signaling Network. FAK canonical signaling pathway was identified by analyzing the core essential gene hits from the screen and was unchanged after analysis was performed on the gene hits after removal of known essential genes. A number of Calpain proteases are enriched in this network. Highlighted nodes represent hits identified in the screen.

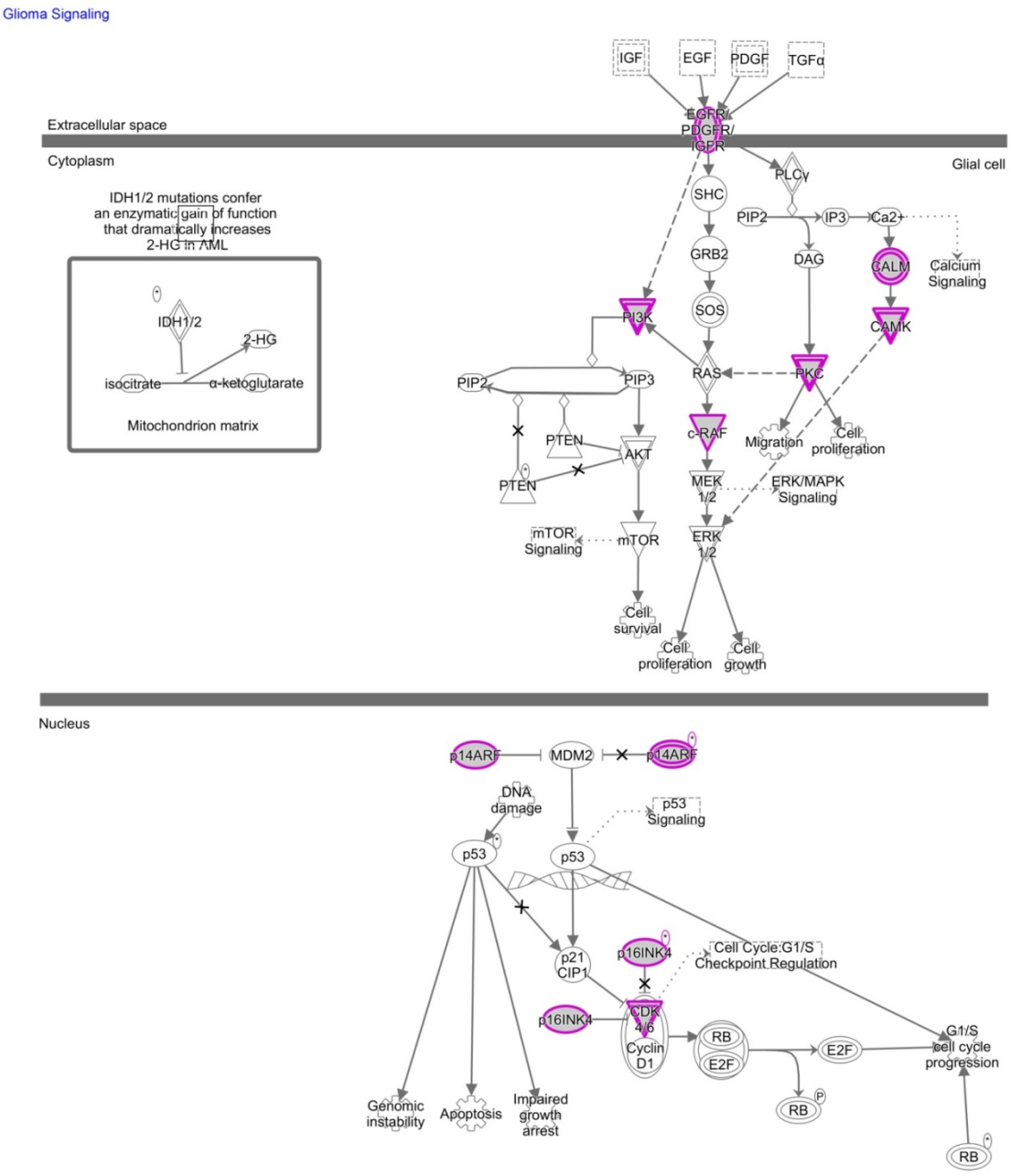

Supplementary Figure S3.4: Glioma Signaling Pathway was one of the top canonical pathways enriched by analyzing top kinases from either cell lines identified by the shRNA screen. Highlighted nodes represent hits identified in the screen.

Chapter 4

Role of SGK1 in GBM-SC Proliferation and Survival

Figure Contributions:

Figure S4.4A was contributed by Surbhi Goel-Bhattacharya.

Introduction

The Serum and Glucocorticoid regulated kinase 1 (SGK1), as the name suggests, was discovered as a transcriptionally induced gene in the presence of serum and glucocorticoids. The list of SGK1 inducers has now been expanded to include a number of different environmental stimuli including oxidative and osmotic stress and UV irradiation [277–279].SGK1 is an AGC kinase family member which includes kinases such as Akt, PDK1, PKC and the S6Kinase [280]. Like other AGC kinases, SGK1 is phosphorylated on its T-loop (Thr256) and hydrophobic motif (Ser422) by upstream kinases (PDKI and mTORC2 respectively) to regulate its kinase activity [281, 282]. Activation of the Wnt pathway and WNK1 have also been shown to regulate SGK1 activity [283]. SGK1 and AKT share a similar consensus target phosphorylation site RXRXXS/T [284]. This indicates that these two kinases should share many downstream targets, which is indeed observed. However, differences in active site conformation, lack of a lipid binding phox domain and presence of a nuclear localization sequence indicates complementary and non-redundant functions of the two proteins [282, 285–287]. The abundance of SGK1 is regulated post-translationally by ubiquitination and degradation by the CHIP and Cullin-1 ubiquitin ligases and the proteasome respectively with a half life of around 30 mins [288–290]. This allows the induction and degradation of SGK1 within 20 mins of exposure to inducing stimuli [291]. The most well described role of SGK1 is the regulation of abundance of the epithelial sodium channel (ENaC) to regulate sodium excretion in the kidney upon stimulation by aldosterone, an antidiuretic hormone [292, 293]. SGK1 regulates degradation of ENaC by phosphorylating and inhibiting ubiquitin ligase NEDD4-2 thereby affecting the Na^+/K^+ movement across the plasma membrane in

the principal cells of the kidney collecting duct. [294, 295]. This molecular function is brought to the fore when a salt-free diet is fed to SGK1 knockout mice, which show a significant loss renal NaCl loss, indicating its importance in the reabsorption of sodium in the kidney due to decrease in ENaC proteins on the plasma membrane [296]. The knockout mouse does not have any other obvious deficiencies, indicating that SGK1 is not essential for cell function and thus may be a suitable drug target for GBMs due to the low potential of side effects.

The primary role of SGK1 in tumor development is as a regulator of cell death through multiple different mechanisms. SGK1 is a part of a cytoprotective signaling network regulating the balance of pro- and anti-apoptotic proteins [291, 297]. The anti-apoptotic activity of SGK1 is mediated through the phosphorylation of FOXO3a and IKKβ. SGK1 phosphorylates FOXO3 preferentially at Ser315, with Akt acting on Ser258, to sequester the transcription factor in the nucleus in 293T cells [287, 298]. FOXO3 regulates a number of pro-apoptotic proteins such as Bim and TRAIL and its sequestration in the cytoplasm by SGK1 maintains cellular survival [299]. Regulation of NF-κB by SGK1 was shown in breast cancer [300, 301]. NF-κB is a key transcription factor for maintaining the expression of anti-apoptotic proteins such as the Bcl2 family protein, Bcl-xL as well as Inhibitors of Apoptosis proteins (IAPs). SGK1 phosphorylates and activates IKKβ, which in turn phosphorylates inhibitor of NF-κB, IK-β. This allows for translocation of NF-κB into the nucleus for target gene transcription. p53 reacts to cellular stress and can function as an activator of apoptosis [302]. SGK1 has been shown to activate MDM2 dependent degradation of p53, leading to inhibition of its role in apoptosis [302]. Interestingly, SGK1 has been shown to be transcriptionally upregulated

in a p53 dependent mechanism, thus uncovering a feedback loop for the regulation of its function [299, 303]. Regulation of cell death by the JNK pathway was demonstrated using the neuroblastoma cell lines SH-SY5Y, treated with neurotoxins to generate reactive oxygen species (ROS). Overexpression of SGK1 decreased generation of ROS and rescued the cell death phenotype [304]. SEK1, an inhibitor of JNK activity is a direct target of SGK1 and is the mechanism through which SGK1 may modulate c-jun transcription [305]. In addition to regulating cell death by apoptosis, SGK1 also mediates Ca2+ mediated necrotic cell death in a CAM Kinase II dependent manner [306]. Due to its ability to mediate survival, mice lacking SGK1 are unable to form tumors in the colon in response to chemical carcinogenesis [307]. SGK1 also promotes radioresistance in GBM cells lines, with knockdown of SGK1 leading to decreased survival and increased radiosensitivity [308]. Recurrent mutations in SGK1 have also been uncovered in Hodgkin's lymphomas, although it is not clear if they are of a functional significance [309]. In breast cancer cells treated with AKT inhibitor, overexpressed SGK1 mediated the resistance of the cells unresponsive to Akt inhibition, indicating that this redundancy with Akt may be functionally significant [310].

SGK1 importance in tumor development is not limited to its pro survival function. Increase in SGK1 expression was observed in invasive breast cancer cells, compared to the non invasive cell types [311]. Further, SGK1 participated in glucocorticoid or CSF1 dependent increase in motility and invasiveness of breast cancer cells [312]. SGK1 is overexpressed in a variety of cancers [291]. Additionally it may play an important role in angiogenesis during tumor development. Zarripashneh et al showed the role of SGK1 in endothelial cell migration and angiogenesis following myocardial infarction [313]. It has

also been demonstrated to protect endothelial cells against oxidative stress and apoptosis under hyperglycemic conditions [314].

In order to better understand the role of SGK1 in GBM-SCs, we have validated the screening hit SGK1 in GBM-SC lines using shRNA, Crispr and a SGK1 specific inhibitor. We have also tested the SGK1 requirement of traditional glioma cell lines, fibroblasts as well as normal neural stem cell lines. We further attempted to elucidate the mechanism behind the loss in viability of GBM-SCs and the molecular pathways involved.

Results

SGK1 is an Essential Gene for GBM-SC Viability

SGK1 was the only kinase hit which was common to all the tested conditions in the pooled shRNA screen as well as in GS6-22 cell lines under normoxic conditions in the arrayed kinome screen. This overlap, in addition to the availability of a SGK1 specific inhibitor, motivated investigation of the role of SGK1 in GBM stem cell biology.

SGK1 was validated as a gene important for GBM-SC proliferation and survival using 3 different reagents; shRNA, SGK1 specific inhibitor and Crispr. To ensure that SGK1 was not scored as a hit due to off-target effects of the screening library shRNAs, we used independent kinase hairpins (from a different shRNA library) to deplete SGK1 mRNA. GBM-SCs were transduced with lentivirus encoding the shRNA hairpins targeting SGK1. Following 48h of puromycin selection and 4 days incubation, cell lysates were prepared for RNA isolation and western blotting. mRNA abundance of SGK1 was measured using qPCR and protein levels were assayed using western blotting by a SGK1 specific antibody. 3 distinct hairpins were able to achieve gene expression knockdown by at least 60%, with 2 hairpins working more efficiently, depleting SGK1 protein by more than 75% of the scrambled control (Figure 4.1A). This was concordant with the amount of decrease in the SGK1 mRNA level (Figure 4.1B). Viability of GBM-SCs after treatment with shRNAs was measured using the prestoblue viability assay. Depletion of SGK1 protein by shRNA led to a significant decrease in cell viability of GS6-22 and MGG 8 cell lines (Figure 4.1C, D). Similar sensitivity to knockdown was observed in three additional patient derived GBM-SC lines

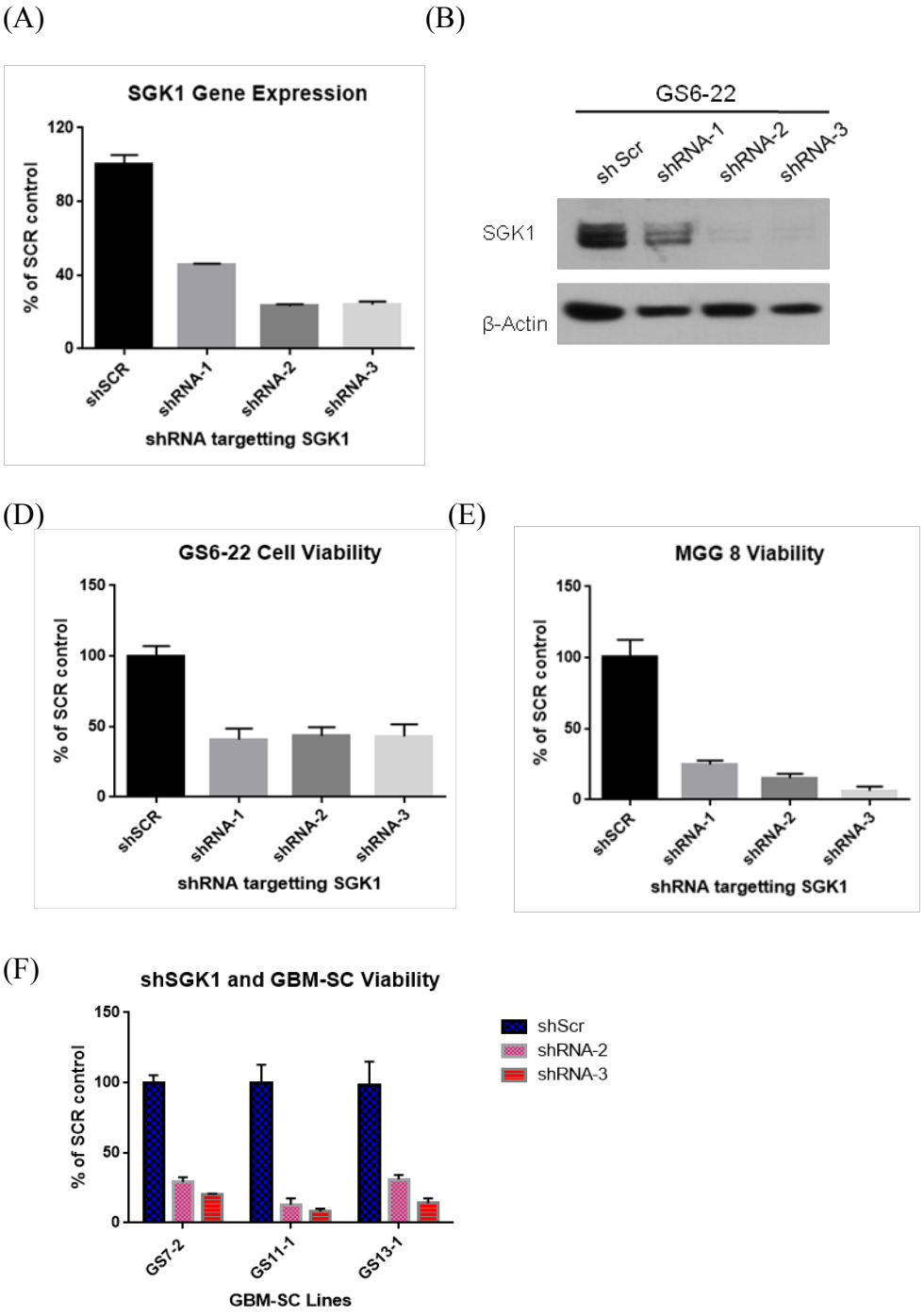

Figure 4.1: Validation of SGK1 as a hit using shRNA. (A) SGK1 mRNA abundance was quantified by qPCR after depletion with SGK1 shRNAs. (B) Western blotting for cell lysates after SGK1 knock down using three hairpins. β-actin is used as a loading control. (C-E) Cell viability assay was performed on cells transduced with shRNAs to SGK1 or scrambled control using Prestoblue viability assay. Cell growth was measured 7-10 days after puromycin selection depending on the cell line used.

(Figure 4.1E). All three hairpins showed a similar growth phenotype indicating that even ~60% protein depletion is sufficient for cells to lose viability.

For additional validation of SGK1 as a hit using Crispr, two guide RNAs targeting exon 1 in the SGK1 gene locus were designed and cloned into lentivirus constructs also expressing Cas9 protein. Expression of small guide RNAs abolished SGK1 protein expression and resulted in a severe loss of viability in GS6-22 cell line (Figure 4.2A,B). MGG 8 and GS11-1 cell lines were also susceptible to knock out of SGK1 by the guide RNAs to SGK1 as determined by prestoblue cell viability assay (Figure 4.2C).

Kinases may be important to the cells not only due to their enzymatic function, but also due to their structural role in cellular processes, as seen in the case of psuedo kinases. To determine whether the kinase activity for SGK1 is required for maintaining cell viability of GBM-SCs, we treated GS6-22 and MGG 8 with commercially available SGK1 specific inhibitor, GSK650394 [259]. Treatment with the inhibitor decreased cell growth in both cell lines at both 5μM and 10μM concentration, with MGG 8 cells demonstrating higher sensitivity to drug treatment (Figure 4.3A,B and C). Interestingly, the effect of the drug is not apparent until 4 days of treatment, after which GBM-SC viability decreases drastically.

The requirement of SGK1 for in vivo tumor growth was assayed using an intracranial xenograft mouse model. Luciferase-tagged MGG 8 cells were transduced with SGK1 shRNA or scrambled sequence lentivirus, subjected to puromycin selection and viable cells counted. 50,000 cells per mouse were injected into female NCR nude mice using stereotactic intracranial injections with MGG 8 cells containing either scrambled

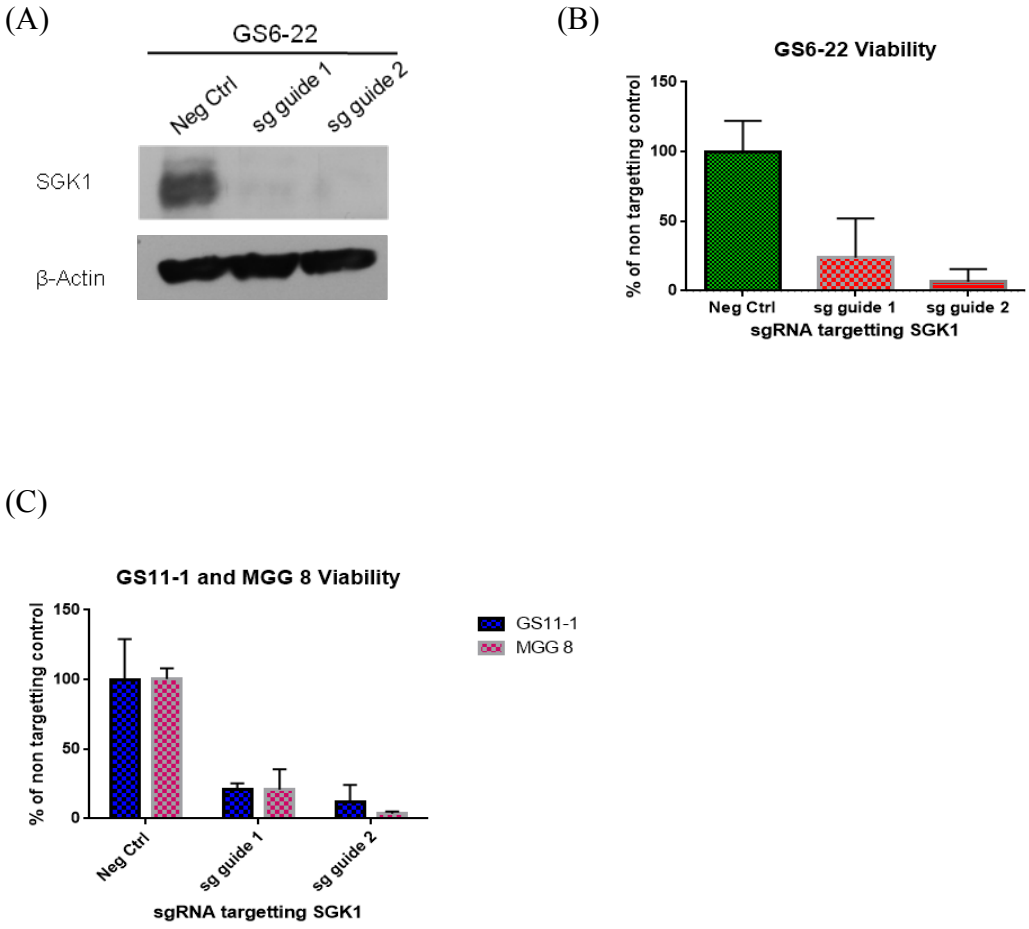

Figure 4.2: SGK1 knock out using Crispr/Cas9 system in GBM-SC lines. (A) Western blot was performed to test efficiency of small guide RNAs to knock out SGK1 in GS6-22 cell lines. β-actin was used as a loading control. (B-C) Relative numbers of viable cells were measured by prestoblue assay after expression of CRISPR/Cas9 guide RNAs to SGK1 in (B) GS6-22, (C) GS11-1 and MGG 8 cell lines. A non-targeting guide sequence (Neg Ctrl) was used as a negative control for the western blot and the prestoblue assays.

(A)

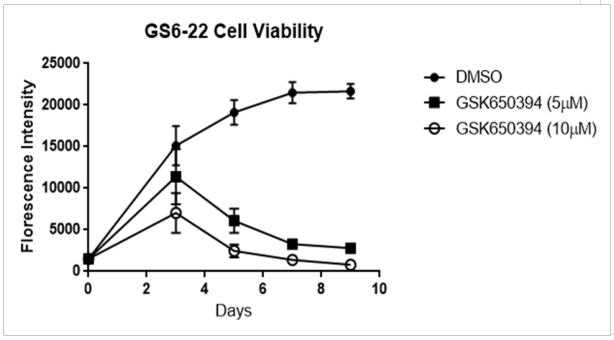

(B)

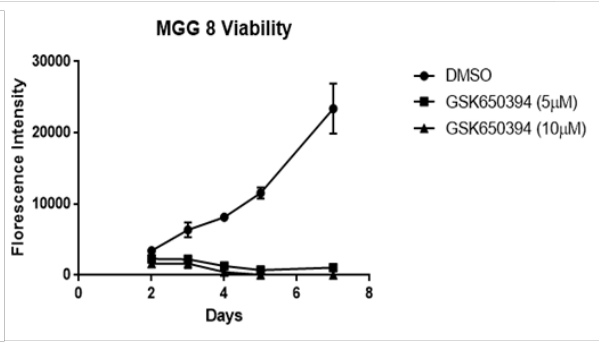

(C)

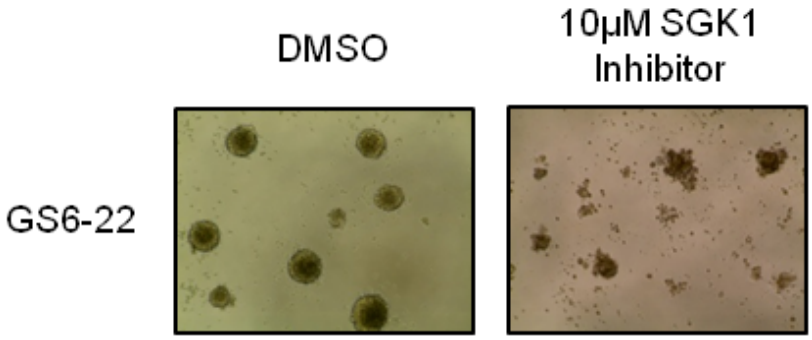

Figure 4.3: SGK1 Kinase activity is important for GBM-SC survival. GSK650394 was added to GBM-SC cultures at a concentration of 5μM and 10μM for different time durations. (A) Relative numbers of viable cells were measured by the prestoblue assay for GS6-22 (A) and MGG 8 (B) cell lines treated with the inhibitor. (C) Image of GS6-22 cell lines after treatment with the 10μM SGK1 inhibitor for 5 days and images were taken using the EVOS inverted microscope at 10X magnification.

control or SGK1 knockdown (n=11 for shScr, n=10 for shRNA-1, n=11 for shRNA-2). The time to death for the mice was noted and Kaplan Meier survival curve was plotted. SGK1 depletion led to a significant increase in survival of the mouse xenografts as compared to the scrambled control, indicating the importance of SGK1 for *in vivo* tumor growth (Figure 4.4). The SGK1 shRNA treated cells were able to form tumors in some mice, although it is not clear if this was due to growth of MGG 8 cell population resistant to SGK1 inhibition or if the cells re-expressed SGK1.

Phenotype of SGK1 knockdown is specific to glioblastoma stem cells

In order for a drug to have high efficacy, it is important to target GBM-SC population of the tumor along with the tumor bulk. To represent the bulk tumor and more differentiated glioma cell types, we tested effect of SGK1 knock down and inhibition on serum glioma lines. These are the traditional, widely used cell lines derived from GBM patients. However, they do not posses stem like characteristics and are grown in presence of 10-15% serum in the culture media. Guide RNAs targeting SGK1 cloned into Cas9 expressing lentiviruses were used to knock out SGK1 in U251, U373 and A172 glioma cell lines. Although efficient SGK1 protein knockout was achieved, U251 cells proliferation and survival were not affected by depletion of SGK1 as compared non-targeting guide RNA control (Figure 4.5 A,B). U373 and A172 cell lines were also refractory to SGK1 knockout (Figure 4.5 C). Although A172 shows a trend of sensitivity to the guide RNAs, this cell line overcomes the proliferation defect after passaging and grows at a rate similar to the non-targeting control (data not shown). Similar results were

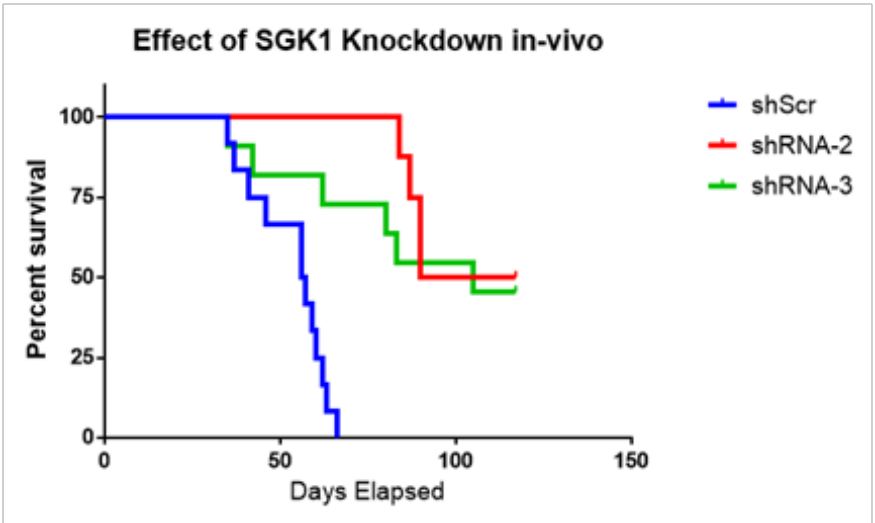

Figure 4.4: SGK1 knock down provides survival benefit using *in vivo* xenograft model. Nude mice were injected intracranially using stereotactic injections with 50,000 cells of the MGG 8 line containing either scrambled control (shScr) or hairpin targeting SGK1 (shRNA-2, shRNA-3). Figure shows a Kaplan-Meier survival curve for mice with MGG 8 cells with scrambled or SGK1 knock down hairpins. Mice with shRNA targeting SGK1 have a significant survival benefit compared to the control ($p<0.04$).

(A)

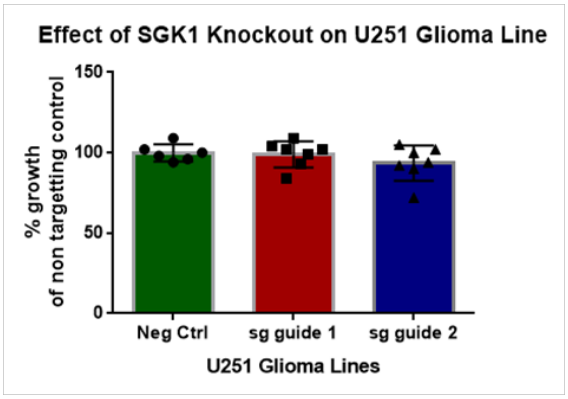

(B)

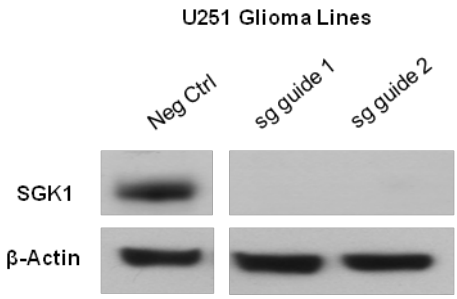

(C)

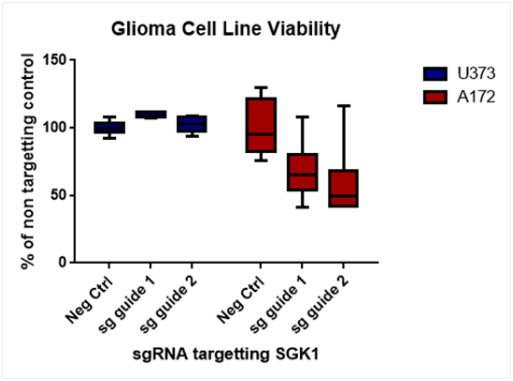

Figure 4.5: Effect of SGK1 Knockout by Crispr on Glioma Serum Lines. Glioma cell lines were infected with lentivirus encoding Cas9 protein and small guide RNAs targeting SGK1 gene locus. (A) Cell viability of U251 cell lines by MTS assay after SGK1 knockout using 2 independent guide RNAs measured 5 days post puromycin selection. (B) Western blot showing efficiency of SGK1 knock out by Crispr. β-actin was used as loading control. (C) Effect of small guides targeting SGK1 on cell viability in U373 and A172 cell viability was tested by MTS assay 5 days after selection with puromycin compared to the non-targeting control.

obtained using the small molecule SGK1 inhibitor, GSK650394, at the concentrations at which GBM-SCs were not able to survive. However, the cell lines are sensitive to higher concentration of the drug, which is likely due to the effect of the drug on off-target kinases similar to SGK1. This difference in sensitivity is not due to absence of SGK1 expression from the cell lines used (Supplementary Figure SS4.1A). SGK1 is expressed in neural stem cells, GBM-SCs as well as in the glioma lines tested. Interestingly, using Oncomine to analyze various GBM-SC and serum cell line data using the Lee study database, we observed that the serum lines, which are insensitive to SGK1 depletion, actually have the highest level of expression of SGK1 (Supplementary Figure S4.1B,C) [121].

Undifferentiated Cell Types are Selectively Sensitive to SGK1 Inhibition

Side effects developed in response to chemotherapeutic drugs are an important concern during cancer treatment. These side effects are due to the effect of the drugs on normal cell types in the body. To investigate the importance of SGK1 in normal human cells, we treated human fibroblast cell lines and normal neural progenitor cells with the SGK1 inhibitor. Hs27 cell fibroblast lines were refractory to SGK1 inhibition (Figure 4.6A). Interestingly, normal neural progenitor lines, H04 and SW06, showed decreased viability when treated with GSK650394 (Figure 4.6B). Although the effect was not as pronounced as observed in GBM-SCs, these cells display sensitivity to SGK1 inhibition. To test the importance of Akt in these cells, as a point of reference, we used Akt specific inhibitor MK2206. We observed a dramatic loss of cell viability in the normal neural progenitor cells as well as in various tested glioma cell lines (Figure 4.6B, data not shown).

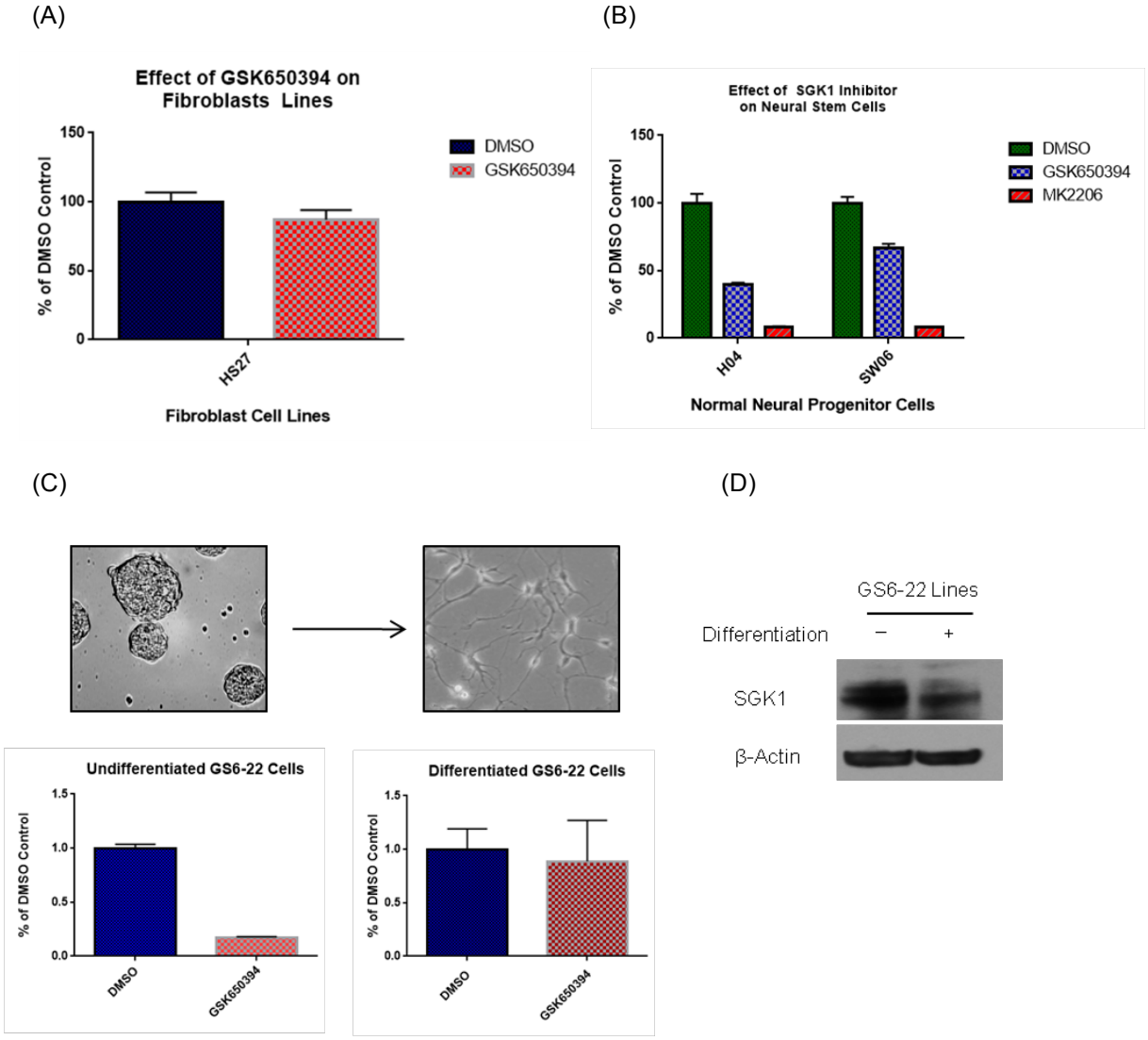

Figure 4.6: Effect of SGK1 inhibitor on non cancer cell lines and differentiated GBM-SCs. (A) Hs27 fibroblast cell lines were treated with 10μM GSK650394 or DMSO control for 5 days and viability was measured using MTS assay. (B) H04 and SW06 normal neural progenitor cell lines were also (C) GS6-22 cells were plated on laminin coated plates and were grown with SCM or were differentiated using 2% serum in DMEM. After completion of differentiation, 10μM GSK650394 was added to undifferentiated cells 2 days after plating and to differentiated cells upon completion of differentiation protocol. Relative cell viability was measured by prestoblue assay. (D) Western blot for SGK1 protein abundance before and after differentiation. β-actin was used as loading control.

Due to the sensitivity of GBM-SCs and normal neural progenitors to loss of SGK1 but the lack of it in the non-stem cell lines, we hypothesized that SGK1 is differentially important in the stem-like cells but not in differentiated cell types. To test this, we differentiated GS6-22 cell lines using 2% serum containing media on laminin, and compared the effect of the GSK650394 on the differentiated GS6-22 cells to the undifferentiated GS6-22 grown on laminin (Figure 4.6C). Interestingly, we observed a loss of sensitivity of GBM-SCs to SGK1 inhibition upon differentiation, indicating that SGK1 loses critical role in upon differentiation (Figure 4.6 C). The SGK1 protein is expressed in differentiated cells, although the expression is reduced compared to the undifferentiated GBM-SCs (Figure 4.6D).

SGK1 is required for cellular survival of GBM-SCs

The reduced number of viable cells observed due to SGK1 depletion may be due to either the loss of proliferation or due to effect of SGK1 on cell survival of the GBM-SCs. SGK1 depletion did not impact the expression of known stem cell markers (Supplementary Figure S4.2). As SGK1 is a known pro-survival kinase, we tested the effect of SGK1 depletion on apoptosis. When cells undergo apoptosis, there is an increase in the flipping of the phosphotidylserine to the cell surface, which may be detected by binding of fluorescent-tagged Annexin V to this lipid. Annexin V binding is an early apoptosis marker. This early event is followed by an increase in cell membrane permeability, which can be detected by incorporation of propidium iodide (PI) into the nucleus of the cell. Apoptotic cells in the population are double positive for Annexin V

(A)

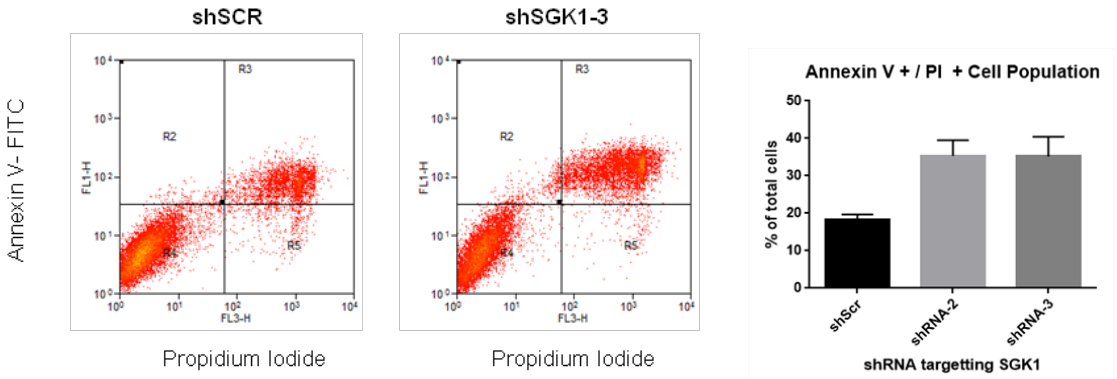

(B)

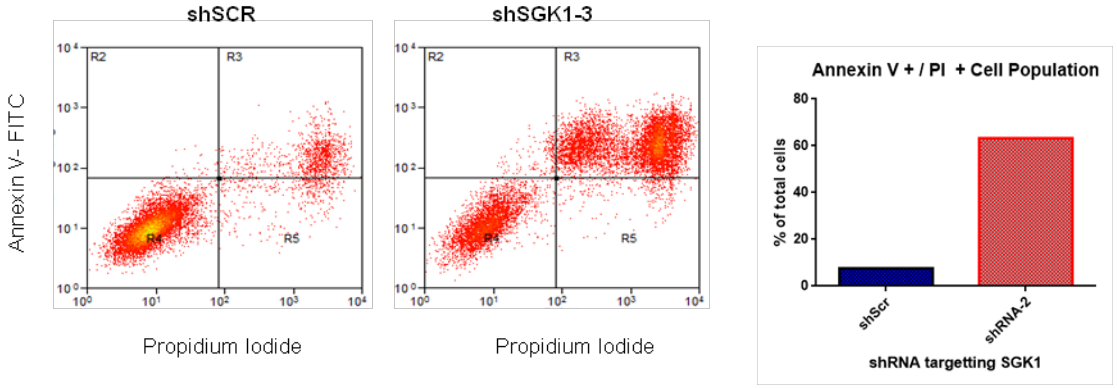

Figure 4.7: Effect of shSGK1 on Annexin V/PI apoptotic population in GS6-22.GS 6-22 Cell line was transduced with shSGK1 or shScrambled lentivirus and puromycin was used to select uninfected cells. Annexin V-GFP and PI were used to stain cells at day 4 (A) and day 5 (B) post selection and number of events in R3 quadrant containing the Annexin V and PI double positive cells were quantified.

and PI staining. To determine whether SGK1 depletion leads to an increase in this population of cells, we transduced shRNA to SGK1 into GS6-22 cells and following 4 days of selection, assayed for Annexin V and PI apoptosis markers by flow cytometry. A significant increase in the Annexin V / PI double positive cell population was detected in SGK1 knockdown cells as compared to the scrambled control (Figure 4.7 A). The number of cells in this population increases with time at day 5 of treatment (Figure 4.7B). Treatment with GSK650394 also increases the number of apoptotic cells in GBM-SCs (Supplementary Figure S4.3A). However, only a small percentage of U251 cells are positive for this marker (12% as compared to 60% at day 5), demonstrating the differential sensitivity between stem and non-stem GBM cell lines (Supplementary Figure S4.3B).

Mechanism of SGK1-dependent Cell Death is Not Caspase-3 Mediated

The canonical pathway for apoptosis induction is via the caspase cascade[315]. Internal or external death stimuli lead to cleavage and activation of caspases in the cells leading to cleavage of downstream substrates such as cleavage of poly ADP ribose polymerase (PARP) by active caspase 3[316]. This change can be detected and used a marker for cell death by apoptosis. Upon knockdown of SGK1 by shRNA, we observed induction of the cleaved form of PARP, indicating activation of the caspase cascade (Figure 4.8A). Although we do observe a decrease in the total caspase -3 and -9 (Figure 4.8 B), we are unable to detect the presence of or any increase in the cleaved form of the caspases. It is possible that the cleaved forms of these enzymes are quickly degraded by the proteasome

thereby preventing their detection. However, addition of proteasome inhibitor MG132 for 24 hours does not enable detection of the cleaved forms of the caspases. Interestingly, the

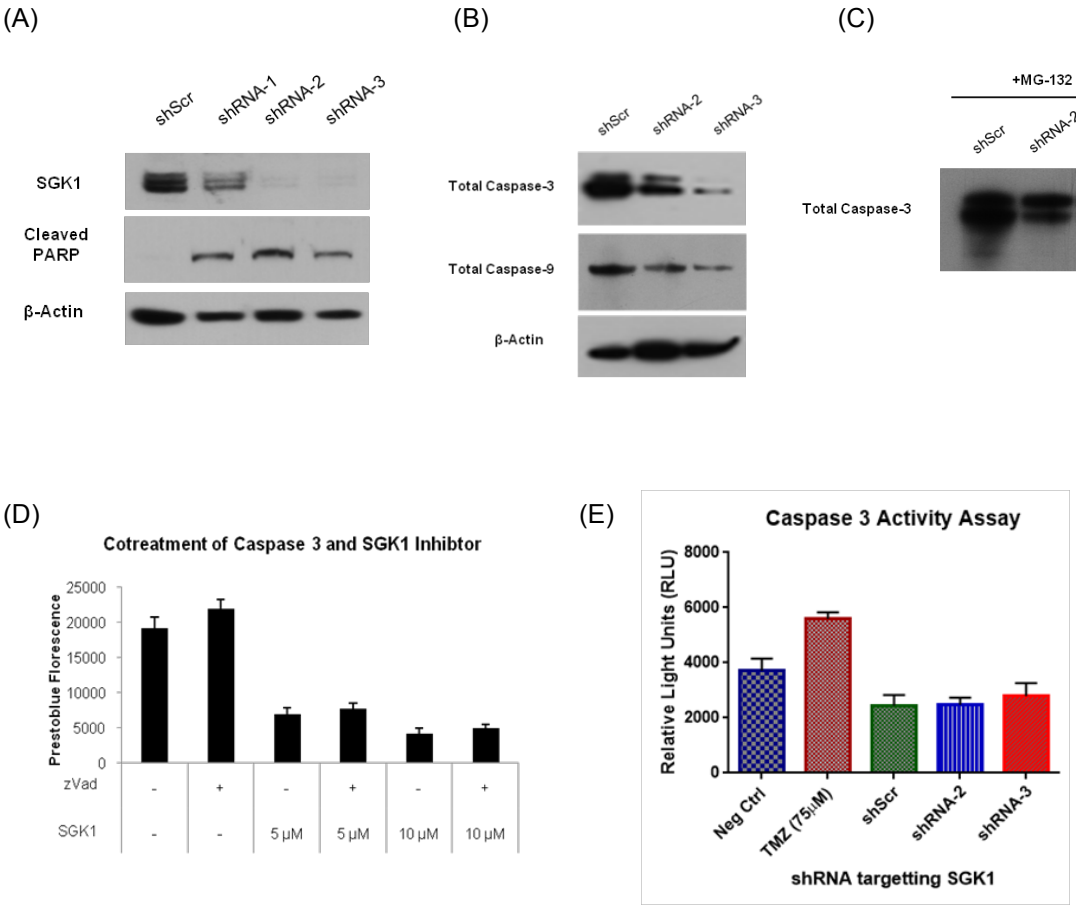

Figure 4.8: Role of Caspase -3 cascade of apoptotic cell death in SGK1 depleted GBM-SCs. (A) Western blotting to test for induction of cleaved isoform of PARP, a marker for apoptotic cell death, in SGK1 knock down GS6-22 cell line. β-actin was used as loading control. (B) Testing activation of caspase 3 and -9 by detection of cleaved form of enzyme by western blotting. β-actin was used as loading control. (C) Cells were treated with MG132 proteasome inhibitor for 24 hrs in cells with SGK1 control or knock down lentivirus. Western blotting was performed to measure abundance of cleaved caspase 3 under above conditions. (D) Relative number of viable cells was determined by prestoblue assay of GS6-22 cells co treated with SGK1 inhibitor (GSK650394) and z-Vad-Fmk, a pan caspase inhibitor. (E) Caspase -3 and -7 activity assay was performed on shSGK1 cells compared to the shScr. Neg Ctrl represents DMSO treated. Temozolomide (TMZ) treatment was used a positive control for induction of apoptosis dependent on caspase activation.

amount of decrease of total caspase-3 upon SGK1 knockdown is attenuated (Figure 4.8C). This leads us to speculate that the mechanism of cell death by SGK1 depletion may not be caspase dependent. In concordance with this data, we do not see a rescue of the cell death phenotype when we co-treat the cells with the SGK1 inhibitor and q-Vd-OPh, an irreversible pan caspase inhibitor (Figure 4.8 D) [262]. Further using an assay for caspase-3 and -7 activation, no increase in activity of these enzymes was detected upon depletion of SGK1 by shRNA (Figure 4.8E). As a control, to show that we can detect cleaved caspase-3, we added YAP inhibitor, Verteporfin and TMZ as a positive control in the q-Vd-OPh and caspase activity assays respectively. TMZ increases the caspase-3 and -7 activity as expected in the assay. Treatment with vertoporfin induced the cleavage of caspase-3 and PARP in GBM-SCs. The former shows that cleaved caspase-3 can be detected in the cell lines upon induction of apoptosis (SupplementaryFigureS4.4A). Further, the induction of PARP by Vertoporfin is decreased by treatment with caspase inhibitor q-Vd-OPh, showing that q-Vd-OPh is active in GBM-SCs (Supplementary Figure S4.4B). .

Regulation of Survival Pathways by SGK1 in GBM-SCs is Unclear

FOXO3a and NF-κB pathways are two such known signaling cascades downstream of SGK1, which may activate apoptosis upon depletion of SGK1. SGK1 specifically phosphorylates FOXO3a, a pro-apoptotic transcription factor, on residue serine 315 (S315) and sequesters it in the cytoplasm, preventing induction of apoptosis [287]. We hypothesized that depletion of SGK1 should decrease S315 phosphorylation and increase FOXO3 in cytoplasm. However, an increase in phospho S315 FOXO3a was observed in SGK1 depleted cells, indicating compensation by other cellular kinases for the loss of

SGK1 to retain FOXO3a in the cytoplasm (Figure 4.9 A). Further, we tested the transcriptional activity of FOXO3a by assaying known FOXO3a targets involved in induction of apoptosis by qPCR. No dramatic change in FOXO3a target genes was observed at 24hrs of treatment with SGK1 inhibitor. Even though a few genes do show an increase at 24hrs, that effect is lost by 48hrs (Figure 4.9 B). As SGK1 has been reported to affect the localization of FOXO3a, we tested the presence of FOXO3a in different cellular compartments by immunofluorescence staining. Although, there is a small increase in nuclear FOXO3a upon treatment with the GSK650394 inhibitor compared to DMSO control, no such increase was observed upon SGK1 shRNA addition (Figure 4.9 C). Taken together, these results indicate that FOXO3a is not likely to be the primary mechanism of cell death due to SGK1 depletion.

The NF-κB pathway is an important pro survival pathway in the cell. Downstream target genes of NF-κB include various Bcl2 family members, which are known anti apoptotic proteins[301]. SGK1 has been previously shown to phosphorylate and activate IKKβ, which in turn phosphorylates inhibitory scaffold protein IKβ. This enables release of NF-κB into the nucleus for transcription of genes important in maintenance of cellular viability. To study the effect of SGK1 on the NF-κB pathway, we assayed the subcellular localization of NF-κB as well as the gene expression of downstream targets. The subcellular localization of NF-κB remained unchanged upon SGK1 shRNA treatment compared to the scrambled control (Figure 4.10 A). NF-κB regulates the transcription of several Bcl2 family members of anti-apoptotic proteins and genes important in cellular survival. If NF-κB is sequestered out of the nucleus, there would be a change in the gene

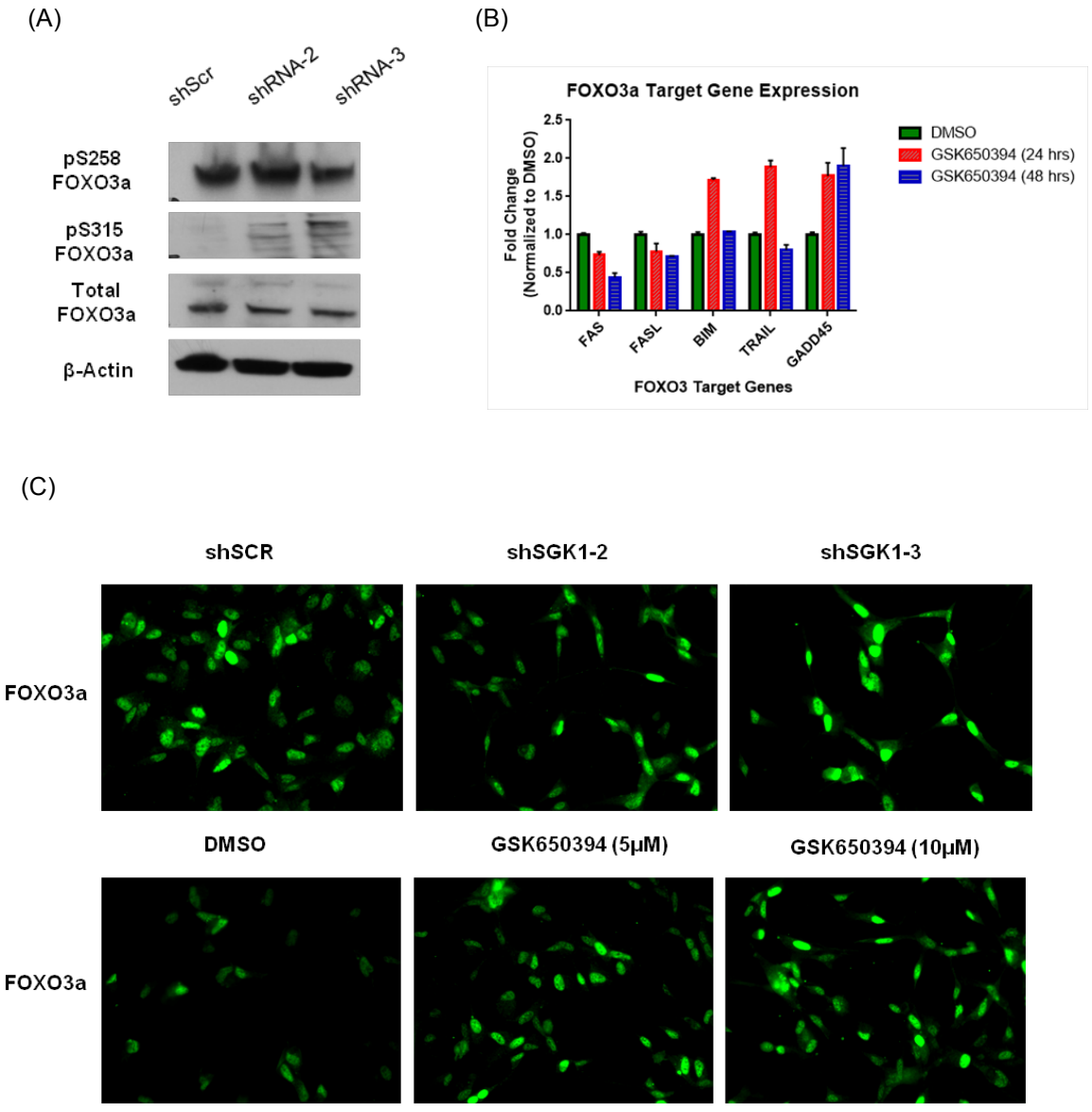

Figure 4.9: Role of FOXO3A in SGK1 inhibition induced cell death. (A) Phosphorylation sites on FOXO3a were assayed using phospho specific antibodies by western blotting. β-actin was used as loading control. (B) FOXO3a downstream target gene expression of pro-apoptotic genes was measured using qPCR. Values were normalized to the B2M control. (C) Immunofluorescence staining of FOXO3a in response to treatment with inhibitor or shRNA targeting SGK1.

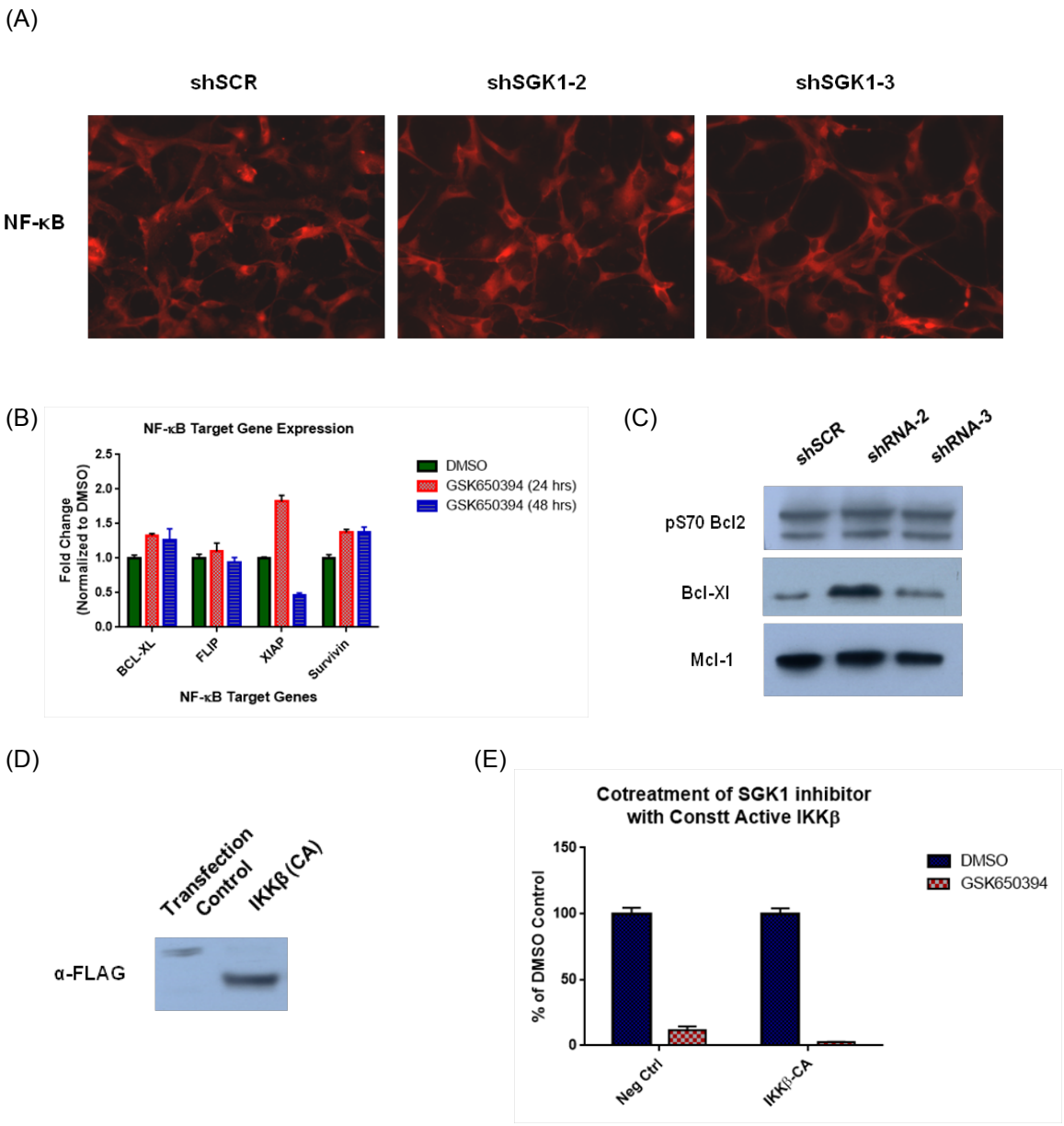

Figure 4.10: Role of NF-κB in SGK1 inhibition induced cell death. (A) Immunofluorescence staining of NF-κB to visualize subcellular localization in response to treatment with shRNA targeting SGK1. (B) NF-κB downstream anti-apoptotic target gene expression was measured using qPCR. Values were normalized to B2M control. (C) Western blotting to test expression of pro-apoptotic gene targets of NF-κB. (D) Western blotting to check for transfection efficiency of Flag-tagged constitutively active IKKβ kinase (IKKβ-CA) in GS6-22 cell line. (E) Prestoblue Viability assay to measure difference in growth in untransfected (Neg ctrl) and IKKβ-CA in response to treatment with SGK1 inhibitor (10μM). Inhibitor treated samples have been normalized to the DMSO control of that group.

expression of its targets which we measured using gene specific primers using qPCR. The expression of anti-apoptotic NF-κB target genes was not significantly reduced by treatment with the SGK1 inhibitor at 24 and 48 hrs after treatment with inhibitor (Figure 4.10 B). As SGK1has been reported to activate this pathway by activating IKKβ, constitutive activation of IKKβ should rescue the apoptotic effect upon SGK1 inhibition. To confirm this, we transfected constitutively active IKKβ (IKKβ -CA) into GBM-SCs (Figure 4.10 C). This however did not rescue the cell death phenotype observed by SGK1 inhibition (Figure 4.10 D). This shows that NF-κB pathway likely does not mediate the cell death induced by SGK1 knockdown in GS6-22 cells.

Other signaling pathways such as Wnt, p53 and JNK may be involved in the induction of cell death by SGK1 depletion. SGK1 affects the stability of β-catenin and p53 by phosphorylation of upstream negative regulators, GSK-3β and MDM2 respectively (Figure 4.11)[302, 317]. To examine this, the abundance of β-catenin and p53after knockdown of SGK1 by shRNA was determined by western blotting. There was no significant change observed in the abundance of either protein in response to SGK1 depletion (Figure 4.11 A,B). Furthermore, treatment of p53 depleted cells with SGK1 inhibitor resulted in similar sensitivity observed the un-transduced GS6-22 and MGG 8 cell lines, ruling out the involvement of p53-dependent apoptosis induction.

Another hypothesis for this phenomenon was the JNK/p38 stress pathway dependent apoptosis induction. SGK1 is regulated by various environmental stressors, and may play a key role in maintaining survival in the presence of basal levels of these factors. JNK and p38 are stress MAP kinases and have been shown to be activated during cell death SGK1 has been shown to negatively regulate JNK activity by phosphorylating upstream

kinase SEK1 [304, 305]. Co-treatment the GS6-22 cell line with either the JNK or p38 inhibitors with GSK650394, however, was unable to rescue to the phenotype observed upon treatment (Figure 4.11 C,D). Although more definitive experiments need to be performed to definitively rule out these pathways, these preliminary data suggest that these pathways may not influence the mechanism of cell death induced by SGK1 depletion and inhibition. Further investigation is required to elucidate the pathways by which SGK1 maintains survival of GBM stem cells.

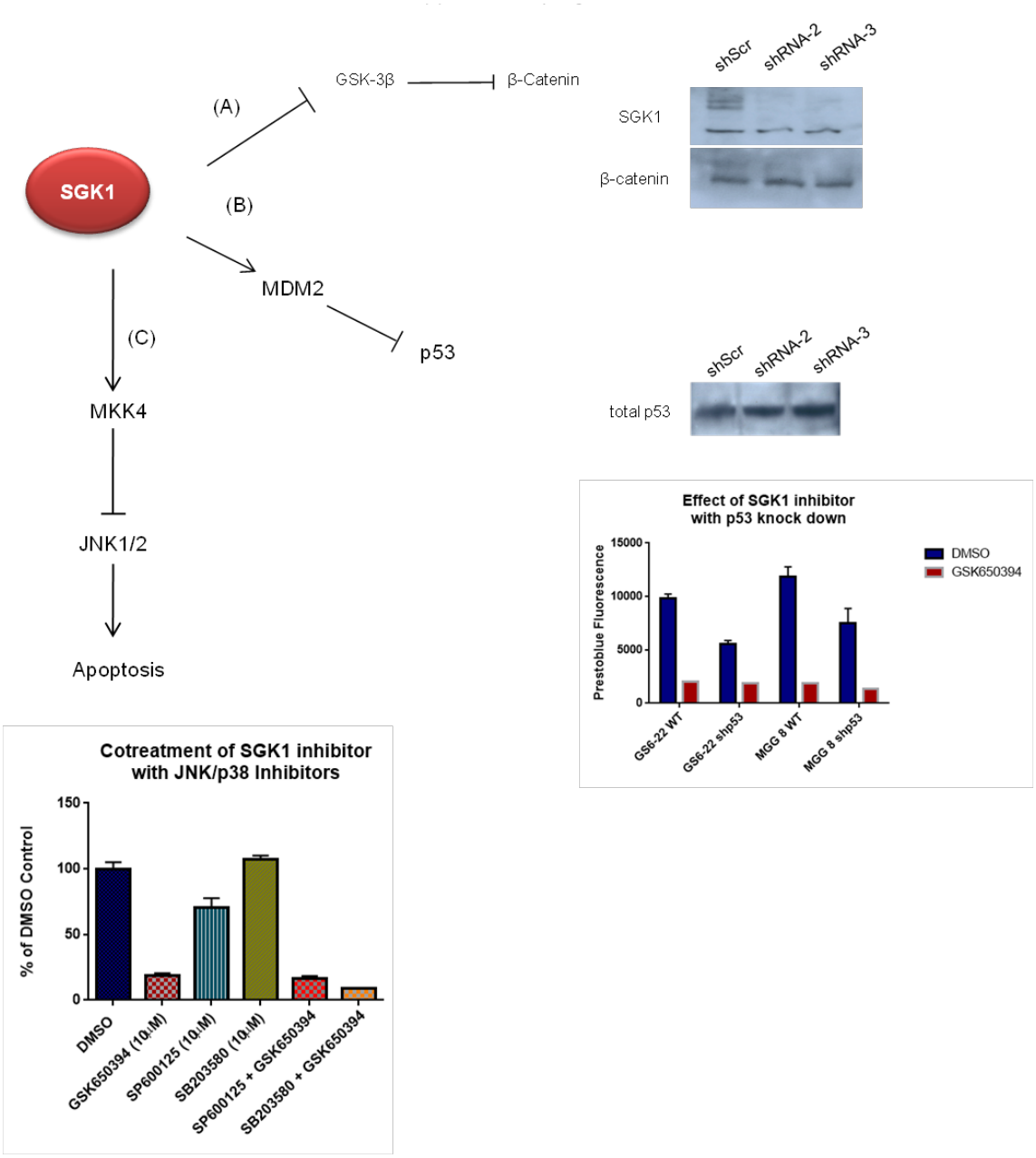

Figure 4.11: Effect of β-Catenin, p53 and JNK pathway on SGK1 inhibition induced cell death. In GS6-22 cells, (A) Abundance of β-catenin was tested in response to SGK1 knock down by shRNA using specific antibody. (B) p53 protein levels were tested by western blotting for investigating different in abundance upon SGK1 inhibitor treatment. p53 was knocked down using shRNA lentivirus and SGK1 inhibitor was added to the wild type and knock down cell lines. Viability was measured using prestoblue viability reagent. (C) Cotreatment of GSK650394 (SGK1 inhibitor) with, JNK inhibitor (SP600125) and p38 inhibitor (SB203580) was performed in GS6-22 cell lines and cell viability was measured using prestoblue viability assay.

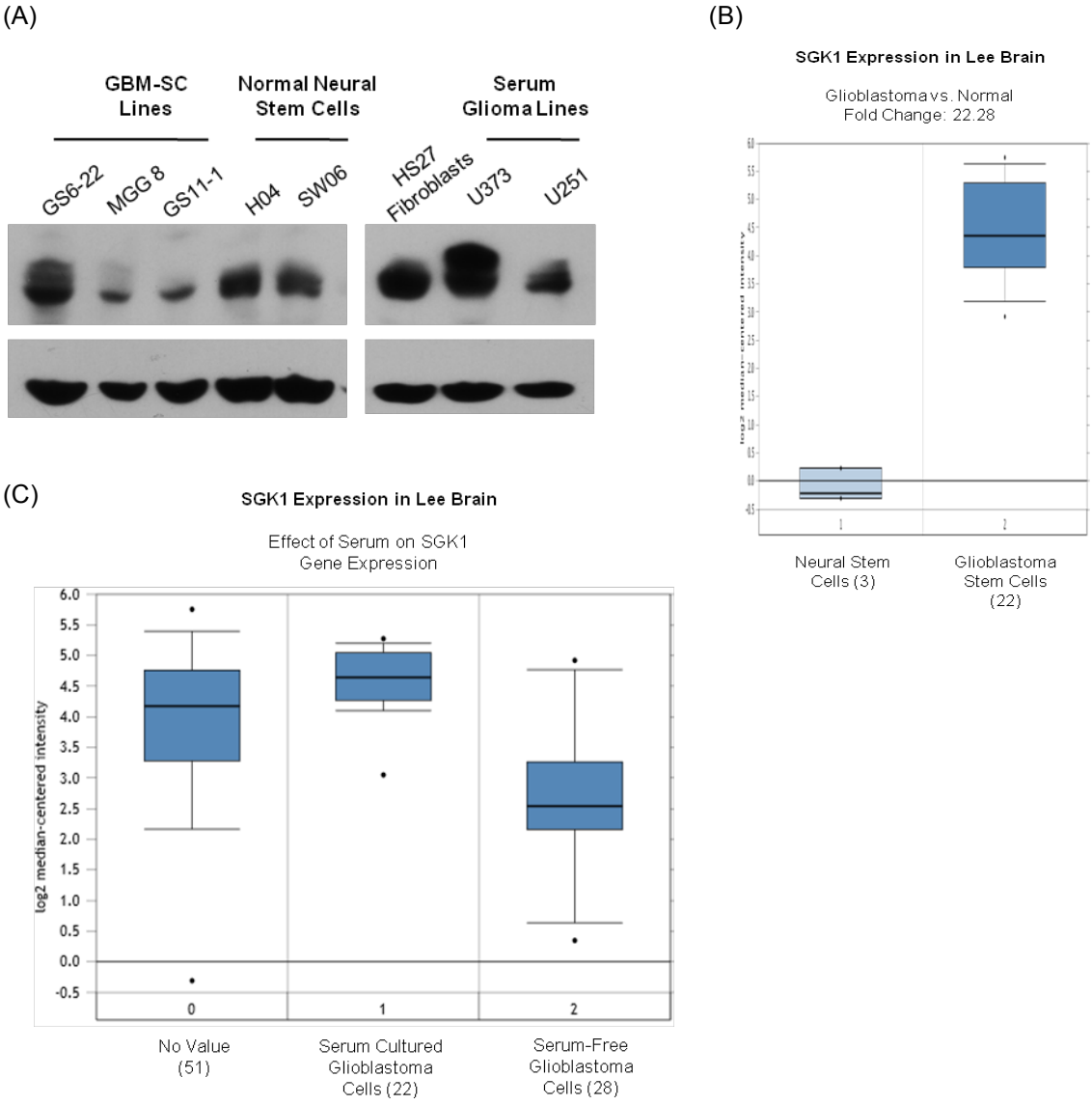

Supplementary Figure S4.1: Expression of SGK1 in various cell lines. (A) Western blot showing SGK1 abundance in the cell lines used including GBM-SCs, serum glioma line, HS27 fibroblast line and normal neural progenitor cells. (B) Data mining Lee Brain database in Oncomine to compare expression of SGK1 between normal neural stem cells and GBM stem cells. (C) Comparison of expression of SGK1 in serum-cultured and serum-free glioma lines by Oncomine using the Lee Brain database.

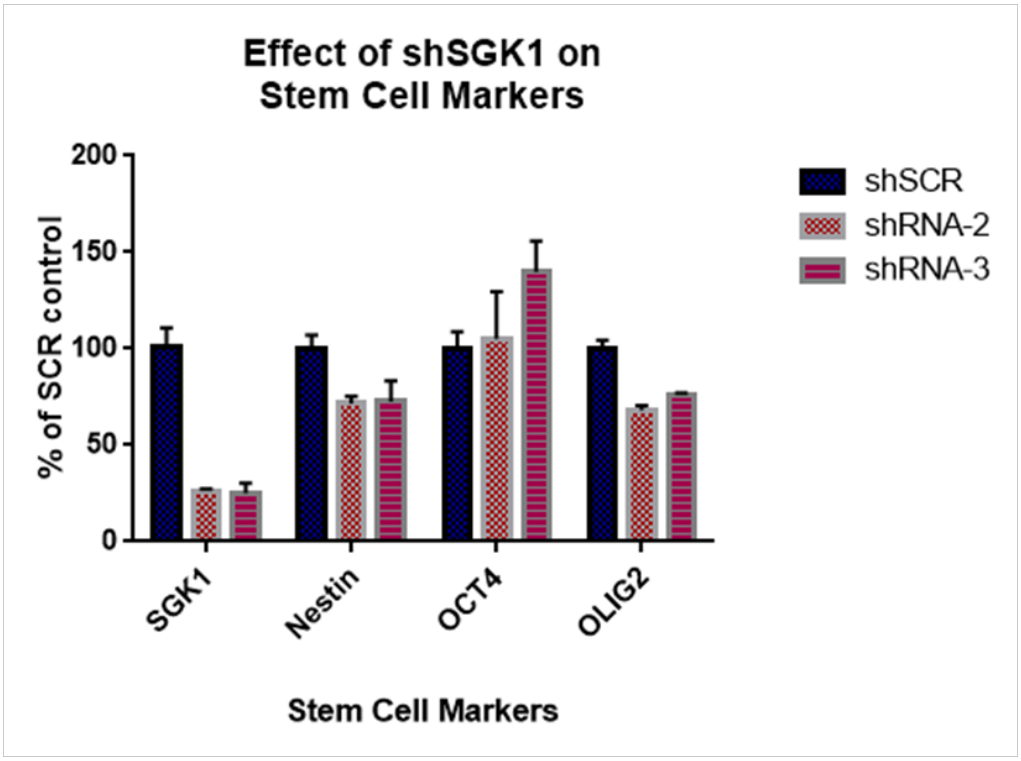

Supplementary Figure S4.2: SGK1 knockdown does not affect stem cell marker expression. GS6-22 cells were transduced with lentivirus with SGK1 shRNA or scrambled hairpin. After puromycin selection, RNA was extracted and gene expression changes were measured using qPCR.

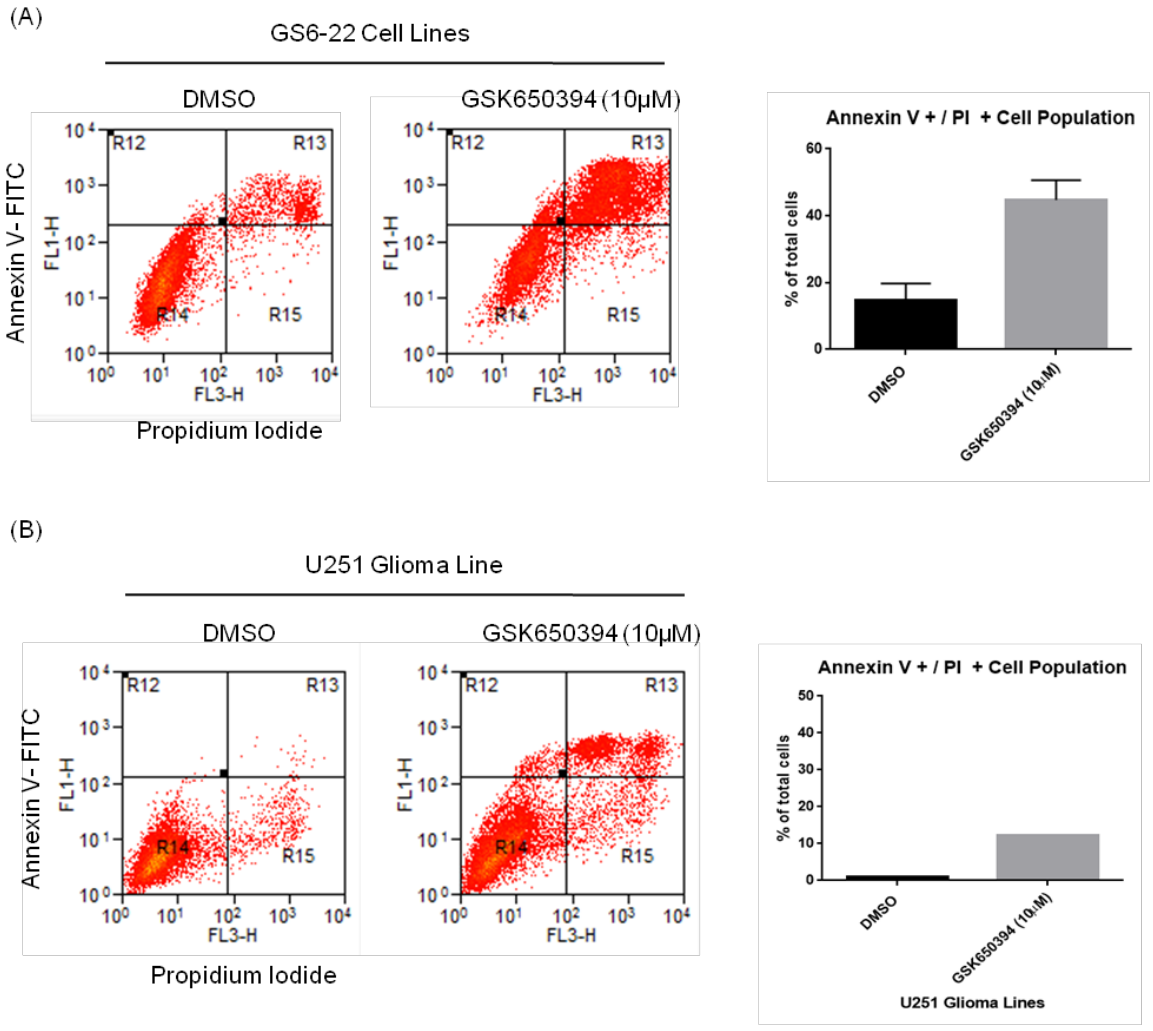

Supplementary Figure S4.3: Comparison of Annexin V/PI stained population after SGK1 inhibitor treatment. GS6-22 (A) and U251 (B) cell lines were treated with GSK650394 (10µM) or DMSO control for 4 days. Following this, cells were double stained with Annexin V-GFP and PI and amount of staining was assessed using flow cytometry. Quadrant R13, representing the double positive population of cells was quantified and graphed.

(A)

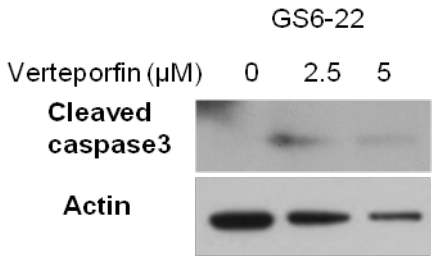

(B)

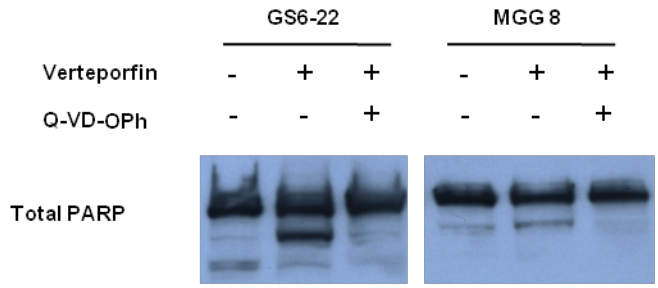

Supplementary Figure S4.4: Detection of cleaved caspase 3 and PARP after Verteporfin treatment. GS6-22 and MGG 8 lines were treated with apoptosis inducer Verteporfin and pan caspase inhibitor, q-VD-OPh for 24 hrs. Western blot to was performed to detect (A) cleaved form of Caspase 3 (B) cleaved and full-length PARP protein levels in GBM-SC treated with Vertoporfin and q-VD-OPh as indicated.

Chapter 5

Identification of molecular markers of GBM-Stem Cells

Figure Contributions:

The following people contributed to the work for Monoclonal antibody screening (Figure 1, 2A,B): Mike Boncaldo, Forrest White, Maureen Sherry-Lynes, Caitlyn Synder, Douglas Jefferson, Shelley Grubman, Willem Louis and Brent Cochran

Experiments in the Figures 5.4 and 5.5C were performed by Colleen Flanagan.

Experiments in the Figures 5.7 and 5.9 were performed by Dorjee Norbu.

Other important contributions on this work were made by Sean Koerner, Alex Neil, and Brendan Waldoch.

Introduction

The primary marker used for identification of GBM-SCs from a tumor population has been CD133 [88, 100, 102]. However, previous studies have shown that CD133 may not be the best marker due to its responsiveness to various external stimuli in both stem cells and non stem populations [174]. Further, various studies have also found that using CD133 as a marker may lead to false negatives as CD133- populations in some tumors may possess stem-like characteristics similar to CD133+ cells as well as give rise to neurospheres expressing CD133. These cells are postulated to be the true progenitor cell population [183]. Further, in the hierarchical stem cell models, there may be cells present that are in the path to terminal differentiate, but have not lost all their stem cell characteristics, such as transit amplifying cells. There is a need to identify additional markers, specific to the various types of stem-like cells represented in the tumor, which may be used in place of or in conjunction with CD133. To this end, we generated monoclonal antibodies against GBM stem cells in culture. These may have use as putative biomarkers to various stem states of the tumor cells and may possibly be used for therapeutically targeting this population.

Results

Generation and Screening of Novel Monoclonal Antibodies

To isolate markers specific for the undifferentiated state of GBM-SCs, mice were immunized with a mixture of fixed and live GS6-22 and GS7-2 cell lines, two patient derived GBM-SC cell lines. Antibody producing B-cells from these mice were then fused with immortalized tumor cells to make antibody producing and immortal hybridoma cells. Cells were separated to clone hybridoma cells producing antibodies against a single antigen. 800 monoclonal antibodies were isolated from different clones for use in the screening described below (Figure 5.1).

GBM-SC cell lines were differentiated by removal of the growth factors and addition of 2% serum to the growth medium. This differentiates the GBM-SC lines leading to decrease in stem cell marker expression and a corresponding increase in expression of differentiation markers [74]. GS6-22 GBM stem cells were seeded into 96 well laminin coated plates at 5000 cells/well and cultured for 1 week in either stem cell media or differentiation media. Cells were then fixed with 4% paraformaldehyde and stained with the monoclonal antibodies using goat anti--mouse IgG coupled to PE as a secondary antibody for visualization. Antibody concentrations and staining times were the same across samples as was the image exposure time and aperture using the imageXpress microscope. Thus, differences in signal intensity should only reflect differences in antibody binding. The antibodies that detected their respective antigen in the undifferentiated state but not after differentiation were considered a screening hit and a putative stem cell marker. 10 candidate monoclonal antibodies were identified which

(A)

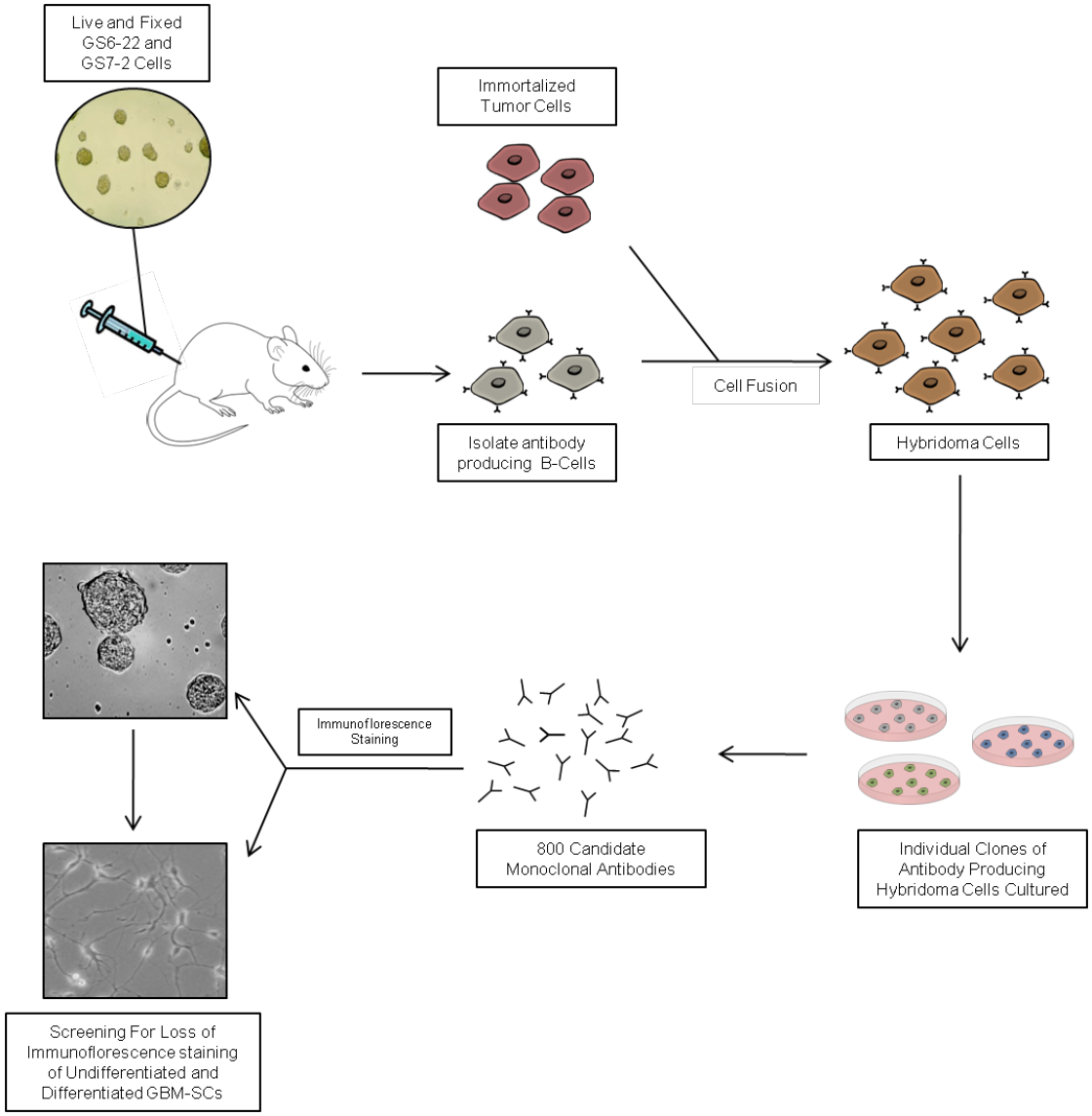

Figure 5.1: Schematic of the screening strategy. Diagram showing the steps taken to generate and isolate novel monoclonal antibodies by immunizing mice with live and fixed GS6-22 and GS7-2 cell lines and screening undifferentiated and differentiated GBM-SCs for loss of staining in the latter group.

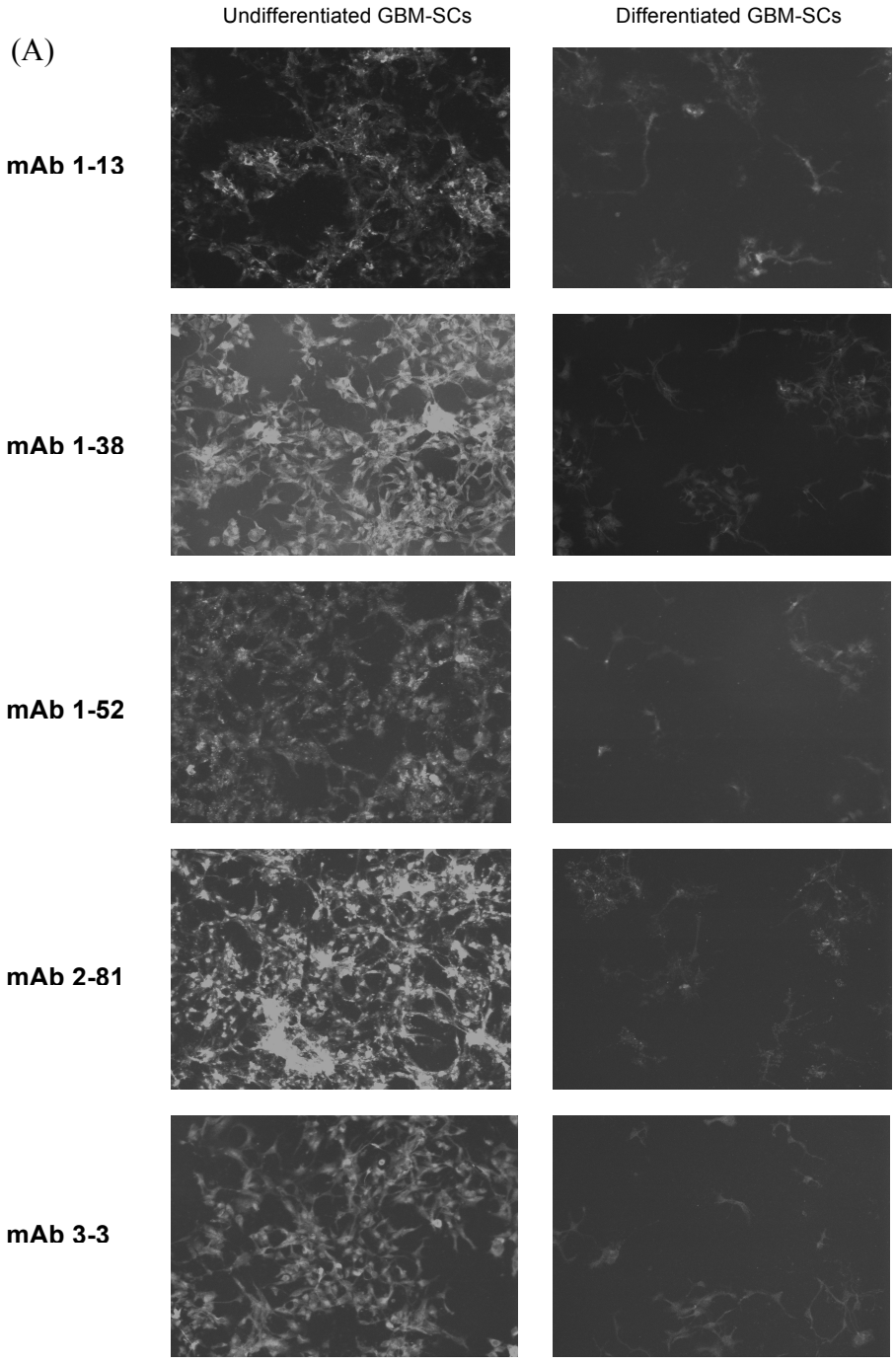

Figure 5.2A: Representative differential staining of differentiated and undifferentiated glioblastoma stem cells by monoclonal antibodies. GS6-22 GBM stem cells were grown as undifferentiated or differentiated cells on laminin. Indicated monoclonal antibodies were used to stain the cells Differences in signal intensity should only reflect differences in antibody binding. Results for mAbs 1-13, 1-38, 1-52, 2-81, 3-3 are shown.

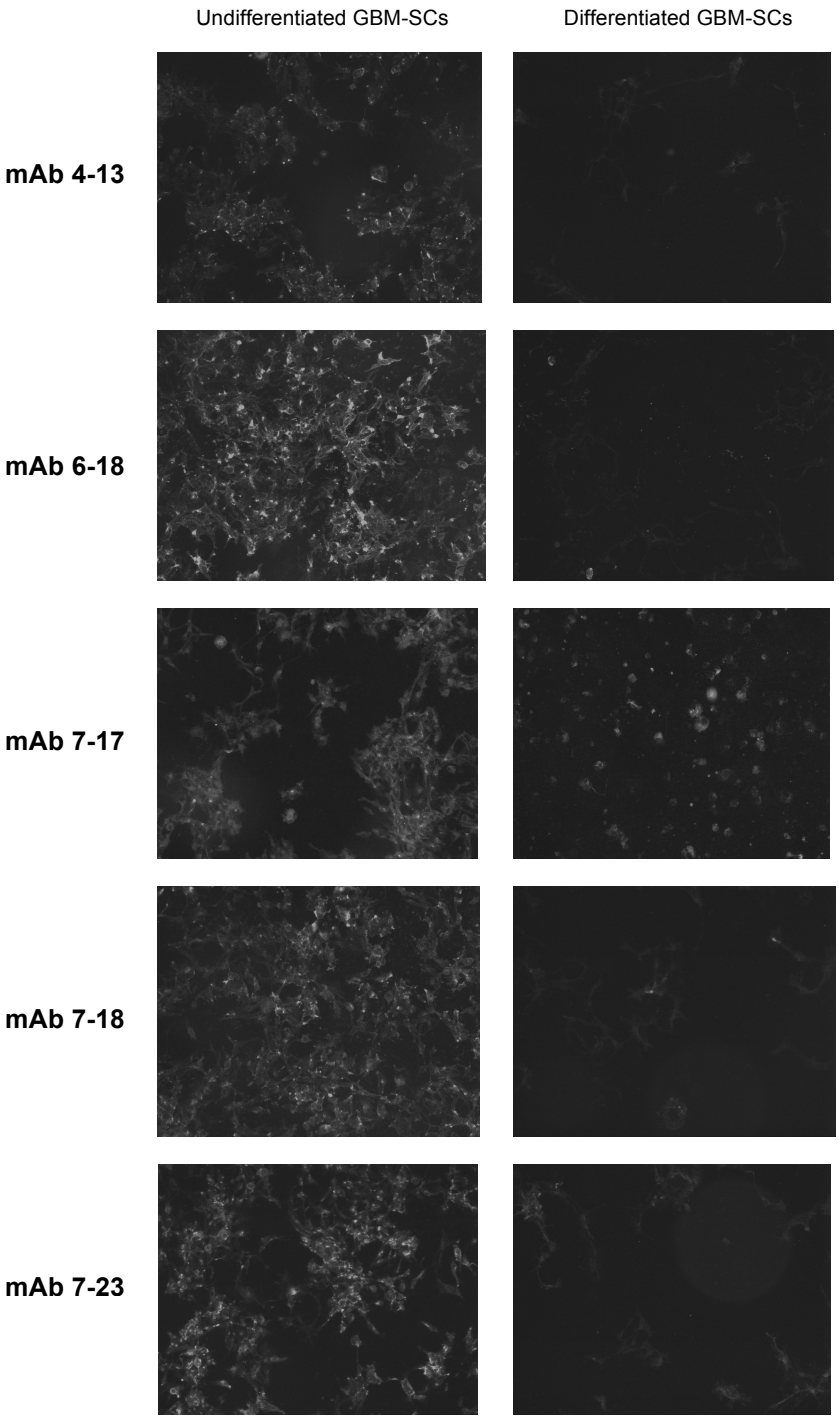

Figure 5.2B: Screening of Undifferentiated and Differentiated GBM-SCs. Same as 5.2A. Results for mAbs 4-13, 6-18, 7-17, 7-18 and 7-23 are shown.

were able to stain undifferentiated GS6-22 and GS7-2 cells, but the staining significantly decreased upon differentiation of the cell line (Figure 5.2A, B). These candidate antibodies were selected for further characterization.

Monoclonal Antibodies are Specific to Stem Cell Populations

To confirm that the antibodies were able to detect the denatured antigen, extracts of undifferentiated and differentiated GBM stem cells were assayed by western blotting. Using this method, we were also able to confirm the stem cell specificity of staining for these antibodies observed during the screen. 5 out of the 10 candidates were able to detect their respective antigens by western blotting. These 5 antibodies detected antigens of at least 4 different molecular weights and were specific to undifferentiated GS6-22 and GS7-2 stem cell lines from both the GS6-22 and GS7-2 cell lines, but not in differentiated cells from the same cell line (Figure 5.3). This indicates that at least 4 different antigens are recognized by these 5 antibodies. mAbs 1-38 and 7-17 recognize proteins of 56 KDa that could be identical, but mAb 7-17 also recognizes a second smaller protein that may or may not be a derivative of the larger 56 KDa protein. The β-actin loading control for the GS6-22 differentiated sample was low, but there was no antigen detected in this lysate. Although the pattern of staining was similar to GS7-2 cell lines, western blotting with a more even loading is required to conclusively exclude the presence of the antigen in the differentiated GS6-22 lysates. However, the immunofluorescent staining would indicate the antigen is indeed down-regulated upon differentiation. This indicates that the expression of these antigens is specific to the undifferentiated state of the GBM-SCs and is independent of the secondary structure of the antigen.

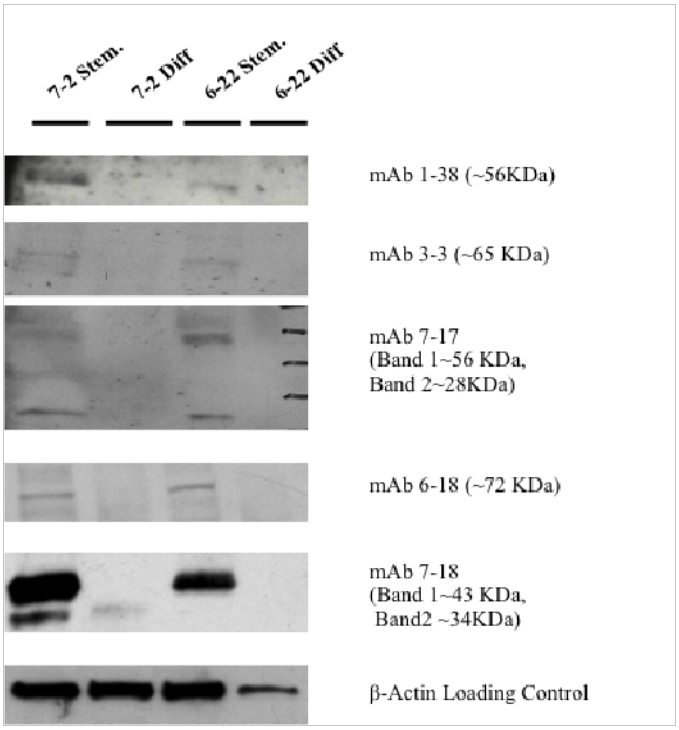

Figure 5.3: Expression of antigens in GS6-22 and GS7-2 before and after differentiation. (A) Western blotting was performed using the monoclonal antibodies as the primary antibody on undifferentiated and differentiated GS6-22 and GS7-2 protein lysates. β-actin was used as a loading control.

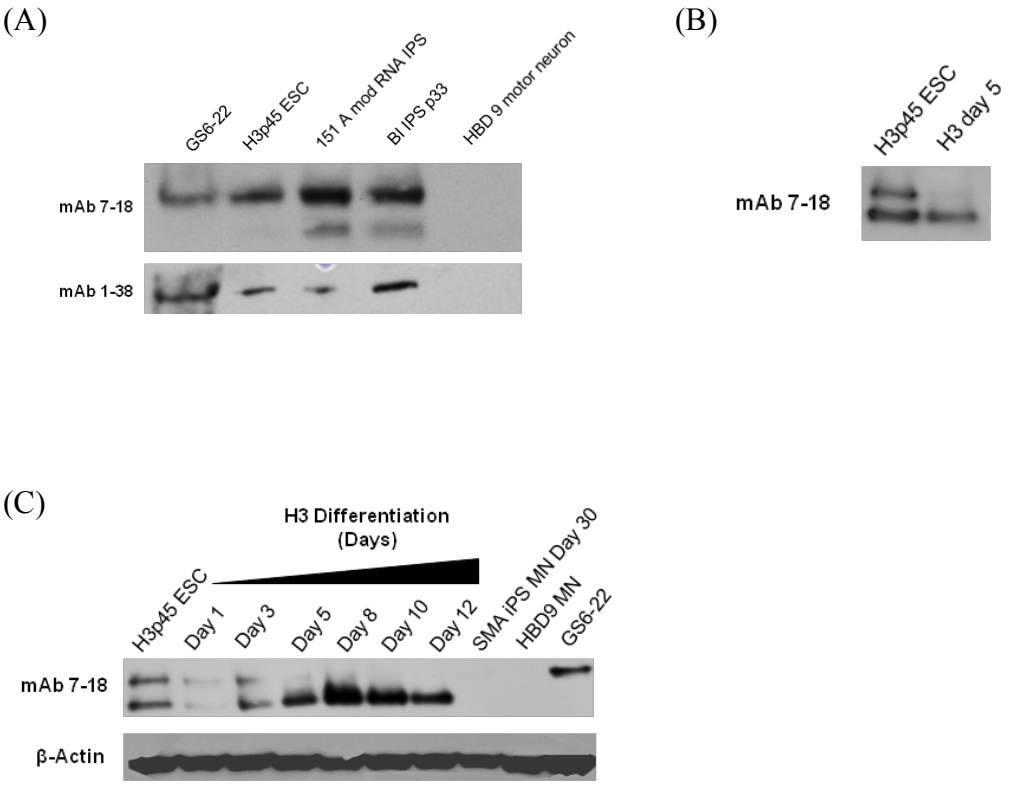

Figure 5.4: Expression of mAb 1-38 and 7-18 antigens in embryonic stem cells:(A) Western blot showing the presence of antigen for mAb 7-18 and 1-38 in GS6-22, H3 embryonic stem cell lines as well as in two iPS lines: 151 A mod RNA iPS and BI iPS cells. Fully differentiated HBD9 or motor neuron line showed no staining. (B) Western blot for mAb 7-18 antigen in H3 embryonic cells and partially differentiated H3 cells. (C) Western blotting showing mAb 7-18 antigen expression over a time course of H3 differentiation with SMA iPS motor neurons and HBD9 motor neurons as terminally differentiated lysates. GS6-22 lysate was used a positive control and β-Actin was used as loading control.

As these antigens are specific to the stem cell population, we investigated their presence in embryonic and induced pluripotent stem cell lines. H3 embryonic stem cells, 151 A mod induced Pluripotent Stem (iPS) cells and BI IPS stem cells were tested for the presence of the antigens detected by the monoclonal antibodies. A differentiated motor neuron produced from HBD 9 ES cell lines, was also assayed for the same. Interestingly, mAb 7-18 and mAb 1-38 antibodies detected the presence of their antigen in all the undifferentiated cell lines, but were not able to detect it in the differentiated HBD 9 motor neuron lysate (Figure 5.4A). Differentiated H3 cells showed similar results when immunoblotted by mAb7-18 (Figure 5.4B). To determine the point at which the antigen is lost during differentiation, we procured lysates of H3 embryonic cells at different time points during differentiation. The abundance of the antigen for mAb7-18 decreases over the course of differentiation, with the staining completely lost upon complete differentiation. SMA iPS cells that were completely differentiated to motor neurons also show no expression of antigen for mAb 7-18 (Figure 5.4C). Two bands are observed in the lysates, which may indicate the presence of posttranslational modification, or alternate splice variants of the antigen detected by mAb 7-18. The upper band is the first to decrease in abundance as early as Day 1 and 3, suggesting that this isoform may have a special function in the stem cell state.

Candidate Antibodies Do Stain Other Cancer Cell Types

To determine if the antigens are specific to GBM-SCs, we assayed various cancer and normal non stem cell lines, which are grown in serum containing medium by western blotting and immunofluorescence. Although, mAb1-38 did not stain any of the tested cell lines by western blotting, presence of the antigens was detected in HS27, MCF7 and

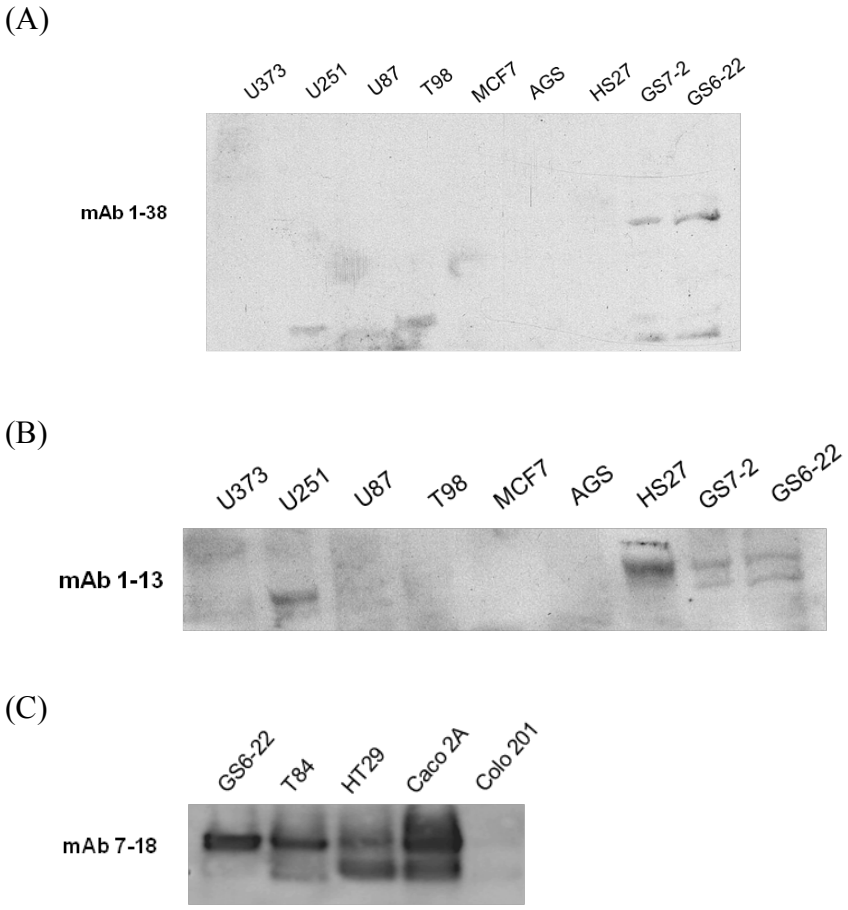

Figure 5.5: Expression of antigens for mAbs in serum cell lines. Western blot with staining for antigen of mAb 1-38 (A) and mAb 1-13 (B) in various glioma (U373, U251, U87, T98), breast cancer (MCF7), gastric cancer (AGS) and fibroblast (HS27) cell lines. GS7-2 and GS6-22 lysates were used as positive controls. (C) Expression of antigen in various recognized by mAb7-18 in colorectal cancer lines (T84, HT29, CaCo2A, Colo201) was tested using western blot by mAb7-18 antibody.

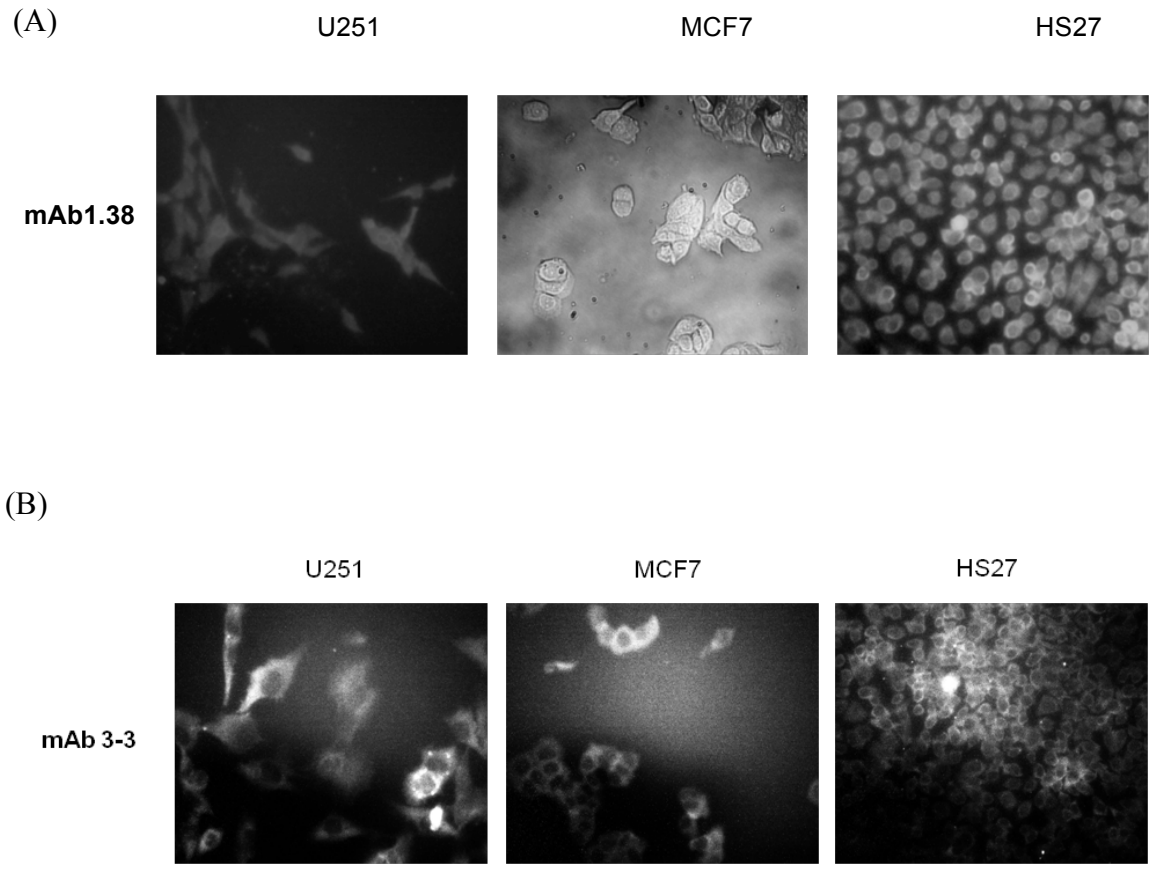

Figure 5.6 A-B: Immunofluorescence staining of serum cell lines. Various serum lines were stained using mAbs by immunofluorescence and imaged using a Zeiss Microscope. The antigen for mAb 1-38 (A) and mAb 3-3 (B) was expressed in various serum lines.

U251 cell lines by immunofluorescence (Figure 5.5A, Figure 5.6A). mAb1-13 staining by western blotting was detected in U251 glioma cells as well as in HS27 fibroblast cell lines (Figure 5.5B) and mAb 3-3 was able to stain U251, MCF7 and Hs27 cell lines by immunofluorescence (Figure 5.6B). The other monoclonals were not able to detect the antigens in these cell lines by immunofluorescence. Four colorectal cancer cell lines were also stained by western blotting with mAb 7-18. 3 out of 4 tested colorectal cell lines were positive for the presence of the antigen of mAb 7-18 (Figure 5.5C). Taken together, these results show that although these antibodies do show some specificity to undifferentiated stem cells, but the antigens are not exclusively expressed in stem cell populations and may have a functional role in other more differentiated cells.

Identification of Antigen for mAb 7-18

In order to assess the utility of the antibodies as a cell surface marker or therapeutic, it is necessary to identify the antigens recognized by the antibodies. mAb 7-18 was chosen for initial characterization due to its ability to detect its antigen by western blotting in various undifferentiated stem cell lysates. Furthermore, the antigen for mAb 7-18 is expressed at a level higher than observed with the other candidate antibodies which should help with purification and identification.. Our goal was to affinity purify the antigen with the cognate monoclonal antibody and then identify the antigen by mass spectrometry.

First, we confirmed that mAb 7-18 antibody was binding a protein antigen. Antibodies often detect post translational modifications (like glycosylation) due to their contribution to the protein's structure. We inhibited the addition of N-like glycosylation by addition of tunicamycin to GS6-22 cells prior to collection of cellular lysates, Although one of the

bands did decrease upon addition of tunicamycin, the smaller antigen was detected by mAb 7-18 indicating that the antigen bound is likely a protein (Supplementary Figure S5.1).

Lysates from GS6-22 cells were used to immunoprecipitate the antigen for mAb 7-18. Antibody was conjugated to protein A/G composite beads. As the band detected by mAb7-18 in western blots is close to ~50KDa in size, the conjugated antibody was crosslinked to the beads using Disuccinimidylsuberate (DSS). This prevents the antibody from being eluted with the antigen and reduces the amount of antibody is detected during staining of the eluted protein. The heavy chain of the antibody is 55kDa in size and would contaminate the eluted antigen band after staining the proteins on the gel. The antigen was successfully immunoprecipitated by the beads and was detected by western blotting with mAb 7-18 (Supplementary Figure S5.2A). However, the amount of antigen isolated was not enough for detection by SYPRO Ruby staining, which was required for detection of the protein by mass spectrometry (Supplementary Figure 5.2B). This was likely due to small amount of starting material obtained from GBM-SC lysates.

To scale up the amount of antigen, we used the colorectal cancer cell lines, T84 and CaCo2A, as starting material for the purification as they also express the antigen of interest and can be grown more easily in larger quantities than the GBM stem cells. A large scale immunoaffinity column was setup and cell lysate was passed through the column by gravitational flow. Elution was performed in high salt conditions (4M Magnesium sulfate) and eluate fractions were collected sequentially. The presence of antigen in the eluate was detected using western blotting as well as by SYPRO Ruby staining. We were able to successfully isolate and detect the antigen for mAb 7-18 using

both methods, with eluate 3 possessing the highest amount of antigen (Figure 5.7A,B). The resultant band was cut from the gel and sent for mass spectrometry analysis.

Various candidate peptides were identified by mass spec analysis (Figure 5.8A). In order to identify the antigen for mAb 7-18, we applied the known selection criteria based on previous experimental data. The antigen for mAb7-18 is detected at ~50 KDa on a western blot and is present on the cell surface (see below). As the protein is broken down into smaller peptides for mass spectrometry analysis, a single protein will be divided into many smaller peptide chains. Detection of only one or two unique peptide sequences for a given protein increases its probability of being a false positive. For this reason, multiple unique peptides must be detected for the protein by mass spectrometry for positive identification of the protein. By investigating the top hits from the results, only the Coxsackie virus and Adenovirus Receptor (CXADR) protein matched these criteria. Further, to ensure that this protein was a potential candidate antigen and not a common contaminant in mass spec analyses, we used the Crapome database to probe the top 20 candidate genes [318]. The crapome database catalogs the various contaminants commonly detected by mass spectrometry, which can obscure the data that it generates. Mass spectrometry is sensitive enough to detect the presence of small amount of contaminants, and this proves to be a drawback during the data analysis. By cataloging the contaminants, the Crapome database helps in the separation of true hits from false positives [318]. CXADR is not a common contaminant and was found in only 2/411 experiments in the database (Figure 5.8B). All these data together suggested that CXADR was a strong candidate for the mAb 7-18 antigen.

(A) (B)

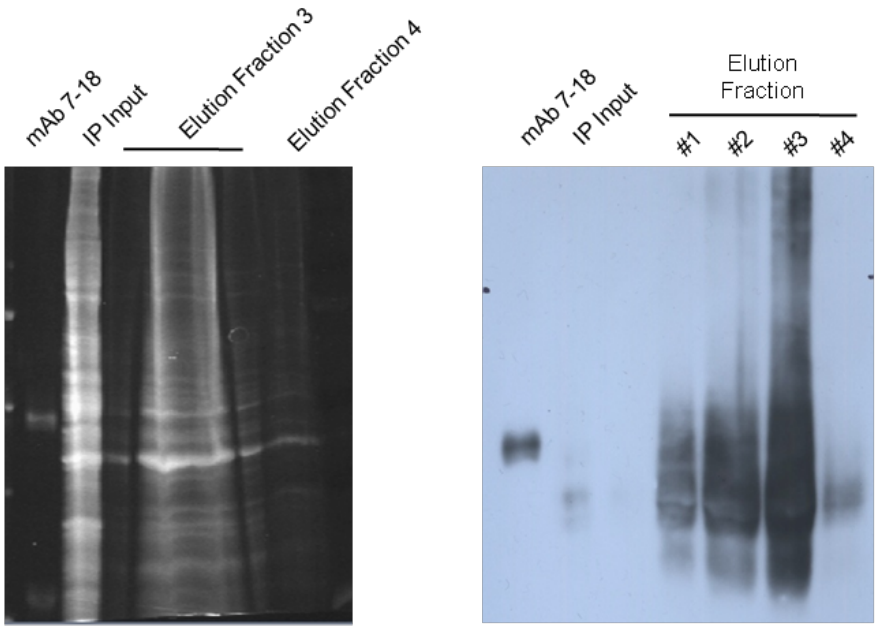

Figure 5.7: Large-scale immunoaffinity purification of mAb 7-18 antigen.mAb- 7-18 was bound to a G-bead column and crosslinked using DSS. T84 and Caco2A lysate was bound to the column and following elution, sequential fractions of the eluate were collected. (A) SYPRO Ruby gel staining of proteins found in fraction 3 and 4 of eluate. Input lysate and mAb 7-18 only were used as a positive control for gel staining and for correct analysis of eluate band size respectively. Heavy chain of denatured mAb 7-18 runs at ~55 KDa. (B) Western blotting of elution fractions 1-4. IP input and mAb 7-18 only were used as controls for staining antigen and antibody respectively to analyze correct size of antigen in eluate lanes.

(A)

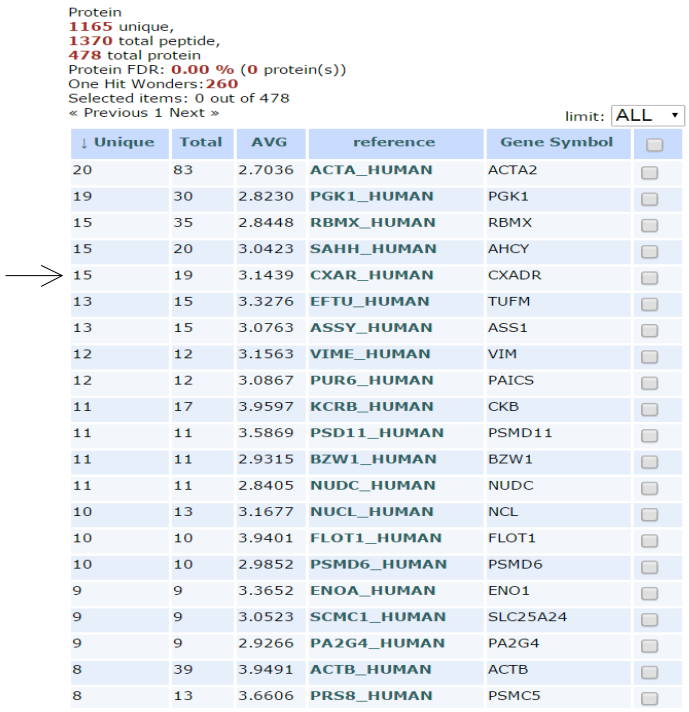

Protein
1165 unique,
1370 total peptide,
478 total protein
Protein FDR: 0.00 % (0 protein(s))
One Hit Wonders:260
Selected items: 0 out of 478
« Previous 1 Next »
limit: ALL

↓ Unique	Total	AVG	reference	Gene Symbol
20	83	2.7036	ACTA_HUMAN	ACTA2
19	30	2.8230	PGK1_HUMAN	PGK1
15	35	2.8448	RBMX_HUMAN	RBMX
15	20	3.0423	SAHH_HUMAN	AHCY
15	19	3.1439	CXAR_HUMAN	CXADR
13	15	3.3276	EFTU_HUMAN	TUFM
13	15	3.0763	ASSY_HUMAN	ASS1
12	12	3.1563	VIME_HUMAN	VIM
12	12	3.0867	PUR6_HUMAN	PAICS
11	17	3.9597	KCRB_HUMAN	CKB
11	11	3.5869	PSD11_HUMAN	PSMD11
11	11	2.9315	BZW1_HUMAN	BZW1
11	11	2.8405	NUDC_HUMAN	NUDC
10	13	3.1677	NUCL_HUMAN	NCL
10	10	3.9401	FLOT1_HUMAN	FLOT1
10	10	2.9852	PSMD6_HUMAN	PSMD6
9	9	3.3652	ENOA_HUMAN	ENO1
9	9	3.0523	SCMC1_HUMAN	SLC25A24
9	9	2.9266	PA2G4_HUMAN	PA2G4
8	39	3.9491	ACTB_HUMAN	ACTB
8	13	3.6606	PRS8_HUMAN	PSMC5

(B)

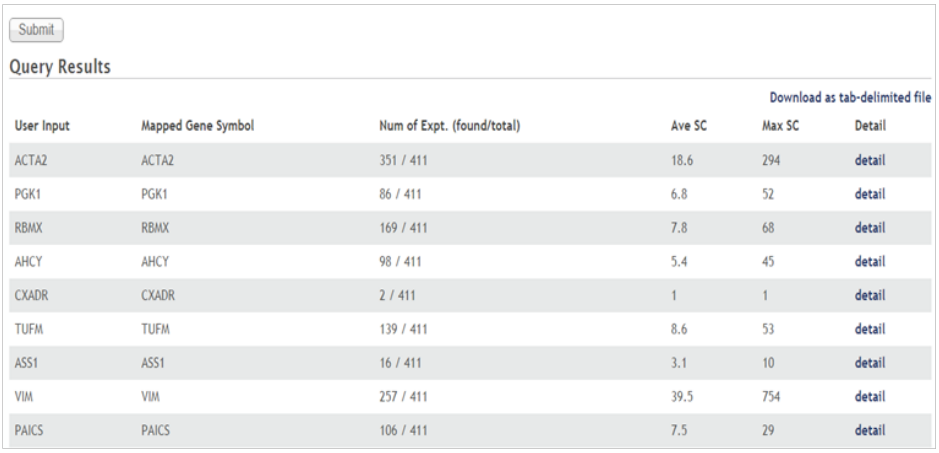

Submit

Query Results

Download as tab-delimited file

User Input	Mapped Gene Symbol	Num of Expt. (found/total)	Ave SC	Max SC	Detail
ACTA2	ACTA2	351 / 411	18.6	294	detail
PGK1	PGK1	86 / 411	6.8	52	detail
RBMX	RBMX	169 / 411	7.8	68	detail
AHCY	AHCY	98 / 411	5.4	45	detail
CXADR	CXADR	2 / 411	1	1	detail
TUFM	TUFM	139 / 411	8.6	53	detail
ASS1	ASS1	16 / 411	3.1	10	detail
VIM	VIM	257 / 411	39.5	754	detail
PAICS	PAICS	106 / 411	7.5	29	detail

Figure 5.8: Data Analysis of Mass Spectrometry Results. (A) Putative candidate antigen was chosen by high number of unique hits, presence on plasma membrane and approximate size of ~50KDa. (B) The top 20 hits were input into Crapome database to analyze frequency of hits of each protein found in other unrelated mass spec analyses. Column 3 represent number of times the candidate protein occurs in different mass spec results. CXADR is only identified in 2 out of 411 studies, indicating that it's not a common mass spectrometry contaminant.

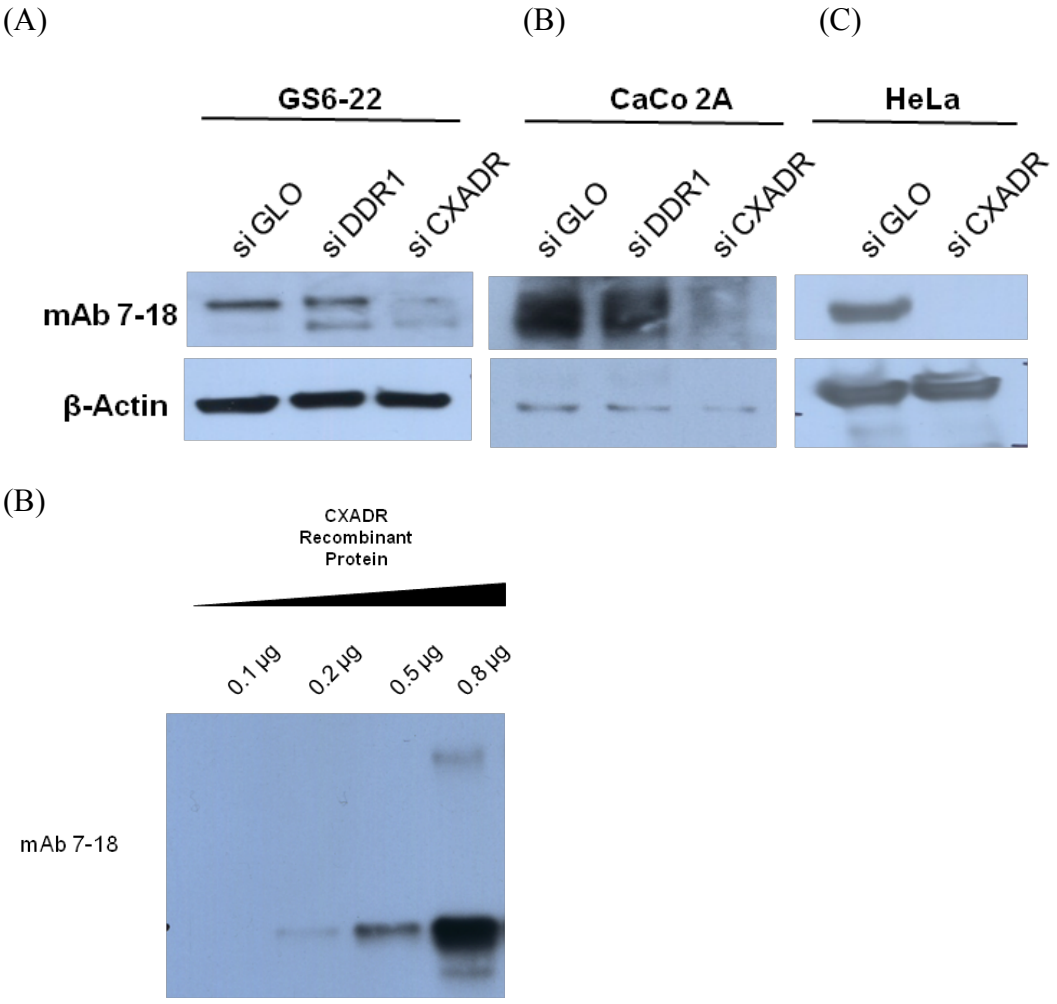

Figure 5.9: Validation of CXADR as putative antigen of mAb 7-18. (A) CXADR protein was knocked down using siRNA targeting CXADR mRNA and expression of mAb 7-18 antigen was tested. siDDR1 was used as a positive control for transfection and knockdown. (B) Recombinant CXADR protein was commercially acquired and was run of SDS-PAGE gel followed by western with mAb 7-18. Detection of CXADR by mAb 7-18 confirm the antigen identity of mAB7-18 as CXADR.

To further test this, CXADR was knocked down using siRNA in the GBM-SC line GS6-22, and other cancer cell lines such as Caco2A and HeLa. The protein was detected using mAb 7-18 antibody. If CXADR is the antigen for this antibody, its expression should be reduced by the siRNA. Indeed, mAb7-18 was able to detect a decrease in expression of CXADR protein in the lysates of siRNA transfected cells (Figure 3.9A). Death Domain Receptor 1 (DDR1) was used a positive control for testing transfection efficiency of siRNA, as it has been used by others in the lab to efficiently knock down DDR1 protein. Further, a commercially available recombinant CXADR protein was run on a SDS PAGE gel and mAb 7-18 was used to detect its presence by western blotting. mAb7-18 successfully detected the recombinant CXADR protein by western and the staining increased with the concentration of the protein loaded(Figure 5.9B). A minimum of 200ng of CXADR was required for detection by mAb 7-18. Taken together, these data show that the antigen for mAb 7-18 is CXADR. The potential role of CXADR in cellular viability of GBM-SCs was tested using the siRNA pool targeting CXADR mRNA. No effect on cellular growth was observed upon knockdown of siRNA in GS6-22 and MGG 8 cell lines (Supplementary Figure S5.3). However, the role of CXADR in invasion and other cellular processes of GBM-SCs is unknown. The identification of the target antigens for the other monoclonal antibodies is currently under investigation.

Using Candidate Monoclonal Antibodies as Therapeutics

Antibodies have successfully been used as therapeutics against various cancers[319–321]. Bevacizumab, an anti-VEGF antibody, has shown promise by increasing progression free survival in GBM patients, individually as well as in conjunction with TMZ [12, 13].

Monoclonal antibodies against immune system checkpoint inhibitors are currently used in cancer therapy to boost the body's immune response to the tumor [322]. Identification of novel targets which may be targeted by the candidate monoclonal antibodies may lead to the development of new therapeutics for GBMs.

Candidate Monoclonal Antibodies Bind to Cell Surface Antigens

The ability of the candidate antibodies to be used as a therapeutic may depend on its ability to detect and bind its antigen in a tumor mass. This would require the epitope to be present on the outer surface of the cell membrane which may be bound by the antibody. More importantly, the antigens should be present not only in patient derived cell lines, but also should be expressed in the tumor.

To determine whether the monoclonals bind to the antigens on the cell surface, we performed live cell staining on three GBM-SC lines; GS6-22, GS7-2 and GS11-1. All ten candidate antibodies detect their antigens on the cell surface to different extents on each cell line (Figure5.10). 5 out of 10 antibodies detect cell surface antigens on GS6-22 cells, whereas all the monoclonals detect their antigens on the surface of GS7-2 and GS11-1 cell lines (Supplementary Figure S5.4 and S5.5). This points to the heterogeneity that is observed between GBM patients and in stem cell lines derived from their tumors. We tested the ability of these monoclonal antibodies to function directly as inhibitory antibodies against the GBM-SC lines. This could entail functional blocking of a receptor or other antigen target by the monoclonal leading to reduction in cellular growth or viability. GBM-SCs were treated with 10ug/ml antibody in stem cell culture conditions and growth and viability was measured using prestoblue viability assay. We did not

observe any decrease in cell proliferation and survival upon treatment of GBM-SCs with the naked antibody in any of the 10 candidate monoclonals (Supplementary Figure S5.6).

Internalization of Antigen Bound Monoclonal Antibodies

Antibodies may be conjugated with drugs which may be too toxic for treatment by themselves. An antibody specific to cancer cells would ensure targeted delivery of the toxin and death in cancer cells specifically. In order for drug-conjugated monoclonals to function, they usually need to be endocytosed by the cells, which occurs when the antibodies are bound to their respective targets. To determine if the antibodies are potential candidates for this approach, we used GS6-22 and GS7-2 cell lines to determine whether the antibody bound to the antigens is internalized by the cells. To assay this, we allowed the antibodies to bind the cells. Following binding, the cells were either incubated at 4°C as a control to block internalization or at 37°C for 2 hrs to allow for internalization.. Bound antibodies would be internalized if the cell endocytoses the antigen. This process would be significantly slower at 4°C, but would proceed at 37°C. The secondary antibody is then applied to both at the end of the incubation and the percentage of cells stained by the antibody is determined by flow cytometry. Interestingly, all the antibodies tested in GS6-22 (5 out of 5) were internalized by the cells as observed by the loss of staining after incubation at 37°C (Figure 5.11 A,B). In contrast, only 1 out of 5 antibodies showed this decrease in GS7-2 cells (Figure 5.11 C). This is likely due to different in times taken by each cell to internalize the antigens from the cell surface. Taken together, these results indicate that these antibodies may be used to make drug-conjugated monoclonals, although further experiments are required to test the efficacy of this approach for each antibody.

	% Live cells stained (FACS)		
	GS6-22	GS7-2	GS11-1
1-13	2	20	14
1-38	0	17	10
1-52	95	31	6
2-81	0	10	ND
3-3	0	15	8
4-13	0	16	14
6-18	5	24	41
7-17	88	86	16
7-18	88	94	11
7-23	0	8	5

Figure 5.10: Summary of Antigens on Cell Surface of GBM-SCs. LiveGS6-22, GS7-2 and GS11-1 were stained using primary candidate monoclonals and fluorescent secondary antibodies. Cells positive for immunofluorescence were detected using flow cytometry and percent of positive cells in population was determined. (A) Table with the percentages of cells showing cell surface presence of the respective antigens.

mAbs Detect Antigens in Human Tumor Tissue Sections

The expression of the antigens in the primary tumor is important for the monoclonals to be considered for either markers or as therapeutic candidates. Using immunohistochemical staining, we tested the expression of candidate antibodies in human GBM tumor sections. 7 out of the 10 antibodies detected their respective antigens in the GBM tumors, with mAb 6-18 staining 4 out of 5 patient tumors tested (Figure 5.12). Out of the antibodies that stained human GBMs, 5 mAbs were used to stain 70 GBM tissue sections on a tissue array. All the 5 tested mAbs were able to detect their antigen albeit at different quantities and intensities on the array (Figure 5.12). A composite of the staining observed with different antibodies on individual human GBM tumors and tissue arrays is shown below (Figure 5.13A, B and C). The antibodies also showed different patterns of staining. mAb 1-13 stained a subpopulation of cells, which were present around the blood vessels in some tumors. This antibody may stain an antigen which may be enriched in GBM-SC derived endothelial cells (Figure 5.13 A). mAb 4-13 also stained a subpopulation of cells, rather than the entire tumor, which may represent the more undifferentiated cells in the tumor population (Figure 5.13A). The pattern of staining for mAb 1-38 was more diverse, with only subpopulations stained in some tumor, and whole tumor sections stained in other (figure 5.13 B). A similar pattern was observed with mAb 6-18, which strongly stained many sections and tissue punches from the array (Figure 5.13 C). These results indicate that at least some these antigens may detect a subpopulation of cells which may be more undifferentiated in phenotype consistent with the cancer stem cell hypothesis. The extent of staining may be determined

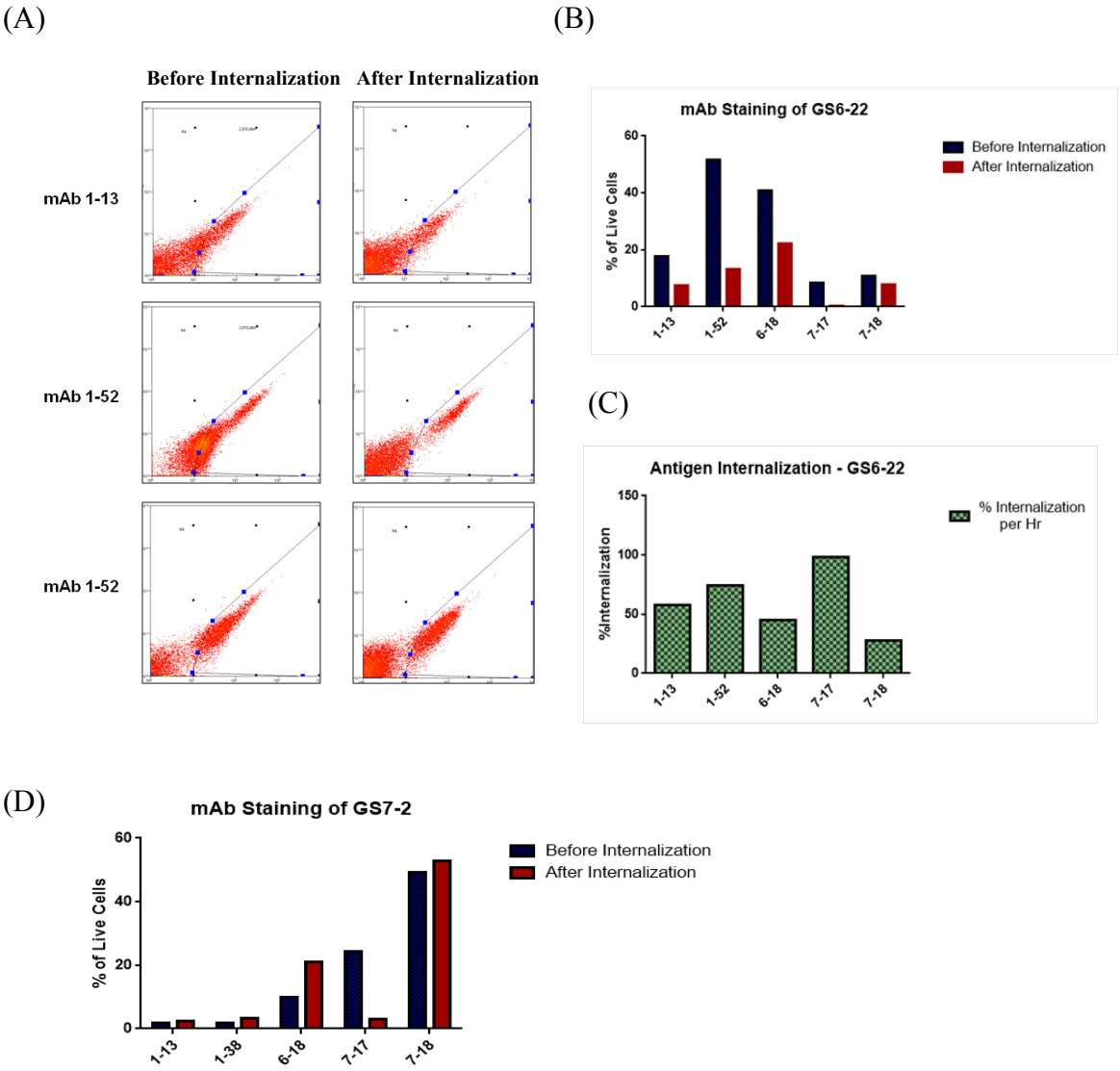

Figure 5.11: Antigen internalization by GS6-22 and GS7-2 cell lines. Cells were bound with candidate mAbs and were allowed to internalize at 37°C or kept at 4°C as control for 2 hrs. Fluorescent secondary antibody was used to stain the remainder mAb on cellular surface and positive cells were measured by FACS. (A) 3 representative mAbs showing FACS plots for GS6-22 stained before internalization (incubation at 4°C) and after internalization (incubation at 37°C). (B) Quantification of before and after internalization cell staining in GS6-22 cell line. (C) Analysis of internalization in GS6-22 represented in percent of internalization per hour. (D)Quantification of before and after internalization cell staining in GS7-2 cell line.

	HuGBM Tumor Slices (n=5)	Tissue Array (% tumors stained; n=70)
1-13	3/5	15
1-38	2/5	87.5
1-52	0/5	ND
2-81	0/5	ND
3-3	2/5	ND
4-13	2/5	10
6-18	4/5	15
7-17	3/5	ND
7-18	0/5	ND
7-23	2/5	32.5

Figure 5.12: Summary of IHC staining of human tissue sections by mABs. Five Human GBM (HuGBM) tumor slices were stained with all monoclonal candidate antibodies and number of positively stained section are represented in column 2. Monoclonals which stained HuGBM tumors were used to stain GBM tissue arrays containing 70 GBM tumor punches. Percentage of positive sections in the tissue arrays are represented in column 3.

by the genetic makeup of the tumor and its aggressiveness and the percent of tumor stem cells in the population of tumor cells. As the antigens for the antibodies are present in tumor tissue samples, we tested if other cancers may also express these antigens. Tissue specific stem cells often express similar antigens in different tissues. 5 candidate antibodies were used to stain tissue arrays containing sections with cancer and surrounding normal tissues for breast, colon, lung and prostate. 3 out of the 5 antibodies detected their antigen in breast tumors, whereas 2 antibodies stained cells in colon, lung and prostate tumors. None of the antibodies showed staining in the matched normal tissues (Supplementary Figure S5.7, S5.8). Only mAb 7-23 was able to stain all 4 tumor tissue types, but did not stain the normal tissue sections. These results show that the antigens are specifically expressed in tumor tissue as compared to normal, making these antibodies attractive prospective candidates for drug development to target tumors in addition to glioblastoma.

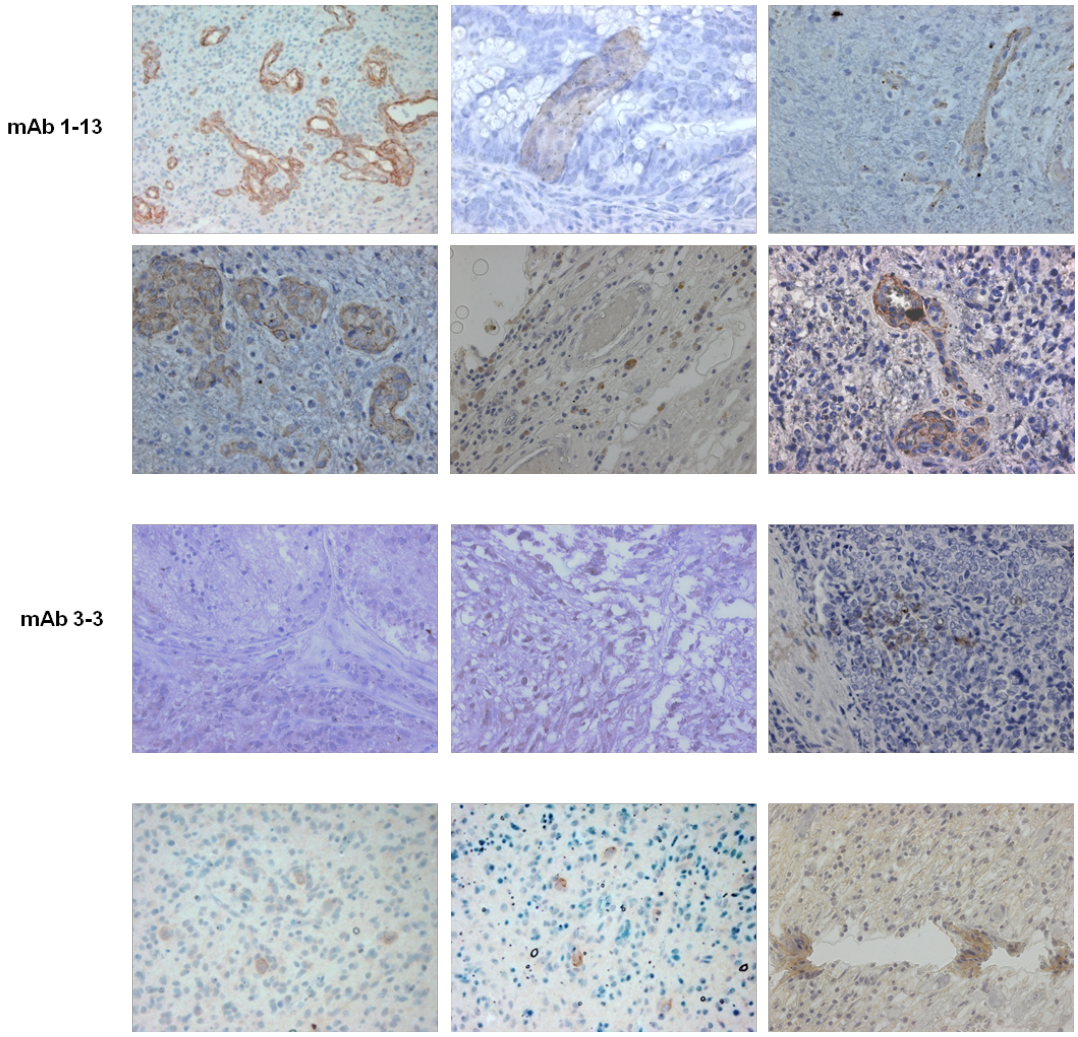

Figure 5.13A: Composite of positively stained section in HuGBM tumor slices and tissue arrays for mAb 1-13 and 3-3. HuGBM tumor sections and tissue arrays were stained with the candidate monoclonal antibodies indicated followed by secondary binding of a horseradish peroxidase (HRP) conjugated anti-mouse secondary antibody. The presence of the antigen antibody interaction was detected using DAB (stains positive regions brown in color) as a colorimetric stain.

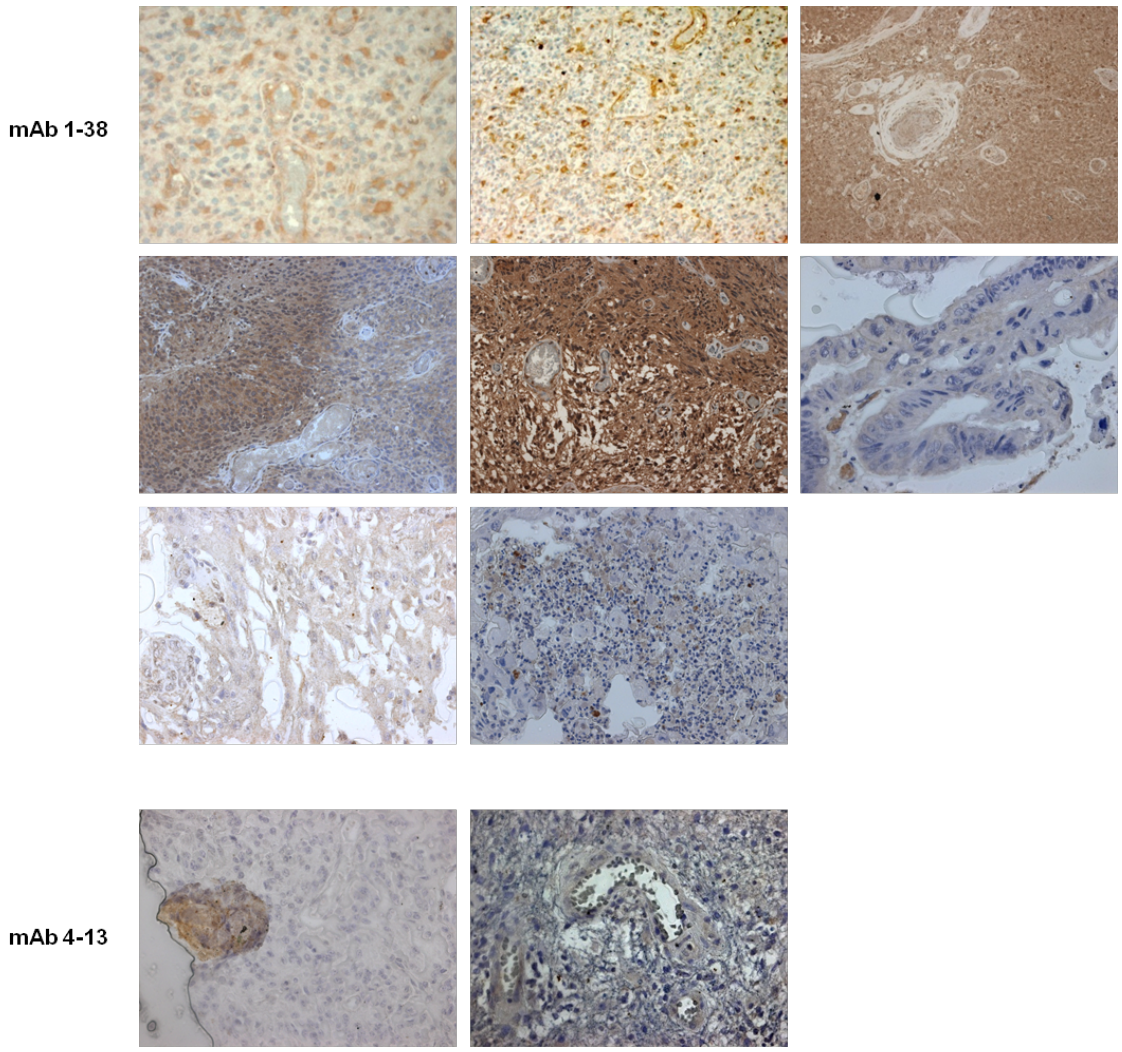

Figure 5.13B: Composite of positively stained sections in HuGBM tumor slices and tissue arrays for mAb 1-38 and 4-13. HuGBM tumor sections and tissue arrays were stained with the candidate monoclonal antibodies indicated followed by secondary binding of a horseradish peroxidase (HRP) conjugated anti-mouse secondary antibody. The presence of the antigen antibody interaction was detected using DAB (stains positive regions brown in color) as a colorimetric stain.

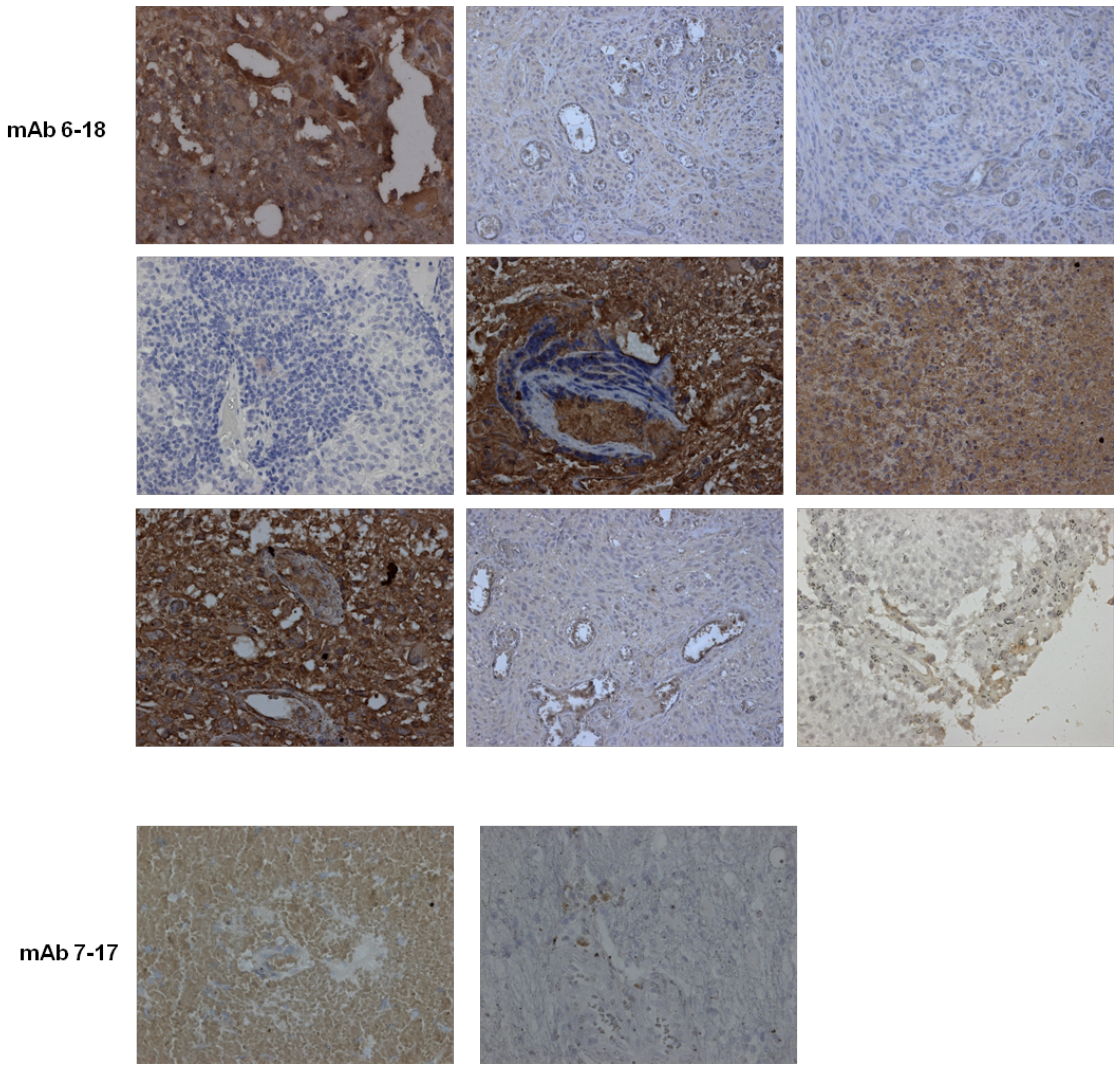

Figure 5.13C: Composite of positively stained sections in HuGBM tumor slices and tissue arrays for mAb 6-18 and 7-17. HuGBM tumor sections and tissue arrays were stained with the candidate monoclonal antibodies indicated followed by secondary binding of a horseradish peroxidase (HRP) conjugated anti-mouse secondary antibody. The presence of the antigen antibody interaction was detected using DAB (stains positive regions brown in color) as a colorimetric stain.

Monoclonal antibodies were generated against GBM-SCs with the aim of identifying novel molecular markers for this subpopulation of tumor cells which in addition might be used as potential therapeutics to target these important cells. These antibodies were specific for undifferentiated GBM-SCs and did not detect the antigens in GBM-SCs after differentiation. However, the antigens for a few of the antibodies can also be detected in non-stem cell lines, which is a disadvantage for their use as a marker – though this is a common problem for existing stem cell markers such as CD133. Monoclonal antibodies offer specificity to the antigen which is difficult to achieve using chemical inhibitors. The ability of these monoclonals to bind cell surface antigens which are internalized, may be an important characteristic for determining whether these may be good candidates to be used as drug-conjugated monoclonals. Further, their ability to detect antigens in different cancer types, but not in normal tissues, may be important for their application in multiple tumor types and as therapeutics with fewer side effects. The identity of the antigens recognized by the antibodies, except for mAb 7-18 which we have shown to recognize CXADR, is currently unknown. In order to evaluate the application of these antibodies as either markers or therapeutics, it is vital to identify the putative antigens and study the role they play in GBM-SC biology. The significant of CXADR will be discussed further in the next chapter.

(A)

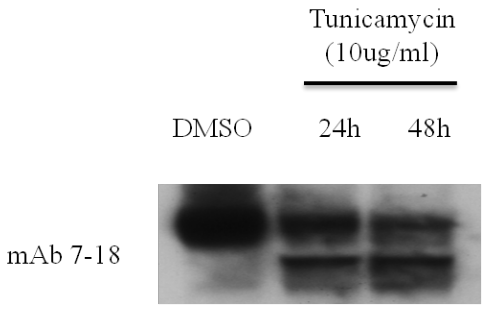

Supplementary Figure S5.1: Effect of tunicamycin on mAb 7-18 Antigen. GS6-22 cells were treated with inhibitor of N-linked glycosylation, Tunicamycin at 10µg/ml or DMSO for 24hrs and 48hrs. Lysates were collected and western blot was performed to detect antigen to mAb 7-18.

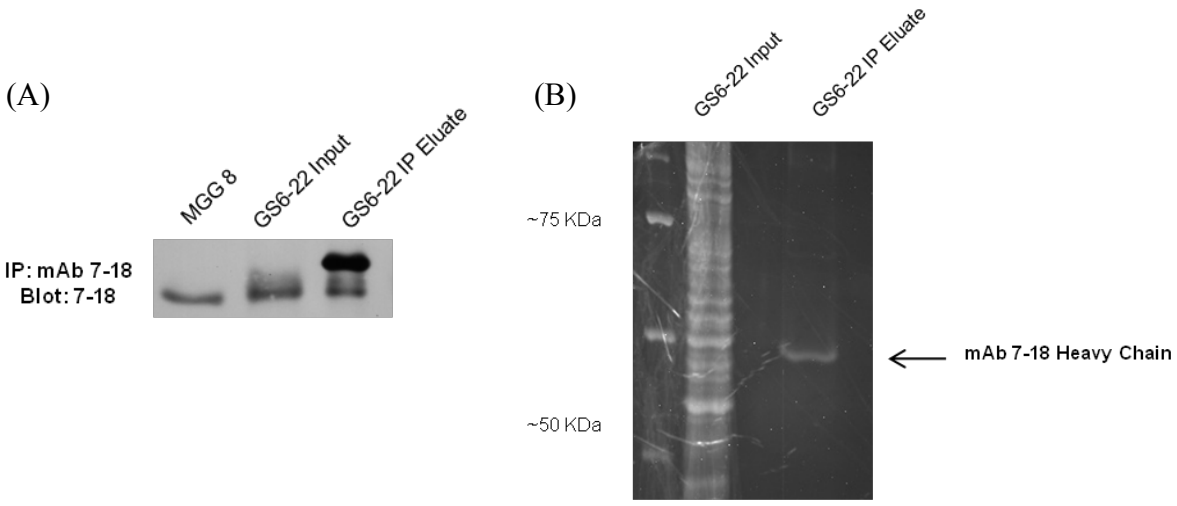

Supplementary Figure S5.2: Immunoprecipitation of mAb 7-18 antigen using GS6-22 lysates. Immunoprecipitation (IP) using mAb 7-18 was performed on GS6-22 cell lysates. The eluate from the IP was analyzed by western blotting and SYPRO Ruby protein gel staining. (A) Western blot of immunoprecipitation and immunoblotting of GS6-22 lysates using mAb 7-18.(B) SYPRO Ruby gel staining of mAb 7-18 immunoprecipitation eluate and GS6-22 input lysate.

(A)

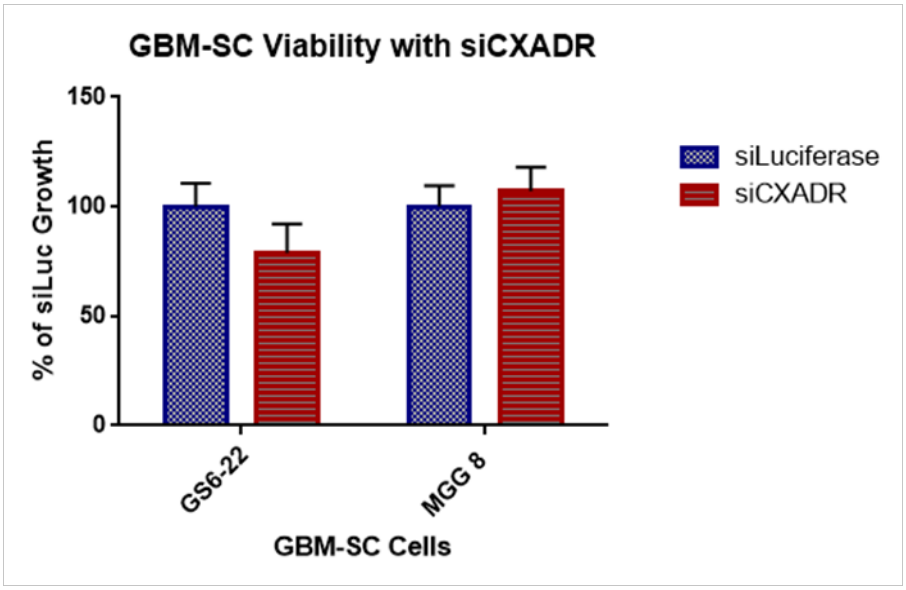

Supplementary Figure S5.3: Relative viable cell number of GBM-SCs after transfection with siCXADR. (A) CXADR protein was knocked down in GS6-22 and MGG 8 cell lines using siRNA and cell viability was measured after 5 days of siRNA treatment using prestoblue viability assay.

(A)

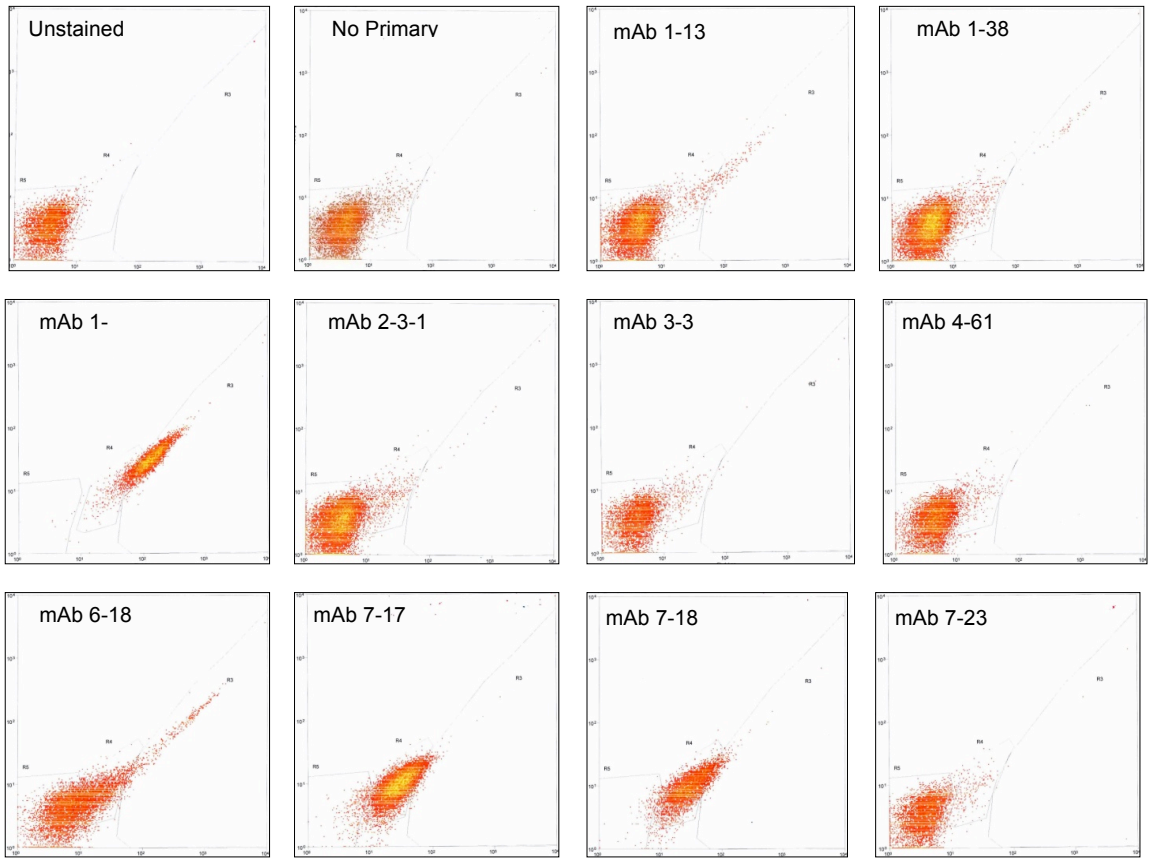

(B)

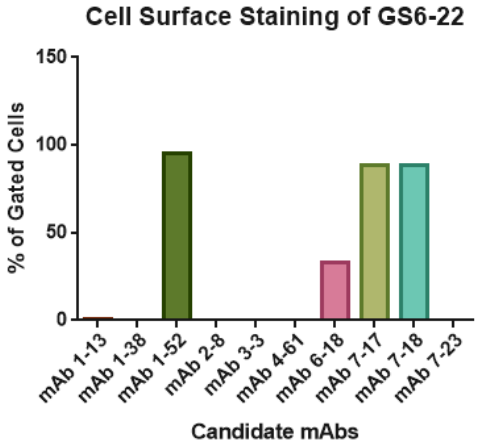

Supplementary Figure S5.4: Live cell staining of GS6-22 cells with candidate mAbs. (A) Candidate monoclonal were used to surface stain GS6-22 cell lines and after addition of fluorescently labeled secondary, positive cells were measured by FACS. (B) Quantification of the live cell surface staining using the monoclonals.

(A)

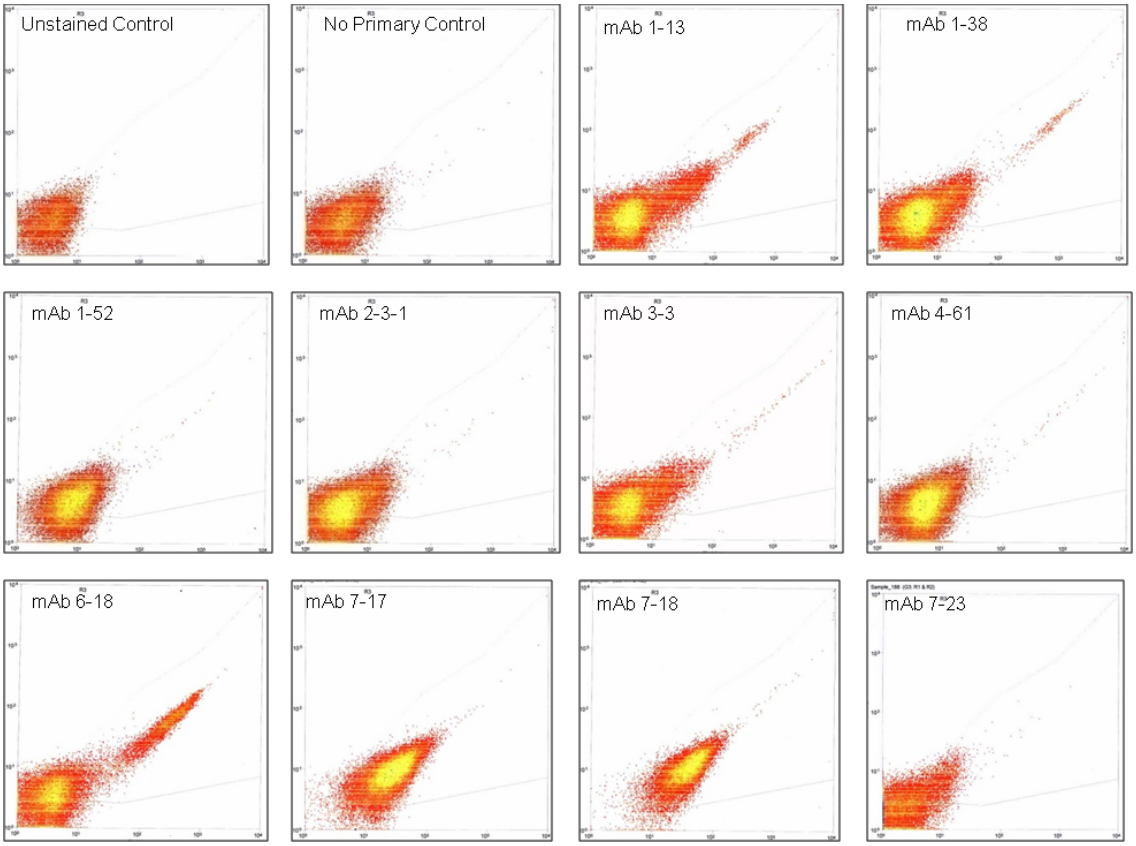

(B)

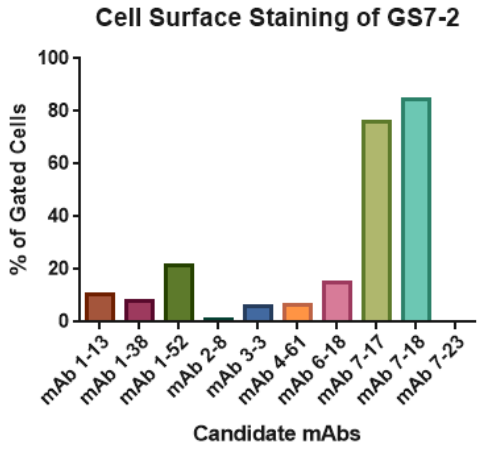

Supplementary Figure S5.5: Live cell staining of GS7-2 cells with candidate mAbs. (A) Candidate monoclonal were used to surface stain GS7-2 cell lines and after addition of fluorescent labeled secondary, positive cells were measured by FACS. (B) Quantification of the live cell surface staining using the monoclonals.

(A)

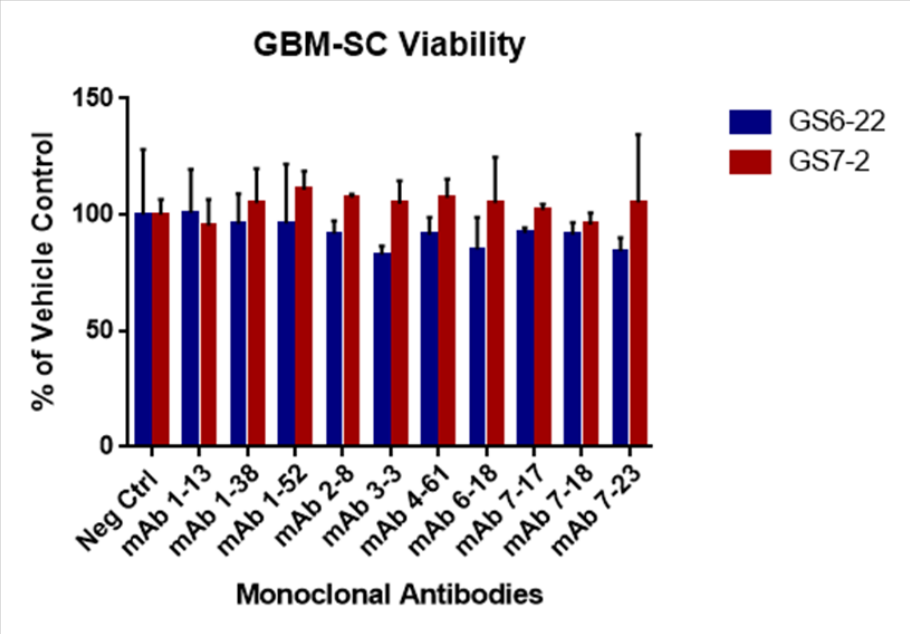

Supplementary Figure S5.6: Relative numbers of viable GBM-SCs treated with mAbs as naked antibodies. (A) mAbs were added to GS6-22 and GS7-2s at a concentration of 10µg/ml and effect on live cell number was measured after 5 days using the prestoblue assay.

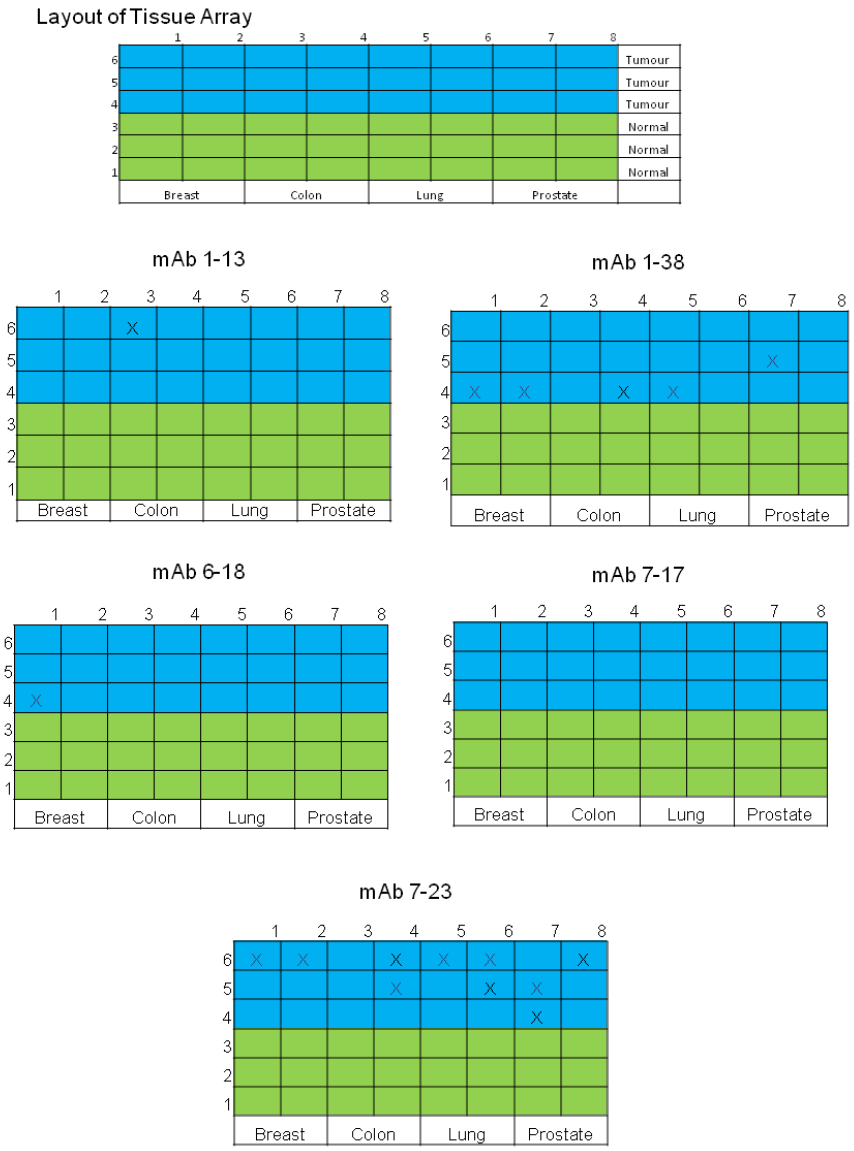

Supplementary Figure S5.7: Summary of staining of tumor and normal tissues. Tissue arrays (US Biomax Inc) containing tumor and normal tissue punches from the breast, colon, lung and prostate organs were stained by selected mAbs by IHC. Each cell represents a section. Blue Cells represent cancer tissue and Green cells are normal tissues. "X" denotes positive staining in the marked cell.

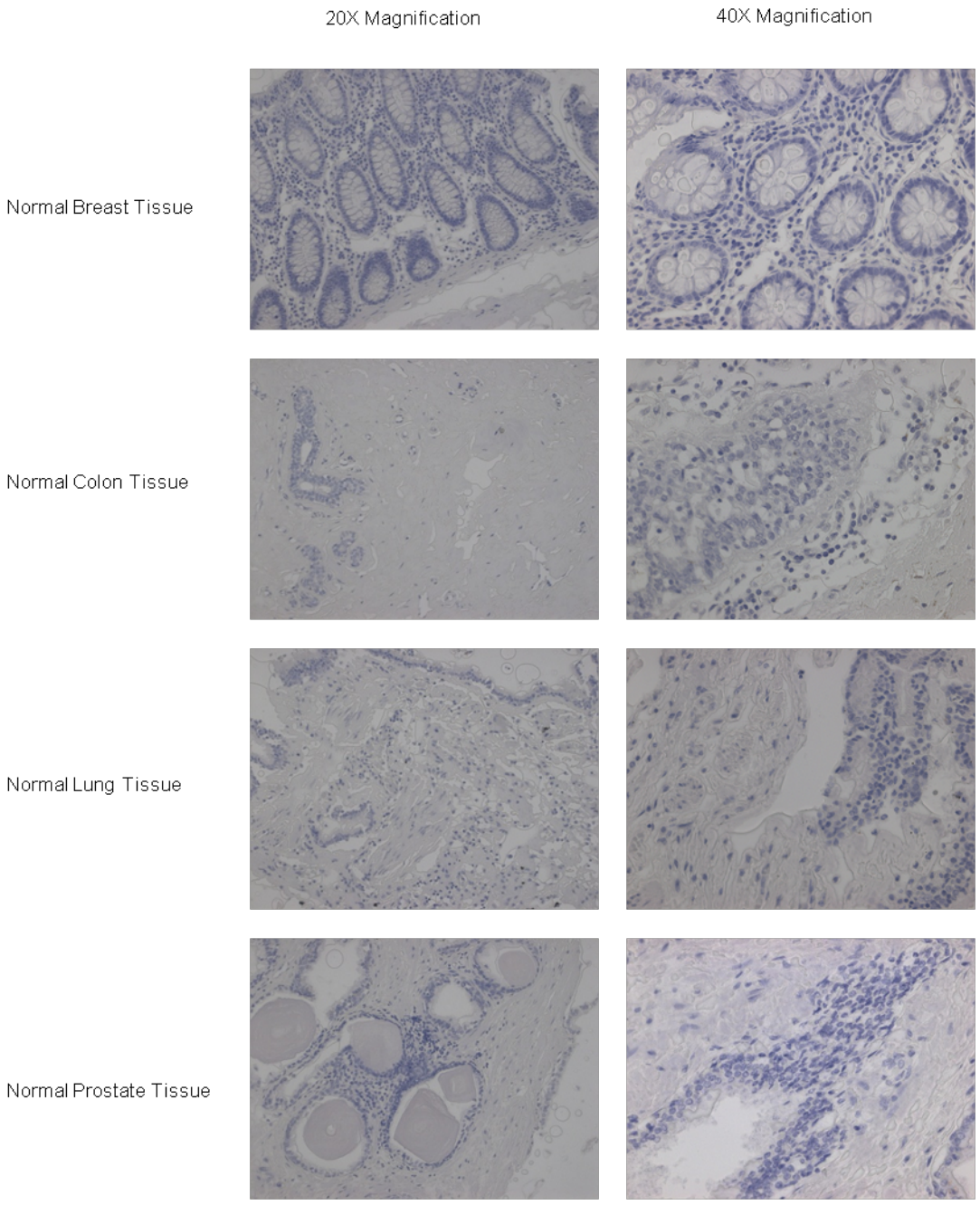

Supplementary Figure S5.8: IHC Staining of Normal Tissue Types. Normal section from Breast, Colon, Lung and Prostate tissue in tissue array (US Biomax Inc) stained using 5 antibodies viz mAbs 1-13, 1-38, 6-18, 7-17 and 7-23. None of the antibodies detected their antigens in normal tissues.

Chapter 6

Discussion and Future Directions

6.1 Pooled shRNA screening of GBM-SCs

GBM-SCs are important targets for drug discovery since they are resistant to treatment with conventional chemo- and radio-therapy and are thought to be responsible for tumor relapse [140, 151]. The enrichment of these populations in hypoxic niches further enhances these properties leading to incomplete tumor clearance and disease recurrence in the patients [230]. Hypoxic conditions in the microenvironment may change the dependency of the cells on particular genetic factors as it does the ability of these cells to resist chemical and radiological treatment [323]. Besides the known involvement of the Hypoxia Inducible Factors (HIFs) in cellular hypoxia response, the pathways important for the cells to survive in hypoxic conditions remain poorly understood [324]. In order to effectively target GBM-SCs, a better understanding is required of the genes important for their proliferation and survival under normal oxygen conditions and how these dependencies change under hypoxia. A good genetic target for drug development should possess the quality of being targetable using small molecule inhibitors as well as be required for GBM-SC proliferation and survival in both normoxic and hypoxic conditions. In addition, the inhibition of the target gene should not be detrimental to other normal cells in the body.

RNAi screening approaches have been used successfully to identify vulnerabilities of in vitro cancer cell lines and have led to the development of novel therapeutics against various types of cancer. Pooled shRNA screening allows for the high throughput testing of the cells dependence on specific genes without robotics and at a relatively low cost. This type of screening relies on the integration of one lentiviral shRNA construct per target cell, so that only one gene is targeted in a single cellular clone. This integrated

clone can be tagged with a molecular barcode for easy identification and enumeration of every shRNA hairpin from the pool of cells, all with different integrants.

Using this methodology, we tested the effect of knockdown of ~10,000 genes on the proliferation and survival of two separate patient derived GBM-SC lines under normoxic and hypoxic conditions. Data analysis was performed using two distinct methods to determine the concordance of hits using the two different algorithms.

6.1.1 Comparing MAD and BAGEL Algorithms for Data Analysis

The MAD analysis utilizes a robust Z-score to identify the hairpins which are 3 median absolute deviations from the mean of the population. In this analysis determinations for each hairpin were made separately and genes were considered hits if at least 2 hairpins met the >3MAD and <0.5 fold change cutoff. The 0.5 fold depletion was imposed to identify the genes with significant effects on cell proliferation.

The Bayesian Analysis using the BAGEL algorithm calculates a Bayes Factor for each gene to estimate the probability of its essentiality by determining whether a test gene's mean fold change is more likely to be closer to the known essential genes within the dataset or to the non essential genes [267]. The known essential and non essential gene lists have been predetermined using data from numerous previous screens [271]. The essential gene list includes genes such as those commonly used in the basal transcription and translation machinery. These genes would be expected to be scored as hits in a viability screen, due to their requirement in various housekeeping cellular functions irrespective of the tissue of origin. The non essential gene list comprise of the genes that had no effect on cellular proliferation or survival as determined by the previous published

screens. By using the internal data from the screen for this predetermined gene list as a comparison of the test genes, this allows for robust testing of the requirement of that gene to the cell.

The bayes factor calculation of the BAGEL algorithm combines the effect of all targeting hairpins to generate the score. For example, if cell viability is reduced by a fold change of 0.65, but is consistent in 4 out of 5 hairpins, the gene will be deemed essential as opposed to a gene targeted by 2 out of 5 hairpins which are effective with fold changes of 0.4. The BAGEL method thus may miss some genes which may be true positives, but are lost due to averaging the effects of less active hairpins targeting the gene. Any given hairpin may or may not effectively knockdown the expression of its cognate gene, so a lack of inhibitory effect of a given hairpin is not significant in the absence of expression information.

This is in contrast to the MAD analysis in which we require only 2 effective hairpins to score as a hit. Two shRNAs are required to minimize the number of false positives due to off-target effects, but to retain most true positives. Of course, true positives that had only a single effective shRNA would be excluded by the two hairpin requirement. In the absence of more detailed knockdown data and off-target information, no RNAi analysis method will be perfect in identifying hits In comparison to other statistical methods such as BAGEL which rely on information from all targeting hairpins, using the MAD analysis reduces the number false negative hits missed although there may be a higher probability of finding more false positives. Comparison of hits from multiple cell lines in triplicate, should overcome this disadvantage to some extent. Using this criteria increases the probability of detecting essential genes which would be missed by other analysis

methods which lay high emphasis on the number of active hairpins targeting the gene. One such example I have found in this thesis, is SGK1, which was validated as a definitive hit in Chapter 4. SGK1 did not score as a hit using BAGEL, however was included in the MAD analysis hit list, which led to its identification as an essential gene from the screen. SGK1 was a hit in both cell lines and under both conditions by MAD analysis.

6.1.2 Core Essential Genes in GBM-SCs

The stringent cutoff applied for the MAD analysis resulted in 81 total hits common to both cell lines and both conditions. Removing the fold change<0.5 cutoff drastically increases the number of hits but includes hairpins which were only reduced by 30% in abundance compared to the reference control and are thus have reduced significance in the biological context. For instance, to achieve a 50% growth reduction over 4 doublings, requires only a 15% decrease in doubling time per cell division. For this screen, we would like to find targets that are most likely to have a significant anti-tumor effect. This pattern emerged due to the clustering of all the hairpins around the mean with most of them not having a significant effect. Due to the long doubling time and relatively low saturation density of the GBM-SCs in culture (>24hrs), the duration of the experiment was probably not enough to allow appropriate number of doublings required to create adequate separation of the weakly inhibitory hairpins from the rest of the population. This would lead to a narrower distribution of the data with a low number of hairpins on the tail, which translates to a lower number of hits. This effect was even more apparent in the hypoxic condition, in which cells proliferate at a slower rate than in normoxia, for both cell lines. We attempted to adjust this difference by increasing growth duration for cells

in the hypoxic conditions. However, this shorter duration and smaller number of doublings has the advantage of biasing the screen for stronger rather than weaker hits. Further, the hit rate of the screen may also be influenced by ineffectiveness of the targeting shRNA sequences and vector. As the multiplicity of infection in the screening is 0.5 to maximize single integrants, it is also possible that the amount shRNA expression from the single integrated vector is not enough to significantly deplete enough of the target protein to produce a phenotype. Additionally, the numerous redundancies in the signaling pathways also adds to the complexity as the knockdown of one protein may not be enough to produce a phenotype. This may explain why some expected target genes such as AKT1 were not detected in our screen.

The core essential genes included ones which are required for core processes in cells such as transcription, translation and proteasomal degradation. To exclude these genes from the analysis, we compared the essential genes from the screening to the predefined list of known genes believed to be essential for cellular survival based on multiple screens, which were used as an internal control training set for the BAGEL algorithm [267]. The high 50% overlap in these hits indicate the enrichment of genes which produce an expected growth phenotype upon knockdown. The targeting of these pathways is not ideal due to their critical functions in the normal cells of the body, inhibition of which could lead to many side-effects. However, the current standard of care for GBM includes localized radiation followed by DNA damaging agent TMZ, which also does not distinguish between normal and cancer cells, but affects the latter more due to their mitotic index. Similarly, targeting these core processes, is not ideal, but may be effective due to the dysregulation and hyperactivation of these pathways in cancer tissues [44,

325]. Inhibitors targeting mRNA translation are currently being investigated, with candidate drug 4Ei-1 directly inhibiting the cap dependent assembly of the ribosomal complexes [326, 327]. Further, upstream regulators of translational machinery assembly such as mTOR, may be targeted in order to affect machinery assembly. Inhibiting the proteasome has proved a successful strategy with many inhibitors currently in preclinical trial and some like Bortezomib (or Velcade), that have been approved for use in the clinic for multiple myeloma [328]. The proteasome shows increased activity in cancer cells and inhibitors were shown to affect ~60 cell lines but did not affect quiescent or terminally differentiated cells [329, 330].

6.1.3 Pathways Regulated by Essential and Hypoxia Specific Hits

Ingenuity pathway analysis of the core essential genes identified Protein ubiquitination, EIF2, EIF4 and Ran signaling as the top canonical pathways, which was expected due to the abundance of proteasome and ribosomal protein hits. The Ran pathway has previously been shown to play an important role in the survival of GBM-SCs, which may be particularly sensitive to Ran inhibition [272]. Removal of the known essential genes from this set, depleted the ribosomal genes as well as the Ran pathway genes, indicating its importance in various different cell types as well (Figure 3.3B). Interestingly, hypoxia signaling was one of the enriched pathways in this core list, implying that the genes required for signaling under hypoxic conditions are also active under normoxic conditions. We postulate that this may be due to the existence of a psuedohypoxic state in the GBM-SCs, which drives the hypoxic signaling network and makes the cells sensitive to the disruption of this pathway. This psuedohypoxic state may be driven in part by the constitutive expression of HIF2α in the GS6-22 and MGG 8 cell lines (data not shown).

The constitutive expression of HIFs in GBM-SCs and their dependence on these factors for survival has also been previously described [189, 250, 252]. In line with this analysis, comparison of the normoxic and hypoxic hit lists showed that ~70% of the genes identified as hits under hypoxic conditions were also enriched under normoxia (Figure 3.1D). In the pathway analysis, the calpain proteases, several of which were identified as a core essential hits in the screen, were enriched in a number of signaling pathways including Focal Adhesion Kinase (FAK) signaling. Calpains have been shown to be required for GBM cell invasion and regulate cell motility through matrix metalloproteinase 2 in GBM cell lines [331, 332]. However, they likely have additional functions in GBM-SC as our screening assay did not score cell motility. FAK also plays a similar role in GBM and has shown to be important in cancer cell survival and TMZ sensitivity in preclinical models [333]. The presence of multiple hits in one signaling cascade (like EGFR signaling) would indicate its importance in the two GBM cell lines as well as the addiction of the cells to this pathway. Intriguingly, none of the key GBM pathways described by the TCGA were highly enriched by the hits in our common list of hits. This indicates that different GBM-SCs and tumors may have dependencies on different pathways for proliferation and survival. Further, many of these key pathways are likely to possess redundancies in signaling [38] and thus knockdown of one protein may not produce a defect in growth or loss of survival. For instance, there are 3 AKT isoforms. It is interesting in this regard that inhibition of the related SGK1 protein has such a profound effect on GBM-SC survival by itself.

Comparison of the hits derived from GS6-22 and MGG 8, showed that a little over one-third of the hits were common to both cell lines (39% and 32% respectively) under

normoxic conditions. Under hypoxic conditions, only 17% of hits in GS6-22 were also identified in MGG 8 cell lines. Although such a limited similarity was unexpected, it was also not as surprising. The heterogeneity between different GBM tumors is high, and a tumor may be in one of the 4 gene expression subtypes as defined by the TCGA [9, 19, 22]. Although, computationally these subtypes are distinct, biologically these subtypes are more fluid and may change depending on the microenvironment of the tumor region [229]. Further, one tumor may contain different tumor populations from multiple subtypes. These cell lines have been derived from different patient tumors, and although mutational and epigenetic landscape of these cells is under investigation, they may rely on different signaling pathways for proliferation and survival. This is both a major challenge and an opportunity for targeted therapies and personalized medicine as there are likely more targets specific to a single GBM than are common between any two tumors. On a more technical note, the variability in knockdown of the same hairpin on different cell lines has also been demonstrated [334]. This could also be a factor in the difference in the hits observed between the two cell lines.

RBX1 and KIF11, the top core essential genes from the screen were independently validated to be important in GBM-SC proliferation and survival. Both proteins have been shown to play a role in cancer biology although RBX1 has not been studied in context of GBMs. Ring-box 1 (RBX1) is an important component of the SCF E3 ubiquitin ligase complex, which targets up to 20% of cellular proteins for ubiquitination and degradation including key cell cycle regulators and transcription factors [335, 336]. RBX1 has been found to be essential for maintaining genomic integrity and has been shown to be important for proliferation and survival of cancer cells [337, 338]. Gastric cancers with

high RBX1 expression have a poorer prognosis [339].Kinesin family 11 (KIF11) is a motor protein which binds to microtubules during the M-phase and anaphase of cell division and is essential for proper chromosomal segregation [340]. KIF11 has been targeted in cancer cells by the use of different small molecule compounds and work is ongoing in preclinical GBM models for KIF11 as a therapeutic target [341].

6.1.4 Comparison of the Kinase Hits from RNAi Screening

Kinases contribute to the tumorigenicity due to their key roles in the various cellular signaling pathways. Kinases have become a popular drug discovery targets with more than 25 approved oncology drugs [342]. To specifically identify the essential kinases from the screen, we utilized two approaches. First, we compared the list of hits in the pooled screen from all conditions. PLK1, STK36 and SGK1 were identified as the only essential kinases common to both cell lines in both normoxic and hypoxic conditions. This highlights the heterogeneity between the GBM-SC lines, with each line having different dependencies and probably distinct compensatory mechanisms. Polo-like Kinase 1 (PLK1) plays important role in mitotic progression during cell division. PLK1 is overexpressed in various cancer types and is a popular target for development of inhibitors for clinical use [343]. Numerous published siRNA screens have also identified PLK1 as a hit, indicating its importance in cellular survival [275]. STK36 is a serine threonine kinase with putative role in survival as a part of the Sonic Hedgehog signaling by regulating localization of the Gli transcription factors [344]. Lastly, Serum and Glucocorticoid regulated Kinase 1, an AGC kinase family member, is upregulated by various external stimuli, and is a known pro survival kinase [278, 291].

We further compared the kinase hits in the GS6-22 under normoxic conditions to hits obtained from an independent well by well kinome screen performed on the same cell line under normoxia. We found that out of 30 hits in the pooled screen, only 4 hits were common to both the screening methodologies. It was somewhat surprising that hits from the screening of the same cell line using 2 libraries was so discordant, though this discordance between libraries has been noted in other RNAi screens [275, 345]. The efficiency of targeting hairpins and the MOIs of the experiment are variables which are known to affect hit rate and selection [346]. Out of the 4 hits, Cyclin Dependent Kinase 4 and VEGF Receptor 2, have been extensively studied in cancer, especially in the context of GBMs and are known to play an important role in tumor maintenance [9, 347]. Cyclin dependent kinase like 5 (CDKL5), located on the X chromosome, has been associated with Rett syndrome and X-linked infantile spasms. CDKL5 is developmentally expressed as well as in the mature neural cells in the adult brain [348, 349]. The role of CDKL5 in cancer is currently not clear and further work is required to elucidate the sensitivity possessed by GBM-SCs for depletion of CDKL5.Although most kinases identified from these analyses are already known to play a role in GBMs, the role of CDKL5 and STK36 in GBM and GBM-SCs is unclear and warrants further investigation. SGK1 was the only kinase identified in both screens, and was thus chosen for further investigation for its role in GBM-SCs.

6.1.5 SGK1 is required for GBM-SC proliferation and survival

SGK1 is a transcriptionally induced gene in the presence of a number of different environmental stimuli including oxidative and osmotic stress and UV irradiation [277, 278]. The primary role of SGK1 in tumor development is as a regulator of cell death.

Previously, SGK1 has been shown to be part of a cytoprotective signaling network regulating the balance of pro- and anti-apoptotic proteins through the FOXO3 and NF-κB cascades [291].

In a recent kinome screen to identify genetic targets regulating mTOR1 activity in NF2-deficient meningiomas. mTOR1 is constitutively active in NF2 deficient cells and kinome screen revealed SGK1 as a key regulator of mTOR1 in an mTOR2 dependent, but AKT and S6 Kinase independent manner. Sensitivity of the meningiomas to mTORC1/2 inhibitors as well as SGK1 inhibitor suggests this is a potential therapeutic target for this cancer [350]. In another kinome and phosphatome screen to identify GBM-SC vulnerabilities, SGK1 was one of the hits of the screen which significantly increased cell death as measured by PI staining [351]. Although, this study did not validate SGK1 as a hit, the identification of SGK1 as a cell survival kinase increases our confidence in it as a bona fide target for GBM-SCs.

Using shRNA, Crispr and a SGK1 specific inhibitor, we validated the importance of SGK1 in GBM-SC proliferation and survival. Interestingly, this dependence was not observed in the traditional glioma serum lines. The growth of A172 cells decreased by approximately 40%, however the resistant population proliferates and can be propagated. It is possible that the cell culture conditions (serum free, growth factor rich) alter the pathways that are required for the survival of these cells. PI-3-Kinase can be stimulated by growth factors, and dependence on downstream effectors of PI-3-Kinase pathways may be enriched in such a model. This is certainly true for PDK1 and Akt inhibition as well, which produce an even more robust phenotype than with SGK1 inhibition. Traditional glioma lines are grown in 10% serum, which itself contains factors

stimulating these pathways. Further, these cells may possess mutations keeping these pathways in the activated state irrespective of the presence of growth factors in the media. Interestingly, H04 and SW06 normal neural progenitor cells were cultured in 5% serum conditions, but they do show sensitivity to SGK1 inhibition to some extent suggesting that the serum does not cause the difference in SGK1 dependence. The inhibitory effect on neural stem cells is a concern for use of SGK1 inhibitor as a therapeutic due to potential toxicity. However, these progenitor cells do not show the same level of toxicity as the GBM-SCs, meaning that the drug could possibly be used at a dosage which would preferentially target the cancer cell population. Moreover, it is likely that most normal adult NSC's are quiescent and likely would be more resistant to killing by SGK1 inhibition in this state (though this needs further testing). Although PDK1 and AKT inhibition gives a more robust phenotype in GBM-SCs, they also affect the normal neural stem cells, differentiated GBM-SCs and other glioma lines equally. SGK1 inhibition, however, is specific to the GBM-SCs and this sensitivity is lost upon their differentiation. Furthermore, normal fibroblast cell line Hs27 was also unaffected by SGK1 inhibition. This would suggest that the toxicity and side-effects to the drug may not be as detrimental as in the case of PDK1 and AKT inhibitors. This indicates, that although SGK1 inhibitor may have limited single agent therapeutic, it may be combined with a drug which is able to affect the bulk of the tumor like TMZ. This is underscored by the clinical trials results for Akt inhibitor, Perifosine, in GBM. The clinical trial did not recapitulate its effectiveness from preclinical studies and has failed. It is currently being combined with other inhibitors to test efficacy in patients [352]. This highlights a

recurring problem of resistance in GBMs, and a better understanding of the pathways are required to devise more effective therapeutics.

The effect of SGK1 inhibition differentially on undifferentiated and differentiated GBM-SCs is intriguing as it suggests that the stem cells preferentially depend on SGK1 for survival. The induction of differentiation will significantly reduce the number of cycling cells in population. If SGK1 also has a role in cell cycle progression in GBM-SCs, as has been previously shown, then differentiated cells would not require SGK1 as they are in a growth arrested state[353].

6.1.6 Mechanism of Cell Death on SGK1 Depletion

We have demonstrated that SGK1 depletion and inhibition leads to an increase in annexin V and PI staining measured by FACS analysis. This induction of apoptosis is further evidenced by the increase in PARP cleavage. PARP is a downstream target of effector caspases and its cleavage is a marker for caspase dependent cell death. However, we do not observe an increase in the activity or the presence of cleaved form of Caspase 3 and 9. Although total Caspase protein decreases, which may be rescued using proteasome inhibitor MG132, the cleaved/active form of these enzymes are not detected. This is further confirmed by the observation that addition of pan caspase inhibitors, Z-vad-FMK and q-Vd-OPh do not rescue this phenotype. Furthermore, signaling cascades including FOXO3, NF-κB, JNK, p53, which regulate apoptosis were examined in this study. No change in FOXO3 and NF-κB target gene transcription or subcellular localization was observed on SGK1 depletion or inhibition. It is possible that there might not be just one responsible pathway for this phenomena and that other pathways may compensate for the

deficiency in the one of the pathways. However, not even a partial rescue of the phenotype was observed upon co-inhibition of SGK1 and p53, JNK and p38 MAPK, indicating that the mechanism may be independent of these pathways. This evidence as well as a lack of a true Annexin V positive only subpopulation of cells in FACS, suggests that cells may be dying by a either a non-apoptotic form of cell death or a non-canonical apoptotic pathway.

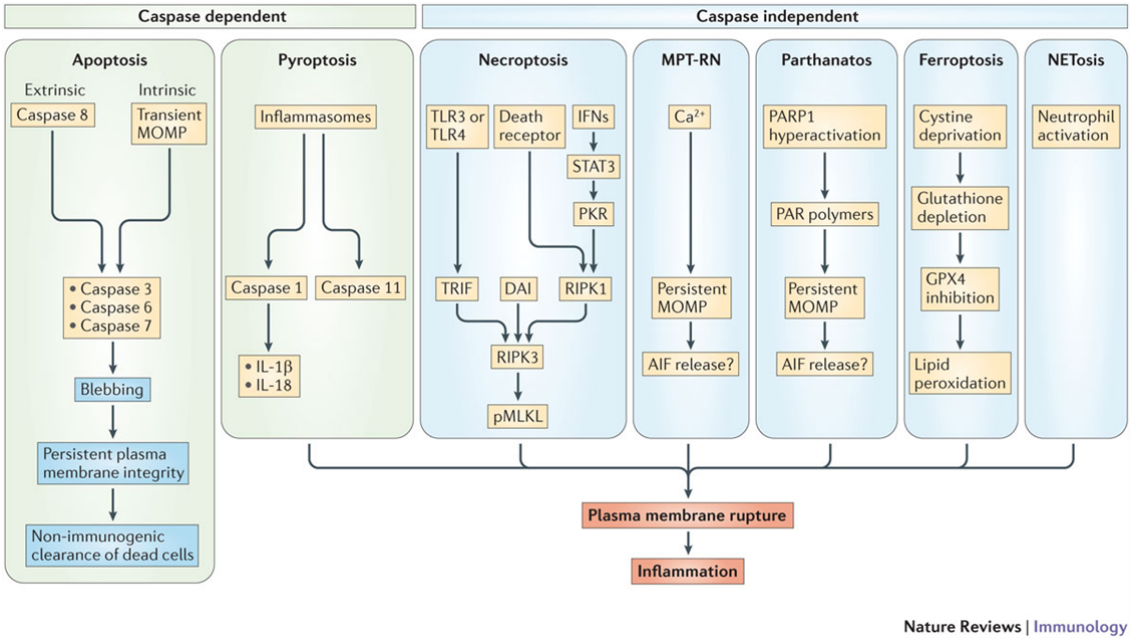

Figure 6.1: Mechanisms of cell death. Regulated cell death may occur by 7 distinct mechanisms, five of which are caspase independent. Figure adapted from Linkermann et al. Nature Reviews Immunology. 14,759–767(2014).

Cells with blockade in the apoptotic cascade, often revert to cell death by necrosis. GBMs have been shown to be highly resistant to apoptotic stimuli [7]. Blockage of apoptosis by caspase inhibition or caspase activator Apaf-1 deletion, leads to a decrease in apoptosis but also causes a concomitant increase in death by necrosis [315]. Decrease in ATP levels

and mitochondrial dysfunction lead to plasma membrane rupture and cell death. This switch between apoptosis and necrosis is enforced by a Bcl2 family member, BCL2L12 [354, 355]. This protein is found to be overexpressed in GBMs and is an effective repressor of the caspase cascades [356]. SGK1 has been shown to mediate necrotic cell death in breast cancer cells and this may represent the alternate mechanism of cell death in GBM-SCs [306]. There are 5 other alternate mechanisms of cell death: Caspase 1 dependent pyroptosis. RIPK1 dependent necroptosis, mitochondrial permeability transition-mediated regulated necrosis (MPT-RN), ferroptosis and NET release-associated cell death (which is known as NETosis) (Figure 6.1) [357]. Of these MPT-RN is mediated by excess calcium release in the cells. SGK1 has been demonstrated to be sensitive to intracellular Ca^{2+} and thus this may present a testable hypothesis of cell death in GBM-SCs [306].

6.1.7 Future Directions

In chapter 3, we identified a number of core essential genes for the two patient derived GBM-SC lines as well as genes that are exclusively important under hypoxia. Many of the core essential genes may have important cellular functions in normal tissue types as well. Thus, pooled screening of the 10,000 genes in normal cell lines such as fibroblasts and normal neural progenitor cells, may provide us with the hits which may have a critical function in the normal cells of the body. However, it's not certain that a list generated by such a screen would greatly improve on the list of core essential genes already identified or found in the CRSIPR screen of NSCs conducted by other labs [358, 359]. Inhibition of these targets in normal cells may lead to more side effects of therapeutics.. Thus, this approach may be used to exclude such hits from the GBM-SC

screen for target identification which is cancer specific. However, the hit by hit approach to examining the effects of gene inhibition on non-GBM cells that I have taken in this thesis for SGK1 might be a better way of examining this given the uncertainties of RNAi screening. In addition, screening GBM-SCs, normal fibroblast and neural stem cell lines using the Cellecta module 3 for further 5000 genes may identify additional targets which may be of interest. The hypoxia specific genes enable the cells to survive under hypoxic stress. Investigation of their role in GBM-SCs will be important in understanding how the GBM-SCs respond to the surrounding microenvironment.

The data from chapter 4 have demonstrated the importance of SGK1 in cellular survival of GBM-SCs. Further investigation is required to better understand the function of SGK1 in GBM-SCs. Although its known role is as a pro-survival kinase, it is likely not the only role it plays in GBMs. The reason for stimulation of cell death in GBM-SCs is unclear. The role of SGK1 in maintenance of Na^+/K^+ homoeostasis may not be limited to kidney cells, and it may play this role, especially in the brain. Further, its role in regulation and cytoprotection from ROS in the cells may be important for GBM-SCs due to the hypoxic microenvironment of their growth. A role for SGK1 in cell cycle progression has also been found in other cancers which may be relevant to GBMs and should be further investigated.

In addition to testing these processes separately, a large scale genomic and proteomic approach needs to be taken to identify the genes and proteins which are regulated upon SGK1 inhibition and depletion. This may help to understand the pathways that are regulated by SGK1 in GBM-SCs and in the development of adjunct therapies for SGK1 inhibition resistant tumor populations. Comparing the role of SGK1 in GBM-SCs to its

effect on non-stem cell lines such as traditional glioma lines, normal fibroblasts as well as serum lines derived from the same patient tumor as the GBM-SCs, may shine light on its specific role pertaining to the stem cell population. Further, this may be extended to other stem cell cultures such as normal neural stem cells, embryonic stem cells and iPS cells to evaluate whether this process is limited to primitive cell types. The role of SGK1 in cells may be confounded by the presence of AKT, due to some degree of functional redundancy of the two proteins. SGK1 and AKT share many substrates, however, their they do have unique targets as well. A phospho-proteomic approach to determine SGK1 specific substrates would further enhance our knowledge of the role SGK1 plays in GBM-SC growth and survival. There is also a gap in knowledge about the in vivo role of SGK1 in tumorigenesis. Although Oncomine analysis of the TCGA did not detect any overexpression of SGK1 mRNA in the tumors, the activity of the kinase may be aberrant in cancer cells, which would negate the need of overexpression or mutation of SGK1. Further, its regulation by ubiquitination and subsequent degradation in normal cells, may be hampered in the tumors, with gene expression or mutational changes in the proteins affecting this process to increase SGK1 stability in the tumor cells. The protein expression and activation of signaling cascades downstream of SGK1 in patient tumors will inform us of its importance in the tumor maintenance. Further, assaying sections from different tumor grades of gliomas will show if SGK1 also has a role in lower grade gliomas or if its role is exclusively in GBMs. Using the SGK1 knockout mouse model may also be useful in understanding its role in tumor development. Knockout of SGK1 in different mouse genetic models of GBM, such as p53/NF1 null, PDGF overexpression or

EGFRvIII mutant mice may further help in elucidating its role in the initiation and maintenance of GBMs.

6.2 Novel Monoclonal Antibodies Recognizing GBM-SCs

6.2.1 Candidate Monoclonals as Molecular Markers

The current GBM-SC molecular markers have many shortcomings. The primary marker CD133, is not able to detect all stem cell populations in GBMs, it changes in expression in response to environmental stimuli, and is also present in many other cell types. There is a need for identification of novel cell surface markers which would be able to detect stem cells specifically. An ideal stem cell marker for isolation of GBM-SCs should (i) able to detect antigen on cell surface, (ii) only detect the antigen in stem cells and not after differentiation, (iii) should not be expressed or at least presented on the cell surface in normal or cancer serum cell lines which do not possess stem cell characteristics, (iv) should only be responsive to changes in stemness and not to microenvironmental fluctuations and (v) should be expressed in subpopulations of tumor cells.

In Chapter 5, we have generated 10 novel monoclonal antibodies to specifically recognize GBM-SCs. This was done by immunizing the mice with fixed and live GBM-SCs, and generating monoclonal antibodies using hybridoma technology. Each antibody was screened against undifferentiated and differentiated GBM-SCs and the antibodies which were specific for the undifferentiated GBM-SCs were considered candidate stem cell antibodies. 10 monoclonal antibodies were identified which recognize antigens on the undifferentiated GBM-SCs but the staining is lost or significantly reduced upon differentiation. 5 of the 10 antibodies detected their denatured antigens undifferentiated

stem cell lysates, but not in differentiated cell lysates when used for western blotting. At least 4 of these antibodies detected bands at different sizes and thus are likely to recognize distinct antigens. Of these, mAb7-18 and mAb1-38 detected stained human embryonic stem cells and induced pluripotent stem cells positively by western blotting. The mAb 7-18 antigen progressively decreased upon differentiation, making it a promising candidate for further investigation. mAb 1-13, mAb 1-38, mAb3-3 and mAb7-18 also detected their antigen in other serum lines by immunofluorescence staining and western blotting (mAb 1-38 and mAb 7-18). Although this is a disadvantage, it is possible that the antigens have different subcellular localization which changes with stemness and thus these antigens merit further investigation. They may also be useful as markers in the GBM context.

In order to use the candidate mAbs for therapeutic applications, it is important to identify the antigenic protein that each recognizes. mAb 7-18 was chosen due to its higher level of expression and detection in GBM-SCs by western blotting. This suggested that a greater amount of starting material would be available for immunopurification. As mAb 7-18 antigen was also found to be present in colorectal cancer lines, we used lysates from those cultures as well to increase the amount of the antigen in the source material. Using immunoaffinity purification followed by mass spectrometry and subsequent experiments, we were able to identify the antigen for mAb 7-18 as Coxsackie virus and adenovirus receptor or CXADR (or hCAR).

6.2.2 Coxsackie virus and Adenovirus Receptor

CXADR is an evolutionarily conserved member of the Ig superfamily and was discovered as a receptor to process adenoviral and grp B coxsackievirus infections [360–362] More importantly, CXADR's role is critical during embryonic development and regeneration [363]. CXADR is highly expressed in the brain and the heart during development [364–366]. CXADR deficiency causes embryonic lethality in mice at E11.5-13.5 due to defects in cardiomyocyte development and heart function [366–368]. Interestingly, primitive hematopoietic progenitor cells lack the expression of CXADR which is in contrast to human and mouse embryonic stem cells as well as in induced pluripotent stem cells [365, 369, 370]. This suggests a different role in distinct cellular lineages. In addition to demonstrating tissue specificity, Honda et al also showed high expression of CXADR mRNA and protein in the brain during development, which is lost after birth of the mouse pup [364]. Further, CXADR expression is only found in the ependymal cells in the adult brain, but is expressed in neurosphere cultures of neural stem cells indicating that proliferating primitive cells may be the cells in the lineage marked by CXADR [371]. CXADR expression was also observed in expression data derived from blastocysts and human ESCs in which CXADR was highly expressed in the undifferentiated cells [372–374]. CXADR mRNA levels increased in pre-implantation embryos but is quickly downregulated upon different implantation [374]. Functionally, CXADR is a member of the intracellular tight junction protein complex. The transmembrane protein associates with structural and signaling components such as JAM-L, ZO-1, β-catenin and MUPP1 and has been shown to signal through the PI-3-Kinase pathway [375–378]. Forced expression in glioma and rhabdomyosarcoma cell lines

reveal a tumor suppressive and anti-migratory role of CXADR in cellular function [379, 380]. A recent paper utilized CXADR as a marker for an undifferentiated cell type in the hematopoietic lineage. The authors evaluated CXADR as a marker of cells differentiating into cardiac lineage or hematopoietic lineage, from mesodermal pluripotent stem cells. CXADR presence successfully predicted the tropism of CXADR+ cells to differentiation into the cardiac lineage, whereas the CXADR- cells were committed to the hematopoietic lineage [381].

Further experiments are required to evaluate the suitability of CXADR as a marker for GBM-SCs and whether it can be used to mark normal neural stem cells. Firstly, its expression and localization in different tissues in adult mice is required to check whether it is present in different stem cells niches of the body. Secondly, coexpression studies with cell surface markers as well as internal stem cell markers such as CD133 and nestin in GBM-SC cultures as well as tumor sample and section, should be performed to evaluate the overlap between the two populations. Further, sorting by mAb7-18 should be able to isolate highly tumorigenic cellular populations which are CXADR+ and not the CXADR- cells. Although we could not detect CXADR expressing cells in the 5 human GBM tissue sections tested, its expression should to be examined in the more GBM tissue samples as well as in other cancer tissue types. In order to better understand its functional role in the cell and to determine its responsiveness to other stimuli, the function of CXADR needs to be further investigated.

Western blotting of CXADR shows the presence of two distinct bands by western blotting. These two bands may be due to post translational modification or splice variants. Although, both of these phenomena occur for CXADR, we found that after

treatment with tunicamycin, a glycosylation inhibitor, the upper band represents a N-linked glycosylation modification on the CXADR protein. These suggest that mAb 7-18 detects the protein specifically and not the sugar residue. Interestingly, it is this upper band which is progressively lost during differentiation and the protein is completely lost upon terminal differentiation. The presence of the sugar residue is not unique to CXADR as CD133 glycosylation is thought to be the mark of stemness and not its mRNA or protein expression [167].

A number of markers are used to distinguish cancer stem cells from the non stem cell population of tumors. The hierarchy of progenitor cells within the cancer stem cell population is not well understood for GBM and the lack of reliable markers is part of the problem. We have identified 10 novel monoclonal antibodies, which may mark some of these populations within the cancer stem cell lineage and indeed the founding clone as well, enabling us to study this phenomena in more detail. CXADR is a putative cancer stem cell marker due to its expression in a wide variety of undifferentiated cells and the lack of it after differentiation as shown in this thesis as well as in the literature. Although, it has the disadvantage of being expressed in other serum cancer cell lines, further investigation into its post translational modifications and regulation may give further insight into its use as a stem cell marker.

6.2.3 Candidate Monoclonals as Therapeutics

Antibodies have successfully been used as therapeutics against various cancers. These affect tumor growth by blocking key signaling molecules (eg. Bevacizumab binds to and blocks VEGF), cell surface receptors (eg. Trastuzumab, antibody targeting EGFR) or

they may be conjugated with a toxin which takes effect once the receptor bound antibody is internalized by the cell via endocytosis (eg. Brentuximab) [319, 382, 383]. Bevacizumab, an anti-VEGF antibody, has shown promise by increasing progression free survival in GBM patients, individually as well as in conjunction with TMZ, although there is no increase in overall survival [12, 13]. Monoclonal antibodies as immune system checkpoint inhibitors are currently used in cancer therapy to boost the body's immune response to the tumor [322]. Identification of novel targets which may be targeted by the candidate monoclonal antibodies may lead to the development of new therapeutics for GBMs. Further, specificity to the GBM stem cell population may allow selective toxicity to this cell population, which is thought to maintain tumor growth and progression. To function as a therapeutic, certain features of the mAb need to be tested; (i) GBM tissue staining to check for its ability to detect its antigen in the tumor (ii) ability to detect cell surface antigen (iii) ability to function as a naked antibody to directly block growth, or should be able to be internalized into the cells. If a toxin is conjugated with an internalized mAb, it will be processed by the cell's lysosomal compartment, which will lead to the release of the toxin, resulting in cytotoxicity. (iv) should not detect antigen in normal tissue.

We have generated 10 monoclonal antibodies which detect subpopulations of cells within the GBM-SCs in culture. All the antibodies detected the antigen on the surface of GBM-SCs as measured by live cell FACS analysis, although not all antibodies were able to stain all three GBM-SC lines tested. In fact, the amount of staining varied for all the antibodies tested. This indicates heterogeneity in the cell surface proteins present in each tumor, suggesting that there may not be one protein which is uniformly detected in all

tumors to be used as a marker. 5 antibodies showing cell surface staining in GS6-22 and GS7-2 cells were used to test for internalization of their binding antigen. The rate of internalization varied between the antibodies as well as according to the cell lines. This indicates the differential rate of receptor or surface protein clearance by each cell line which may be a factor to consider during development of mAbs as toxin conjugated therapeutics. GS7-2 cells showed a high stability and low clearance of 4 out of 5 cell surface proteins tested. The successful internalization in GS6-22 of all 5 antibodies tested, shows that they may potentially be used for toxin conjugated therapeutics.

7 out of 10 candidate monoclonal antibodies were able to successfully stain positive some of the human GBM tumor sections by immunohistochemistry. Of these, 5 antibodies were selected on the basis of cell surface staining and IHC data and were used to stain 70 GBM tumor sections on a tissue array. Additionally, these antibodies were also used to stain other tissue tumors as well as normal tissues using tissue array slides. The heterogeneity between the tumors is apparent in that none of the antibodies were able to stain all the 5 tumor sections tested. Furthermore, any given antibody did not exhibit the same pattern of staining in all of the sections it stained positively, implying that it was picking up different number and type of positive cellular populations in each section. This further highlights that one marker or therapeutic may not target all GBM tumors alike and development of combinatorial protocols is required. Alternatively, this may indicate GBM stem cells in intermediate states of differentiation. Interestingly, none of the antibodies tested were able to stain the normal tissue sections, which is an advantage for further development of these monoclonals as therapeutics.

CXADR expression in human GBMs and other cancer or normal tissues has not been extensively tested. Although it did not stain the 5 human GBM tumor sections, mAb 7-18 does detect CXADR on the cellular surface of live cells. The importance of CXADR in cardiac development and in cardiac conduction in adult mice has been shown[384]. Since it is also likely that CXADR is the receptor for coxsackievirus mediated myocarditis in humans and mice, this will likely rule out its use as a toxin conjugated therapeutic due the high risk of cardiotoxicity in humans [384, 385].

6.2.4 Future Directions

The generation of monoclonals specific to GBM-SCs has allowed us to evaluate their roles as markers and as therapeutics. In both applications, the knowledge of the antigen for each antibody is critical. The identity of the antigens for 9 out of 10 antibodies is still unknown and further identification is required for validation of each antibody, especially because they might be recognizing an antigen which is already used as a stem cell marker.

Large scale immunopurification offers the most effective methodology for this purpose although the source material may vary for each antigen. Flank tumors may provide a rich source of antigen as many of them are not expressed strongly in cell culture and require a large number of cells for detection by western. In addition to immunoaffinity purification, phage display libraries may be utilized for antigen identification. By making phage display libraries from GBM-SC mRNA, which are subsequently expressed on surface of phage particle, it is possible to screen for phages which bind each of the antibodies.

As stated above, for the antibodies to be used as markers, assays used to test for stemness such as ability to differentiate into specific lineages and high tumorigenicity, must be performed on the antibody enriched cells from culture. Further analysis of tumor cell populations using fresh tumor specimens will allow identification of positive population from GBMs, which can then be subsequently tested for tumorigenicity. The staining of GBM stem cells with other known stem cell markers will also be an important step in the further characterization of these antibodies.

Further investigation of the role of CXADR and its post translational modification will be required to identify its role in GBM-SCs. Although it does not appear to play an important role in their proliferation or self renewal based on limited siRNA experiments, its role in invasiveness is unknown. Invasion into the brain parenchyma is a problem in GBM tumors and is one of the main causes for recurrence. The role of CXADR in the formation and maintenance of tight junctions may make it important in cell motility and cell-cell communications in the tumors.

Thesis Conclusions

In summary, to identify GBM-SC vulnerabilities for better therapeutic targeting, we utilized a pooled shRNA screening approach to identify novel genetic targets. SGK1 was identified as an important gene for survival especially in the GBM-SC population of multiple GBM-SC line and may provide an avenue for therapeutic intervention for GBMs. We also described the identification of 10 novel monoclonal antibodies which detect proteins in GBM-SCs, but not in the differentiated populations. These antibodies detect cell surface antigens, are internalized and can stain human tumor tissue sections. Further investigation is required to identify all the antigenic targets of these antibodies and to characterize them as markers for GBM-SCs as well as candidates for targeted therapeutics. The results of this thesis enhance our understanding of GBM stem cells and identify possible new therapeutic targets for this deadly disease.

Bibliography

1. Schwartzbaum, J. A., Fisher, J. L., Aldape, K. D., and Wrensch, M. (2006). Epidemiology and molecular pathology of glioma. Nat Clin Pract Neurol *2*, 494–503; quiz 1 p following 516.

2. Gladson, C. L., Prayson, R. A., and Liu, W. M. (2010). The pathobiology of glioma tumors. Annu Rev Pathol *5*, 33–50.

3. Aldape, K., Zadeh, G., Mansouri, S., Reifenberger, G., and von Deimling, A. (2015). Glioblastoma: pathology, molecular mechanisms and markers. Acta Neuropathol *129*, 829–848.

4. Louis, D. N., Ohgaki, H., Wiestler, O. D., Cavenee, W. K., Burger, P. C., Jouvet, A., Scheithauer, B. W., and Kleihues, P. (2007). The 2007 WHO classification of tumours of the central nervous system. Acta Neuropathol *114*, 97–109.

5. Ostrom, Q. T., Gittleman, H., Farah, P., Ondracek, A., Chen, Y., Wolinsky, Y., Stroup, N. E., Kruchko, C., and Barnholtz-Sloan, J. S. (2013). CBTRUS statistical report: Primary brain and central nervous system tumors diagnosed in the United States in 2006-2010. Neuro Oncol *15 Suppl 2*, ii1–i56.

6. Ostrom, Q. T., Gittleman, H., Fulop, J., Liu, M., Blanda, R., Kromer, C., Wolinsky, Y., Kruchko, C., and Barnholtz-Sloan, J. S. (2015). CBTRUS Statistical Report: Primary Brain and Central Nervous System Tumors Diagnosed in the United States in 2008-2012. Neuro Oncol *17 Suppl 4*, iv1–iv62.

7. Furnari, F. B., Fenton, T., Bachoo, R. M., Mukasa, A., Stommel, J. M., Stegh, A., Hahn, W. C., Ligon, K. L., Louis, D. N., Brennan, C., et al. (2007). Malignant astrocytic glioma: genetics, biology, and paths to treatment. Genes Dev *21*, 2683–2710.

8. Stupp, R., Hegi, M. E., Mason, W. P., van den Bent, M. J., Taphoorn, M. J. B., Janzer, R. C., Ludwin, S. K., Allgeier, A., Fisher, B., Belanger, K., et al. (2009). Effects of radiotherapy with concomitant and adjuvant temozolomide versus radiotherapy alone on survival in glioblastoma in a randomised phase III study: 5-year analysis of the EORTC-NCIC trial. Lancet Oncol *10*, 459–466.

9. Brennan, C. W., Verhaak, R. G. W., McKenna, A., Campos, B., Noushmehr, H., Salama, S. R., Zheng, S., Chakravarty, D., Sanborn, J. Z., Berman, S. H., et al. (2013). The somatic genomic landscape of glioblastoma. Cell *155*, 462–477.

10. Gaspar, L. E., Fisher, B. J., Macdonald, D. R., LeBer, D. V., Halperin, E. C., Schold, S. C., and Cairncross, J. G. (1992). Supratentorial malignant glioma: patterns of recurrence and implications for external beam local treatment. Int J Radiat Oncol Biol Phys *24*, 55–57.

11. Stupp, R., Mason, W. P., van den Bent, M. J., Weller, M., Fisher, B., Taphoorn, M. J. B., Belanger, K., Brandes, A. A., Marosi, C., Bogdahn, U., et al. (2005). Radiotherapy plus concomitant and adjuvant temozolomide for glioblastoma. N Engl J Med *352*, 987–996.

12. Chinot, O. L., Wick, W., Mason, W., Henriksson, R., Saran, F., Nishikawa, R., Carpentier, A. F., Hoang-Xuan, K., Kavan, P., Cernea, D., et al. (2014). Bevacizumab plus radiotherapy-temozolomide for newly diagnosed glioblastoma. N Engl J Med *370*, 709–722.

13. Gilbert, M. R., Dignam, J. J., Armstrong, T. S., Wefel, J. S., Blumenthal, D. T., Vogelbaum, M. A., Colman, H., Chakravarti, A., Pugh, S., Won, M., et al. (2014). A randomized trial of bevacizumab for newly diagnosed glioblastoma. N Engl J Med *370*, 699–708.

14. Ohgaki, H., and Kleihues, P. (2013). The definition of primary and secondary glioblastoma. Clin Cancer Res *19*, 764–772.

15. Yan, H., Parsons, D. W., Jin, G., McLendon, R., Rasheed, B. A., Yuan, W., Kos, I., Batinic-Haberle, I., Jones, S., Riggins, G. J., et al. (2009). IDH1 and IDH2 mutations in gliomas. N Engl J Med *360*, 765–773.

16. Parsons, D. W., Jones, S., Zhang, X., Lin, J. C.-H., Leary, R. J., Angenendt, P., Mankoo, P., Carter, H., Siu, I.-M., Gallia, G. L., et al. (2008). An integrated genomic analysis of human glioblastoma multiforme. Science *321*, 1807–1812.

17. Kannan, K., Inagaki, A., Silber, J., Gorovets, D., Zhang, J., Kastenhuber, E. R., Heguy, A., Petrini, J. H., Chan, T. A., and Huse, J. T. (2012). Whole-exome sequencing identifies ATRX mutation as a key molecular determinant in lower-grade glioma. Oncotarget *3*, 1194–1203.

18. Cancer Genome Atlas Research Network (2008). Comprehensive genomic characterization defines human glioblastoma genes and core pathways. Nature *455*, 1061–1068.

19. Cancer Genome Atlas Research Network, Brat, D. J., Verhaak, R. G. W., Aldape, K. D., Yung, W. K. A., Salama, S. R., Cooper, L. A. D., Rheinbay, E., Miller, C. R., Vitucci, M., et al. (2015). Comprehensive, Integrative Genomic Analysis of Diffuse Lower-Grade Gliomas. N Engl J Med *372*, 2481–2498.

20. Raudino, G., Caffo, M., Caruso, G., Alafaci, C., Raudino, F., Marventano, V., Romano, A., Montemagno, F., Belvedere, M., Maria, F., et al. (2013). From Gliomagenesis to Multimodal Therapeutic Approaches into High-Grade Glioma Treatment. In Evolution of the Molecular Biology of Brain Tumors and the Therapeutic Implications, T. Lichtor, ed. (InTech).

21. Phillips, H. S., Kharbanda, S., Chen, R., Forrest, W. F., Soriano, R. H., Wu, T. D., Misra, A., Nigro, J. M., Colman, H., Soroceanu, L., et al. (2006). Molecular subclasses of high-grade glioma predict prognosis, delineate a pattern of disease progression, and resemble stages in neurogenesis. Cancer Cell *9*, 157–173.

22. Verhaak, R. G. W., Hoadley, K. A., Purdom, E., Wang, V., Qi, Y., Wilkerson, M. D., Miller, C. R., Ding, L., Golub, T., Mesirov, J. P., et al. (2010). Integrated genomic analysis identifies clinically relevant subtypes of glioblastoma characterized by abnormalities in PDGFRA, IDH1, EGFR, and NF1. Cancer Cell *17*, 98–110.

23. Mischel, P. S., Nelson, S. F., and Cloughesy, T. F. (2003). Molecular analysis of glioblastoma: pathway profiling and its implications for patient therapy. Cancer Biol Ther *2*, 242–247.

24. Freije, W. A., Castro-Vargas, F. E., Fang, Z., Horvath, S., Cloughesy, T., Liau, L. M., Mischel, P. S., and Nelson, S. F. (2004). Gene expression profiling of gliomas strongly predicts survival. Cancer Res *64*, 6503–6510.

25. Cairncross, J. G., Ueki, K., Zlatescu, M. C., Lisle, D. K., Finkelstein, D. M., Hammond, R. R., Silver, J. S., Stark, P. C., Macdonald, D. R., Ino, Y., et al. (1998). Specific genetic predictors of chemotherapeutic response and survival in patients with anaplastic oligodendrogliomas. J Natl Cancer Inst *90*, 1473–1479.

26. Aldape, K. D., Ballman, K., Furth, A., Buckner, J. C., Giannini, C., Burger, P. C., Scheithauer, B. W., Jenkins, R. B., and James, C. D. (2004). Immunohistochemical detection of EGFRvIII in high malignancy grade astrocytomas and evaluation of prognostic significance. J Neuropathol Exp Neurol *63*, 700–707.

27. Ceccarelli, M., Barthel, F. P., Malta, T. M., Sabedot, T. S., Salama, S. R., Murray, B. A., Morozova, O., Newton, Y., Radenbaugh, A., Pagnotta, S. M., et al. (2016). Molecular Profiling Reveals Biologically Discrete Subsets and Pathways of Progression in Diffuse Glioma. Cell *164*, 550–563.

28. Esteller, M., Hamilton, S. R., Burger, P. C., Baylin, S. B., and Herman, J. G. (1999). Inactivation of the DNA repair gene O6-methylguanine-DNA

methyltransferase by promoter hypermethylation is a common event in primary human neoplasia. Cancer Res *59*, 793–797.

29. Tisdale, M. J. (1987). Antitumour imidazotetrazines—XV. Biochem Pharmacol *36*, 457–462.

30. Watts, G. S., Pieper, R. O., Costello, J. F., Peng, Y. M., Dalton, W. S., and Futscher, B. W. (1997). Methylation of discrete regions of the O6-methylguanine DNA methyltransferase (MGMT) CpG island is associated with heterochromatinization of the MGMT transcription start site and silencing of the gene. Mol Cell Biol *17*, 5612–5619.

31. Hegi, M. E., Diserens, A.-C., Gorlia, T., Hamou, M.-F., de Tribolet, N., Weller, M., Kros, J. M., Hainfellner, J. A., Mason, W., Mariani, L., et al. (2005). MGMT gene silencing and benefit from temozolomide in glioblastoma. N Engl J Med *352*, 997–1003.

32. Wick, W., Platten, M., Meisner, C., Felsberg, J., Tabatabai, G., Simon, M., Nikkhah, G., Papsdorf, K., Steinbach, J. P., Sabel, M., et al. (2012). Temozolomide chemotherapy alone versus radiotherapy alone for malignant astrocytoma in the elderly: the NOA-08 randomised, phase 3 trial. Lancet Oncol *13*, 707–715.

33. Noushmehr, H., Weisenberger, D. J., Diefes, K., Phillips, H. S., Pujara, K., Berman, B. P., Pan, F., Pelloski, C. E., Sulman, E. P., Bhat, K. P., et al. (2010). Identification of a CpG island methylator phenotype that defines a distinct subgroup of glioma. Cancer Cell *17*, 510–522.

34. Dang, L., White, D. W., Gross, S., Bennett, B. D., Bittinger, M. A., Driggers, E. M., Fantin, V. R., Jang, H. G., Jin, S., Keenan, M. C., et al. (2009). Cancer-associated IDH1 mutations produce 2-hydroxyglutarate. Nature *462*, 739–744.

35. Xu, W., Yang, H., Liu, Y., Yang, Y., Wang, P., Kim, S.-H., Ito, S., Yang, C., Wang, P., Xiao, M.-T., et al. (2011). Oncometabolite 2-hydroxyglutarate is a competitive inhibitor of α-ketoglutarate-dependent dioxygenases. Cancer Cell *19*, 17–30.

36. Yang, H., Ye, D., Guan, K.-L., and Xiong, Y. (2012). IDH1 and IDH2 mutations in tumorigenesis: mechanistic insights and clinical perspectives. Clin Cancer Res *18*, 5562–5571.

37. Sottoriva, A., Spiteri, I., Shibata, D., Curtis, C., and Tavaré, S. (2013). Single-molecule genomic data delineate patient-specific tumor profiles and cancer stem cell organization. Cancer Res *73*, 41–49.

38. Patel, A. P., Tirosh, I., Trombetta, J. J., Shalek, A. K., Gillespie, S. M., Wakimoto, H., Cahill, D. P., Nahed, B. V., Curry, W. T., Martuza, R. L., et al. (2014). Single-cell RNA-seq highlights intratumoral heterogeneity in primary glioblastoma. Science *344*, 1396–1401.

39. Hanahan, D., and Weinberg, R. A. (2011). Hallmarks of cancer: the next generation. Cell *144*, 646–674.

40. Vogelstein, B., and Kinzler, K. W. (2015). The Path to Cancer --Three Strikes and You're Out. N Engl J Med *373*, 1895–1898.

41. Dunn, G. P., Rinne, M. L., Wykosky, J., Genovese, G., Quayle, S. N., Dunn, I. F., Agarwalla, P. K., Chheda, M. G., Campos, B., Wang, A., et al. (2012). Emerging insights into the molecular and cellular basis of glioblastoma. Genes Dev *26*, 756–784.

42. Bieging, K. T., Mello, S. S., and Attardi, L. D. (2014). Unravelling mechanisms of p53-mediated tumour suppression. Nat Rev Cancer *14*, 359–370.

43. Malumbres, M., and Barbacid, M. (2009). Cell cycle, CDKs and cancer: a changing paradigm. Nat Rev Cancer *9*, 153–166.

44. Chen, H.-Z., Tsai, S.-Y., and Leone, G. (2009). Emerging roles of E2Fs in cancer: an exit from cell cycle control. Nat Rev Cancer *9*, 785–797.

45. Crespo, I., Vital, A. L., Gonzalez-Tablas, M., Patino, M. del C., Otero, A., Lopes, M. C., de Oliveira, C., Domingues, P., Orfao, A., and Tabernero, M. D. (2015). Molecular and Genomic Alterations in Glioblastoma Multiforme. Am J Pathol *185*, 1820–1833.

46. Lemmon, M. A., and Schlessinger, J. (2010). Cell signaling by receptor tyrosine kinases. Cell *141*, 1117–1134.

47. Brennan, C., Momota, H., Hambardzumyan, D., Ozawa, T., Tandon, A., Pedraza, A., and Holland, E. (2009). Glioblastoma subclasses can be defined by activity among signal transduction pathways and associated genomic alterations. PLoS ONE *4*, e7752.

48. Hurtt, M. R., Moossy, J., Donovan-Peluso, M., and Locker, J. (1992). Amplification of epidermal growth factor receptor gene in gliomas: histopathology and prognosis. J Neuropathol Exp Neurol *51*, 84–90.

49. Ekstrand, A. J., Sugawa, N., James, C. D., and Collins, V. P. (1992). Amplified and rearranged epidermal growth factor receptor genes in human glioblastomas reveal

deletions of sequences encoding portions of the N- and/or C-terminal tails. Proc Natl Acad Sci U S A *89*, 4309–4313.

50. Wong, A. J., Ruppert, J. M., Bigner, S. H., Grzeschik, C. H., Humphrey, P. A., Bigner, D. S., and Vogelstein, B. (1992). Structural alterations of the epidermal growth factor receptor gene in human gliomas. Proc Natl Acad Sci U S A *89*, 2965–2969.

51. Huang, H. S., Nagane, M., Klingbeil, C. K., Lin, H., Nishikawa, R., Ji, X. D., Huang, C. M., Gill, G. N., Wiley, H. S., and Cavenee, W. K. (1997). The enhanced tumorigenic activity of a mutant epidermal growth factor receptor common in human cancers is mediated by threshold levels of constitutive tyrosine phosphorylation and unattenuated signaling. J Biol Chem *272*, 2927–2935.

52. Shinojima, N., Tada, K., Shiraishi, S., Kamiryo, T., Kochi, M., Nakamura, H., Makino, K., Saya, H., Hirano, H., Kuratsu, J.-I., et al. (2003). Prognostic value of epidermal growth factor receptor in patients with glioblastoma multiforme. Cancer Res *63*, 6962–6970.

53. Nishikawa, R., Sugiyama, T., Narita, Y., Furnari, F., Cavenee, W. K., and Matsutani, M. (2004). Immunohistochemical analysis of the mutant epidermal growth factor, ΔEGFR, in glioblastoma. Brain Tumor Pathol *21*, 53–56.

54. Inda, M.-M., Bonavia, R., Mukasa, A., Narita, Y., Sah, D. W. Y., Vandenberg, S., Brennan, C., Johns, T. G., Bachoo, R., Hadwiger, P., et al. (2010). Tumor heterogeneity is an active process maintained by a mutant EGFR-induced cytokine circuit in glioblastoma. Genes Dev *24*, 1731–1745.

55. Ozawa, T., Brennan, C. W., Wang, L., Squatrito, M., Sasayama, T., Nakada, M., Huse, J. T., Pedraza, A., Utsuki, S., Yasui, Y., et al. (2010). PDGFRA gene rearrangements are frequent genetic events in PDGFRA-amplified glioblastomas. Genes Dev *24*, 2205–2218.

56. Dai, C., Celestino, J. C., Okada, Y., Louis, D. N., Fuller, G. N., and Holland, E. C. (2001). PDGF autocrine stimulation dedifferentiates cultured astrocytes and induces oligodendrogliomas and oligoastrocytomas from neural progenitors and astrocytes in vivo. Genes Dev *15*, 1913–1925.

57. Stommel, J. M., Kimmelman, A. C., Ying, H., Nabioullin, R., Ponugoti, A. H., Wiedemeyer, R., Stegh, A. H., Bradner, J. E., Ligon, K. L., Brennan, C., et al. (2007). Coactivation of receptor tyrosine kinases affects the response of tumor cells to targeted therapies. Science *318*, 287–290.

58. Du, J., Bernasconi, P., Clauser, K. R., Mani, D. R., Finn, S. P., Beroukhim, R., Burns, M., Julian, B., Peng, X. P., Hieronymus, H., et al. (2009). Bead-based profiling of tyrosine kinase phosphorylation identifies SRC as a potential target for glioblastoma therapy. Nat Biotechnol *27*, 77–83.

59. Lathia, J. D., Gallagher, J., Heddleston, J. M., Wang, J., Eyler, C. E., Macswords, J., Wu, Q., Vasanji, A., McLendon, R. E., Hjelmeland, A. B., et al. (2010). Integrin alpha 6 regulates glioblastoma stem cells. Cell Stem Cell *6*, 421–432.

60. Mitra, S. K., and Schlaepfer, D. D. (2006). Integrin-regulated FAK-Src signaling in normal and cancer cells. Curr Opin Cell Biol *18*, 516–523.

61. Vanhaesebroeck, B., Stephens, L., and Hawkins, P. (2012). PI3K signalling: the path to discovery and understanding. Nat Rev Mol Cell Biol *13*, 195–203.

62. Courtney, K. D., Corcoran, R. B., and Engelman, J. A. (2010). The PI3K pathway as drug target in human cancer. J Clin Oncol *28*, 1075–1083.

63. Sasaki, H., Zlatescu, M. C., Betensky, R. A., Ino, Y., Cairncross, J. G., and Louis, D. N. (2001). PTEN is a target of chromosome 10q loss in anaplastic oligodendrogliomas and PTEN alterations are associated with poor prognosis. Am J Pathol *159*, 359–367.

64. Wang, X., Trotman, L. C., Koppie, T., Alimonti, A., Chen, Z., Gao, Z., Wang, J., Erdjument-Bromage, H., Tempst, P., Cordon-Cardo, C., et al. (2007). NEDD4-1 is a proto-oncogenic ubiquitin ligase for PTEN. Cell *128*, 129–139.

65. Zheng, H., Ying, H., Yan, H., Kimmelman, A. C., Hiller, D. J., Chen, A.-J., Perry, S. R., Tonon, G., Chu, G. C., Ding, Z., et al. (2008). p53 and Pten control neural and glioma stem/progenitor cell renewal and differentiation. Nature *455*, 1129–1133.

66. Kwon, C.-H., Zhao, D., Chen, J., Alcantara, S., Li, Y., Burns, D. K., Mason, R. P., Lee, E. Y.-H. P., Wu, H., and Parada, L. F. (2008). Pten haploinsufficiency accelerates formation of high-grade astrocytomas. Cancer Res *68*, 3286–3294.

67. Chow, L. M. L., Endersby, R., Zhu, X., Rankin, S., Qu, C., Zhang, J., Broniscer, A., Ellison, D. W., and Baker, S. J. (2011). Cooperativity within and among Pten, p53, and Rb pathways induces high-grade astrocytoma in adult brain. Cancer Cell *19*, 305–316.

68. Corral, T., Jiménez, M., Hernández-Muñoz, I., Pérez de Castro, I., and Pellicer, A. (2003). NF1 modulates the effects of Ras oncogenes: evidence of other NF1 function besides its GAP activity. J Cell Physiol *197*, 214–224.

69. Sandsmark, D. K., Zhang, H., Hegedus, B., Pelletier, C. L., Weber, J. D., and Gutmann, D. H. (2007). Nucleophosmin mediates mammalian target of rapamycin-dependent actin cytoskeleton dynamics and proliferation in neurofibromin-deficient astrocytes. Cancer Res *67*, 4790–4799.

70. Banerjee, S., Byrd, J. N., Gianino, S. M., Harpstrite, S. E., Rodriguez, F. J., Tuskan, R. G., Reilly, K. M., Piwnica-Worms, D. R., and Gutmann, D. H. (2010). The neurofibromatosis type 1 tumor suppressor controls cell growth by regulating signal transducer and activator of transcription-3 activity in vitro and in vivo. Cancer Res *70*, 1356–1366.

71. Bajenaru, M. L., Zhu, Y., Hedrick, N. M., Donahoe, J., Parada, L. F., and Gutmann, D. H. (2002). Astrocyte-specific inactivation of the neurofibromatosis 1 gene (NF1) is insufficient for astrocytoma formation. Mol Cell Biol *22*, 5100–5113.

72. Alcantara Llaguno, S., Chen, J., Kwon, C.-H., Jackson, E. L., Li, Y., Burns, D. K., Alvarez-Buylla, A., and Parada, L. F. (2009). Malignant astrocytomas originate from neural stem/progenitor cells in a somatic tumor suppressor mouse model. Cancer Cell *15*, 45–56.

73. Carro, M. S., Lim, W. K., Alvarez, M. J., Bollo, R. J., Zhao, X., Snyder, E. Y., Sulman, E. P., Anne, S. L., Doetsch, F., Colman, H., et al. (2010). The transcriptional network for mesenchymal transformation of brain tumours. Nature *463*, 318–325.

74. Sherry, M. M., Reeves, A., Wu, J. K., and Cochran, B. H. (2009). STAT3 is required for proliferation and maintenance of multipotency in glioblastoma stem cells. Stem Cells *27*, 2383–2392.

75. Konnikova, L., Kotecki, M., Kruger, M. M., and Cochran, B. H. (2003). Knockdown of STAT3 expression by RNAi induces apoptosis in astrocytoma cells. BMC Cancer *3*, 23.

76. Bhat, K. P. L., Salazar, K. L., Balasubramaniyan, V., Wani, K., Heathcock, L., Hollingsworth, F., James, J. D., Gumin, J., Diefes, K. L., Kim, S. H., et al. (2011). The transcriptional coactivator TAZ regulates mesenchymal differentiation in malignant glioma. Genes Dev *25*, 2594–2609.

77. Raychaudhuri, B., Han, Y., Lu, T., and Vogelbaum, M. A. (2007). Aberrant constitutive activation of nuclear factor kappaB in glioblastoma multiforme drives invasive phenotype. J Neurooncol *85*, 39–47.

78. Bredel, M., Scholtens, D. M., Yadav, A. K., Alvarez, A. A., Renfrow, J. J., Chandler, J. P., Yu, I. L. Y., Carro, M. S., Dai, F., Tagge, M. J., et al. (2011). NFKBIA deletion in glioblastomas. N Engl J Med *364*, 627–637.

79. Habib, A. A., Chatterjee, S., Park, S. K., Ratan, R. R., Lefebvre, S., and Vartanian, T. (2001). The epidermal growth factor receptor engages receptor interacting protein and nuclear factor-kappa B (NF-kappa B)-inducing kinase to activate NF-kappa B. Identification of a novel receptor-tyrosine kinase signalosome. J Biol Chem *276*, 8865–8874.

80. Vescovi, A. L., Galli, R., and Reynolds, B. A. (2006). Brain tumour stem cells. Nat Rev Cancer *6*, 425–436.

81. Beck, B., and Blanpain, C. (2013). Unravelling cancer stem cell potential. Nat Rev Cancer *13*, 727–738.

82. Venere, M., Fine, H. A., Dirks, P. B., and Rich, J. N. (2011). Cancer stem cells in gliomas: identifying and understanding the apex cell in cancer's hierarchy. Glia *59*, 1148–1154.

83. Stiles, C. D., and Rowitch, D. H. (2008). Glioma stem cells: a midterm exam. Neuron *58*, 832–846.

84. Quintana, E., Shackleton, M., Foster, H. R., Fullen, D. R., Sabel, M. S., Johnson, T. M., and Morrison, S. J. (2010). Phenotypic heterogeneity among tumorigenic melanoma cells from patients that is reversible and not hierarchically organized. Cancer Cell *18*, 510–523.

85. Somervaille, T. C. P., Matheny, C. J., Spencer, G. J., Iwasaki, M., Rinn, J. L., Witten, D. M., Chang, H. Y., Shurtleff, S. A., Downing, J. R., and Cleary, M. L. (2009). Hierarchical maintenance of MLL myeloid leukemia stem cells employs a transcriptional program shared with embryonic rather than adult stem cells. Cell Stem Cell *4*, 129–140.

86. Taylor, M. D., Poppleton, H., Fuller, C., Su, X., Liu, Y., Jensen, P., Magdaleno, S., Dalton, J., Calabrese, C., Board, J., et al. (2005). Radial glia cells are candidate stem cells of ependymoma. Cancer Cell *8*, 323–335.

87. Bonnet, D., and Dick, J. E. (1997). Human acute myeloid leukemia is organized as a hierarchy that originates from a primitive hematopoietic cell. Nat Med *3*, 730–737.

88. Singh, S. K., Clarke, I. D., Terasaki, M., Bonn, V. E., Hawkins, C., Squire, J., and Dirks, P. B. (2003). Identification of a cancer stem cell in human brain tumors. Cancer Res *63*, 5821–5828.

89. Eppert, K., Takenaka, K., Lechman, E. R., Waldron, L., Nilsson, B., van Galen, P., Metzeler, K. H., Poeppl, A., Ling, V., Beyene, J., et al. (2011). Stem cell gene expression programs influence clinical outcome in human leukemia. Nat Med *17*, 1086–1093.

90. Beier, D., Hau, P., Proescholdt, M., Lohmeier, A., Wischhusen, J., Oefner, P. J., Aigner, L., Brawanski, A., Bogdahn, U., and Beier, C. P. (2007). CD133(+) and CD133(-) glioblastoma-derived cancer stem cells show differential growth characteristics and molecular profiles. Cancer Res *67*, 4010–4015.

91. Magee, J. A., Piskounova, E., and Morrison, S. J. (2012). Cancer stem cells: impact, heterogeneity, and uncertainty. Cancer Cell *21*, 283–296.

92. Rahman, M., Deleyrolle, L., Vedam-Mai, V., Azari, H., Abd-El-Barr, M., and Reynolds, B. A. (2011). The cancer stem cell hypothesis: failures and pitfalls. Neurosurgery *68*, 531–45; discussion 545.

93. Quintana, E., Shackleton, M., Sabel, M. S., Fullen, D. R., Johnson, T. M., and Morrison, S. J. (2008). Efficient tumour formation by single human melanoma cells. Nature *456*, 593–598.

94. Suvà, M. L., Rheinbay, E., Gillespie, S. M., Patel, A. P., Wakimoto, H., Rabkin, S. D., Riggi, N., Chi, A. S., Cahill, D. P., Nahed, B. V., et al. (2014). Reconstructing and reprogramming the tumor-propagating potential of glioblastoma stem-like cells. Cell *157*, 580–594.

95. Heddleston, J. M., Li, Z., McLendon, R. E., Hjelmeland, A. B., and Rich, J. N. (2009). The hypoxic microenvironment maintains glioblastoma stem cells and promotes reprogramming towards a cancer stem cell phenotype. Cell Cycle *8*, 3274–3284.

96. Lathia, J. D., Mack, S. C., Mulkearns-Hubert, E. E., Valentim, C. L. L., and Rich, J. N. (2015). Cancer stem cells in glioblastoma. Genes Dev *29*, 1203–1217.

97. Masters, J. R. W., and Köberle, B. (2003). Curing metastatic cancer: lessons from testicular germ-cell tumours. Nat Rev Cancer *3*, 517–525.

98. Poulikakos, P. I., and Rosen, N. (2011). Mutant BRAF melanomas--dependence and resistance. Cancer Cell *19*, 11–15.

99. Villanueva, J., Vultur, A., Lee, J. T., Somasundaram, R., Fukunaga-Kalabis, M., Cipolla, A. K., Wubbenhorst, B., Xu, X., Gimotty, P. A., Kee, D., et al. (2010). Acquired resistance to BRAF inhibitors mediated by a RAF kinase switch in melanoma can be overcome by cotargeting MEK and IGF-1R/PI3K. Cancer Cell *18*, 683–695.

100. Singh, S. K., Hawkins, C., Clarke, I. D., Squire, J. A., Bayani, J., Hide, T., Henkelman, R. M., Cusimano, M. D., and Dirks, P. B. (2004). Identification of human brain tumour initiating cells. Nature *432*, 396–401.

101. Hemmati, H. D., Nakano, I., Lazareff, J. A., Masterman-Smith, M., Geschwind, D. H., Bronner-Fraser, M., and Kornblum, H. I. (2003). Cancerous stem cells can arise from pediatric brain tumors. Proc Natl Acad Sci U S A *100*, 15178–15183.

102. Galli, R., Binda, E., Orfanelli, U., Cipelletti, B., Gritti, A., De Vitis, S., Fiocco, R., Foroni, C., Dimeco, F., and Vescovi, A. (2004). Isolation and characterization of tumorigenic, stem-like neural precursors from human glioblastoma. Cancer Res *64*, 7011–7021.

103. Hambardzumyan, D., Parada, L. F., Holland, E. C., and Charest, A. (2011). Genetic modeling of gliomas in mice: new tools to tackle old problems. Glia *59*, 1155–1168.

104. Alcantara Llaguno, S. R., Wang, Z., Sun, D., Chen, J., Xu, J., Kim, E., Hatanpaa, K. J., Raisanen, J. M., Burns, D. K., Johnson, J. E., et al. (2015). Adult Lineage-Restricted CNS Progenitors Specify Distinct Glioblastoma Subtypes. Cancer Cell *28*, 429–440.

105. Friedmann-Morvinski, D., Bushong, E. A., Ke, E., Soda, Y., Marumoto, T., Singer, O., Ellisman, M. H., and Verma, I. M. (2012). Dedifferentiation of neurons and astrocytes by oncogenes can induce gliomas in mice. Science *338*, 1080–1084.

106. Seri, B., García-Verdugo, J. M., Collado-Morente, L., McEwen, B. S., and Alvarez-Buylla, A. (2004). Cell types, lineage, and architecture of the germinal zone in the adult dentate gyrus. J Comp Neurol *478*, 359–378.

107. Doetsch, F., García-Verdugo, J. M., and Alvarez-Buylla, A. (1999). Regeneration of a germinal layer in the adult mammalian brain. Proc Natl Acad Sci U S A *96*, 11619–11624.

108. Suh, H., Consiglio, A., Ray, J., Sawai, T., D'Amour, K. A., and Gage, F. H. (2007). In vivo fate analysis reveals the multipotent and self-renewal capacities of Sox2+ neural stem cells in the adult hippocampus. Cell Stem Cell *1*, 515–528.

109. Ming, G., and Song, H. (2005). Adult neurogenesis in the mammalian central nervous system. Annu Rev Neurosci *28*, 223–250.

110. Chenn, A., and McConnell, S. K. (1995). Cleavage orientation and the asymmetric inheritance of Notch1 immunoreactivity in mammalian neurogenesis. Cell *82*, 631–641.

111. Reynolds, B. A., and Weiss, S. (1992). Generation of neurons and astrocytes from isolated cells of the adult mammalian central nervous system. Science *255*, 1707–1710.

112. Gritti, A., Parati, E. A., Cova, L., Frolichsthal, P., Galli, R., Wanke, E., Faravelli, L., Morassutti, D. J., Roisen, F., Nickel, D. D., et al. (1996). Multipotential stem cells from the adult mouse brain proliferate and self-renew in response to basic fibroblast growth factor. J Neurosci *16*, 1091–1100.

113. Vescovi, A. L., Parati, E. A., Gritti, A., Poulin, P., Ferrario, M., Wanke, E., Frölichsthal-Schoeller, P., Cova, L., Arcellana-Panlilio, M., Colombo, A., et al. (1999). Isolation and cloning of multipotential stem cells from the embryonic human CNS and establishment of transplantable human neural stem cell lines by epigenetic stimulation. Exp Neurol *156*, 71–83.

114. Ignatova, T. N., Kukekov, V. G., Laywell, E. D., Suslov, O. N., Vrionis, F. D., and Steindler, D. A. (2002). Human cortical glial tumors contain neural stem-like cells expressing astroglial and neuronal markers in vitro. Glia *39*, 193–206.

115. Pollard, S. M., Yoshikawa, K., Clarke, I. D., Danovi, D., Stricker, S., Russell, R., Bayani, J., Head, R., Lee, M., Bernstein, M., et al. (2009). Glioma stem cell lines expanded in adherent culture have tumor-specific phenotypes and are suitable for chemical and genetic screens. Cell Stem Cell *4*, 568–580.

116. Pastrana, E., Silva-Vargas, V., and Doetsch, F. (2011). Eyes wide open: a critical review of sphere-formation as an assay for stem cells. Cell Stem Cell *8*, 486–498.

117. Singh, S., and Dirks, P. B. (2007). Brain tumor stem cells: identification and concepts. Neurosurg Clin N Am *18*, 31–8, viii.

118. Tunici, P., Bissola, L., Lualdi, E., Pollo, B., Cajola, L., Broggi, G., Sozzi, G., and Finocchiaro, G. (2004). Genetic alterations and in vivo tumorigenicity of neurospheres derived from an adult glioblastoma. Mol Cancer *3*, 25.

119. Inda, M.-D.-M., Bonavia, R., and Seoane, J. (2014). Glioblastoma multiforme: a look inside its heterogeneous nature. Cancers (Basel) *6*, 226–239.

120. Ligon, K. L., Huillard, E., Mehta, S., Kesari, S., Liu, H., Alberta, J. A., Bachoo, R. M., Kane, M., Louis, D. N., Depinho, R. A., et al. (2007). Olig2-regulated lineage-restricted pathway controls replication competence in neural stem cells and malignant glioma. Neuron *53*, 503–517.

121. Lee, J., Kotliarova, S., Kotliarov, Y., Li, A., Su, Q., Donin, N. M., Pastorino, S., Purow, B. W., Christopher, N., Zhang, W., et al. (2006). Tumor stem cells derived from glioblastomas cultured in bFGF and EGF more closely mirror the phenotype and genotype of primary tumors than do serum-cultured cell lines. Cancer Cell *9*, 391–403.

122. McKay, R. (1997). Stem cells in the central nervous system. Science *276*, 66–71.

123. Li, A., Walling, J., Kotliarov, Y., Center, A., Steed, M. E., Ahn, S. J., Rosenblum, M., Mikkelsen, T., Zenklusen, J. C., and Fine, H. A. (2008). Genomic changes and gene expression profiles reveal that established glioma cell lines are poorly representative of primary human gliomas. Mol Cancer Res *6*, 21–30.

124. Wakimoto, H., Mohapatra, G., Kanai, R., Curry, W. T., Yip, S., Nitta, M., Patel, A. P., Barnard, Z. R., Stemmer-Rachamimov, A. O., Louis, D. N., et al. (2012). Maintenance of primary tumor phenotype and genotype in glioblastoma stem cells. Neuro Oncol *14*, 132–144.

125. Modrek, A. S., Bayin, N. S., and Placantonakis, D. G. (2014). Brain stem cells as the cell of origin in glioma. World J Stem Cells *6*, 43–52.

126. Holland, E. C. (2000). Glioblastoma multiforme: the terminator. Proc Natl Acad Sci U S A *97*, 6242–6244.

127. Uhrbom, L., Dai, C., Celestino, J. C., Rosenblum, M. K., Fuller, G. N., and Holland, E. C. (2002). Ink4a-Arf loss cooperates with KRas activation in astrocytes and neural progenitors to generate glioblastomas of various morphologies depending on activated Akt. Cancer Res *62*, 5551–5558.

128. Lindberg, N., Kastemar, M., Olofsson, T., Smits, A., and Uhrbom, L. (2009). Oligodendrocyte progenitor cells can act as cell of origin for experimental glioma. Oncogene *28*, 2266–2275.

129. Liu, C., Sage, J. C., Miller, M. R., Verhaak, R. G. W., Hippenmeyer, S., Vogel, H., Foreman, O., Bronson, R. T., Nishiyama, A., Luo, L., et al. (2011). Mosaic analysis with double markers reveals tumor cell of origin in glioma. Cell *146*, 209–221.

130. Geha, S., Pallud, J., Junier, M.-P., Devaux, B., Leonard, N., Chassoux, F., Chneiweiss, H., Daumas-Duport, C., and Varlet, P. (2010). NG2+/Olig2+ cells are

the major cycle-related cell population of the adult human normal brain. Brain Pathol *20*, 399–411.

131. Bachoo, R. M., Maher, E. A., Ligon, K. L., Sharpless, N. E., Chan, S. S., You, M. J., Tang, Y., DeFrances, J., Stover, E., Weissleder, R., et al. (2002). Epidermal growth factor receptor and Ink4a/Arf: convergent mechanisms governing terminal differentiation and transformation along the neural stem cell to astrocyte axis. Cancer Cell *1*, 269–277.

132. Bruggeman, S. W. M., Hulsman, D., Tanger, E., Buckle, T., Blom, M., Zevenhoven, J., van Tellingen, O., and van Lohuizen, M. (2007). Bmi1 controls tumor development in an Ink4a/Arf-independent manner in a mouse model for glioma. Cancer Cell *12*, 328–341.

133. Doetsch, F., Verdugo, J. M.-G., Caille, I., Alvarez-Buylla, A., Chao, M. V., and Casaccia-Bonnefil, P. (2002). Lack of the cell-cycle inhibitor p27Kip1 results in selective increase of transit-amplifying cells for adult neurogenesis. J Neurosci *22*, 2255–2264.

134. Hardee, M. E., and Zagzag, D. (2012). Mechanisms of glioma-associated neovascularization. Am J Pathol *181*, 1126–1141.

135. Soda, Y., Marumoto, T., Friedmann-Morvinski, D., Soda, M., Liu, F., Michiue, H., Pastorino, S., Yang, M., Hoffman, R. M., Kesari, S., et al. (2011). Transdifferentiation of glioblastoma cells into vascular endothelial cells. Proc Natl Acad Sci U S A *108*, 4274–4280.

136. Ricci-Vitiani, L., Pallini, R., Biffoni, M., Todaro, M., Invernici, G., Cenci, T., Maira, G., Parati, E. A., Stassi, G., Larocca, L. M., et al. (2010). Tumour vascularization via endothelial differentiation of glioblastoma stem-like cells. Nature *468*, 824–828.

137. Zhao, Y., Dong, J., Huang, Q., Lou, M., Wang, A., and Lan, Q. (2010). Endothelial cell transdifferentiation of human glioma stem progenitor cells in vitro. Brain Res Bull *82*, 308–312.

138. Dong, J., Zhao, Y., Huang, Q., Fei, X., Diao, Y., Shen, Y., Xiao, H., Zhang, T., Lan, Q., and Gu, X. (2011). Glioma stem/progenitor cells contribute to neovascularization via transdifferentiation. Stem Cell Rev *7*, 141–152.

139. Meyer, M., Reimand, J., Lan, X., Head, R., Zhu, X., Kushida, M., Bayani, J., Pressey, J. C., Lionel, A. C., Clarke, I. D., et al. (2015). Single cell-derived clonal analysis of human glioblastoma links functional and genomic heterogeneity. Proc Natl Acad Sci U S A *112*, 851–856.

140. Chen, J., Li, Y., Yu, T.-S., McKay, R. M., Burns, D. K., Kernie, S. G., and Parada, L. F. (2012). A restricted cell population propagates glioblastoma growth after chemotherapy. Nature *488*, 522–526.

141. Blough, M. D., Westgate, M. R., Beauchamp, D., Kelly, J. J., Stechishin, O., Ramirez, A. L., Weiss, S., and Cairncross, J. G. (2010). Sensitivity to temozolomide in brain tumor initiating cells. Neuro Oncol *12*, 756–760.

142. Eramo, A., Ricci-Vitiani, L., Zeuner, A., Pallini, R., Lotti, F., Sette, G., Pilozzi, E., Larocca, L. M., Peschle, C., and De Maria, R. (2006). Chemotherapy resistance of glioblastoma stem cells. Cell Death Differ *13*, 1238–1241.

143. Clement, V., Sanchez, P., de Tribolet, N., Radovanovic, I., and Ruiz i Altaba, A. (2007). HEDGEHOG-GLI1 signaling regulates human glioma growth, cancer stem cell self-renewal, and tumorigenicity. Curr Biol *17*, 165–172.

144. Beier, D., Röhrl, S., Pillai, D. R., Schwarz, S., Kunz-Schughart, L. A., Leukel, P., Proescholdt, M., Brawanski, A., Bogdahn, U., Trampe-Kieslich, A., et al. (2008). Temozolomide preferentially depletes cancer stem cells in glioblastoma. Cancer Res *68*, 5706–5715.

145. Mihaliak, A. M., Gilbert, C. A., Li, L., Daou, M.-C., Moser, R. P., Reeves, A., Cochran, B. H., and Ross, A. H. (2010). Clinically relevant doses of chemotherapy agents reversibly block formation of glioblastoma neurospheres. Cancer Lett *296*, 168–177.

146. Bleau, A.-M., Hambardzumyan, D., Ozawa, T., Fomchenko, E. I., Huse, J. T., Brennan, C. W., and Holland, E. C. (2009). PTEN/PI3K/Akt pathway regulates the side population phenotype and ABCG2 activity in glioma tumor stem-like cells. Cell Stem Cell *4*, 226–235.

147. Lamoral-Theys, D., Le Mercier, M., Le Calvé, B., Rynkowski, M. A., Bruyère, C., Decaestecker, C., Haibe-Kains, B., Bontempi, G., Dubois, J., Lefranc, F., et al. (2010). Long-term temozolomide treatment induces marked amino metabolism modifications and an increase in TMZ sensitivity in Hs683 oligodendroglioma cells. Neoplasia *12*, 69–79.

148. Liu, G., Yuan, X., Zeng, Z., Tunici, P., Ng, H., Abdulkadir, I. R., Lu, L., Irvin, D., Black, K. L., and Yu, J. S. (2006). Analysis of gene expression and chemoresistance of CD133+ cancer stem cells in glioblastoma. Mol Cancer *5*, 67.

149. Beier, D., Schulz, J. B., and Beier, C. P. (2011). Chemoresistance of glioblastoma cancer stem cells--much more complex than expected. Mol Cancer *10*, 128.

150. Tamura, K., Aoyagi, M., Wakimoto, H., Ando, N., Nariai, T., Yamamoto, M., and Ohno, K. (2010). Accumulation of CD133-positive glioma cells after high-dose irradiation by Gamma Knife surgery plus external beam radiation. J Neurosurg *113*, 310–318.

151. Bao, S., Wu, Q., McLendon, R. E., Hao, Y., Shi, Q., Hjelmeland, A. B., Dewhirst, M. W., Bigner, D. D., and Rich, J. N. (2006). Glioma stem cells promote radioresistance by preferential activation of the DNA damage response. Nature *444*, 756–760.

152. Ropolo, M., Daga, A., Griffero, F., Foresta, M., Casartelli, G., Zunino, A., Poggi, A., Cappelli, E., Zona, G., Spaziante, R., et al. (2009). Comparative analysis of DNA repair in stem and nonstem glioma cell cultures. Mol Cancer Res *7*, 383–392.

153. McCord, A. M., Jamal, M., Williams, E. S., Camphausen, K., and Tofilon, P. J. (2009). CD133+ glioblastoma stem-like cells are radiosensitive with a defective DNA damage response compared with established cell lines. Clin Cancer Res *15*, 5145–5153.

154. Bhat, K. P. L., Balasubramaniyan, V., Vaillant, B., Ezhilarasan, R., Hummelink, K., Hollingsworth, F., Wani, K., Heathcock, L., James, J. D., Goodman, L. D., et al. (2013). Mesenchymal differentiation mediated by NF-κB promotes radiation resistance in glioblastoma. Cancer Cell *24*, 331–346.

155. Wang, J., Wakeman, T. P., Lathia, J. D., Hjelmeland, A. B., Wang, X.-F., White, R. R., Rich, J. N., and Sullenger, B. A. (2010). Notch promotes radioresistance of glioma stem cells. Stem Cells *28*, 17–28.

156. Venere, M., Hamerlik, P., Wu, Q., Rasmussen, R. D., Song, L. A., Vasanji, A., Tenley, N., Flavahan, W. A., Hjelmeland, A. B., Bartek, J., et al. (2013). Therapeutic targeting of constitutive PARP activation compromises stem cell phenotype and survival of glioblastoma-initiating cells. Cell Death Differ.

157. Fuentealba, L. C., Obernier, K., and Alvarez-Buylla, A. (2012). Adult neural stem cells bridge their niche. Cell Stem Cell *10*, 698–708.

158. Merkle, F. T., Tramontin, A. D., García-Verdugo, J. M., and Alvarez-Buylla, A. (2004). Radial glia give rise to adult neural stem cells in the subventricular zone. Proc Natl Acad Sci U S A *101*, 17528–17532.

159. Zhang, S., and Cui, W. (2014). Sox2, a key factor in the regulation of pluripotency and neural differentiation. World J Stem Cells *6*, 305–311.

160. Takahashi, K., and Yamanaka, S. (2006). Induction of pluripotent stem cells from mouse embryonic and adult fibroblast cultures by defined factors. Cell *126*, 663–676.

161. Hägerstrand, D., He, X., Bradic Lindh, M., Hoefs, S., Hesselager, G., Ostman, A., and Nistér, M. (2011). Identification of a SOX2-dependent subset of tumor- and sphere-forming glioblastoma cells with a distinct tyrosine kinase inhibitor sensitivity profile. Neuro Oncol *13*, 1178–1191.

162. Brescia, P., Richichi, C., and Pelicci, G. (2012). Current strategies for identification of glioma stem cells: adequate or unsatisfactory? J Oncol *2012*, 376894.

163. Yin, A. H., Miraglia, S., Zanjani, E. D., Almeida-Porada, G., Ogawa, M., Leary, A. G., Olweus, J., Kearney, J., and Buck, D. W. (1997). AC133, a novel marker for human hematopoietic stem and progenitor cells. Blood *90*, 5002–5012.

164. Miraglia, S., Godfrey, W., Yin, A. H., Atkins, K., Warnke, R., Holden, J. T., Bray, R. A., Waller, E. K., and Buck, D. W. (1997). A novel five-transmembrane hematopoietic stem cell antigen: isolation, characterization, and molecular cloning. Blood *90*, 5013–5021.

165. Horn, P. A., Tesch, H., Staib, P., Kube, D., Diehl, V., and Voliotis, D. (1999). Expression of AC133, a novel hematopoietic precursor antigen, on acute myeloid leukemia cells. Blood *93*, 1435–1437.

166. Corbeil, D., Röper, K., Hellwig, A., Tavian, M., Miraglia, S., Watt, S. M., Simmons, P. J., Peault, B., Buck, D. W., and Huttner, W. B. (2000). The human AC133 hematopoietic stem cell antigen is also expressed in epithelial cells and targeted to plasma membrane protrusions. J Biol Chem *275*, 5512–5520.

167. Kemper, K., Sprick, M. R., de Bree, M., Scopelliti, A., Vermeulen, L., Hoek, M., Zeilstra, J., Pals, S. T., Mehmet, H., Stassi, G., et al. (2010). The AC133 epitope, but not the CD133 protein, is lost upon cancer stem cell differentiation. Cancer Res *70*, 719–729.

168. Uchida, N., Buck, D. W., He, D., Reitsma, M. J., Masek, M., Phan, T. V., Tsukamoto, A. S., Gage, F. H., and Weissman, I. L. (2000). Direct isolation of human central nervous system stem cells. Proc Natl Acad Sci U S A *97*, 14720–14725.

169. O'Brien, C. A., Pollett, A., Gallinger, S., and Dick, J. E. (2007). A human colon cancer cell capable of initiating tumour growth in immunodeficient mice. Nature *445*, 106–110.

170. Rebetz, J., Tian, D., Persson, A., Widegren, B., Salford, L. G., Englund, E., Gisselsson, D., and Fan, X. (2008). Glial progenitor-like phenotype in low-grade glioma and enhanced CD133-expression and neuronal lineage differentiation potential in high-grade glioma. PLoS ONE *3*, e1936.

171. Thon, N., Damianoff, K., Hegermann, J., Grau, S., Krebs, B., Schnell, O., Tonn, J.-C., and Goldbrunner, R. (2010). Presence of pluripotent CD133+ cells correlates with malignancy of gliomas. Mol Cell Neurosci *43*, 51–59.

172. Zeppernick, F., Ahmadi, R., Campos, B., Dictus, C., Helmke, B. M., Becker, N., Lichter, P., Unterberg, A., Radlwimmer, B., and Herold-Mende, C. C. (2008). Stem cell marker CD133 affects clinical outcome in glioma patients. Clin Cancer Res *14*, 123–129.

173. Lathia, J. D., Hitomi, M., Gallagher, J., Gadani, S. P., Adkins, J., Vasanji, A., Liu, L., Eyler, C. E., Heddleston, J. M., Wu, Q., et al. (2011). Distribution of CD133 reveals glioma stem cells self-renew through symmetric and asymmetric cell divisions. Cell Death Dis *2*, e200.

174. Campos, B., and Herold-Mende, C. C. (2011). Insight into the complex regulation of CD133 in glioma. Int J Cancer *128*, 501–510.

175. Cheray, M., Petit, D., Forestier, L., Karayan-Tapon, L., Maftah, A., Jauberteau, M.-O., Battu, S., Gallet, F. P., and Lalloué, F. (2011). Glycosylation-related gene expression is linked to differentiation status in glioblastomas undifferentiated cells. Cancer Lett *312*, 24–32.

176. Pallini, R., Ricci-Vitiani, L., Banna, G. L., Signore, M., Lombardi, D., Todaro, M., Stassi, G., Martini, M., Maira, G., Larocca, L. M., et al. (2008). Cancer stem cell analysis and clinical outcome in patients with glioblastoma multiforme. Clin Cancer Res *14*, 8205–8212.

177. Laks, D. R., Visnyei, K., and Kornblum, H. I. (2010). Brain tumor stem cells as therapeutic targets in models of glioma. Yonsei Med J *51*, 633–640.

178. Zhang, M., Song, T., Yang, L., Chen, R., Wu, L., Yang, Z., and Fang, J. (2008). Nestin and CD133: valuable stem cell-specific markers for determining clinical outcome of glioma patients. J Exp Clin Cancer Res *27*, 85.

179. Kim, K.-J., Lee, K.-H., Kim, H.-S., Moon, K.-S., Jung, T.-Y., Jung, S., and Lee, M.-C. (2011). The presence of stem cell marker-expressing cells is not prognostically significant in glioblastomas. Neuropathology *31*, 494–502.

180. Christensen, K., Schrøder, H. D., and Kristensen, B. W. (2008). CD133 identifies perivascular niches in grade II-IV astrocytomas. J Neurooncol *90*, 157–170.

181. Kase, M., Minajeva, A., Niinepuu, K., Kase, S., Vardja, M., Asser, T., and Jaal, J. (2013). Impact of CD133 positive stem cell proportion on survival in patients with glioblastoma multiforme. Radiol Oncol *47*, 405–410.

182. Wang, J., Sakariassen, P. Ø., Tsinkalovsky, O., Immervoll, H., Bøe, S. O., Svendsen, A., Prestegarden, L., Røsland, G., Thorsen, F., Stuhr, L., et al. (2008). CD133 negative glioma cells form tumors in nude rats and give rise to CD133 positive cells. Int J Cancer *122*, 761–768.

183. Chen, R., Nishimura, M. C., Bumbaca, S. M., Kharbanda, S., Forrest, W. F., Kasman, I. M., Greve, J. M., Soriano, R. H., Gilmour, L. L., Rivers, C. S., et al. (2010). A hierarchy of self-renewing tumor-initiating cell types in glioblastoma. Cancer Cell *17*, 362–375.

184. Sun, Y., Kong, W., Falk, A., Hu, J., Zhou, L., Pollard, S., and Smith, A. (2009). CD133 (Prominin) negative human neural stem cells are clonogenic and tripotent. PLoS ONE *4*, e5498.

185. Lottaz, C., Beier, D., Meyer, K., Kumar, P., Hermann, A., Schwarz, J., Junker, M., Oefner, P. J., Bogdahn, U., Wischhusen, J., et al. (2010). Transcriptional profiles of CD133+ and CD133- glioblastoma-derived cancer stem cell lines suggest different cells of origin. Cancer Res *70*, 2030–2040.

186. Barrantes-Freer, A., Renovanz, M., Eich, M., Braukmann, A., Sprang, B., Spirin, P., Pardo, L. A., Giese, A., and Kim, E. L. (2015). CD133 Expression Is Not Synonymous to Immunoreactivity for AC133 and Fluctuates throughout the Cell Cycle in Glioma Stem-Like Cells. PLoS ONE *10*, e0130519.

187. Brescia, P., Ortensi, B., Fornasari, L., Levi, D., Broggi, G., and Pelicci, G. (2013). CD133 is essential for glioblastoma stem cell maintenance. Stem Cells *31*, 857–869.

188. Wei, Y., Jiang, Y., Zou, F., Liu, Y., Wang, S., Xu, N., Xu, W., Cui, C., Xing, Y., Liu, Y., et al. (2013). Activation of PI3K/Akt pathway by CD133-p85 interaction promotes tumorigenic capacity of glioma stem cells. Proc Natl Acad Sci U S A *110*, 6829–6834.

189. Soeda, A., Park, M., Lee, D., Mintz, A., Androutsellis-Theotokis, A., McKay, R. D., Engh, J., Iwama, T., Kunisada, T., Kassam, A. B., et al. (2009). Hypoxia promotes expansion of the CD133-positive glioma stem cells through activation of HIF-1alpha. Oncogene *28*, 3949–3959.

190. Griguer, C. E., Oliva, C. R., Gobin, E., Marcorelles, P., Benos, D. J., Lancaster, J. R., and Gillespie, G. Y. (2008). CD133 is a marker of bioenergetic stress in human glioma. PLoS ONE *3*, e3655.

191. Capela, A., and Temple, S. (2006). LeX is expressed by principle progenitor cells in the embryonic nervous system, is secreted into their environment and binds Wnt-1. Dev Biol *291*, 300–313.

192. Capela, A., and Temple, S. (2002). LeX/ssea-1 is expressed by adult mouse CNS stem cells, identifying them as nonependymal. Neuron *35*, 865–875.

193. Thomson, J. A., Itskovitz-Eldor, J., Shapiro, S. S., Waknitz, M. A., Swiergiel, J. J., Marshall, V. S., and Jones, J. M. (1998). Embryonic stem cell lines derived from human blastocysts. Science *282*, 1145–1147.

194. Son, M. J., Woolard, K., Nam, D.-H., Lee, J., and Fine, H. A. (2009). SSEA-1 is an enrichment marker for tumor-initiating cells in human glioblastoma. Cell Stem Cell *4*, 440–452.

195. Kahlert, U. D., Bender, N. O., Maciaczyk, D., Bogiel, T., Bar, E. E., Eberhart, C. G., Nikkhah, G., and Maciaczyk, J. (2012). CD133/CD15 defines distinct cell subpopulations with differential in vitro clonogenic activity and stem cell-related gene expression profile in in vitro propagated glioblastoma multiforme-derived cell line with a PNET-like component. Folia Neuropathol *50*, 357–368.

196. Kenney-Herbert, E., Al-Mayhani, T., Piccirillo, S. G. M., Fowler, J., Spiteri, I., Jones, P., and Watts, C. (2015). CD15 Expression Does Not Identify a Phenotypically or Genetically Distinct Glioblastoma Population. Stem Cells Transl Med *4*, 822–831.

197. Graus-Porta, D., Blaess, S., Senften, M., Littlewood-Evans, A., Damsky, C., Huang, Z., Orban, P., Klein, R., Schittny, J. C., and Müller, U. (2001). Beta1-class integrins regulate the development of laminae and folia in the cerebral and cerebellar cortex. Neuron *31*, 367–379.

198. Fortunel, N. O., Otu, H. H., Ng, H.-H., Chen, J., Mu, X., Chevassut, T., Li, X., Joseph, M., Bailey, C., Hatzfeld, J. A., et al. (2003). Comment on " 'Stemness': transcriptional profiling of embryonic and adult stem cells" and "a stem cell molecular signature". Science *302*, 393; author reply 393.

199. Hall, P. E., Lathia, J. D., Caldwell, M. A., and Ffrench-Constant, C. (2008). Laminin enhances the growth of human neural stem cells in defined culture media. BMC Neurosci *9*, 71.

200. Schonberg, D. L., Lubelski, D., Miller, T. E., and Rich, J. N. (2014). Brain tumor stem cells: Molecular characteristics and their impact on therapy. Mol Aspects Med *39*, 82–101.

201. Ogden, A. T., Waziri, A. E., Lochhead, R. A., Fusco, D., Lopez, K., Ellis, J. A., Kang, J., Assanah, M., McKhann, G. M., Sisti, M. B., et al. (2008). Identification of A2B5+CD133- tumor-initiating cells in adult human gliomas. Neurosurgery *62*, 505–14; discussion 514.

202. Han, Y., Wang, H., Huang, Y., Cheng, Z., Sun, T., Chen, G., Xie, X., Zhou, Y., and Du, Z. (2015). Isolation and characteristics of CD133⍰/A2B5+ and CD133⍰/A2B5⍰ cells from the SHG139s cell line. Mol Med Report *12*, 7949–7956.

203. Nie, S., Gurrea, M., Zhu, J., Thakolwiboon, S., Heth, J. A., Muraszko, K. M., Fan, X., and Lubman, D. M. (2015). Tenascin-C: a novel candidate marker for cancer stem cells in glioblastoma identified by tissue microarrays. J Proteome Res *14*, 814–822.

204. He, J., Liu, Y., Zhu, T., Zhu, J., Dimeco, F., Vescovi, A. L., Heth, J. A., Muraszko, K. M., Fan, X., and Lubman, D. M. (2012). CD90 is identified as a candidate marker for cancer stem cells in primary high-grade gliomas using tissue microarrays. Mol Cell Proteomics *11*, M111.010744.

205. Liu, J. K., Lubelski, D., Schonberg, D. L., Wu, Q., Hale, J. S., Flavahan, W. A., Mulkearns-Hubert, E. E., Man, J., Hjelmeland, A. B., Yu, J., et al. (2014). Phage display discovery of novel molecular targets in glioblastoma-initiating cells. Cell Death Differ *21*, 1325–1339.

206. Anido, J., Sáez-Borderías, A., Gonzàlez-Juncà, A., Rodón, L., Folch, G., Carmona, M. A., Prieto-Sánchez, R. M., Barba, I., Martínez-Sáez, E., Prudkin, L., et al. (2010). TGF-β Receptor Inhibitors Target the CD44(high)/Id1(high) Glioma-Initiating Cell Population in Human Glioblastoma. Cancer Cell *18*, 655–668.

207. Brown, D. V., Daniel, P. M., D'Abaco, G. M., Gogos, A., Ng, W., Morokoff, A. P., and Mantamadiotis, T. (2015). Coexpression analysis of CD133 and CD44 identifies proneural and mesenchymal subtypes of glioblastoma multiforme. Oncotarget *6*, 6267–6280.

208. Flüh, C., Hattermann, K., Mehdorn, H. M., Synowitz, M., and Held-Feindt, J. (2016). Differential expression of CXCR4 and CXCR7 with various stem cell markers in paired human primary and recurrent glioblastomas. Int J Oncol.

209. Iacopino, F., Angelucci, C., Piacentini, R., Biamonte, F., Mangiola, A., Maira, G., Grassi, C., and Sica, G. (2014). Isolation of cancer stem cells from three human glioblastoma cell lines: characterization of two selected clones. PLoS ONE *9*, e105166.

210. Gargiulo, G., Cesaroni, M., Serresi, M., de Vries, N., Hulsman, D., Bruggeman, S. W., Lancini, C., and van Lohuizen, M. (2013). In vivo RNAi screen for BMI1 targets identifies TGF-β/BMP-ER stress pathways as key regulators of neural- and malignant glioma-stem cell homeostasis. Cancer Cell *23*, 660–676.

211. Soroceanu, L., Murase, R., Limbad, C., Singer, E., Allison, J., Adrados, I., Kawamura, R., Pakdel, A., Fukuyo, Y., Nguyen, D., et al. (2013). Id-1 is a key transcriptional regulator of glioblastoma aggressiveness and a novel therapeutic target. Cancer Res *73*, 1559–1569.

212. Zhang, W., Liu, Y., Hu, H., Huang, H., Bao, Z., Yang, P., Wang, Y., You, G., Yan, W., Jiang, T., et al. (2015). ALDH1A3: A Marker of Mesenchymal Phenotype in Gliomas Associated with Cell Invasion. PLoS ONE *10*, e0142856.

213. Pointer, K. B., Clark, P. A., Zorniak, M., Alrfaei, B. M., and Kuo, J. S. (2014). Glioblastoma cancer stem cells: Biomarker and therapeutic advances. Neurochem Int *71*, 1–7.

214. Cavazos, D. A., and Brenner, A. J. (2016). Hypoxia in astrocytic tumors and implications for therapy. Neurobiol Dis *85*, 227–233.

215. Evans, S. M., Judy, K. D., Dunphy, I., Jenkins, W. T., Hwang, W.-T., Nelson, P. T., Lustig, R. A., Jenkins, K., Magarelli, D. P., Hahn, S. M., et al. (2004). Hypoxia is important in the biology and aggression of human glial brain tumors. Clin Cancer Res *10*, 8177–8184.

216. Keith, B., and Simon, M. C. (2007). Hypoxia-inducible factors, stem cells, and cancer. Cell *129*, 465–472.

217. Gustafsson, M., Zheng, X., Pereira, T., Gradin, K., Jin, S., Lundkvist, J., Ruas, J., Poellinger, L., Lendahl, U., and Bondesson, M. (2005). Hypoxia requires notch signaling to maintain the undifferentiated cell state. Dev Cell *9*, 617–628.

218. Evans, S. M., Jenkins, K. W., Jenkins, W. T., Dilling, T., Judy, K. D., Schrlau, A., Judkins, A., Hahn, S. M., and Koch, C. J. (2008). Imaging and analytical methods as applied to the evaluation of vasculature and hypoxia in human brain tumors. Radiation research *170*, 677–90. Available at: http://www.pubmedcentral.nih.gov/articlerender.fcgi?artid=2629387&tool=pmcentrez&rendertype=abstract.

219. Dewhirst, M. W., Cao, Y., and Moeller, B. (2008). Cycling hypoxia and free radicals regulate angiogenesis and radiotherapy response. Nat Rev Cancer *8*, 425–437.

220. Brat, D. J., Castellano-Sanchez, A. A., Hunter, S. B., Pecot, M., Cohen, C., Hammond, E. H., Devi, S. N., Kaur, B., and Van Meir, E. G. (2004). Pseudopalisades in glioblastoma are hypoxic, express extracellular matrix proteases, and are formed by an actively migrating cell population. Cancer Res *64*, 920–927.

221. Carmeliet, P., and Jain, R. K. (2000). Angiogenesis in cancer and other diseases. Nature *407*, 249–257.

222. Brat, D. J., and Van Meir, E. G. (2004). Vaso-occlusive and prothrombotic mechanisms associated with tumor hypoxia, necrosis, and accelerated growth in glioblastoma. Laboratory investigation; a journal of technical methods and pathology *84*, 397–405. Available at: http://dx.doi.org/10.1038/labinvest.3700070.

223. Jain, R. K. (2013). Normalizing tumor microenvironment to treat cancer: bench to bedside to biomarkers. J Clin Oncol *31*, 2205–2218.

224. Burger, P. C., and Green, S. B. (1987). Patient age, histologic features, and length of survival in patients with glioblastoma multiforme. Cancer *59*, 1617–1625.

225. Spence, A. M., Muzi, M., Swanson, K. R., O'Sullivan, F., Rockhill, J. K., Rajendran, J. G., Adamsen, T. C. H., Link, J. M., Swanson, P. E., Yagle, K. J., et al. (2008). Regional hypoxia in glioblastoma multiforme quantified with [18F]fluoromisonidazole positron emission tomography before radiotherapy: correlation with time to progression and survival. Clin Cancer Res *14*, 2623–2630.

226. Jensen, R. L. (2009). Brain tumor hypoxia: tumorigenesis, angiogenesis, imaging, pseudoprogression, and as a therapeutic target. J Neurooncol *92*, 317–335.

227. Gray, L. H., Conger, A. D., Ebert, M., Hornsey, S., and Scott, O. C. (1953). The concentration of oxygen dissolved in tissues at the time of irradiation as a factor in radiotherapy. Br J Radiol *26*, 638–648.

228. Pistollato, F., Abbadi, S., Rampazzo, E., Persano, L., Della Puppa, A., Frasson, C., Sarto, E., Scienza, R., D'avella, D., and Basso, G. (2010). Intratumoral hypoxic gradient drives stem cells distribution and MGMT expression in glioblastoma. Stem Cells *28*, 851–862.

229. Karsy, M., Guan, J., Jensen, R., Huang, L. E., and Colman, H. (2015). The impact of hypoxia and mesenchymal transition on glioblastoma pathogenesis and cancer stem cells regulation. World Neurosurg.

230. Fidoamore, A., Cristiano, L., Antonosante, A., d Angelo, M., Di Giacomo, E., Astarita, C., Giordano, A., Ippoliti, R., Benedetti, E., and Cimini, A. (2016). Glioblastoma Stem Cells Microenvironment: The Paracrine Roles of the Niche in Drug and Radioresistance. Stem Cells Int *2016*, 6809105.

231. Cooper, L. A. D., Gutman, D. A., Chisolm, C., Appin, C., Kong, J., Rong, Y., Kurc, T., Van Meir, E. G., Saltz, J. H., Moreno, C. S., et al. (2012). The tumor microenvironment strongly impacts master transcriptional regulators and gene expression class of glioblastoma. Am J Pathol *180*, 2108–2119.

232. Semenza, G. L., and Wang, G. L. (1992). A nuclear factor induced by hypoxia via de novo protein synthesis binds to the human erythropoietin gene enhancer at a site required for transcriptional activation. Mol Cell Biol *12*, 5447–5454.

233. Lee, J.-W., Bae, S.-H., Jeong, J.-W., Kim, S.-H., and Kim, K.-W. (2004). Hypoxia-inducible factor (HIF-1)alpha: its protein stability and biological functions. Exp Mol Med *36*, 1–12.

234. Maxwell, P. H., Wiesener, M. S., Chang, G. W., Clifford, S. C., Vaux, E. C., Cockman, M. E., Wykoff, C. C., Pugh, C. W., Maher, E. R., and Ratcliffe, P. J. (1999). The tumour suppressor protein VHL targets hypoxia-inducible factors for oxygen-dependent proteolysis. Nature *399*, 271–275.

235. Semenza, G. L. (2012). Hypoxia-inducible factors in physiology and medicine. Cell *148*, 399–408.

236. Jaakkola, P., Mole, D. R., Tian, Y. M., Wilson, M. I., Gielbert, J., Gaskell, S. J., von Kriegsheim, A., Hebestreit, H. F., Mukherji, M., Schofield, C. J., et al. (2001). Targeting of HIF-alpha to the von Hippel-Lindau ubiquitylation complex by O2-regulated prolyl hydroxylation. Science *292*, 468–472.

237. Ohh, M., Park, C. W., Ivan, M., Hoffman, M. A., Kim, T. Y., Huang, L. E., Pavletich, N., Chau, V., and Kaelin, W. G. (2000). Ubiquitination of hypoxia-inducible factor requires direct binding to the beta-domain of the von Hippel-Lindau protein. Nat Cell Biol *2*, 423–427.

238. Wenger, R. H., Stiehl, D. P., and Camenisch, G. (2005). Integration of oxygen signaling at the consensus HRE. Sci STKE *2005*, re12.

239. Raval, R. R., Lau, K. W., Tran, M. G. B., Sowter, H. M., Mandriota, S. J., Li, J.-L., Pugh, C. W., Maxwell, P. H., Harris, A. L., and Ratcliffe, P. J. (2005). Contrasting properties of hypoxia-inducible factor 1 (HIF-1) and HIF-2 in von Hippel-Lindau-associated renal cell carcinoma. Mol Cell Biol *25*, 5675–5686.

240. Wiesener, M. S., Jürgensen, J. S., Rosenberger, C., Scholze, C. K., Hörstrup, J. H., Warnecke, C., Mandriota, S., Bechmann, I., Frei, U. A., Pugh, C. W., et al. (2003). Widespread hypoxia-inducible expression of HIF-2alpha in distinct cell populations of different organs. FASEB J *17*, 271–273.

241. Covello, K. L., Kehler, J., Yu, H., Gordan, J. D., Arsham, A. M., Hu, C.-J., Labosky, P. A., Simon, M. C., and Keith, B. (2006). HIF-2alpha regulates Oct-4: effects of hypoxia on stem cell function, embryonic development, and tumor growth. Genes Dev *20*, 557–570.

242. Sowter, H. M., Raval, R. R., Moore, J. W., Ratcliffe, P. J., and Harris, A. L. (2003). Predominant role of hypoxia-inducible transcription factor (Hif)-1alpha versus Hif-2alpha in regulation of the transcriptional response to hypoxia. Cancer Res *63*, 6130–6134.

243. Lau, K. W., Tian, Y.-M., Raval, R. R., Ratcliffe, P. J., and Pugh, C. W. (2007). Target gene selectivity of hypoxia-inducible factor-alpha in renal cancer cells is conveyed by post-DNA-binding mechanisms. Br J Cancer *96*, 1284–1292.

244. Ryan, H. E., Lo, J., and Johnson, R. S. (1998). HIF-1 alpha is required for solid tumor formation and embryonic vascularization. EMBO J *17*, 3005–3015.

245. Ramírez-Bergeron, D. L., and Simon, M. C. (2001). Hypoxia-inducible factor and the development of stem cells of the cardiovascular system. Stem Cells *19*, 279–286.

246. Sathornsumetee, S., Cao, Y., Marcello, J. E., Herndon, J. E., McLendon, R. E., Desjardins, A., Friedman, H. S., Dewhirst, M. W., Vredenburgh, J. J., and Rich, J. N. (2008). Tumor angiogenic and hypoxic profiles predict radiographic response and survival in malignant astrocytoma patients treated with bevacizumab and irinotecan. J Clin Oncol *26*, 271–278.

247. Inukai, M., Hara, A., Yasui, Y., Kumabe, T., Matsumoto, T., and Saegusa, M. (2015). Hypoxia-mediated cancer stem cells in pseudopalisades with activation of hypoxia-inducible factor-1α/Akt axis in glioblastoma. Hum Pathol *46*, 1496–1505.

248. Piccirillo, S. G. M., Combi, R., Cajola, L., Patrizi, A., Redaelli, S., Bentivegna, A., Baronchelli, S., Maira, G., Pollo, B., Mangiola, A., et al. (2009). Distinct pools of

cancer stem-like cells coexist within human glioblastomas and display different tumorigenicity and independent genomic evolution. Oncogene *28*, 1807–1811.

249. Blazek, E. R., Foutch, J. L., and Maki, G. (2007). Daoy medulloblastoma cells that express CD133 are radioresistant relative to CD133- cells, and the CD133+ sector is enlarged by hypoxia. Int J Radiat Oncol Biol Phys *67*, 1–5.

250. Seidel, S., Garvalov, B. K., Wirta, V., von Stechow, L., Schänzer, A., Meletis, K., Wolter, M., Sommerlad, D., Henze, A.-T., Nistér, M., et al. (2010). A hypoxic niche regulates glioblastoma stem cells through hypoxia inducible factor 2 alpha. Brain *133*, 983–995.

251. Bar, E. E., Lin, A., Mahairaki, V., Matsui, W., and Eberhart, C. G. (2010). Hypoxia increases the expression of stem-cell markers and promotes clonogenicity in glioblastoma neurospheres. Am J Pathol *177*, 1491–1502.

252. Heddleston, J. M., Li, Z., Lathia, J. D., Bao, S., Hjelmeland, A. B., and Rich, J. N. (2010). Hypoxia inducible factors in cancer stem cells. Br J Cancer *102*, 789–795.

253. Li, Z., Bao, S., Wu, Q., Wang, H., Eyler, C., Sathornsumetee, S., Shi, Q., Cao, Y., Lathia, J., McLendon, R. E., et al. (2009). Hypoxia-inducible factors regulate tumorigenic capacity of glioma stem cells. Cancer Cell *15*, 501–513.

254. Semenza, G. L. (2016). The hypoxic tumor microenvironment: A driving force for breast cancer progression. Biochim Biophys Acta *1863*, 382–391.

255. Ravi, R., Mookerjee, B., Bhujwalla, Z. M., Sutter, C. H., Artemov, D., Zeng, Q., Dillehay, L. E., Madan, A., Semenza, G. L., and Bedi, A. (2000). Regulation of tumor angiogenesis by p53-induced degradation of hypoxia-inducible factor 1alpha. Genes Dev *14*, 34–44.

256. Narita, T., Yin, S., Gelin, C. F., Moreno, C. S., Yepes, M., Nicolaou, K. C., and Van Meir, E. G. (2009). Identification of a novel small molecule HIF-1alpha translation inhibitor. Clin Cancer Res *15*, 6128–6136.

257. Lou, Y., McDonald, P. C., Oloumi, A., Chia, S., Ostlund, C., Ahmadi, A., Kyle, A., Auf dem Keller, U., Leung, S., Huntsman, D., et al. (2011). Targeting tumor hypoxia: suppression of breast tumor growth and metastasis by novel carbonic anhydrase IX inhibitors. Cancer Res *71*, 3364–3376.

258. Meng, F., Bhupathi, D., Sun, J. D., Liu, Q., Ahluwalia, D., Wang, Y., Matteucci, M. D., and Hart, C. P. (2015). Enhancement of hypoxia-activated prodrug TH-302 anti-tumor activity by Chk1 inhibition. BMC Cancer *15*, 422.

259. Sherk, A. B., Frigo, D. E., Schnackenberg, C. G., Bray, J. D., Laping, N. J., Trizna, W., Hammond, M., Patterson, J. R., Thompson, S. K., Kazmin, D., et al. (2008). Development of a small-molecule serum- and glucocorticoid-regulated kinase-1 antagonist and its evaluation as a prostate cancer therapeutic. Cancer Res *68*, 7475–7483.

260. Peters, T., Lindenmaier, H., Haefeli, W. E., and Weiss, J. (2006). Interaction of the mitotic kinesin Eg5 inhibitor monastrol with P-glycoprotein. Naunyn Schmiedebergs Arch Pharmacol *372*, 291–299.

261. Vandenabeele, P., Vanden Berghe, T., and Festjens, N. (2006). Caspase inhibitors promote alternative cell death pathways. Sci STKE *2006*, pe44.

262. Caserta, T. M., Smith, A. N., Gultice, A. D., Reedy, M. A., and Brown, T. L. (2003). Q-VD-OPh, a broad spectrum caspase inhibitor with potent antiapoptotic properties. Apoptosis *8*, 345–352.

263. Bennett, B. L., Sasaki, D. T., Murray, B. W., O'Leary, E. C., Sakata, S. T., Xu, W., Leisten, J. C., Motiwala, A., Pierce, S., Satoh, Y., et al. (2001). SP600125, an anthrapyrazolone inhibitor of Jun N-terminal kinase. Proc Natl Acad Sci U S A *98*, 13681–13686.

264. Underwood, D. C., Osborn, R. R., Kotzer, C. J., Adams, J. L., Lee, J. C., Webb, E. F., Carpenter, D. C., Bochnowicz, S., Thomas, H. C., Hay, D. W., et al. (2000). SB 239063, a potent p38 MAP kinase inhibitor, reduces inflammatory cytokine production, airways eosinophil infiltration, and persistence. J Pharmacol Exp Ther *293*, 281–288.

265. Sanjana, N. E., Shalem, O., and Zhang, F. (2014). Improved vectors and genome-wide libraries for CRISPR screening. Nat Methods *11*, 783–784.

266. Chung, N., Zhang, X. D., Kreamer, A., Locco, L., Kuan, P.-F., Bartz, S., Linsley, P. S., Ferrer, M., and Strulovici, B. (2008). Median absolute deviation to improve hit selection for genome-scale RNAi screens. J Biomol Screen *13*, 149–158.

267. Hart, T., and Moffat, J. (2015). BAGEL: A computational framework for identifying essential genes from pooled library screens. bioRxiv. Available at: http://biorxiv.org/content/biorxiv/early/2015/11/27/033068.full.pdf.

268. Cetin, A., Komai, S., Eliava, M., Seeburg, P. H., and Osten, P. (2006). Stereotaxic gene delivery in the rodent brain. Nat Protoc *1*, 3166–3173.

269. Lima, F. R. S., Kahn, S. A., Soletti, R. C., Biasoli, D., Alves, T., da Fonseca, A. C. C., Garcia, C., Romão, L., Brito, J., Holanda-Afonso, R., et al. (2012).

Glioblastoma: therapeutic challenges, what lies ahead. Biochim Biophys Acta *1826*, 338–349.

270. Persano, L., Rampazzo, E., Basso, G., and Viola, G. (2013). Glioblastoma cancer stem cells: role of the microenvironment and therapeutic targeting. Biochem Pharmacol *85*, 612–622.

271. Hart, T., Brown, K. R., Sircoulomb, F., Rottapel, R., and Moffat, J. (2014). Measuring error rates in genomic perturbation screens: gold standards for human functional genomics. Mol Syst Biol *10*, 733.

272. Guvenc, H., Pavlyukov, M. S., Joshi, K., Kurt, H., Banasavadi-Siddegowda, Y. K., Mao, P., Hong, C., Yamada, R., Kwon, C.-H., Bhasin, D., et al. (2013). Impairment of glioma stem cell survival and growth by a novel inhibitor for Survivin-Ran protein complex. Clin Cancer Res *19*, 631–642.

273. Fabbro, D. (2015). 25 years of small molecular weight kinase inhibitors: potentials and limitations. Mol Pharmacol *87*, 766–775.

274. Cohen, P., and Alessi, D. R. (2013). Kinase drug discovery--what's next in the field? ACS Chem Biol *8*, 96–104.

275. Bhinder, B., and Djaballah, H. (2013). Systematic analysis of RNAi reports identifies dismal commonality at gene-level and reveals an unprecedented enrichment in pooled shRNA screens. Comb Chem High Throughput Screen *16*, 665–681.

276. Buehler, E., Chen, Y.-C., and Martin, S. (2012). C911: A bench-level control for sequence specific siRNA off-target effects. PLoS ONE *7*, e51942.

277. Leong, M. L. L., Maiyar, A. C., Kim, B., O'Keeffe, B. A., and Firestone, G. L. (2003). Expression of the serum- and glucocorticoid-inducible protein kinase, Sgk, is a cell survival response to multiple types of environmental stress stimuli in mammary epithelial cells. J Biol Chem *278*, 5871–5882.

278. Webster, M. K., Goya, L., Ge, Y., Maiyar, A. C., and Firestone, G. L. (1993). Characterization of sgk, a novel member of the serine/threonine protein kinase gene family which is transcriptionally induced by glucocorticoids and serum. Mol Cell Biol *13*, 2031–2040.

279. Mikosz, C. A., Brickley, D. R., Sharkey, M. S., Moran, T. W., and Conzen, S. D. (2001). Glucocorticoid receptor-mediated protection from apoptosis is associated with induction of the serine/threonine survival kinase gene, sgk-1. J Biol Chem *276*, 16649–16654.

280. Pearce, L. R., Komander, D., and Alessi, D. R. (2010). The nuts and bolts of AGC protein kinases. Nat Rev Mol Cell Biol *11*, 9–22.

281. García-Martínez, J. M., and Alessi, D. R. (2008). mTOR complex 2 (mTORC2) controls hydrophobic motif phosphorylation and activation of serum- and glucocorticoid-induced protein kinase 1 (SGK1). Biochem J *416*, 375–385.

282. Kobayashi, T., Deak, M., Morrice, N., and Cohen, P. (1999). Characterization of the structure and regulation of two novel isoforms of serum- and glucocorticoid-induced protein kinase. Biochem J *344 Pt 1*, 189–197.

283. Xu, B.-E., Stippec, S., Lazrak, A., Huang, C.-L., and Cobb, M. H. (2005). WNK1 activates SGK1 by a phosphatidylinositol 3-kinase-dependent and non-catalytic mechanism. J Biol Chem *280*, 34218–34223.

284. Sakoda, H., Gotoh, Y., Katagiri, H., Kurokawa, M., Ono, H., Onishi, Y., Anai, M., Ogihara, T., Fujishiro, M., Fukushima, Y., et al. (2003). Differing roles of Akt and serum- and glucocorticoid-regulated kinase in glucose metabolism, DNA synthesis, and oncogenic activity. J Biol Chem *278*, 25802–25807.

285. Park, J., Leong, M. L., Buse, P., Maiyar, A. C., Firestone, G. L., and Hemmings, B. A. (1999). Serum and glucocorticoid-inducible kinase (SGK) is a target of the PI 3-kinase-stimulated signaling pathway. EMBO J *18*, 3024–3033.

286. Buse, P., Tran, S. H., Luther, E., Phu, P. T., Aponte, G. W., and Firestone, G. L. (1999). Cell cycle and hormonal control of nuclear-cytoplasmic localization of the serum- and glucocorticoid-inducible protein kinase, Sgk, in mammary tumor cells. A novel convergence point of anti-proliferative and proliferative cell signaling pathways. J Biol Chem *274*, 7253–7263.

287. Brunet, A., Park, J., Tran, H., Hu, L. S., Hemmings, B. A., and Greenberg, M. E. (2001). Protein kinase SGK mediates survival signals by phosphorylating the forkhead transcription factor FKHRL1 (FOXO3a). Mol Cell Biol *21*, 952–965.

288. Gao, D., Wan, L., Inuzuka, H., Berg, A. H., Tseng, A., Zhai, B., Shaik, S., Bennett, E., Tron, A. E., Gasser, J. A., et al. (2010). Rictor forms a complex with Cullin-1 to promote SGK1 ubiquitination and destruction. Mol Cell *39*, 797–808.

289. Brickley, D. R., Mikosz, C. A., Hagan, C. R., and Conzen, S. D. (2002). Ubiquitin modification of serum and glucocorticoid-induced protein kinase-1 (SGK-1). J Biol Chem *277*, 43064–43070.

290. Belova, L., Brickley, D. R., Wu, W., and Conzen, S. D. (2006). The role of serum and glucocorticoid-inducible kinase-1 (SGK-1) in breast cancer. Cancer Res. Available at: http://cancerres.aacrjournals.org/content/66/8_Supplement/1001.3.

291. Lang, F., Böhmer, C., Palmada, M., Seebohm, G., Strutz-Seebohm, N., and Vallon, V. (2006). (Patho)physiological significance of the serum- and glucocorticoid-inducible kinase isoforms. Physiol Rev *86*, 1151–1178.

292. Blazer-Yost, B. L., Păunescu, T. G., Helman, S. I., Lee, K. D., and Vlahos, C. J. (1999). Phosphoinositide 3-kinase is required for aldosterone-regulated sodium reabsorption. Am J Physiol *277*, C531–C536.

293. Rossier, B. C. (2002). Hormonal regulation of the epithelial sodium channel ENaC: N or P(o)? J Gen Physiol *120*, 67–70.

294. Snyder, P. M., Olson, D. R., Kabra, R., Zhou, R., and Steines, J. C. (2004). cAMP and serum and glucocorticoid-inducible kinase (SGK) regulate the epithelial Na(+) channel through convergent phosphorylation of Nedd4-2. J Biol Chem *279*, 45753–45758.

295. Náray-Fejes-Tóth, A., and Fejes-Tóth, G. (2000). The sgk, an aldosterone-induced gene in mineralocorticoid target cells, regulates the epithelial sodium channel. Kidney Int *57*, 1290–1294.

296. Wulff, P., Vallon, V., Huang, D. Y., Völkl, H., Yu, F., Richter, K., Jansen, M., Schlünz, M., Klingel, K., Loffing, J., et al. (2002). Impaired renal Na(+) retention in the sgk1-knockout mouse. J Clin Invest *110*, 1263–1268.

297. Lang, F., and Voelkl, J. (2013). Therapeutic potential of serum and glucocorticoid inducible kinase inhibition. Expert Opin Investig Drugs *22*, 701–714.

298. Richards, J. S., Sharma, S. C., Falender, A. E., and Lo, Y. H. (2002). Expression of FKHR, FKHRL1, and AFX genes in the rodent ovary: evidence for regulation by IGF-I, estrogen, and the gonadotropins. Mol Endocrinol *16*, 580–599.

299. You, H., Jang, Y., You-Ten, A. I., Okada, H., Liepa, J., Wakeham, A., Zaugg, K., and Mak, T. W. (2004). p53-dependent inhibition of FKHRL1 in response to DNA damage through protein kinase SGK1. Proc Natl Acad Sci U S A *101*, 14057–14062.

300. Tai, D. J. C., Su, C.-C., Ma, Y.-L., and Lee, E. H. Y. (2009). SGK1 phosphorylation of IkappaB Kinase alpha and p300 Up-regulates NF-kappaB activity and increases N-Methyl-D-aspartate receptor NR2A and NR2B expression. J Biol Chem *284*, 4073–4089.

301. Zhang, L., Cui, R., Cheng, X., and Du, J. (2005). Antiapoptotic effect of serum and glucocorticoid-inducible protein kinase is mediated by novel mechanism activating I{kappa}B kinase. Cancer Res *65*, 457–464.

302. Amato, R., D'Antona, L., Porciatti, G., Agosti, V., Menniti, M., Rinaldo, C., Costa, N., Bellacchio, E., Mattarocci, S., Fuiano, G., et al. (2009). Sgk1 activates MDM2-dependent p53 degradation and affects cell proliferation, survival, and differentiation. J Mol Med *87*, 1221–1239.

303. Maiyar, A. C., Huang, A. J., Phu, P. T., Cha, H. H., and Firestone, G. L. (1996). p53 stimulates promoter activity of the sgk. serum/glucocorticoid-inducible serine/threonine protein kinase gene in rodent mammary epithelial cells. J Biol Chem *271*, 12414–12422.

304. Iqbal, S., Howard, S., and LoGrasso, P. V. (2015). Serum- and Glucocorticoid-Inducible Kinase 1 Confers Protection in Cell-Based and in In Vivo Neurotoxin Models via the c-Jun N-Terminal Kinase Signaling Pathway. Mol Cell Biol *35*, 1992–2006.

305. Kim, M. J., Chae, J. S., Kim, K. J., Hwang, S. G., Yoon, K. W., Kim, E. K., Yun, H. J., Cho, J.-H., Kim, J., Kim, B.-W., et al. (2007). Negative regulation of SEK1 signaling by serum- and glucocorticoid-inducible protein kinase 1. EMBO J *26*, 3075–3085.

306. Brickley, D. R., Agyeman, A. S., Kopp, R. F., Hall, B. A., Harbeck, M. C., Belova, L., Volden, P. A., Wu, W., Roe, M. W., and Conzen, S. D. (2013). Serum- and glucocorticoid-induced protein kinase 1 (SGK1) is regulated by store-operated Ca2+ entry and mediates cytoprotection against necrotic cell death. J Biol Chem *288*, 32708–32719.

307. Nasir, O., Wang, K., Föller, M., Gu, S., Bhandaru, M., Ackermann, T. F., Boini, K. M., Mack, A., Klingel, K., Amato, R., et al. (2009). Relative resistance of SGK1 knockout mice against chemical carcinogenesis. IUBMB Life *61*, 768–776.

308. Talarico, C., Dattilo, V., D'Antona, L., Barone, A., Amodio, N., Belviso, S., Musumeci, F., Abbruzzese, C., Bianco, C., Trapasso, F., et al. (2016). SI113, a SGK1 inhibitor, potentiates the effects of radiotherapy, modulates the response to oxidative stress and induces cytotoxic autophagy in human glioblastoma multiforme cells. Oncotarget.

309. Hartmann, S., Schuhmacher, B., Rausch, T., Fuller, L., Döring, C., Weniger, M., Lollies, A., Weiser, C., Thurner, L., Rengstl, B., et al. (2015). Highly recurrent

mutations of SGK1, DUSP2 and JUNB in nodular lymphocyte predominant Hodgkin lymphoma. Leukemia.

310. Sommer, E. M., Dry, H., Cross, D., Guichard, S., Davies, B. R., and Alessi, D. R. (2013). Elevated SGK1 predicts resistance of breast cancer cells to Akt inhibitors. Biochem J *452*, 499–508.

311. Hall, B. A., Kim, T. Y., Skor, M. N., and Conzen, S. D. (2012). Serum and glucocorticoid-regulated kinase 1 (SGK1) activation in breast cancer: requirement for mTORC1 activity associates with ER-alpha expression. Breast Cancer Res Treat *135*, 469–479.

312. Tangir, J., Bonafé, N., Gilmore-Hebert, M., Henegariu, O., and Chambers, S. K. (2004). SGK1, a potential regulator of c-fms related breast cancer aggressiveness. Clin Exp Metastasis *21*, 477–483.

313. Zarrinpashneh, E., Poggioli, T., Sarathchandra, P., Lexow, J., Monassier, L., Terracciano, C., Lang, F., Damilano, F., Zhou, J. Q., Rosenzweig, A., et al. (2013). Ablation of SGK1 impairs endothelial cell migration and tube formation leading to decreased neo-angiogenesis following myocardial infarction. PLoS ONE *8*, e80268.

314. Ferrelli, F., Pastore, D., Capuani, B., Lombardo, M. F., Blot-Chabaud, M., Coppola, A., Basello, K., Galli, A., Donadel, G., Romano, M., et al. (2015). Serum glucocorticoid inducible kinase (SGK)-1 protects endothelial cells against oxidative stress and apoptosis induced by hyperglycaemia. Acta Diabetol *52*, 55–64.

315. Nicotera, P., and Melino, G. (2004). Regulation of the apoptosis-necrosis switch. Oncogene *23*, 2757–2765.

316. Chaitanya, G. V., Steven, A. J., and Babu, P. P. (2010). PARP-1 cleavage fragments: signatures of cell-death proteases in neurodegeneration. Cell Commun Signal *8*, 31.

317. Zhong, W., Oguljahan, B., Xiao, Y., Nelson, J., Hernandez, L., Garcia-Barrio, M., and Francis, S. C. (2014). Serum and glucocorticoid-regulated kinase 1 promotes vascular smooth muscle cell proliferation via regulation of β-catenin dynamics. Cell Signal *26*, 2765–2772.

318. Mellacheruvu, D., Wright, Z., Couzens, A. L., Lambert, J.-P., St-Denis, N. A., Li, T., Miteva, Y. V., Hauri, S., Sardiu, M. E., Low, T. Y., et al. (2013). The CRAPome: a contaminant repository for affinity purification-mass spectrometry data. Nat Methods *10*, 730–736.

319. Teicher, B. A. (2009). Antibody-drug conjugate targets. Curr Cancer Drug Targets *9*, 982–1004.

320. Alley, S. C., Okeley, N. M., and Senter, P. D. (2010). Antibody-drug conjugates: targeted drug delivery for cancer. Curr Opin Chem Biol *14*, 529–537.

321. Kovtun, Y. V., and Goldmacher, V. S. (2007). Cell killing by antibody-drug conjugates. Cancer Lett *255*, 232–240.

322. Korman, A. J., Peggs, K. S., and Allison, J. P. (2006). Checkpoint blockade in cancer immunotherapy. Adv Immunol *90*, 297–339.

323. Bar, E. E. (2011). Glioblastoma, cancer stem cells and hypoxia. Brain pathology (Zurich, Switzerland). Available at: http://onlinelibrary.wiley.com.ezproxy.library.tufts.edu/doi/10.1111/j.1750-3639.2010.00460.x/full.

324. Eales, K. L., Hollinshead, K. E. R., and Tennant, D. A. (2016). Hypoxia and metabolic adaptation of cancer cells. Oncogenesis *5*, e190.

325. Bhat, M., Robichaud, N., Hulea, L., Sonenberg, N., Pelletier, J., and Topisirovic, I. (2015). Targeting the translation machinery in cancer. Nat Rev Drug Discov *14*, 261–278.

326. Ghosh, B., Benyumov, A. O., Ghosh, P., Jia, Y., Avdulov, S., Dahlberg, P. S., Peterson, M., Smith, K., Polunovsky, V. A., Bitterman, P. B., et al. (2009). Nontoxic chemical interdiction of the epithelial-to-mesenchymal transition by targeting cap-dependent translation. ACS Chem Biol *4*, 367–377.

327. Li, S., Jia, Y., Jacobson, B., McCauley, J., Kratzke, R., Bitterman, P. B., and Wagner, C. R. (2013). Treatment of breast and lung cancer cells with a N-7 benzyl guanosine monophosphate tryptamine phosphoramidate pronucleotide (4Ei-1) results in chemosensitization to gemcitabine and induced eIF4E proteasomal degradation. Mol Pharm *10*, 523–531.

328. Allegra, A., Alonci, A., Gerace, D., Russo, S., Innao, V., Calabrò, L., and Musolino, C. (2014). New orally active proteasome inhibitors in multiple myeloma. Leuk Res *38*, 1–9.

329. Adams, J., Palombella, V. J., Sausville, E. A., Johnson, J., Destree, A., Lazarus, D. D., Maas, J., Pien, C. S., Prakash, S., and Elliott, P. J. (1999). Proteasome inhibitors: a novel class of potent and effective antitumor agents. Cancer Res *59*, 2615–2622.

330. (2002). The proteasome: a novel target for cancer chemotherapy. Available at: http://www.nature.com/leu/journal/v16/n4/full/2402417a.html [Accessed March 19, 2016].

331. Jang, H. S., Lal, S., and Greenwood, J. A. (2010). Calpain 2 is required for glioblastoma cell invasion: regulation of matrix metalloproteinase 2. Neurochem Res *35*, 1796–1804.

332. Lal, S., La Du, J., Tanguay, R. L., and Greenwood, J. A. (2012). Calpain 2 is required for the invasion of glioblastoma cells in the zebrafish brain microenvironment. J Neurosci Res *90*, 769–781.

333. Golubovskaya, V. M., Huang, G., Ho, B., Yemma, M., Morrison, C. D., Lee, J., Eliceiri, B. P., and Cance, W. G. (2013). Pharmacologic blockade of FAK autophosphorylation decreases human glioblastoma tumor growth and synergizes with temozolomide. Mol Cancer Ther *12*, 162–172.

334. Boettcher, M., and Hoheisel, J. D. (2010). Pooled RNAi Screens - Technical and Biological Aspects. Curr Genomics *11*, 162–167.

335. Nakayama, K. I., and Nakayama, K. (2006). Ubiquitin ligases: cell-cycle control and cancer. Nat Rev Cancer *6*, 369–381.

336. Soucy, T. A., Smith, P. G., Milhollen, M. A., Berger, A. J., Gavin, J. M., Adhikari, S., Brownell, J. E., Burke, K. E., Cardin, D. P., Critchley, S., et al. (2009). An inhibitor of NEDD8-activating enzyme as a new approach to treat cancer. Nature *458*, 732–736.

337. Jia, L., Bickel, J. S., Wu, J., Morgan, M. A., Li, H., Yang, J., Yu, X., Chan, R. C., and Sun, Y. (2011). RBX1 (RING box protein 1) E3 ubiquitin ligase is required for genomic integrity by modulating DNA replication licensing proteins. J Biol Chem *286*, 3379–3386.

338. Schlabach, M. R., Luo, J., Solimini, N. L., Hu, G., Xu, Q., Li, M. Z., Zhao, Z., Smogorzewska, A., Sowa, M. E., Ang, X. L., et al. (2008). Cancer proliferation gene discovery through functional genomics. Science *319*, 620–624.

339. Migita, K., Takayama, T., Matsumoto, S., Wakatsuki, K., Tanaka, T., Ito, M., Nishiwada, S., and Nakajima, Y. (2014). Prognostic impact of RING box protein-1 (RBX1) expression in gastric cancer. Gastric Cancer *17*, 601–609.

340. Kapitein, L. C., Peterman, E. J. G., Kwok, B. H., Kim, J. H., Kapoor, T. M., and Schmidt, C. F. (2005). The bipolar mitotic kinesin Eg5 moves on both microtubules that it crosslinks. Nature *435*, 114–118.

341. Venere, M., Horbinski, C., Crish, J. F., Jin, X., Vasanji, A., Major, J., Burrows, A. C., Chang, C., Prokop, J., Wu, Q., et al. (2015). The mitotic kinesin KIF11 is a driver of invasion, proliferation, and self-renewal in glioblastoma. Sci Transl Med *7*, 304ra143.

342. Gross, S., Rahal, R., Stransky, N., Lengauer, C., and Hoeflich, K. P. (2015). Targeting cancer with kinase inhibitors. J Clin Invest *125*, 1780–1789.

343. Strebhardt, K., and Ullrich, A. (2006). Targeting polo-like kinase 1 for cancer therapy. Nat Rev Cancer *6*, 321–330.

344. Katoh, Y., and Katoh, M. (2006). Hedgehog signaling pathway and gastrointestinal stem cell signaling network (Review). Int J Mol Med.

345. Buehler, E., Khan, A. A., Marine, S., Rajaram, M., Bahl, A., Burchard, J., and Ferrer, M. (2012). siRNA off-target effects in genome-wide screens identify signaling pathway members. Sci Rep *2*, 428.

346. Bhinder, B., Shum, D., and Djaballah, H. (2014). Comparative Analysis of RNAi Screening Technologies at Genome-Scale Reveals an Inherent Processing Inefficiency of the Plasmid-Based shRNA Hairpin. Comb Chem High Throughput Screen *17*, 98–113.

347. Yao, X., Ping, Y., Liu, Y., Chen, K., Yoshimura, T., Liu, M., Gong, W., Chen, C., Niu, Q., Guo, D., et al. (2013). Vascular endothelial growth factor receptor 2 (VEGFR-2) plays a key role in vasculogenic mimicry formation, neovascularization and tumor initiation by Glioma stem-like cells. PLoS ONE *8*, e57188.

348. Rusconi, L., Salvatoni, L., Giudici, L., Bertani, I., Kilstrup-Nielsen, C., Broccoli, V., and Landsberger, N. (2008). CDKL5 expression is modulated during neuronal development and its subcellular distribution is tightly regulated by the C-terminal tail. J Biol Chem *283*, 30101–30111.

349. Montini, E., Andolfi, G., Caruso, A., Buchner, G., Walpole, S. M., Mariani, M., Consalez, G., Trump, D., Ballabio, A., and Franco, B. (1998). Identification and characterization of a novel serine-threonine kinase gene from the Xp22 region. Genomics *51*, 427–433.

350. Beauchamp, R., James, M., Wagh, V., DeSouza, P., Zhao, W.-N., Stemmer-Rachamimov, A., Plotkin, S., Gusella, J., Haggarty, S., and Ramesh, V. (2015). Kinome Screen Reveals SGK1 as a Therapeutic Target for NF2: Inhibition of mTORC1/2 is More Effective than Rapamycin. FASEB J. Available at: http://www.fasebj.org/content/29/1_Supplement/889.4.

351. Goidts, V., Bageritz, J., Puccio, L., Nakata, S., Zapatka, M., Barbus, S., Toedt, G., Campos, B., Korshunov, A., Momma, S., et al. (2012). RNAi screening in glioma stem-like cells identifies PFKFB4 as a key molecule important for cancer cell survival. Oncogene *31*, 3235–3243.

352. Wen, P. Y., Lee, E. Q., Reardon, D. A., Ligon, K. L., and Alfred Yung, W. K. (2012). Current clinical development of PI3K pathway inhibitors in glioblastoma. Neuro Oncol *14*, 819–829.

353. Hong, F., Larrea, M. D., Doughty, C., Kwiatkowski, D. J., Squillace, R., and Slingerland, J. M. (2008). mTOR-raptor binds and activates SGK1 to regulate p27 phosphorylation. Mol Cell *30*, 701–711.

354. Stegh, A. H., Kim, H., Bachoo, R. M., Forloney, K. L., Zhang, J., Schulze, H., Park, K., Hannon, G. J., Yuan, J., Louis, D. N., et al. (2007). Bcl2L12 inhibits post-mitochondrial apoptosis signaling in glioblastoma. Genes Dev *21*, 98–111.

355. Stegh, A. H., Kesari, S., Mahoney, J. E., Jenq, H. T., Forloney, K. L., Protopopov, A., Louis, D. N., Chin, L., and DePinho, R. A. (2008). Bcl2L12-mediated inhibition of effector caspase-3 and caspase-7 via distinct mechanisms in glioblastoma. Proc Natl Acad Sci U S A *105*, 10703–10708.

356. Stegh, A. H., Chin, L., Louis, D. N., and DePinho, R. A. (2008). What drives intense apoptosis resistance and propensity for necrosis in glioblastoma? A role for Bcl2L12 as a multifunctional cell death regulator. Cell Cycle *7*, 2833–2839.

357. Linkermann, A., Stockwell, B. R., Krautwald, S., and Anders, H.-J. (2014). Regulated cell death and inflammation: an auto-amplification loop causes organ failure. Nat Rev Immunol *14*, 759–767.

358. Hart, T., Chandrashekhar, M., Aregger, M., Steinhart, Z., Brown, K. R., MacLeod, G., Mis, M., Zimmermann, M., Fradet-Turcotte, A., Sun, S., et al. (2015). High-Resolution CRISPR Screens Reveal Fitness Genes and Genotype-Specific Cancer Liabilities. Cell *163*, 1515–1526.

359. Toledo, C. M., Ding, Y., Hoellerbauer, P., Davis, R. J., Basom, R., Girard, E. J., Lee, E., Corrin, P., Hart, T., Bolouri, H., et al. (2015). Genome-wide CRISPR-Cas9 Screens Reveal Loss of Redundancy between PKMYT1 and WEE1 in Glioblastoma Stem-like Cells. Cell Rep *13*, 2425–2439.

360. Tomko, R. P., Xu, R., and Philipson, L. (1997). HCAR and MCAR: the human and mouse cellular receptors for subgroup C adenoviruses and group B coxsackieviruses. Proc Natl Acad Sci U S A *94*, 3352–3356.

361. Bergelson, J. M., Cunningham, J. A., Droguett, G., Kurt-Jones, E. A., Krithivas, A., Hong, J. S., Horwitz, M. S., Crowell, R. L., and Finberg, R. W. (1997). Isolation of a common receptor for Coxsackie B viruses and adenoviruses 2 and 5. Science *275*, 1320–1323.

362. Bewley, M. C., Springer, K., Zhang, Y. B., Freimuth, P., and Flanagan, J. M. (1999). Structural analysis of the mechanism of adenovirus binding to its human cellular receptor, CAR. Science *286*, 1579–1583.

363. Carson, S. D. (2001). Receptor for the group B coxsackieviruses and adenoviruses: CAR. Rev Med Virol *11*, 219–226.

364. Honda, T., Saitoh, H., Masuko, M., Katagiri-Abe, T., Tominaga, K., Kozakai, I., Kobayashi, K., Kumanishi, T., Watanabe, Y. G., Odani, S., et al. (2000). The coxsackievirus-adenovirus receptor protein as a cell adhesion molecule in the developing mouse brain. Molecular Brain Research *77*, 19–28.

365. Rebel, V. I., Hartnett, S., Denham, J., Chan, M., Finberg, R., and Sieff, C. A. (2000). Maturation and lineage-specific expression of the coxsackie and adenovirus receptor in hematopoietic cells. Stem Cells *18*, 176–182.

366. Chen, J.-W., Zhou, B., Yu, Q.-C., Shin, S. J., Jiao, K., Schneider, M. D., Baldwin, H. S., and Bergelson, J. M. (2006). Cardiomyocyte-specific deletion of the coxsackievirus and adenovirus receptor results in hyperplasia of the embryonic left ventricle and abnormalities of sinuatrial valves. Circ Res *98*, 923–930.

367. Dorner, A. A., Wegmann, F., Butz, S., Wolburg-Buchholz, K., Wolburg, H., Mack, A., Nasdala, I., August, B., Westermann, J., Rathjen, F. G., et al. (2005). Coxsackievirus-adenovirus receptor (CAR) is essential for early embryonic cardiac development. J Cell Sci *118*, 3509–3521.

368. Asher, D. R., Cerny, A. M., Weiler, S. R., Horner, J. W., Keeler, M. L., Neptune, M. A., Jones, S. N., Bronson, R. T., DePinho, R. A., and Finberg, R. W. (2005). Coxsackievirus and adenovirus receptor is essential for cardiomyocyte development. Genesis *42*, 77–85.

369. Tashiro, K., Kawabata, K., Inamura, M., Takayama, K., Furukawa, N., Sakurai, F., Katayama, K., Hayakawa, T., Furue, M. K., and Mizuguchi, H. (2010). Adenovirus vector-mediated efficient transduction into human embryonic and induced pluripotent stem cells. Cell Reprogram *12*, 501–507.

370. Tashiro, K., Inamura, M., Kawabata, K., Sakurai, F., Yamanishi, K., Hayakawa, T., and Mizuguchi, H. (2009). Efficient adipocyte and osteoblast differentiation from

mouse induced pluripotent stem cells by adenoviral transduction. Stem Cells *27*, 1802–1811.

371. Hauwel, M., Furon, E., and Gasque, P. (2005). Molecular and cellular insights into the coxsackie-adenovirus receptor: role in cellular interactions in the stem cell niche. Brain Res Brain Res Rev *48*, 265–272.

372. Adjaye, J., Huntriss, J., Herwig, R., BenKahla, A., Brink, T. C., Wierling, C., Hultschig, C., Groth, D., Yaspo, M.-L., Picton, H. M., et al. (2005). Primary differentiation in the human blastocyst: comparative molecular portraits of inner cell mass and trophectoderm cells. Stem Cells *23*, 1514–1525.

373. Assou, S., Cerecedo, D., Tondeur, S., Pantesco, V., Hovatta, O., Klein, B., Hamamah, S., and De Vos, J. (2009). A gene expression signature shared by human mature oocytes and embryonic stem cells. BMC Genomics *10*, 10.

374. Krivega, M., Geens, M., and Van de Velde, H. (2014). CAR expression in human embryos and hESC illustrates its role in pluripotency and tight junctions. Reproduction *148*, 531–544.

375. Cohen, C. J., Shieh, J. T., Pickles, R. J., Okegawa, T., Hsieh, J. T., and Bergelson, J. M. (2001). The coxsackievirus and adenovirus receptor is a transmembrane component of the tight junction. Proc Natl Acad Sci U S A *98*, 15191–15196.

376. Walters, R. W., Freimuth, P., Moninger, T. O., Ganske, I., Zabner, J., and Welsh, M. J. (2002). Adenovirus fiber disrupts CAR-mediated intercellular adhesion allowing virus escape. Cell *110*, 789–799.

377. Coyne, C. B., Voelker, T., Pichla, S. L., and Bergelson, J. M. (2004). The coxsackievirus and adenovirus receptor interacts with the multi-PDZ domain protein-1 (MUPP-1) within the tight junction. J Biol Chem *279*, 48079–48084.

378. Luissint, A.-C., Lutz, P. G., Calderwood, D. A., Couraud, P.-O., and Bourdoulous, S. (2008). JAM-L-mediated leukocyte adhesion to endothelial cells is regulated in cis by alpha4beta1 integrin activation. J Cell Biol *183*, 1159–1173.

379. Kim, M., Sumerel, L. A., Belousova, N., Lyons, G. R., Carey, D. E., Krasnykh, V., and Douglas, J. T. (2003). The coxsackievirus and adenovirus receptor acts as a tumour suppressor in malignant glioma cells. Br J Cancer *88*, 1411–1416.

380. Majhen, D., Stojanović, N., Špeljko, T., Brozovic, A., De Zan, T., Osmak, M., and Ambriović-Ristov, A. (2011). Increased expression of the coxsackie and adenovirus receptor downregulates αvβ3 and αvβ5 integrin expression and reduces cell adhesion and migration. Life Sci *89*, 241–249.

381. Tashiro, K., Hirata, N., Okada, A., Yamaguchi, T., Takayama, K., Mizuguchi, H., and Kawabata, K. (2015). Expression of coxsackievirus and adenovirus receptor separates hematopoietic and cardiac progenitor cells in fetal liver kinase 1-expressing mesoderm. Stem Cells Transl Med *4*, 424–436.

382. Scott, A. M., Wolchok, J. D., and Old, L. J. (2012). Antibody therapy of cancer. Nat Rev Cancer *12*, 278–287.

383. Sliwkowski, M. X., and Mellman, I. (2013). Antibody therapeutics in cancer. Science *341*, 1192–1198.

384. Marsman, R. F. J., Bezzina, C. R., Freiberg, F., Verkerk, A. O., Adriaens, M. E., Podliesna, S., Chen, C., Purfürst, B., Spallek, B., Koopmann, T. T., et al. (2014). Coxsackie and adenovirus receptor is a modifier of cardiac conduction and arrhythmia vulnerability in the setting of myocardial ischemia. J Am Coll Cardiol *63*, 549–559.

385. Shen, Y., Kan, Q.-C., Xu, W., Chu, Y.-W., and Xiong, S.-D. (2009). Coxsackievirus B3 infection induced viral myocarditis by regulating the expression pattern of chemokines in cardiac myocytes. Iran J Allergy Asthma Immunol *8*, 1–9.